

UNIVERSITY OF IOANNINA

SCHOOL OF INFORMATICS AND TELECOMMUNICATIONS

DEPARTMENT OF INFORMATICS AND TELECOMMUNICATIONS

PhD Thesis

Characterization and Optimization of MIMO Systems for Wireless Communications

Nikolaos Mouziouras

Arta, October 2026

© 2026 Nikolaos Mouziouras
Licensed under the Creative Commons Attribution-NonCommercial-NoDerivatives 4.0 International License.
CC BY-NC-ND 4.0



ΠΑΝΕΠΙΣΤΗΜΙΟ ΙΩΑΝΝΙΝΩΝ

ΤΜΗΜΑ ΠΛΗΡΟΦΟΡΙΚΗΣ ΚΑΙ ΤΗΛΕΠΙΚΟΙΝΩΝΙΩΝ

Διδακτορική Διατριβή

Χαρακτηρισμός και βελτιστοποίηση επιδόσεων διαύλων MIMO για ασύρματα συστήματα επικοινωνιών

Νικόλαος Μουζιούρας

Επιβλέπων Καθηγητής
Κωνσταντίνος Θ. Αγγέλης

Άρτα, Οκτώβριος 2026

CHARACTERIZATION AND OPTIMIZATION OF MIMO SYSTEMS FOR WIRELESS COMMUNICATIONS

Εγκρίθηκε από επταμελή εξεταστική επιτροπή

Άρτα, Οκτώβριος 2026

ΕΠΤΑΜΕΛΗΣ ΕΠΙΤΡΟΠΗ ΑΞΙΟΛΟΓΗΣΗΣ

1. Αγγέλης Κωνσταντίνος
   Καθηγητής Α΄ βαθμίδας (Επιβλέπων)
   Τμήμα Πληροφορικής και Τηλεπικοινωνιών
   Πανεπιστήμιο Ιωαννίνων

2. Οικονόμου Κωνσταντίνος
   Καθηγητής Α΄ βαθμίδας
   Τμήμα Πληροφορικής
   Ιόνιο Πανεπιστήμιο

3. Τσορμπατζόγλου Ανδρέας
   Αναπληρωτής Καθηγητής
   Τμήμα Πληροφορικής και Τηλεπικοινωνιών
   Πανεπιστήμιο Ιωαννίνων

4. Βαρτζιώτης Φώτιος
   Επίκουρος Καθηγητής
   Τμήμα Πληροφορικής και Τηλεπικοινωνιών
   Πανεπιστήμιο Ιωαννίνων

5. Γιαννακέας Νικόλαος
   Αναπληρωτής Καθηγητής
   Τμήμα Πληροφορικής και Τηλεπικοινωνιών
   Πανεπιστήμιο Ιωαννίνων

6. Δουμένης Γρηγόριος
Αναπληρωτής Καθηγητής
Τμήμα Πληροφορικής και Τηλεπικοινωνιών
Πανεπιστήμιο Ιωαννίνων

7. Τσουμάνης Γεώργιος
Επίκουρος Καθηγητής
Τμήμα Πληροφορικής
Ιόνιο Πανεπιστήμιο

Acknowledgements

The completion of this doctoral dissertation marks the end of an important academic journey, one that would not have been possible without the support, guidance and encouragement of many people. First and foremost, I would like to express my sincere gratitude to my supervisor, Professor Constantinos T. Angelis, for his continuous guidance, valuable advice and unwavering support throughout the course of this research. His scientific insight, critical feedback and encouragement played a fundamental role in shaping both this dissertation and my development as a researcher. I would also like to sincerely thank the members of my advisory and examination committee, Associate Professor Andreas Tsormpatzoglou and Professor Constantinos Oikonomou, for their valuable comments, constructive suggestions and encouragement during this doctoral journey. Finally, I would like to express my deepest gratitude to my family and my close friends for their unconditional love, patience, patience, patience and support throughout all these years. Their encouragement and belief in me have been a constant source of strength and motivation.

Abstract

Modern wireless communication systems are evolving toward increasingly heterogeneous, dynamic and resource-constrained operating environments, driven by the requirements of beyond-5G and 6G networks, massive machine-type communications, ultra-reliable services and energy-constrained Internet of Things (IoT) applications. Within this context, Multiple-Input Multiple-Output (MIMO) technology has become a fundamental component of modern wireless communications due to its ability to improve reliability, spectral efficiency, coverage and network capacity. However, much of the existing understanding of MIMO system behavior and optimization relies on idealized assumptions that only partially represent realistic wireless operating conditions.

In non ideal environments, MIMO performance is jointly influenced by propagation characteristics, imperfect channel state information (CSI), reliability requirements, implementation constraints and energy limitations. The interaction of these factors can substantially alter system behavior and limit the applicability of conclusions derived under simplified assumptions. This dissertation addresses these limitations through a systematic investigation of MIMO communication systems under realistic propagation conditions and imperfect CSI, progressing from system characterization to reliability–energy analysis, adaptive transmission and cooperative communication.

The first part of the dissertation investigates MIMO behavior under standardized 3GPP propagation models. The analysis examines the effects of propagation asymmetries, antenna geometry, polarization characteristics, user distribution, mobility and network load on key communication metrics. The results demonstrate that MIMO performance under non ideal propagation conditions is governed by the combined interaction of spatial dimensionality, temporal channel dynamics, propagation heterogeneity and network load. Conditions that enhance channel symmetry and spatial diversity generally improve performance, whereas mobility, propagation asymmetry and unfavorable user distributions can lead to significant degradation.

Building upon this characterization, the dissertation investigates the interaction between communication reliability and energy efficiency. By accounting for retransmissions, hardware-related energy consumption and signal-processing overhead, the analysis demonstrates that increasing the diversity order does not necessarily provide the most energy-efficient solution, since the energy-preferred MIMO configuration depends on propagation conditions, communication reliability and implementation costs. The investigation is further extended to energy-constrained IoT and LPWAN systems, including LoRa-based networks. Under these constrained operating conditions, spatial diversity improves link robustness, while imperfect CSI shifts the reliability transition toward more favorable SNR conditions and reduces the effective reliability advantage of higher-diversity configurations. These effects directly influence retransmission behavior and the energy required for successful packet delivery.

The knowledge obtained from these analyses is subsequently exploited to develop an adap-

tive MIMO diversity-selection framework that dynamically selects the most energy-efficient feasible transmission configuration according to the prevailing operating conditions. The resulting adaptive policy exhibits structured operating regions characterized by progressive diversity activation as propagation conditions, CSI uncertainty and hardware overhead vary. Transition analysis further shows that adaptive evolution occurs predominantly between neighboring diversity configurations, while larger transitions arise selectively near feasibility boundaries. These results demonstrate that adaptive diversity selection can provide reliable and energy-efficient MIMO operation while maintaining structured and continuity-preserving behavior across the considered operating space.

Finally, the dissertation extends the adaptive optimization perspective to cooperative relay-assisted MIMO systems operating under imperfect CSI. The analysis demonstrates that cooperative transmission is not universally beneficial and identifies a harmful cooperation region in which relay-assisted transmission becomes less reliable than direct MIMO communication. This behavior results from the combined effects of residual CSI-induced interference and relay decoding error propagation and becomes more pronounced as channel estimation accuracy deteriorates. To mitigate this effect, a reliability-aware relay activation mechanism is investigated, in which relay participation is controlled according to the estimated quality of the source–relay channel. The resulting adaptive strategy suppresses unreliable relay participation, reduces the harmful cooperation region and preserves the benefits of cooperative diversity when relay conditions are sufficiently reliable.

Collectively, the investigations establish a unified perspective on the characterization and optimization of MIMO communication systems under non-ideal operating conditions. The results demonstrate that effective MIMO operation cannot be described by a universally optimal transmission strategy, since the preferred operating configuration depends on propagation conditions, CSI quality, reliability requirements and implementation constraints. By linking realistic system characterization with reliability–energy analysis, adaptive diversity selection and reliability-aware cooperative operation, this dissertation contributes to the understanding and design of robust and energy-efficient MIMO communication systems for next-generation wireless networks.

Keywords: Multiple-Input Multiple-Output (MIMO), non-ideal wireless propagation, imperfect channel state information, communication reliability, energy efficiency, adaptive MIMO, cooperative MIMO, reliability-aware optimization.

Περίληψη

Τα σύγχρονα ασύρματα συστήματα επικοινωνιών λειτουργούν σε ολοένα πιο σύνθετα, δυναμικά και ετερογενή περιβάλλοντα, καθώς καλούνται να υποστηρίξουν τις αυξανόμενες απαιτήσεις εφαρμογών επόμενης γενιάς, όπως η μαζική συνδεσιμότητα, οι υπερ-αξιόπιστες επικοινωνίες και τα ενεργειακά περιορισμένα δίκτυα του Διαδικτύου των Πραγμάτων (IoT). Στο πλαίσιο αυτό, η τεχνολογία Πολλαπλών Εισόδων–Πολλαπλών Εξόδων (MIMO) έχει αναδειχθεί ως θεμελιώδης τεχνολογία των σύγχρονων ασύρματων επικοινωνιών, λόγω της ικανότητάς της να βελτιώνει την αξιοπιστία επικοινωνίας, τη φασματική αποδοτικότητα, την κάλυψη και τη χωρητικότητα του δικτύου. Ωστόσο, μεγάλο μέρος της υφιστάμενης γνώσης σχετικά με τη συμπεριφορά των συστημάτων MIMO βασίζεται σε ιδεατές παραδοχές που δεν αποτυπώνουν επαρκώς τις πραγματικές συνθήκες λειτουργίας των ασύρματων συστημάτων.

Σε μη ιδανικά ασύρματα περιβάλλοντα, η απόδοση των συστημάτων MIMO επηρεάζεται από τη σύνθετη αλληλεπίδραση μεταξύ ρεαλιστικών συνθηκών διάδοσης και ατελούς πληροφορίας καναλιού, καθώς και από απαιτήσεις αξιοπιστίας, ενεργειακούς περιορισμούς, προσαρμοστικούς μηχανισμούς μετάδοσης και συνεργατικές στρατηγικές επικοινωνίας. Φαινόμενα διάδοσης όπως η χωρική συσχέτιση, η ασυμμετρία καναλιού, η γεωμετρία των κεραιών και η μη ομοιόμορφη κατανομή χρηστών μπορούν να μεταβάλουν σημαντικά τη συμπεριφορά των συστημάτων σε σχέση με τις ιδεατές υποθέσεις μοντελοποίησης. Παρά τη σημαντική πρόοδο της έρευνας στις ασύρματες επικοινωνίες, η συνδυασμένη επίδραση των παραπάνω παραγόντων παραμένει ανεπαρκώς διερευνημένη.

Η παρούσα διατριβή αντιμετωπίζει την πρόκληση αυτή μέσω μιας συστηματικής διερεύνησης συστημάτων MIMO υπό μη ιδανικές συνθήκες διάδοσης και ατελή πληροφορία καναλιού. Η ερευνητική μεθοδολογία ακολουθεί μια προοδευτική προσέγγιση, στην οποία ο ρεαλιστικός χαρακτηρισμός της συμπεριφοράς του συστήματος αποτελεί τη βάση για τη βελτιστοποίηση της απόδοσης, την ανάπτυξη προσαρμοστικών μηχανισμών μετάδοσης και τη μελέτη συνεργατικών τεχνικών επικοινωνίας υπό μη ιδανικές συνθήκες λειτουργίας.

Το πρώτο μέρος της διατριβής επικεντρώνεται στον χαρακτηρισμό της συμπεριφοράς συστημάτων MIMO με χρήση τυποποιημένων τρισδιάστατων μοντέλων καναλιού 3GPP. Η ανάλυση εξετάζει την επίδραση των ασυμμετριών διάδοσης, της γεωμετρίας των κεραιών, των χαρακτηριστικών πόλωσης και της χωρικής κατανομής των χρηστών σε βασικούς δείκτες απόδοσης, αποδεικνύοντας ότι οι ρεαλιστικές συνθήκες ανάπτυξης επηρεάζουν ουσιαστικά τη λειτουργία των συστημάτων και αναδεικνύουν περιορισμούς των ιδεατών μοντέλων καναλιού.

Με βάση τον παραπάνω χαρακτηρισμό, η διατριβή διερευνά τη θεμελιώδη αλληλεπίδραση μεταξύ αξιοπιστίας επικοινωνίας και ενεργειακής αποδοτικότητας. Λαμβάνοντας υπόψη τις επαναμεταδόσεις, την κατανάλωση ενέργειας του υλικού και το κόστος επεξεργασίας σήματος, η ανάλυση αναδεικνύει τους βασικούς συμβιβασμούς αξιοπιστίας–ενέργειας και καταδεικνύει ότι η αύξηση της διαφοριστικής τάξης δεν αποτελεί πάντοτε την ενεργεια-

κά αποδοτικότερη επιλογή, καθώς η προτιμητέα διαμόρφωση MIMO εξαρτάται από τις εκάστοτε συνθήκες λειτουργίας και το σχετικό ενεργειακό κόστος. Η διερεύνηση επεκτείνεται επίσης σε ενεργειακά περιορισμένα δίκτυα IoT και LPWAN, με ιδιαίτερη έμφαση στα συστήματα LoRa, τα οποία αξιοποιούνται τόσο ως αντιπροσωπευτικό παράδειγμα για τη μελέτη της επίδρασης ρεαλιστικών συνθηκών διάδοσης όσο και για τη διερεύνηση των συμβιβασμών μεταξύ αξιοπιστίας και ενεργειακής αποδοτικότητας σε ασύρματα περιβάλλοντα με αυστηρούς ενεργειακούς και επικοινωνιακούς περιορισμούς.

Η γνώση που προκύπτει από τις προηγούμενες αναλύσεις αξιοποιείται στη συνέχεια για την ανάπτυξη προσαρμοστικών στρατηγικών λειτουργίας MIMO, οι οποίες επιλέγουν δυναμικά την καταλληλότερη διαμόρφωση μετάδοσης σύμφωνα με τις εκάστοτε συνθήκες λειτουργίας. Το προτεινόμενο πλαίσιο καταδεικνύει ότι η προσαρμοστική βελτιστοποίηση, βασισμένη στις εκάστοτε περιοχές λειτουργίας του συστήματος, επιτυγχάνει υψηλότερη αξιοπιστία και ενεργειακή αποδοτικότητα σε σχέση με στατικές στρατηγικές μετάδοσης.

Τέλος, η διατριβή επεκτείνει τη φιλοσοφία της προσαρμοστικής βελτιστοποίησης σε συνεργατικά συστήματα MIMO με αναμετάδοση (Cooperative MIMO) υπό ατελή πληροφορία κατάστασης καναλιού (CSI). Η ανάλυση αναδεικνύει το φαινόμενο της επιζήμιας συνεργασίας, σύμφωνα με το οποίο, υπό ορισμένες μη ιδανικές συνθήκες λειτουργίας, η συνεργατική μετάδοση μπορεί να παρουσιάσει χαμηλότερη αξιοπιστία από την απευθείας επικοινωνία MIMO εξαιτίας της συνδυασμένης επίδρασης της αβεβαιότητας του καναλιού και της διάδοσης σφαλμάτων από τον αναμεταδότη. Για την αντιμετώπιση του φαινομένου αυτού προτείνεται ένας μηχανισμός ενεργοποίησης του αναμεταδότη βασισμένος στην αξιοπιστία της επικοινωνίας, ο οποίος επιτρέπει προσαρμοστική συνεργατική λειτουργία ανάλογα με τις επικρατούσες συνθήκες.

Συνολικά, η διατριβή διαμορφώνει ένα ενιαίο πλαίσιο για τον χαρακτηρισμό και τη βελτιστοποίηση συστημάτων MIMO υπό μη ιδανικές συνθήκες λειτουργίας. Τα αποτελέσματα δείχνουν ότι η αξιόπιστη και ενεργειακά αποδοτική λειτουργία των ασύρματων συστημάτων δεν προκύπτει από την εφαρμογή μιας καθολικά βέλτιστης στρατηγικής μετάδοσης, αλλά από τον συνδυασμό ρεαλιστικού χαρακτηρισμού του συστήματος, βελτιστοποίησης βασισμένης στην αξιοπιστία και προσαρμοστικών μηχανισμών λήψης αποφάσεων που ανταποκρίνονται στις εκάστοτε συνθήκες λειτουργίας. Με τον τρόπο αυτό, η διατριβή συμβάλλει τόσο στην κατανόηση όσο και στον σχεδιασμό συστημάτων MIMO για τα ασύρματα δίκτυα επόμενης γενιάς.

Λέξεις-κλειδιά: Συστήματα Πολλαπλών Εισόδων–Πολλαπλών Εξόδων (MIMO), μη ιδανική διάδοση ασύρματων καναλιών, ατελής πληροφορία κατάστασης καναλιού, αξιοπιστία επικοινωνίας, ενεργειακή αποδοτικότητα, προσαρμοστικά συστήματα MIMO, συνεργατικά συστήματα MIMO, βελτιστοποίηση.

Publications Related to This Dissertation

The following publications were produced in the context of the research conducted for this doctoral dissertation.

Journal Publications

1. N. Mouziouras, A. Tsormpatzoglou, and C. T. Angelis, "Performance Analysis of a MIMO System Under Realistic Conditions Using 3GPP Channel Model," *Symmetry*, vol. 17, no. 12, Art. no. 2159, 2025. doi: 10.3390/sym17122159.

2. N. Mouziouras, A. Tsormpatzoglou, and C. T. Angelis, "A Progressive Evaluation of MIMO Techniques in LoRa-Type Wireless Sensor Networks Under Imperfect Channel State Information," *Electronics*, vol. 15, no. 4, Art. no. 867, 2026. doi: 10.3390/electronics15040867.

3. N. Mouziouras, C. T. Angelis, A. Tsormpatzoglou, and E. Spyrou, "Harmful Cooperation in Relay-Assisted MIMO Under Imperfect CSI," *Sensors*, vol. 26, no. 13, Art. no. 4061, 2026. doi: 10.3390/s26134061.

4. N. Mouziouras and C. T. Angelis, "Energy-Efficient MIMO Diversity: Operating Regimes, Hardware Constraints and Geometry-Aware Propagation Effects," *Computer Networks and Communications*, vol. 4, no. 2, pp. 332–357, Sep. 2026.

Conference Publication

1. N. Mouziouras, A. Tsormpatzoglou, G. Tsoumanis, K. Oikonomou and C. T. Angelis, "Adaptive Diversity Selection for Energy-Aware MIMO Systems," presented at the 11th South-East Europe Design Automation, Computer Engineering, Computer Networks and Social Media Conference (SEEDA-CECNSM 2026), Thessaloniki, Greece, Sep. 2026. Proceedings to be submitted for inclusion in IEEE Xplore.

Abbreviations

3GPP	Third Generation Partnership Project
AWGN	Additive White Gaussian Noise
ARQ	Automatic Repeat Request
BER	Bit Error Rate
BLER	Block Error Rate
BPSK	Binary Phase-Shift Keying
BS	Base Station
CDF	Cumulative Distribution Function
CQI	Channel Quality Indicator
CEEM	Channel Estimation Error Model
CEEM-I	Channel Estimation Error Model I
CEEM-II	Channel Estimation Error Model II
CSI	Channel State Information
DF	Decode-and-Forward
DFT	Discrete Fourier Transform
DMT	Diversity–Multiplexing Tradeoff
DoF	Degrees of Freedom
ECDF	Empirical Cumulative Distribution Function
eMBB	enhanced Mobile Broadband
FD-MIMO	Full-Dimension Multiple-Input Multiple-Output
HARQ	Hybrid Automatic Repeat Request
IoT	Internet of Things
LOS	Line-of-Sight
LPWAN	Low-Power Wide-Area Network
LTE	Long-Term Evolution
LTE-A	Long-Term Evolution Advanced
MIESM	Mutual Information Effective SINR Mapping
MIMO	Multiple-Input Multiple-Output
MISO	Multiple-Input Single-Output
ML	Maximum Likelihood
MMSE	Minimum Mean Square Error

mMTC	massive Machine-Type Communications
MRC	Maximal Ratio Combining
NB-IoT	Narrowband Internet of Things
NLOS	Non-Line-of-Sight
PER	Packet Error Rate
QPSK	Quadrature Phase-Shift Keying
RF	Radio Frequency
RMa	Rural Macrocell
SCM	Spatial Channel Model
SF	Spreading Factor
SIMO	Single-Input Multiple-Output
SINR	Signal-to-Interference-plus-Noise Ratio
SISO	Single-Input Single-Output
SLS	System-Level Simulator
SNR	Signal-to-Noise Ratio
STBC	Space–Time Block Coding
SVD	Singular Value Decomposition
TTI	Transmission Time Interval
TXDIV	Transmit Diversity
UE	User Equipment
UMa	Urban Macrocell
UMi	Urban Microcell
URLLC	Ultra-Reliable Low-Latency Communications
ZF	Zero Forcing

Nomenclature

N_t	Number of transmit antennas
N_r	Number of receive antennas
N_s	Number of transmitted spatial streams
$\mathbf{x}$	Transmitted signal vector
$\mathbf{y}$	Received signal vector
$\mathbf{n}$	Additive noise vector
$\mathbf{H}$	Channel matrix
$\hat{\mathbf{H}}$	Estimated channel matrix
$\mathbf{E}$	Channel estimation error matrix
$\mathbf{W}$	Linear detection or equalization matrix
$\mathbf{F}$	Transmit precoding matrix
$\mathbf{I}$	Identity matrix
σ_n^2	Noise variance
σ_e^2	Channel estimation error variance
ρ	Signal-to-noise ratio
r	Channel rank or multiplexing gain, depending on context
C	Achievable channel capacity
d	Diversity order or transmission distance, depending on context
P_e	Symbol or bit error probability
R	Achievable transmission rate
$PL(d)$	Path loss at distance d
d_0	Reference distance for path-loss modeling
n	Path-loss exponent
X_σ	Log-normal shadowing component
σ	Shadowing standard deviation
L	Number of propagation paths or packet length, depending on context
α_l	Amplitude of the l-th propagation path
ϕ_l	Phase of the l-th propagation path
K	Rician K-factor
P_{LOS}	Power of the line-of-sight component

P_{NLOS}	Power of the non-line-of-sight multipath components
γ	Instantaneous SNR or SINR
γ_{th}	Reliability or relay-activation threshold
P_{out}	Outage probability
N_{error}	Number of incorrectly detected bits
N_{total}	Total number of transmitted bits
E_{tx}	Transmission energy per transmission attempt
E_{circuit}	Circuit-related energy consumption
E_{proc}	Signal-processing energy consumption
E_{overhead}	Additional hardware-related energy overhead
E_{total}	Total energy consumed per transmission attempt
$E_{\text{pkt},m}$	Packet-level energy consumption of transmission mode m
E_{succ}	Expected energy required for successful packet delivery
$E_{\text{succ},m}$	Expected energy per successful packet for mode m
α_m	Mode-dependent hardware or circuit-energy overhead
β_m	Mode-dependent signal-processing or complexity-related energy overhead
m	Transmission or diversity mode
m^*	Selected optimal transmission mode
$\mathcal{M}$	Set of candidate transmission modes
$\mathcal{F}$	Set of feasible transmission modes
$J(m)$	Mode-dependent optimization objective
PER_m	Packet error rate of transmission mode m
PER_{th}	Packet-error-rate feasibility threshold
$M(i, j)$	Adaptive operating mode at operating point (i, j)
$D(i, j)$	Transition distance between neighboring operating modes
D_{avg}	Average adaptive transition distance
N_{local}	Number of local adaptive transitions
N_{switch}	Total number of adaptive mode switches
$N_{\text{neighbors}}$	Number of neighboring operating-point comparisons
L_{loc}	Transition locality ratio
A	Abrupt-transition ratio
S	Adaptive stability index
$\mathbf{H}_{SR}$	Source-to-relay channel matrix

$\mathbf{H}_{SD}$	Source-to-destination channel matrix
$\mathbf{H}_{RD}$	Relay-to-destination channel matrix
$\hat{\mathbf{H}}_{SR}$	Estimated source-to-relay channel matrix
$\mathbf{s}$	Transmitted symbol vector
$\hat{\mathbf{s}}_R$	Symbol vector detected and forwarded by the relay
$\mathbf{e}_R$	Relay decoding error vector
γ_{SR}	Estimated source-to-relay channel-quality metric
G_{coop}	Cooperation gain
ΔBER	BER difference between cooperative and direct transmission
$\Delta\text{BER}_{\text{coded}}$	Coded BER difference between cooperative and direct transmission
$\mathbf{i}_{\text{CSI}}$	Residual interference due to CSI uncertainty
SINR_{eff}	Effective post-detection SINR
P_s	Desired signal power
P_{CSI}	Residual interference power due to imperfect CSI
P_n	Post-detection noise power
S_{CSI}	CSI sensitivity metric
$S_{\text{CSI}}^{\text{safe}}$	Stabilized CSI sensitivity metric
G_R^{safe}	Stabilized robustness gain
$\hat{\mathbf{G}}$	Effective estimated channel matrix
$\kappa(\hat{\mathbf{G}})$	Condition number of the effective estimated channel matrix
ϵ	Small positive constant used for numerical stabilization

Contents

Publications Related to This Dissertation x

List of Abbreviations xi

Nomenclature xiii

1 Introduction 1
- 1.1 Evolution of Wireless Communication Systems . . . 1
- 1.2 MIMO Communications as a Key Enabling Technology . . . 2
- 1.3 From Idealized Models to Realistic Wireless Environments . . . 3
- 1.4 The Challenge of Imperfect Channel State Information . . . 4
- 1.5 Reliability Challenges in Modern MIMO Systems . . . 5
- 1.6 Energy Efficiency as a Design Constraint . . . 6
- 1.7 Adaptive Communication as a Key Enabler of Efficient Wireless Operation . 7
- 1.8 Cooperative Communication for Reliability Enhancement in Wireless Networks 8
- 1.9 Research Gap and Problem Statement . . . 10
- 1.10 Research Objectives . . . 11
- 1.11 Main Scientific Contributions . . . 12
- 1.12 Organization of the Thesis . . . 13

2 Theoretical Foundations 16
- 2.1 Fundamentals of MIMO Communications . . . 16
  - 2.1.1 MIMO System Model . . . 16
  - 2.1.2 Spatial Degrees of Freedom in MIMO Systems . . . 17
  - 2.1.3 Diversity Techniques in MIMO Systems . . . 19
  - 2.1.4 Spatial Multiplexing and Throughput Enhancement . . . 21
  - 2.1.5 Linear Detection in MIMO Systems . . . 22
  - 2.1.6 Diversity–Multiplexing Tradeoff . . . 23
- 2.2 Realistic Wireless Propagation and Channel Modeling . . . 24
  - 2.2.1 Limitations of Simplified Channel Models . . . 24
  - 2.2.2 Large-Scale Propagation Effects . . . 25
  - 2.2.3 Small-Scale Fading and Spatial Correlation . . . 27
  - 2.2.4 Realistic Channel Modeling for MIMO Systems . . . 29
  - 2.2.5 Simulation Frameworks for Realistic MIMO Evaluation . . . 31
- 2.3 Channel State Information and Channel Uncertainty . . . 32
  - 2.3.1 CSI in MIMO Communications . . . 32
  - 2.3.2 Modeling CSI Imperfections . . . 34
  - 2.3.3 Impact of Imperfect CSI on MIMO Performance . . . 35
- 2.4 Reliability and Energy Efficiency in Wireless Systems . . . 36

2.4.1 Reliability Metrics in Wireless Communications 36
2.4.2 Energy Consumption and Retransmission Cost in Wireless Systems . 37
2.4.3 Reliability–Energy Trade-offs in MIMO Communications 39
2.4.4 Energy-Constrained Wireless Systems: IoT and LPWAN 40
2.4.5 Adaptive MIMO Operation and Mode Selection 41
2.5 Cooperative MIMO Communications 42
2.5.1 Fundamentals of Cooperative Communications 42
2.5.2 Decode-and-Forward Relaying 44
2.5.3 Benefits and Limitations of Cooperative MIMO 45
2.5.4 Practical Considerations for Cooperative Operation 46
2.6 Chapter Summary 47

3 State of the Art and Research Gaps 49
3.1 Literature Review on Realistic MIMO System Characterization 49
3.2 Literature Review on Reliability–Energy Trade-offs in MIMO and Energy-Constrained Wireless Systems 52
3.3 Literature Review on Adaptive Energy-Aware MIMO Operation 54
3.4 Literature Review on Cooperative MIMO Communications under Realistic Operating Conditions 56
3.5 Research Gaps and Thesis Positioning 58

4 MIMO Performance Characterization Under Realistic Wireless Conditions 61
4.1 Broadband MIMO Characterization Under Realistic Propagation Conditions . 62
4.1.1 Broadband MIMO Simulation Framework 62
4.1.2 Initial Sensitivity Analysis of Key System and Channel Parameters . . 65
4.1.3 Performance Under Realistic Propagation Conditions 70
4.1.4 Cross-Scenario Insights for Broadband MIMO Systems 88
4.2 LoRa-Type MIMO Characterization Under Constrained Operating Conditions 93
4.2.1 Simulation Methodology and System Assumptions 94
4.2.2 Baseline Coverage and Operating-Regime Characterization 97
4.2.3 Diversity-Oriented MIMO Analysis 103
4.2.4 Spatial Multiplexing Analysis 113
4.2.5 LoRa Characterization Discussion and Design Implications 122
4.3 Summary and Conclusions 126

5 Reliability-Aware Energy Optimization in MIMO Systems 129
5.1 Energy-Optimal Operating Regions in MIMO Diversity Systems 130
5.1.1 System Model and Energy Framework 130
5.1.2 Distance-Driven Retransmission Energy and Diversity Gains 132
5.1.3 Hardware-Aware Operating Region Analysis 139
5.1.4 Energy-Optimal Operating Regions and Design Insights 143

5.2 Energy Optimization in Constrained LoRa MIMO Systems 146
5.2.1 System Model and LoRa Energy Framework 147
5.2.2 SNR-Driven Reliability Transition under Imperfect CSI 148
5.2.3 SNR-Driven Energy–Reliability Trade-Off and Mode Switching . . . 151
5.2.4 Impact of System Parameters 153
5.2.5 Energy-Optimal Operating Regions and Design Insights 156
5.3 Summary and Conclusions 159

6 Structured Adaptive Diversity Selection for Energy-Aware MIMO Systems 163
6.1 Adaptive Optimization Framework for Diversity Selection 164
6.1.1 System Model 165
6.1.2 Energy Consumption Model 165
6.1.3 Feasibility-Aware Adaptive Selector 167
6.1.4 Transition and Stability Characterization Framework 169
6.1.5 Learnability Characterization Framework 170
6.1.6 Simulation Setup 171
6.2 Adaptive Operating Behavior and Energy-Efficiency Evaluation 172
6.2.1 Adaptive Operating Region Analysis 172
6.2.2 Adaptive Occupancy Redistribution 174
6.2.3 Transition and Stability Analysis 176
6.2.4 Adaptive Energy Efficiency Analysis 179
6.2.5 Robustness Analysis under CSI Uncertainty 183
6.2.6 Learnability and Policy Approximation 184
6.3 Summary and Conclusions 186

7 Cooperative MIMO under Realistic Operating Impairments 190
7.1 Reliability-Aware Cooperative MIMO Framework and Evaluation Methodology 191
7.2 Cooperative Reliability Analysis and Relay-Activation Evaluation 196
7.2.1 Interference-Limited Cooperative Behavior under Imperfect CSI . . . 196
7.2.2 Comparative Behavior of Direct and Cooperative MIMO under Ideal and Impaired Conditions 199
7.2.3 Harmful Cooperation Region Analysis 202
7.2.4 Reliability-Aware Relay Activation 206
7.2.5 Relay-Activation Threshold Optimization 208
7.2.6 Performance Evaluation of Adaptive Cooperative Operation 210
7.2.7 Antenna Scaling and Cooperative Robustness 212
7.3 Summary and Conclusions 216

8 General Conclusions and Future Research Directions 220
8.1 Principal Scientific Findings 220
8.2 Scientific Contributions and Research Outcomes 224

8.3 Design Implications for MIMO Systems 226
8.4 Limitations and Scope of the Present Work 227
8.5 Future Research Directions 228
8.6 Final Remarks 229

List of Figures

1.1 Conceptual research framework 14

2.1 Basic MIMO communication system model with N_t transmit antennas and N_r receive antennas. 16
2.2 Basic concept of cooperative communication. 43
2.3 Two-phase Decode-and-Forward cooperative relaying 44

4.1 Impact of transmit power on average UE throughput. 67
4.2 Impact of transmit power on average UE spectral efficiency. 67
4.3 Impact of carrier frequency on average UE throughput. 68
4.4 Impact of carrier frequency on average UE spectral efficiency. 68
4.5 Impact of propagation K-factor on average UE throughput. 70
4.6 Impact of propagation K-factor on average UE spectral efficiency. 70
4.7 CDF of average UE throughput for different transmit power and antenna polarization configurations. 72
4.8 CDF of average UE spectral efficiency for different transmit power and antenna polarization configurations. 73
4.9 CDF of UE SINR for different transmit power and antenna polarization configurations. 73
4.10 CDF of average UE throughput for different antenna configurations and polarization settings. 75
4.11 CDF of average UE spectral efficiency for different antenna configurations and polarization settings. 75
4.12 CDF of UE SINR for different antenna configurations and polarization settings. 76
4.13 CDF of average UE throughput for different indoor-user fractions and user mobility levels. 78
4.14 CDF of average UE spectral efficiency for different indoor-user fractions and user mobility levels. 78
4.15 CDF of UE SINR for different indoor-user fractions and user mobility levels. 79
4.16 CDF of average UE throughput for different indoor-user fractions in the indoor office model. 81
4.17 CDF of average UE spectral efficiency for different indoor-user fractions in the indoor office model. 81
4.18 CDF of UE SINR for different indoor-user fractions in the indoor office model. 82
4.19 CDF of average UE throughput for different user densities. 83
4.20 CDF of average UE spectral efficiency for different user densities. 84
4.21 CDF of UE SINR for different user densities. 84
4.22 CDF of average UE throughput for different cell radius values. 86

4.23 CDF of average UE spectral efficiency for different cell radius values. 86
4.24 CDF of UE SINR for different cell radius values. 87
4.25 CDF of received SNR for different cell radius values. 100
4.26 CDF of received SNR for different shadowing standard deviation values. . . . 101
4.27 CDF of received SNR under different spreading-factor allocation margins. . . 102
4.28 BER versus SNR for diversity-oriented MIMO configurations under perfect CSI with SF9. 104
4.29 BER versus SNR for diversity-oriented MIMO configurations under perfect CSI. 104
4.30 BER versus SNR for diversity-oriented MIMO configurations under CEEM-I. 106
4.31 BER versus SNR under different CEEM-I uncertainty levels for the 2×1 and 2×2 configurations. 107
4.32 BER versus SNR under different CEEM-I uncertainty levels for the 4×1 and 4×2 configurations. 108
4.33 BER versus SNR for diversity-oriented MIMO configurations under CEEM-II. 109
4.34 BER versus SNR under different CEEM-II uncertainty levels for the 2×1 and 2×2 configurations. 110
4.35 BER versus SNR under different CEEM-II uncertainty levels for the 4×1 and 4×2 configurations. 111
4.36 BER versus SNR for different transmission mechanisms under perfect CSI. . 114
4.37 BER versus SNR under CEEM-I for different transmission and detection schemes in a 2×2 MIMO configuration: (a) spatial multiplexing with ZF detection, (b) spatial multiplexing with MMSE detection, and (c) STBC transmission. 116
4.38 BER versus SNR for different antenna configurations using spatial multiplexing with MMSE detection. 118
4.39 PER versus SNR for different antenna configurations using spatial multiplexing with MMSE detection. 119
4.40 Normalized goodput versus SNR for different antenna configurations using spatial multiplexing with MMSE detection. 120
4.41 PER versus SNR for different receiver-rank configurations using spatial multiplexing with MMSE detection. 120
4.42 Normalized goodput versus SNR for different receiver-rank configurations using spatial multiplexing with MMSE detection. 121

5.1 PER versus distance for the Indoor LOS scenario. 133
5.2 Energy per successful packet versus distance for the Indoor LOS scenario. . . 134
5.3 PER versus distance under the i.i.d. Rayleigh fading model. 135
5.4 Impact of SNR on energy per successful packet versus distance. 136
5.5 PER versus antenna spacing. 137
5.6 Energy per successful packet versus antenna spacing. 138

5.7 Energy per successful packet versus distance under different hardware-overhead regimes. 141
5.8 Energy per successful packet under different overhead conditions: (a) short-distance regime and (b) long-distance regime. 142
5.9 BER versus SNR for MIMO configurations under perfect and imperfect CSI (SF = 10): (a) Perfect CSI, (b) CEEM-I, (c) CEEM-II. 149
5.10 PER versus SNR for MIMO configurations under perfect and imperfect CSI (SF = 10): (a) Perfect CSI, (b) CEEM-I, (c) CEEM-II. 150
5.11 Normalized energy per successful packet versus SNR for different MIMO configurations under perfect and imperfect CSI (SF = 10): (a) Perfect CSI, (b) CEEM-I, (c) CEEM-II. 152
5.12 Normalized energy per successful packet as a function of PER under perfect and imperfect CSI (SF = 10): (a) Perfect CSI, (b) CEEM-I, (c) CEEM-II. . . 153
5.13 Impact of CSI accuracy on the normalized energy per successful packet versus SNR for different MIMO configurations (SF = 10): (a) 1×1, (b) 1×2, (c) 2×1, (d) 2×2. 154
5.14 Effect of the spreading factor on the normalized energy per successful packet versus SNR for selected MIMO configurations under perfect CSI: (a) 1×2, (b) 2×2. 156
5.15 Energy-optimal MIMO configuration as a function of SNR under different CSI conditions (SF = 10): (a) Perfect CSI, (b) CEEM-I, (c) CEEM-II. 157

6.1 Overall architecture of the proposed adaptive diversity-selection framework with structured operating-region evolution and supplementary policy characterization. 164
6.2 Decision flow of the proposed feasibility-aware adaptive diversity-selection policy. 167
6.3 Adaptive operating-region map of the proposed framework for the representative Moderate hardware-overhead regime with CSI uncertainty variance $\sigma_e^2 = 0.01$. 173
6.4 Adaptive occupancy redistribution of the proposed framework under different operating scenarios. The operating scenarios are denoted as X-σ_e^2, where $X \in \{L, M, H\}$ represents the hardware-overhead regime (Low, Moderate, High), while $\sigma_e^2 \in \{0, 0.01, 0.1\}$ denotes the CSI uncertainty variance. 175
6.5 Observed transition frequencies between adaptive operating modes. 177
6.6 Aggregated distribution of adaptive transition distances between neighboring operating points across all examined CSI uncertainty levels and hardware-overhead regimes, computed from the operating-state indices used by the adaptive selector. 178

6.7 Mean adaptive energy per successful packet transmission of the proposed framework under different CSI uncertainty and hardware-overhead conditions. The operating scenarios are denoted as $X - \sigma_e^2$, where $X \in \{L, M, H\}$ represents the hardware-overhead regime (Low, Moderate, High), while $\sigma_e^2 \in \{0, 0.01, 0.1\}$ denotes the CSI uncertainty variance. 180
6.8 Pairwise comparison of the mean energy per successful packet between each fixed diversity configuration and the proposed adaptive framework under low-overhead operation ($\sigma_e^2 = 0.01$). For each pair, the mean values are evaluated over the common set of operating points for which both the fixed configuration and the adaptive framework remain feasible. 181
6.9 ECDF of the adaptive energy reduction relative to selected fixed operating-mode baselines across the considered operating space. 182
6.10 Adaptive operating-mode maps under increasing CSI uncertainty variance ($\sigma_e^2 = 0$, 0.01, and 0.1), illustrating the redistribution of selected diversity configurations across distance and reference-SNR conditions. 183
6.11 Classification performance of lightweight machine-learning models for adaptive policy approximation. 185

7.1 Architecture of the considered cooperative relay-assisted MIMO system with reliability-aware relay activation under imperfect CSI. 192
7.2 BER performance of the source–relay link under different CSI error variances. 197
7.3 BER performance of cooperative DF MIMO under imperfect relay decoding for different CSI error variances. 198
7.4 BER performance of direct 4×2 MIMO transmission with ZF detection under perfect CSI. 199
7.5 BER performance of cooperative DF 4×2 MIMO transmission under ideal relay operation and perfect CSI. 200
7.6 BER performance of cooperative DF 4×2 MIMO transmission under imperfect CSI for different CSI error variances. 201
7.7 BER comparison of direct MIMO and cooperative DF with imperfect relay decoding for $\sigma_e^2 = 0.01$. 202
7.8 BER comparison of direct MIMO and cooperative DF with imperfect relay decoding for $\sigma_e^2 = 0.1$. 203
7.9 Harmful cooperation region, defined by $\Delta\text{BER} = \text{BER}_{\text{coop}} - \text{BER}_{\text{direct}}$, as a function of SNR for different CSI error variances σ_e^2. Positive values indicate harmful cooperation. The horizontal dashed line indicates the boundary at $\Delta\text{BER} = 0$, separating beneficial and harmful cooperation regions. 204
7.10 Coded harmful cooperation region for $\sigma_e^2 = 0.1$, expressed through $\Delta\text{BER}_{\text{coded}} = \text{BER}_{\text{coop,coded}} - \text{BER}_{\text{direct,coded}}$. Positive values indicate harmful cooperation, while negative values indicate beneficial cooperation. The horizontal dashed line indicates the boundary at $\Delta\text{BER}_{\text{coded}} = 0$. 205

7.11 BER performance of reliability-aware cooperative DF ($\gamma_{\text{th}} = 4$) under different CSI uncertainty levels. 207
7.12 BER vs. SNR for different activation thresholds γ_{th} ($\sigma_e^2 = 0.05$). 210
7.13 BER comparison of direct MIMO, always-on cooperative DF and adaptive reliability-aware cooperative transmission under $\sigma_e^2 = 0.1$ using the optimized relay activation threshold. 211
7.14 BER comparison across different antenna configurations under imperfect CSI ($\sigma_e^2 = 0.1$). 214
7.15 Robustness gain versus CSI error variance 215

List of Tables

4.1 Main simulation parameters used for broadband MIMO characterization under realistic propagation conditions. 63
4.2 Channel performance under varying transmit power and antenna polarization configurations. 71
4.3 Channel performance under varying antenna configurations and polarization settings. 74
4.4 Channel performance under varying indoor-user fractions and user mobility levels. 77
4.5 Channel performance under varying indoor-user fractions in the indoor office propagation model. 80
4.6 Average performance for different cell radius values. 87
4.7 Summary of the main findings for simulations related to system-level parameters (Simulations 1–5). 90
4.8 Summary of the main findings for simulations related to deployment and environmental parameters (Simulations 6–9). 91
4.9 Main simulation parameters used for LoRa-type MIMO characterization under constrained operating conditions. 96
4.10 Baseline simulation parameters used for coverage and operating-regime characterization. 98
4.11 Relative BER reduction achieved by MMSE compared with ZF under CEEM-I. 117
4.12 Summary of the main characterization findings for MIMO operation under constrained LoRa-type conditions. 124

5.1 Main simulation parameters for energy-efficiency evaluation 131
5.2 Energy per successful packet transmission for different antenna configurations 134
5.3 PER across propagation environments 139
5.4 Normalized circuit (α_m) and processing (β_m) energy scaling 140
5.5 Main simulation parameters for LoRa MIMO energy-efficiency evaluation . . 148

6.1 Normalized hardware-overhead parameters for the considered diversity configurations under different hardware-overhead regimes. 166
6.2 Simulation and evaluation parameters. 172

7.1 Simulation parameters. 196
7.2 Impact of Relay-Activation Threshold Selection for $\sigma_e^2 = 0.05$ 209

1 Introduction

This chapter introduces the scientific context, motivation and research scope of the present thesis. It begins with an overview of the evolution of modern wireless communication systems and the role of MIMO technologies in enabling next-generation wireless communications. It subsequently introduces the principal factors governing realistic MIMO system operation, including realistic propagation conditions, imperfect channel state information, communication reliability, energy efficiency, adaptive transmission and cooperative communications.

Building upon this foundation, the chapter identifies the main research gaps addressed in this dissertation, defines the research objectives, summarizes the principal scientific contributions and outlines the overall organization of the thesis.

1.1 Evolution of Wireless Communication Systems

Wireless communication systems have undergone remarkable evolution over the past decades, progressing from simple voice-oriented networks to highly sophisticated communication infrastructures supporting data-intensive, latency-sensitive and large-scale connectivity services. From first-generation (1G) analog systems to broadband fourth-generation (4G) mobile networks, each technological transition has been driven by the continuous growth of user demands, increasing traffic requirements and the need for more efficient spectrum utilization [1, 2].

More recently, fifth-generation (5G) wireless systems introduced a broad set of advanced technologies designed to support diverse and often conflicting communication requirements, including enhanced mobile broadband (eMBB), ultra-reliable low-latency communications (URLLC) and massive machine-type communications (mMTC). Looking ahead, sixth-generation (6G) networks are expected to operate in even more dynamic, intelligent and heterogeneous environments, supporting diverse ecosystems of mobile users, autonomous systems, sensing platforms and machine-type devices. Under such conditions, future communication systems will be required to simultaneously satisfy stringent requirements in terms of throughput, reliability, latency, scalability and energy efficiency, making robust and adaptive wireless operation increasingly important [2–4].

In parallel with the evolution of cellular communications, the rapid growth of the Internet of Things (IoT) has introduced a new class of wireless communication scenarios characterized by limited energy resources, low-cost implementation and long operational lifetimes. Unlike conventional broadband communication systems, many IoT and Low-Power Wide-Area Network (LPWAN) applications prioritize coverage, communication reliability and energy efficiency over raw throughput. Technologies such as LoRa, Sigfox and NB-IoT exemplify this transition toward communication paradigms in which coverage, energy efficiency, communication robustness and long operational lifetime become important design objectives, providing a complementary application domain for investigating reliability–energy trade-offs under stringent resource constraints [5–7].

As wireless systems continue to evolve toward increasingly heterogeneous, dynamic and resource-constrained operating environments, conventional single-antenna communication architectures face growing limitations in satisfying the performance requirements of modern wireless applications. These challenges have led to the widespread adoption of multi-antenna communication techniques capable of exploiting the spatial dimension of the wireless channel. Among these technologies, Multiple-Input Multiple-Output (MIMO) communications have emerged as one of the most influential advances in modern wireless systems, providing significant improvements in communication reliability, spectral efficiency, coverage and overall network capacity [8, 9].

1.2 MIMO Communications as a Key Enabling Technology

The fundamental principle of multi-antenna communication systems is the use of multiple antennas at the transmitter, the receiver, or both. By exploiting the spatial dimension of the wireless channel, MIMO systems create multiple transmission paths between communicating nodes, allowing more efficient utilization of the propagation environment compared to conventional single-antenna systems. Depending on the transmission strategy employed, these additional spatial degrees of freedom can be utilized either to improve communication reliability or to increase data throughput [1, 10, 11].

One of the primary advantages of MIMO communications is their ability to provide spatial diversity gain. Wireless signal propagation is inherently affected by multipath fading, which can significantly degrade communication quality. Diversity techniques exploit multiple signal replicas experiencing different channel conditions in order to reduce the probability of deep fades and improve link robustness. Through appropriate diversity schemes, including receive diversity and transmit diversity techniques such as space–time block coding (STBC), MIMO systems can significantly enhance communication reliability, particularly in challenging propagation environments [12, 13].

In addition to reliability improvements, MIMO systems can also provide spatial multiplexing gain. Spatial multiplexing techniques allow several independent data streams to be transmitted simultaneously over the same frequency band, significantly improving spectral efficiency and system capacity. This capability has made spatial multiplexing a key component of modern broadband wireless communications [8, 9].

The coexistence of diversity and multiplexing capabilities gives rise to one of the fundamental characteristics of MIMO communications: the diversity–multiplexing trade-off. While diversity techniques prioritize communication reliability through redundancy, multiplexing techniques seek to maximize throughput by transmitting multiple independent data streams. Consequently, the selection of an appropriate transmission strategy depends strongly on propagation conditions, channel characteristics and the performance objectives of the communication system [14].

Despite these significant theoretical gains, the practical performance of MIMO systems

depends strongly on the characteristics of the wireless propagation environment, since the achievable diversity and multiplexing gains are strongly influenced by channel rank, spatial correlation and propagation conditions. Consequently, realistic propagation modeling represents a fundamental prerequisite for understanding and accurately evaluating MIMO system behavior under realistic operating conditions.

1.3 From Idealized Models to Realistic Wireless Environments

Theoretical analysis has played a fundamental role in the development of wireless communication systems by enabling tractable performance evaluation under simplified mathematical assumptions. For this reason, a large portion of MIMO research has traditionally relied on simplified assumptions such as independent and identically distributed (i.i.d.) Rayleigh fading [1, 11], uncorrelated antenna elements, perfect channel state information and statistically homogeneous propagation environments. Although such assumptions facilitate analytical treatment and provide useful performance benchmarks, they often fail to capture important characteristics of practical wireless deployments [15].

In realistic wireless environments, communication channels are shaped by multiple interacting factors, including path loss, shadowing, multipath propagation, spatial correlation, antenna geometry, polarization and heterogeneous user distributions [15, 16]. These factors introduce spatial and temporal variations that can significantly alter system behavior compared to idealized predictions. As wireless networks evolve toward increasingly dense and heterogeneous deployments, the limitations of simplified propagation assumptions become progressively more apparent [17].

This discrepancy becomes particularly important in MIMO systems, where communication performance depends strongly on channel structure and spatial characteristics [13]. Geometry-dependent and propagation-dependent effects directly influence channel rank, angular diversity, interference conditions and signal quality. For example, antenna geometry affects spatial correlation and diversity characteristics, while non-uniform user distributions may introduce channel asymmetries that significantly impact resource allocation and overall system efficiency [18]. Consequently, key performance indicators such as signal-to-interference-plus-noise ratio (SINR), spectral efficiency and throughput may differ substantially from those predicted under idealized assumptions.

To capture these practical propagation characteristics and enable representative system-level evaluation, increasingly sophisticated wireless channel models have been developed over the years, including the COST, WINNER and standardized 3GPP frameworks [19,20]. Among these, the three-dimensional channel models specified by the Third Generation Partnership Project (3GPP), particularly TR 36.873 and TR 38.901, have become widely adopted in both academia and industry [16, 17]. These models provide realistic representations of wireless deployments by incorporating line-of-sight and non-line-of-sight propagation, spatial consis-

tency, polarization effects and deployment-dependent propagation characteristics, enabling more representative evaluation of MIMO system performance under the considered operating conditions [16, 17].

Among the various practical factors affecting MIMO system performance, the availability of accurate channel state information plays a particularly important role. Since many advanced MIMO techniques rely heavily on channel knowledge for signal detection, precoding and resource allocation, channel uncertainty introduces an additional source of performance degradation that must be explicitly considered in practical system design.

1.4 The Challenge of Imperfect Channel State Information

The performance of MIMO communication systems depends not only on the characteristics of the wireless propagation environment but also on the availability of accurate channel state information (CSI). Channel knowledge enables transmitters and receivers to adapt their signal-processing strategies according to the prevailing propagation conditions and constitutes a fundamental requirement for many advanced communication techniques, including coherent diversity processing, spatial multiplexing and interference mitigation [1, 11].

In practical wireless systems, CSI is obtained through channel estimation procedures based on pilot or reference signals [21]. The estimated channel information is subsequently used for signal detection, equalization, precoding and resource-allocation decisions. Under ideal conditions, accurate CSI allows MIMO systems to more effectively exploit the available spatial degrees of freedom, thereby improving communication reliability and spectral efficiency [22].

However, perfect channel knowledge is rarely available in realistic communication environments. Channel estimation accuracy is affected by numerous factors, including thermal noise, limited pilot resources, feedback delays, hardware impairments, user mobility and rapidly varying propagation conditions [23]. As a result, the channel information available at the transmitter or receiver inevitably contains estimation errors, introducing uncertainty into the communication process.

The presence of CSI uncertainty can significantly alter the performance of MIMO systems by reducing the gains predicted under ideal channel assumptions. In diversity-oriented transmission schemes, channel estimation errors reduce the effectiveness of combining and diversity mechanisms, thereby limiting the achievable reliability gains. Similarly, spatial multiplexing techniques, which rely heavily on accurate channel knowledge to separate simultaneously transmitted data streams, become particularly sensitive to estimation inaccuracies. Under severe CSI uncertainty, residual interference may remain after signal detection, leading to performance degradation and, in some cases, the appearance of error floors at high signal-to-noise ratios [24]. More generally, the impact of CSI uncertainty extends beyond physical-layer detection accuracy, influencing the effectiveness of communication mechanisms that rely on accurate channel knowledge.

The impact of imperfect CSI becomes even more pronounced in advanced communication

scenarios involving cooperative transmission, adaptive communication strategies and energy-aware system operation. In such environments, channel uncertainty affects not only physical-layer signal detection but also higher-level system decisions, including relay participation, transmission-mode selection and resource allocation. As a result, imperfect CSI may alter system behavior in a non-trivial manner, creating operating conditions in which communication strategies designed under ideal assumptions become suboptimal, inefficient or even detrimental in practice. Consequently, CSI uncertainty represents a fundamental limitation that must be explicitly considered when designing practical wireless communication systems [25, 26].

These observations highlight that imperfect CSI is not merely a channel estimation issue, but a fundamental system-level challenge that directly affects communication reliability, robustness and decision-making in practical wireless systems. As communication systems increasingly operate under stringent reliability requirements, understanding and mitigating the impact of CSI uncertainty becomes essential for designing MIMO frameworks capable of maintaining dependable operation under non-ideal conditions. Consequently, communication reliability emerges as a central design objective that must be jointly considered with channel uncertainty, propagation conditions and system adaptation in MIMO communications.

1.5 Reliability Challenges in Modern MIMO Systems

The increasing complexity and uncertainty of practical wireless environments have made communication reliability one of the most critical performance requirements in modern wireless communication systems [27]. While earlier generations of wireless networks primarily focused on expanding coverage and increasing data rates, contemporary communication infrastructures are increasingly expected to provide highly dependable connectivity under diverse operating conditions. This requirement is particularly important in emerging applications such as industrial automation, autonomous transportation, mission-critical communications, wireless sensor networks and large-scale Internet of Things (IoT) deployments, where communication failures may have significant operational consequences [28, 29].

Achieving reliable wireless communication remains inherently challenging due to the unpredictable nature of the radio propagation environment. Wireless channels are affected by fading, shadowing, interference, user mobility and environmental variability, all of which can degrade signal quality and increase transmission errors [1, 15]. As wireless networks become denser and more heterogeneous, maintaining stable and dependable communication performance becomes increasingly demanding. Nevertheless, the achievable reliability gains ultimately depend on the characteristics of the propagation environment and the accuracy of the available channel information.

Multi-antenna communication techniques provide important mechanisms for improving reliability by exploiting the spatial dimension of the wireless channel. In particular, diversity-oriented MIMO transmission schemes improve communication reliability by increasing the robustness of wireless links against fading and other propagation impairments. As a result,

MIMO technologies have become a key tool for improving communication robustness under challenging propagation conditions [11, 12].

However, the reliability benefits offered by MIMO systems are not always fully achievable in practice. Deployment-dependent propagation environments, spatial correlation, channel asymmetries and imperfect channel state information may significantly reduce the effectiveness of diversity mechanisms and degrade overall system performance [15]. Furthermore, transmission schemes designed to increase spectral efficiency through spatial multiplexing may exhibit increased sensitivity to propagation impairments, channel uncertainty and interference, reflecting an important trade-off between multiplexing gain and communication reliability [14]. Consequently, reliability in MIMO systems must be treated as a broader system-level design objective influencing transmission strategies, resource allocation and communication architecture decisions.

At the same time, improving reliability often requires additional communication resources, including transmission power, bandwidth, redundancy and processing complexity. Consequently, reliability cannot be pursued independently of other system objectives. In particular, the resources required to achieve highly dependable communication may introduce significant energy costs, creating a fundamental interaction between reliability and energy efficiency. This interaction has emerged as a major design challenge in modern wireless communication systems [30].

1.6 Energy Efficiency as a Design Constraint

The pursuit of high communication reliability often comes at the cost of increased resource utilization, including higher transmission power, additional redundancy and greater processing complexity. As a result, communication reliability and energy consumption become inherently coupled in practical wireless systems. Understanding this interaction has therefore become a fundamental challenge in the design of modern wireless communication systems [30, 31].

The rapid growth of wireless connectivity, combined with the increasing number of deployed devices and network infrastructures, has further intensified concerns regarding energy utilization at both the network and device levels. As wireless communication systems continue to evolve, improving energy efficiency has become one of the primary design objectives alongside throughput, latency and communication reliability.

The importance of energy-aware system design is particularly evident in Internet of Things (IoT) and Low-Power Wide-Area Network (LPWAN) applications. Many wireless devices operate under strict energy constraints and are expected to remain functional for extended periods without battery replacement or maintenance. Consequently, even moderate increases in energy consumption may significantly reduce operational lifetime and compromise the practicality of large-scale deployments. Technologies such as LoRa, Sigfox and NB-IoT have therefore been specifically designed to support communication under stringent power limitations, highlighting the growing importance of energy-efficient wireless operation [5–7].

From a broader perspective, energy efficiency has become increasingly important across virtually all wireless communication systems. Mobile terminals, sensor networks, industrial communication platforms and cellular infrastructures must continuously balance communication performance against energy expenditure. This challenge becomes even more significant as future wireless networks are expected to support massive device connectivity, dense deployments and increasingly diverse service requirements [28].

Within this context, MIMO technologies introduce both opportunities and challenges. Multi-antenna transmission schemes can improve communication reliability and link quality, potentially reducing retransmission requirements and increasing communication efficiency. However, these benefits are accompanied by additional energy costs associated with radio-frequency chains, signal-processing operations, circuitry activation and hardware complexity. Consequently, communication strategies that maximize communication performance do not necessarily minimize total energy consumption [32, 33].

Furthermore, meaningful energy-efficiency evaluation extends beyond transmission power alone. In practical wireless systems, overall energy consumption is influenced by retransmission behavior, signal-processing requirements, hardware overhead, circuitry utilization and protocol operation. Consequently, energy efficiency must be assessed from a system-level perspective that jointly considers communication performance and resource expenditure [30].

These observations suggest that no single transmission strategy can be expected to provide optimal performance under all operating conditions. Instead, the relative advantages of different communication schemes depend strongly on the propagation environment, channel quality, reliability requirements and hardware characteristics of the system. Under such circumstances, flexible communication mechanisms capable of adapting their operation to prevailing conditions become increasingly attractive for next-generation wireless networks.

1.7 Adaptive Communication as a Key Enabler of Efficient Wireless Operation

The increasing complexity and variability of modern wireless environments have highlighted the limitations of fixed communication strategies [34]. Wireless systems operate under rapidly changing propagation conditions, fluctuating interference levels, varying user requirements and diverse hardware constraints. Under such conditions, transmission schemes optimized for one operating scenario may become inefficient or unsuitable when network conditions change.

To address these challenges, modern wireless systems increasingly employ adaptive operating principles. Rather than relying on static transmission configurations, adaptive communication frameworks dynamically adjust system parameters according to prevailing channel and network conditions, enabling more efficient resource utilization and improved performance across diverse operating environments [35].

Adaptation may be performed at multiple layers of the communication system, including transmission power control, modulation and coding selection, antenna configuration and re-

source allocation policies. The common objective of these mechanisms is to dynamically adjust system operation in response to changing conditions, often balancing competing performance objectives such as communication reliability, energy efficiency and spectral efficiency under practical implementation constraints [36].

The importance of adaptation becomes particularly evident in MIMO systems, where communication performance depends strongly on propagation conditions, channel uncertainty, reliability requirements and energy constraints. Consequently, a transmission strategy that performs optimally under one set of conditions may become suboptimal under another. Adaptive MIMO frameworks therefore seek to exploit the operating conditions of the wireless environment by dynamically selecting the most suitable transmission configuration according to prevailing channel conditions, communication reliability requirements and energy constraints [37, 38].

More fundamentally, adaptive operation represents the natural response to the operating-condition-dependent behavior of practical wireless systems. As the preceding sections have shown, deployment-dependent propagation conditions, channel uncertainty, communication reliability requirements and energy constraints jointly influence MIMO system performance. Consequently, no single transmission strategy can be expected to remain universally optimal across all operating scenarios. Instead, effective wireless operation increasingly relies on adaptive decision mechanisms capable of selecting the most appropriate communication strategy according to the prevailing operating conditions.

Beyond performance optimization, adaptive communication strategies also provide an effective means of managing fundamental system trade-offs involving reliability, spectral efficiency, energy consumption and implementation complexity. Among the various communication paradigms relevant to adaptive wireless operation, cooperative communication represents a particularly important transmission strategy. By exploiting distributed spatial diversity through relay-assisted transmission, cooperative communication can provide MIMO-like diversity benefits through spatially separated nodes and offers significant potential for improving communication reliability under challenging propagation conditions [39, 40]. However, its effectiveness depends strongly on channel conditions, relay reliability and CSI quality, making cooperative transmission a particularly relevant case for studying MIMO behavior under realistic operating conditions.

1.8 Cooperative Communication for Reliability Enhancement in Wireless Networks

Cooperative communication has emerged as an effective approach for enhancing the performance and reliability of wireless networks without requiring a large increase in physical antenna resources [39, 40]. The fundamental concept behind cooperative transmission is that neighboring wireless nodes can assist one another by forwarding information toward the destination, thereby creating additional communication paths and improving the probability of

successful signal reception. By exploiting the spatial diversity offered by distributed nodes, cooperative communication can provide many of the benefits traditionally associated with multi-antenna systems.

The motivation for cooperative communication originates from the limitations of conventional point-to-point transmission. In practical wireless environments, direct communication links may suffer from severe fading, shadowing, interference or unfavorable propagation conditions. Under such circumstances, the availability of an intermediate relay node can improve communication robustness by providing an alternative transmission path between the source and the destination. As a result, cooperative transmission has been extensively investigated as a means of improving reliability, extending coverage and enhancing overall communication performance [41].

A variety of cooperative transmission protocols have been proposed in the literature. Among them, Decode-and-Forward (DF) relaying has received significant attention due to its conceptual simplicity and practical implementation characteristics [39]. In DF systems, the relay node first decodes the received information and subsequently retransmits a regenerated version of the detected signal toward the destination. Through this process, the destination can potentially benefit from multiple independently faded communication paths, thereby improving reception reliability.

The potential benefits of cooperative communication are well documented. Relay-assisted transmission can increase diversity gain, improve communication robustness and extend network coverage in challenging propagation environments. In addition, cooperative techniques have been investigated in the context of wireless sensor networks, IoT systems and energy-constrained communication scenarios, where reliability enhancement may contribute to improved overall system efficiency [42].

Despite these advantages, cooperative communication does not always guarantee performance improvement. The effectiveness of relay-assisted transmission depends strongly on channel conditions, relay reliability, protocol operation and the accuracy of the available channel state information. In practical systems, relay decoding errors, channel estimation uncertainty and additional signaling overhead may reduce or even negate the expected benefits of cooperation. Furthermore, the introduction of relay nodes increases system complexity and may lead to additional resource consumption that must be carefully considered during system design [39, 40].

Consequently, the conditions under which cooperation remains beneficial represent an important research challenge in modern wireless communications. Since the effectiveness of cooperative transmission depends strongly on channel conditions, relay reliability and channel-state-information accuracy, fixed cooperation strategies may not always provide optimal performance. These observations have motivated increasing interest in adaptive and reliability-aware cooperative communication frameworks capable of adjusting their operation according to prevailing network conditions.

Collectively, the preceding sections demonstrate that MIMO operation is governed by the

interaction of multiple tightly coupled mechanisms. Realistic propagation conditions influence channel characteristics, imperfect CSI affects communication reliability, reliability impacts energy consumption, while these factors jointly determine the suitability of adaptive and cooperative transmission strategies. Consequently, understanding MIMO systems under non-ideal operating conditions requires an integrated perspective that considers these mechanisms collectively rather than in isolation.

1.9 Research Gap and Problem Statement

The preceding sections highlighted the growing importance of MIMO communications in modern wireless systems and discussed several factors that strongly influence system behavior under non-ideal operating conditions, including realistic propagation conditions, channel state information uncertainty, communication reliability requirements, energy constraints and adaptive transmission mechanisms. Although the theoretical foundations of MIMO communications have been extensively established through decades of research under mathematically tractable and idealized assumptions [1,11], practical wireless systems rarely operate under such conditions. In realistic wireless deployments, communication performance is simultaneously influenced by propagation variability, channel estimation errors, implementation constraints and continuously changing operating conditions. Consequently, communication strategies that perform well under idealized assumptions may exhibit substantially different behavior in practical wireless environments.

As wireless systems evolve toward increasingly heterogeneous, dynamic and resource-constrained architectures, understanding MIMO operation under realistic wireless conditions has become a fundamental research challenge. While considerable research has been devoted to individual aspects of MIMO communications, these aspects are often investigated independently and under idealized assumptions. As a result, the joint impact of realistic propagation conditions, channel uncertainty and implementation constraints on MIMO operation remains less comprehensively characterized.

In particular, further investigation is required to understand how realistic propagation asymmetries and deployment-dependent characteristics influence MIMO performance compared to idealized channel assumptions [18, 43]. Furthermore, the impact of imperfect CSI on advanced communication paradigms such as adaptive and cooperative MIMO operation requires further investigation, particularly in scenarios where channel uncertainty fundamentally alters system-level decisions and communication reliability [25, 26]. Finally, although communication reliability, energy efficiency and adaptive transmission have each been extensively studied, their combined interaction under non-ideal operating conditions warrants further investigation, particularly toward the development of optimization strategies capable of supporting practical wireless deployments.

Addressing these limitations is essential for future wireless communication systems expected to operate under stringent reliability requirements, limited energy resources and highly

diverse propagation environments. More importantly, effective optimization under practical wireless operating conditions requires a thorough understanding of the mechanisms governing MIMO system behavior before robust transmission strategies can be developed.

Motivated by these challenges, this dissertation investigates the behavior of MIMO communication systems under realistic propagation conditions and imperfect channel state information. More specifically, it examines how realistic propagation effects, channel uncertainty, communication reliability requirements and implementation constraints jointly influence MIMO system behavior, and how this understanding provides the foundation for the development of energy-efficient, adaptive and cooperative transmission strategies for realistic wireless environments.

The practical operating conditions considered in this dissertation do not aim to encompass the full range of impairments and constraints encountered in contemporary wireless systems. Instead, the thesis focuses on a selected set of interacting factors—realistic propagation characteristics, imperfect CSI, reliability requirements and implementation-related energy costs—that directly influence the effectiveness of MIMO diversity, adaptation and cooperative transmission. This scope enables these factors to be examined within a common framework while preserving a clear progression from system characterization to operating-condition-dependent optimization.

Through this progression, the dissertation aims to establish a coherent framework for understanding and optimizing MIMO operation under non-ideal wireless conditions, enabling robust, reliable and energy-efficient communication across diverse wireless deployment scenarios.

1.10 Research Objectives

The overarching objective of this thesis is to characterize and optimize MIMO communication systems under realistic propagation conditions and imperfect channel state information (CSI), with particular emphasis on communication reliability, energy efficiency and adaptive operation under non-ideal wireless conditions. To achieve this objective, the thesis pursues the following specific research goals:

- To investigate and characterize the behavior of wireless communication systems under realistic operating conditions, with particular emphasis on broadband MIMO and energy-constrained LPWAN environments, quantifying the influence of deployment-dependent characteristics, channel uncertainty and practical implementation constraints on fundamental performance metrics.

- To identify and analyze the trade-offs between communication reliability, energy efficiency and implementation complexity in practical wireless communication systems, including both broadband MIMO and energy-constrained IoT/LPWAN communication environments.

- To develop adaptive MIMO communication strategies capable of exploiting the identified operating regions by dynamically selecting robust and energy-efficient transmission configurations according to the prevailing wireless conditions.
- To extend the characterization-driven optimization approach to cooperative relay-assisted MIMO systems by investigating the impact of imperfect CSI and relay reliability, identifying the operating conditions under which cooperation becomes detrimental and developing reliability-aware mitigation strategies for cooperative communication under imperfect CSI.

1.11 Main Scientific Contributions

Contribution 1 – Realistic Characterization of MIMO and Energy-Constrained Wireless Systems

This thesis provides a systematic characterization of wireless system behavior under selected realistic operating conditions using standardized 3GPP channel models, advanced system-level simulation platforms and complementary energy-constrained LPWAN scenarios. The analysis demonstrates that deployment-related characteristics, particularly propagation asymmetries, antenna geometry, polarization, user distribution and realistic channel impairments, influence key performance metrics such as SINR, spectral efficiency, throughput and communication reliability. Beyond improving the realism of performance evaluation, the obtained results provide a deeper understanding of the physical mechanisms governing wireless system behavior and establish the characterization foundation upon which the subsequent optimization frameworks are developed.

Contribution 2 – Characterization of Reliability–Energy Trade-offs for Wireless Optimization

This thesis characterizes the interaction between communication reliability and energy efficiency under the considered wireless operating conditions by explicitly accounting for retransmission behavior, hardware-related energy consumption and signal-processing overhead. The obtained results demonstrate that maximizing communication reliability does not necessarily minimize total energy consumption when practical implementation constraints are considered. Furthermore, the analysis identifies distinct operating regions that support operating-condition-dependent optimization by revealing the conditions under which different diversity configurations become preferable according to the prevailing reliability requirements and energy constraints. The investigation is further extended to energy-constrained IoT and LPWAN communication environments, demonstrating that the identified reliability–energy trade-offs remain equally important in highly resource-limited wireless systems.

Contribution 3 – Development of Adaptive Transmission Strategies for MIMO Systems under Realistic Operating Conditions

Building upon the operating regions identified through the preceding characterization and

optimization analyses, this thesis develops an adaptive MIMO transmission framework capable of dynamically selecting appropriate transmission configurations according to prevailing wireless conditions. The proposed framework translates the identified reliability–energy trade-offs into adaptive system operation, enabling robust and energy-efficient communication across diverse wireless environments. The obtained results demonstrate that adaptive transmission strategies provide an effective mechanism for exploiting the operating-condition-dependent behavior of MIMO systems under realistic operating conditions while maintaining stable communication performance.

Contribution 4 – Reliability-Aware Adaptive Cooperative Communication under Practical Wireless Impairments

This thesis extends the proposed optimization principles to cooperative relay-assisted MIMO systems operating under imperfect CSI. The analysis identifies and characterizes the harmful cooperation phenomenon, demonstrating that cooperative transmission may under specific operating conditions become less reliable than direct MIMO communication due to the combined effects of channel estimation uncertainty and relay error propagation. Based on these observations, a reliability-aware relay activation mechanism is developed to selectively enable cooperation according to prevailing communication conditions, thereby mitigating harmful cooperation and extending adaptive optimization principles to cooperative MIMO operation.

1.12 Organization of the Thesis

Collectively, the scientific contributions presented above form a coherent progression rather than a set of independent research outcomes. The investigations presented throughout this dissertation follow a progressive research methodology in which realistic system characterization provides the foundation for understanding the mechanisms governing MIMO behavior under realistic conditions, identifying the associated performance trade-offs and developing robust optimization strategies for realistic wireless operation. This overall scientific progression is summarized in Figure 1.1, which illustrates how the individual research directions are integrated within the unified research framework of the dissertation.

The remainder of this thesis is organized as follows.

Chapter 2 presents the theoretical foundations and technical background required for the subsequent analyses. It introduces the fundamental principles of MIMO communications, wireless propagation modeling, imperfect channel state information, communication reliability, energy efficiency and adaptive transmission concepts. Particular emphasis is placed on the practical mechanisms that influence MIMO system behavior under realistic wireless operating conditions.

Chapter 3 reviews the state of the art and establishes the scientific context of the thesis. The chapter critically examines existing research on realistic MIMO system modeling, communication reliability, energy-efficient wireless design, adaptive transmission and cooper-

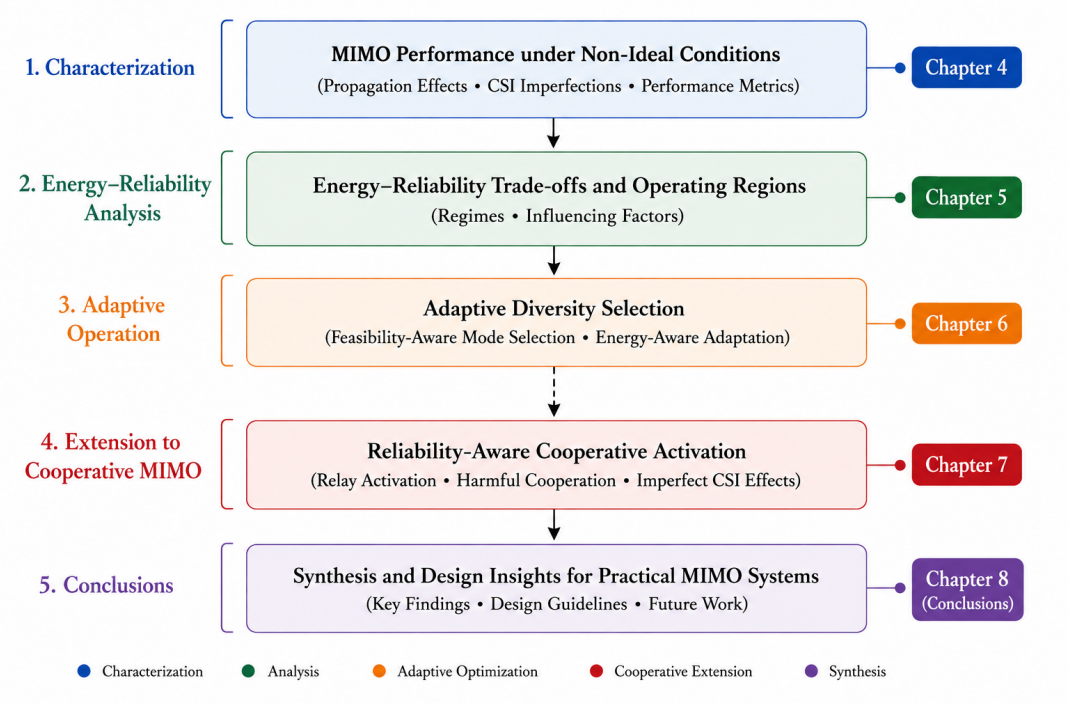


Figure 1.1. Conceptual research framework

ative communications, identifying the principal research gaps that motivate the investigations presented in this dissertation.

Chapter 4 investigates the behavior of MIMO systems under realistic wireless propagation conditions using standardized 3GPP channel models and advanced system-level simulation frameworks. The analysis identifies the dominant mechanisms governing system performance under the considered realistic propagation conditions by examining the impact of antenna geometry, polarization characteristics, user-distribution asymmetries and propagation effects on key performance metrics, thereby establishing the characterization foundation for the subsequent optimization studies.

Chapter 5 investigates the interaction between communication reliability and energy efficiency under practical operating conditions. The analysis characterizes the fundamental reliability–energy trade-offs governing both broadband MIMO and energy-constrained IoT/LPWAN communication systems while explicitly accounting for imperfect CSI, retransmission behavior, hardware-related energy consumption and signal-processing overhead. Based on these analyses, distinct operating regions are identified to support system optimization.

Chapter 6 develops adaptive MIMO transmission strategies that exploit the operating regions identified in the previous chapter. The proposed adaptive framework dynamically selects appropriate transmission configurations according to prevailing wireless conditions, communication reliability requirements and implementation constraints, enabling robust and energy-efficient system operation across diverse practical wireless environments.

Chapter 7 extends the proposed optimization principles to cooperative relay-assisted MIMO

communications operating under imperfect CSI. The chapter investigates the limitations of cooperative transmission under realistic wireless impairments, identifies the harmful cooperation region and develops a reliability-aware relay activation strategy that enables adaptive cooperative operation according to the prevailing communication conditions. The influence of antenna scaling on cooperative system robustness is also investigated.

Finally, Chapter 8 summarizes the principal scientific findings and contributions of the dissertation. It synthesizes the results obtained throughout the characterization and optimization studies, discusses their implications for the design of MIMO communication systems operating under realistic wireless conditions and outlines promising directions for future research.

2 Theoretical Foundations

This chapter presents the theoretical foundations required for the remainder of this thesis. It introduces the fundamental principles of MIMO communications and discusses key theoretical concepts and practical factors relevant to wireless system performance, including realistic propagation environments, channel state information uncertainty, communication reliability, energy efficiency, adaptive transmission strategies and cooperative communication mechanisms. Together, these concepts establish the scientific and technical foundation for the analyses, methodologies and communication frameworks developed in the subsequent chapters. Although the primary focus of this dissertation is on MIMO communications, several of the theoretical concepts discussed in this chapter, particularly those related to communication reliability, energy efficiency and adaptive operation, are equally relevant to energy-constrained wireless systems such as LPWAN technologies. This broader perspective provides the theoretical basis for the analyses presented later for both broadband MIMO and LoRa-based communication systems.

2.1 Fundamentals of MIMO Communications

2.1.1 MIMO System Model

A Multiple-Input Multiple-Output (MIMO) communication system employs multiple antennas at both the transmitter and receiver in order to exploit the spatial dimension of the wireless channel [11, 13]. Compared to conventional single-antenna systems, MIMO architectures introduce additional spatial degrees of freedom that can be exploited to improve communication reliability, increase spectral efficiency and enhance overall system performance [8, 9]. The basic structure of a MIMO communication system is illustrated in Figure 2.1.

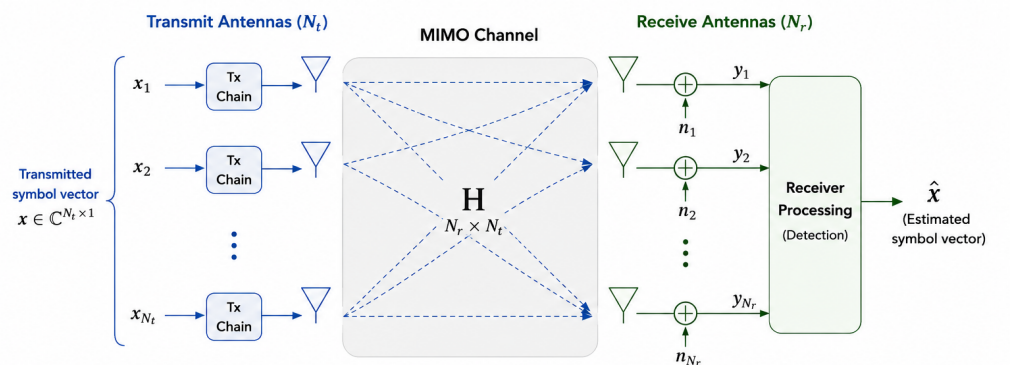


Figure 2.1. Basic MIMO communication system model with N_t transmit antennas and N_r receive antennas.

Figure 2.1 illustrates the basic signal flow in a MIMO communication system. The transmitted symbols are simultaneously mapped onto the N_t transmit antennas and propagate through the wireless channel, represented by the matrix $\mathbf{H}$. Each receive antenna observes a

superposition of the transmitted signal components weighted by the corresponding channel coefficients, together with additive noise. The resulting N_r received signals are jointly processed at the receiver to estimate the transmitted symbol vector. This representation highlights the fundamental role of the MIMO channel matrix in coupling the transmitted and received signal vectors and forms the basis for the mathematical model introduced below. Under the commonly adopted narrowband flat-fading assumption, the discrete-time complex baseband input–output relationship of a MIMO system is expressed as [1, 11]

$$\mathbf{y} = \mathbf{H}\mathbf{x} + \mathbf{n} \tag{2.1}$$

where $\mathbf{x} \in \mathbb{C}^{N_t \times 1}$ denotes the transmitted signal vector, $\mathbf{y} \in \mathbb{C}^{N_r \times 1}$ denotes the received signal vector, $\mathbf{H} \in \mathbb{C}^{N_r \times N_t}$ denotes the channel matrix and $\mathbf{n} \in \mathbb{C}^{N_r \times 1}$ denotes the additive white Gaussian noise (AWGN) vector, commonly modeled as

$$\mathbf{n} \sim \mathcal{CN}(0, \sigma_n^2 \mathbf{I}_{N_r}).$$

The MIMO channel matrix is given by

$$\mathbf{H} = \begin{bmatrix} h_{11} & h_{12} & \cdots & h_{1N_t} \\ h_{21} & h_{22} & \cdots & h_{2N_t} \\ \vdots & \vdots & \ddots & \vdots \\ h_{N_r1} & h_{N_r2} & \cdots & h_{N_rN_t} \end{bmatrix} \tag{2.2}$$

where each coefficient h_{ij} represents the complex channel gain between the j-th transmit antenna and the i-th receive antenna. Depending on the adopted channel model, these coefficients may incorporate the effects of large-scale propagation and small-scale fading, including path loss, shadowing, multipath fading and phase variations [15].

The received signal at each antenna is therefore formed by the superposition of all transmitted signal components as shaped by the wireless channel. The structure and properties of $\mathbf{H}$, particularly its rank, spatial correlation and conditioning characteristics, strongly influence the achievable performance of the MIMO system.

Under favorable propagation conditions, a well-conditioned high-rank channel enables efficient exploitation of spatial multiplexing, while highly correlated or rank-deficient channels reduce the achievable spatial gains [11, 13]. This system model provides the mathematical foundation for MIMO communication analysis and serves as the basis for understanding diversity-oriented transmission and spatial multiplexing techniques.

2.1.2 Spatial Degrees of Freedom in MIMO Systems

The principal advantage of MIMO communication systems lies in their ability to exploit the spatial dimension of the wireless channel [11,13]. Unlike conventional single-antenna systems, which cannot exploit multiple antenna dimensions for spatial processing, MIMO systems

utilize multiple transmit and receive antennas to provide additional spatial degrees of freedom (DoF). These spatial resources enable more flexible transmission and reception strategies, allowing wireless systems to improve communication reliability, increase throughput and enhance overall system efficiency.

The maximum number of available spatial degrees of freedom is fundamentally bounded by the number of antennas at the transmitter and receiver [11]:

$$\mathrm{DoF}_{\max} = \min(N_t, N_r) \tag{2.3}$$

This quantity represents the maximum number of independent spatial channels that can theoretically be supported by the MIMO system. In practice, however, the effective number of usable spatial degrees of freedom depends primarily on the characteristics of the channel matrix $\mathbf{H}$, particularly its rank, spatial correlation properties and propagation conditions. The rank of the channel matrix is defined as

$$r_H = \mathrm{rank}(\mathbf{H}) \tag{2.4}$$

and determines the number of independent spatial streams that can be supported. Accordingly, the number of simultaneously transmitted spatial streams N_s satisfies

$$N_s \leq r_H \leq \min(N_t, N_r) \tag{2.5}$$

Under favorable propagation conditions, where the channel matrix has high rank and low spatial correlation, multiple parallel spatial channels can be established between transmitter and receiver. This behavior can be interpreted through the singular value decomposition (SVD) of the channel matrix [1, 11]:

$$\mathbf{H} = \mathbf{U}\mathbf{\Sigma}\mathbf{V}^H \tag{2.6}$$

where $\mathbf{U}$ and $\mathbf{V}$ are unitary matrices and $\mathbf{\Sigma}$ contains the singular values of the channel. Through appropriate transmit and receive transformations, the non-zero singular values define parallel spatial eigenchannels, which determine the effective spatial resources available for communication.

For a MIMO channel with perfect CSI at the receiver and equal power allocation across the transmit antennas, the instantaneous achievable capacity can be expressed as [9]

$$C = \log_2 \det\left(\mathbf{I}_{N_r} + \frac{\rho}{N_t}\mathbf{H}\mathbf{H}^H\right) \tag{2.7}$$

where ρ denotes the signal-to-noise ratio. This expression highlights that channel rank, channel conditioning and spatial correlation strongly influence the achievable spectral efficiency and is primarily used here to illustrate the dependence of MIMO capacity on channel rank and spatial structure.

The spatial resources provided by MIMO systems can be exploited primarily through spa-

tial diversity and spatial multiplexing. Spatial diversity improves communication reliability by leveraging multiple independently faded signal paths, thereby reducing sensitivity to fading and improving reception robustness. Spatial multiplexing, in contrast, enables multiple independent data streams to be transmitted simultaneously, significantly increasing throughput and spectral efficiency [8].

The competing objectives of spatial diversity and spatial multiplexing give rise to the fundamental diversity–multiplexing trade-off in MIMO communications. Diversity-oriented transmission prioritizes robustness against fading, whereas spatial multiplexing exploits the available spatial dimensions to increase transmission rate. In the information-theoretic sense, the diversity–multiplexing trade-off characterizes the fundamental relationship between achievable diversity gain and multiplexing gain [14]. In practical systems, the preferred balance between these objectives depends on channel conditions, communication requirements and the quality of the available channel state information.

2.1.3 Diversity Techniques in MIMO Systems

One of the most important advantages of MIMO communication systems is their ability to improve communication reliability through diversity [11, 13]. In wireless environments, signal quality is often degraded by multipath fading and other propagation impairments, which may cause severe fluctuations in received signal strength. Diversity techniques mitigate the effects of fading by providing multiple independently or weakly correlated observations of the transmitted signal, thereby reducing the probability of simultaneous signal degradation across all diversity branches.

The fundamental principle of diversity relies on exploiting independently or weakly correlated signal observations across the time, frequency or spatial domains [1]. Time diversity exploits observations transmitted at different time instants, whereas frequency diversity distributes information across sufficiently separated frequency components. In MIMO systems, particular emphasis is placed on spatial diversity, since multiple antennas enable diversity gains without necessarily requiring additional time or frequency resources. By combining signal observations affected by statistically independent or weakly correlated fading conditions, wireless systems can significantly improve reception robustness and reduce transmission error probability. The resulting improvement in communication reliability is commonly referred to as diversity gain.

The effectiveness of diversity is commonly characterized by the diversity order d, which determines the asymptotic slope of the error probability curve with increasing signal-to-noise ratio [44]. At sufficiently high SNR, the error probability exhibits the asymptotic behavior

$$P_e \propto \mathrm{SNR}^{-d} \tag{2.8}$$

where d denotes the diversity order. A higher diversity order therefore leads to faster error-probability reduction and improved communication robustness. Diversity gain is conceptually distinct from array gain: diversity gain improves the asymptotic robustness of the link against

fading, whereas array gain improves the effective received signal strength through coherent combining or transmission.

For an ideal uncorrelated MIMO channel, a full-diversity transmission scheme can achieve a maximum diversity order of [11]

$$d_{\max} = N_t N_r \tag{2.9}$$

indicating that the potential diversity order increases with the number of antennas at both the transmitter and receiver.

In MIMO systems, diversity is primarily achieved through spatial diversity using multiple antennas at the transmitter, receiver or both. Receiver diversity employs multiple receive antennas to obtain several independently faded versions of the transmitted signal, which are then combined to improve detection reliability. A widely used receive-diversity technique is maximal ratio combining (MRC), in which the received signals are coherently weighted according to the corresponding channel coefficients and combined as [1]

$$y = \sum_{i=1}^{N_r} w_i y_i, \tag{2.10}$$

where y_i denotes the received signal at the i-th antenna and, for equal noise variance across the receive branches, the combining weights are chosen proportionally to the complex conjugate of the corresponding channel coefficients, i.e., $w_i \propto h_i^*$. Transmit diversity improves communication robustness by transmitting redundant signal components across multiple transmit antennas using suitable coding or signal design techniques. A widely used example is Space-Time Block Coding (STBC), particularly the Alamouti scheme [12], where two symbols are transmitted across two antennas and two time slots according to

$$\mathbf{X} = \begin{bmatrix} x_1 & -x_2^* \\ x_2 & x_1^* \end{bmatrix} \tag{2.11}$$

where the rows correspond to the transmit antennas and the columns to consecutive time slots.

This structure enables transmit-side diversity while maintaining relatively low decoding complexity. Joint transmit–receive diversity further enhances reliability by simultaneously exploiting spatial diversity at both ends of the communication link. Under ideal uncorrelated MIMO conditions, this configuration enables diversity gains up to the full diversity order.

Diversity-oriented MIMO transmission plays a central role in communication scenarios where reliability is prioritized over throughput, particularly in wireless systems operating under challenging propagation conditions or stringent quality-of-service requirements. However, the effectiveness of diversity mechanisms depends strongly on the degree of channel independence among antenna paths. Spatial correlation, propagation asymmetry and imperfect channel state information may significantly reduce the achievable diversity gain in practical wireless

environments [15].

2.1.4 Spatial Multiplexing and Throughput Enhancement

Spatial multiplexing enables a MIMO system to transmit multiple independent data streams simultaneously over the same time–frequency resources, thereby increasing spectral efficiency and throughput without requiring additional bandwidth [8, 9].

Under ideal channel conditions, spatial multiplexing enables MIMO systems to achieve substantial capacity gains compared to conventional single-stream systems. By transmitting multiple independent data streams simultaneously over parallel spatial channels, throughput can increase significantly without requiring additional bandwidth or transmission power. In such cases, channel capacity scales approximately with the number of effective spatial streams [9, 11].

For spatial multiplexing, the transmitted signal vector contains N_s independent data streams and can be represented as

$$\mathbf{s} = \begin{bmatrix} s_1 & s_2 & \cdots & s_{N_s} \end{bmatrix}^T, \tag{2.12}$$

where, as established in Section 2.1.2, the number of simultaneously transmitted streams is constrained by the rank of the MIMO channel.

In the simplest case, where one independent stream is transmitted from each active transmit antenna, the received signal follows the conventional MIMO input–output model given in (2.1). The receiver must then separate the simultaneously transmitted streams by exploiting the spatial structure of the channel.

At high SNR, the capacity of a MIMO channel with r_H effective independent spatial dimensions exhibits the asymptotic scaling behavior

$$C(\rho) = r_H \log_2(\rho) + O(1), \tag{2.13}$$

where ρ denotes the signal-to-noise ratio, $r_H = \operatorname{rank}(\mathbf{H})$, and $O(1)$ represents terms that remain bounded as $\rho \to \infty$. This relation illustrates the fundamental multiplexing advantage of MIMO systems, since each additional usable spatial dimension can contribute to the growth of the achievable rate.

However, the effectiveness of spatial multiplexing depends strongly on the characteristics of the wireless channel. Efficient multiplexing requires sufficiently independent spatial channels, high channel rank and favorable channel conditioning in order to reliably separate the simultaneously transmitted data streams at the receiver [13].

These requirements also introduce important practical challenges. Since multiple streams are transmitted over the same time–frequency resources, reliable signal detection becomes significantly more complex and requires appropriate receiver processing to separate the simultaneously transmitted streams. Linear detection techniques such as Zero-Forcing (ZF) and Minimum Mean Square Error (MMSE), which are particularly relevant to the analyses

developed later in this thesis, are discussed in the following subsection. In addition, imperfect channel state information, spatial correlation and unfavorable propagation conditions may increase residual inter-stream interference and substantially degrade system performance [15].

Consequently, spatial multiplexing offers substantial throughput advantages under favorable operating conditions, but typically at the cost of increased signal-processing complexity and reduced robustness compared to diversity-oriented transmission. This creates an important trade-off between throughput and reliability in MIMO system design [14].

2.1.5 Linear Detection in MIMO Systems

Signal detection is a fundamental task in MIMO communication systems, where the receiver must recover the transmitted signal vector from the received observations [1, 11]. Due to the multi-antenna nature of MIMO channels, the received signal generally consists of a superposition of multiple transmitted signal components, making reliable detection a non-trivial problem. Considering the MIMO input–output model given in (2.1), the objective of the receiver is to estimate the transmitted signal vector $\mathbf{x}$ from the received vector $\mathbf{y}$.

Among the various detection methods available for MIMO systems, linear detection techniques are widely used due to their relatively low computational complexity and practical implementation feasibility [13]. Two common linear detectors are the Zero-Forcing (ZF) and Minimum Mean Square Error (MMSE) detectors.

The ZF detector attempts to eliminate inter-stream interference by applying the pseudo-inverse of the channel matrix [11]. The ZF equalization matrix is given by

$$\mathbf{W}_{\mathrm{ZF}} = \left(\mathbf{H}^H\mathbf{H}\right)^{-1}\mathbf{H}^H, \tag{2.14}$$

provided that $\mathbf{H}^H\mathbf{H}$ is nonsingular, as in the case of a full-column-rank channel with $N_r \geq N_t$. The estimated transmitted signal vector is then obtained as

$$\hat{\mathbf{x}} = \mathbf{W}_{\mathrm{ZF}}\mathbf{y}. \tag{2.15}$$

Equivalently, using the Moore–Penrose pseudo-inverse, the ZF estimate may be written as

$$\hat{\mathbf{x}} = \mathbf{H}^{\dagger}\mathbf{y}. \tag{2.16}$$

Under perfect CSI and a full-column-rank channel, ZF detection can eliminate inter-stream interference in the linear model. However, channel inversion may lead to significant noise enhancement, particularly when the channel matrix is ill-conditioned.

The MMSE detector addresses this limitation by balancing interference suppression and noise amplification [1]. Assuming spatially white noise and normalized unit-power transmitted symbols, the MMSE equalization matrix is expressed as

$$\mathbf{W}_{\mathrm{MMSE}} = \left(\mathbf{H}^H\mathbf{H} + \sigma_n^2\mathbf{I}_{N_t}\right)^{-1}\mathbf{H}^H, \tag{2.17}$$

where σ_n^2 denotes the noise variance. The corresponding detected signal vector is

$$\hat{\mathbf{x}} = \mathbf{W}_{\text{MMSE}}\mathbf{y}. \tag{2.18}$$

Compared with ZF detection, MMSE detection generally provides improved robustness in noisy environments because it does not attempt to completely cancel inter-stream interference at the expense of excessive noise amplification.

The performance of both ZF and MMSE detectors depends strongly on channel conditioning and CSI accuracy. Under imperfect CSI, the same detector structures are constructed using the estimated channel matrix $\hat{\mathbf{H}}$ instead of the true channel matrix $\mathbf{H}$, resulting in residual inter-stream interference and degraded detection reliability [22]. This sensitivity is particularly relevant to the analyses developed later in this thesis, where the robustness of MIMO transmission is evaluated under different levels of channel estimation uncertainty.

2.1.6 Diversity–Multiplexing Tradeoff

The preceding discussion highlights that MIMO communication systems offer multiple mechanisms for improving wireless performance, primarily through diversity-oriented transmission and spatial multiplexing. However, these transmission strategies pursue fundamentally different performance objectives and therefore introduce an inherent trade-off in MIMO system design [11].

Diversity-oriented transmission prioritizes communication reliability and robustness against fading, whereas spatial multiplexing aims to increase spectral efficiency and throughput by transmitting multiple independent data streams. The fundamental relationship between these two objectives is formally characterized by the diversity–multiplexing tradeoff (DMT), which provides an asymptotic framework for quantifying the balance between reliability and transmission rate in MIMO channels [14].

The diversity gain characterizes the asymptotic rate at which the error probability decreases with increasing signal-to-noise ratio and is defined as

$$d = -\lim_{\text{SNR}\to\infty} \frac{\log P_e(\text{SNR})}{\log \text{SNR}}, \tag{2.19}$$

where $P_e(\text{SNR})$ denotes the error probability. A larger diversity gain therefore corresponds to a faster asymptotic reduction in error probability as the SNR increases.

The multiplexing gain characterizes the asymptotic rate at which the transmission rate increases with SNR and is defined as

$$r = \lim_{\text{SNR}\to\infty} \frac{R(\text{SNR})}{\log \text{SNR}}, \tag{2.20}$$

where $R(\text{SNR})$ denotes the transmission rate. A larger multiplexing gain therefore reflects a greater ability to exploit the available spatial dimensions for increasing the achievable data rate.

For an i.i.d. Rayleigh fading MIMO channel, the optimal diversity–multiplexing trade-off is characterized by the piecewise-linear curve connecting the points [14]

$$(k, (N_t - k)(N_r - k)), \qquad k = 0, 1, \ldots, \min(N_t, N_r). \tag{2.21}$$

This relation demonstrates that diversity gain and multiplexing gain cannot be simultaneously maximized. At $r = 0$, the maximum diversity gain is $N_t N_r$, corresponding to operation that prioritizes reliability. As the multiplexing gain increases, the maximum achievable diversity gain progressively decreases, reaching zero at the maximum multiplexing gain $r = \min(N_t, N_r)$. The DMT therefore provides a fundamental asymptotic characterization of the competing reliability and rate benefits offered by MIMO systems.

From a system-design perspective, this fundamental trade-off reflects the competing objectives of reliability-oriented and throughput-oriented MIMO operation. Reliability-critical systems typically favor diversity-oriented transmission, whereas throughput-driven systems place greater emphasis on spatial multiplexing. The preferred operating strategy therefore depends on communication requirements, channel conditions and the characteristics of the propagation environment.

Under non-ideal MIMO operating conditions, the achievable balance between reliability and throughput may deviate substantially from that predicted under idealized DMT assumptions. Spatial correlation, propagation asymmetry and imperfect channel state information can affect channel rank, detection performance and the achievable diversity and multiplexing benefits [15]. These effects motivate the evaluation of MIMO transmission strategies under realistic propagation and channel estimation conditions.

2.2 Realistic Wireless Propagation and Channel Modeling

2.2.1 Limitations of Simplified Channel Models

Theoretical analysis of wireless communication systems has commonly relied on simplified channel models in order to enable tractable mathematical analysis and facilitate performance evaluation. Among the most commonly used models are the Additive White Gaussian Noise (AWGN) channel and idealized fading models such as independent and identically distributed (i.i.d.) Rayleigh fading [1, 15]. These models have played a central role in establishing the theoretical foundations of wireless communications and have provided valuable insight into the fundamental behavior of MIMO systems.

The AWGN model assumes that signal impairment arises solely from additive Gaussian noise, without accounting for multipath propagation, fading or propagation variability. Under the AWGN assumption, the received signal can be represented in its simplest form as

$$y = x + n, \tag{2.22}$$

where n denotes complex Gaussian noise modeled as

$$n \sim \mathcal{CN}(0, \sigma_n^2). \tag{2.23}$$

This model provides a useful baseline by isolating the effect of additive noise from propagation-induced channel variations.

Although useful for baseline performance analysis, this model neglects many critical characteristics of practical wireless channels. Similarly, idealized i.i.d. Rayleigh fading models incorporate small-scale fading effects and are widely used to analyze MIMO systems under rich-scattering conditions [11]. Under the conventional i.i.d. Rayleigh fading assumption, the entries of the MIMO channel matrix are modeled as independent complex Gaussian random variables,

$$h_{ij} \sim \mathcal{CN}(0, 1), \tag{2.24}$$

so that

$$\mathbf{H} \in \mathbb{C}^{N_r \times N_t}, \qquad [\mathbf{H}]_{ij} \overset{\text{i.i.d.}}{\sim} \mathcal{CN}(0, 1). \tag{2.25}$$

Consequently, the channel magnitudes $|h_{ij}|$ follow a Rayleigh distribution, while the channel coefficients are statistically independent across transmit–receive antenna pairs.

Despite their analytical convenience, conventional i.i.d. Rayleigh models do not explicitly capture important deployment-dependent characteristics such as spatial correlation, antenna geometry, polarization and location-dependent propagation conditions.

While these simplified assumptions are useful for theoretical analysis, they often fail to accurately represent realistic wireless propagation environments. In practical systems, individual wireless links are shaped by complex interactions among path loss, shadowing, multipath propagation, antenna geometry and polarization effects [15]. At the system level, variations in user locations and deployment geometry further introduce heterogeneous propagation conditions across the network. These factors can substantially influence channel rank, spatial correlation and overall MIMO performance.

As a result, conclusions derived under simplified channel assumptions may not always generalize to practical wireless systems. This limitation becomes particularly important in modern MIMO communications, where system performance depends strongly on realistic channel structure and spatial propagation characteristics. Consequently, meaningful assessment of MIMO performance requires channel models capable of capturing the complexity and variability of practical wireless propagation environments [15].

2.2.2 Large-Scale Propagation Effects

Large-scale propagation effects describe the average signal attenuation behavior over relatively large transmission distances and represent one of the most fundamental factors affecting wireless communication performance [1, 45]. Unlike small-scale fading, which causes rapid fluctuations in signal amplitude due to multipath propagation, large-scale effects determine

the overall channel strength and strongly influence the average received signal quality.

One of the primary large-scale propagation effects is path loss, which describes the reduction in signal power as the distance between transmitter and receiver increases. Path loss is influenced by transmission distance, carrier frequency, environmental characteristics and propagation conditions. In practical wireless systems, increased distance typically results in lower received signal power, reduced signal-to-noise ratio and degraded communication performance [45].

A widely used model for large-scale path loss is the log-distance path loss model with log-normal shadowing [1], expressed as

$$PL(d) = PL(d_0) + 10n \log_{10}\left(\frac{d}{d_0}\right) + X_{\text{sh}}, \tag{2.26}$$

where $PL(d)$ denotes the path loss at distance d in dB, $PL(d_0)$ is the path loss at a reference distance d_0, n is the path loss exponent determined by the propagation environment, and X_{sh} represents the random variation introduced by shadowing.

In addition to distance-dependent attenuation, wireless propagation is affected by shadowing, which represents variations in received signal power caused by obstacles such as buildings, terrain and other environmental obstructions. Shadowing introduces slow variations in received signal strength and may create significant differences in channel quality among users located in different physical environments. In the dB domain, log-normal shadowing is commonly represented by a zero-mean Gaussian random variable,

$$X_{\text{sh}} \sim \mathcal{N}(0, \sigma_{\text{sh}}^2), \tag{2.27}$$

where σ_{sh} denotes the shadowing standard deviation in dB and characterizes the severity of large-scale signal variations caused by environmental obstructions [15].

Another important factor is the propagation condition between transmitter and receiver, commonly classified as Line-of-Sight (LOS) or Non-Line-of-Sight (NLOS). LOS conditions typically exhibit lower path loss and a stronger deterministic propagation component, whereas NLOS conditions generally introduce additional attenuation, scattering and multipath propagation due to obstruction. Although LOS propagation often improves received signal strength, its impact on MIMO performance also depends on the resulting spatial channel structure and correlation characteristics. In practical channel models, LOS and NLOS conditions are often characterized by different path loss exponents, shadowing statistics and fading behavior [16, 17].

These large-scale propagation effects play a central role in realistic MIMO system evaluation because they strongly influence channel quality, link reliability and user-specific communication conditions. In practical wireless deployments, large-scale propagation variations frequently create channel asymmetries among users, making realistic propagation modeling essential for accurate system-level performance analysis [15].

2.2.3 Small-Scale Fading and Spatial Correlation

In addition to large-scale propagation effects, wireless channels are strongly influenced by small-scale fading, which causes rapid fluctuations in received signal amplitude and phase over short time intervals, frequencies or spatial displacements [15,45]. Small-scale fading primarily arises from multipath propagation, where transmitted signals reach the receiver through multiple paths caused by reflection, diffraction and scattering from surrounding objects.

Under a narrowband flat-fading representation, the complex channel coefficient can be modeled as the superposition of multiple propagation components [1]:

$$h = \sum_{l=1}^{L} \alpha_l e^{-j\phi_l}, \tag{2.28}$$

where L denotes the number of resolvable propagation components, α_l represents the amplitude of the l-th component and ϕ_l denotes its corresponding phase.

As these multipath components combine constructively or destructively at the receiver, significant variations in instantaneous signal strength may occur. Such fluctuations can substantially affect communication reliability and constitute one of the primary challenges in wireless system design.

Another important characteristic of small-scale propagation is delay dispersion, which arises from multipath components arriving at different delays. Delay spread may introduce frequency-selective fading and inter-symbol interference, particularly in broadband communication systems. A commonly used measure is the root-mean-square (RMS) delay spread, τ_{rms}, which is related to the coherence bandwidth of the channel. In general, coherence bandwidth is inversely related to the delay spread and may be approximately characterized as

$$B_c \propto \frac{1}{\tau_{\text{rms}}}, \tag{2.29}$$

where B_c denotes the coherence bandwidth. Signals whose bandwidth is substantially smaller than B_c generally experience approximately flat fading, whereas signals with bandwidth comparable to or larger than B_c may experience frequency-selective fading [15, 45].

Temporal channel variations constitute another important aspect of small-scale fading, particularly in mobile wireless environments. Relative motion between the transmitter, receiver and surrounding scatterers introduces Doppler shifts in the received multipath components. For a propagation component arriving at angle θ, the Doppler shift may be expressed as

$$f_D = \frac{v}{\lambda}\cos(\theta), \tag{2.30}$$

where v denotes the relative velocity and λ is the carrier wavelength. The maximum Doppler shift is therefore given by

$$f_{D,\max} = \frac{v}{\lambda}. \tag{2.31}$$

The temporal stability of the wireless channel is commonly characterized by the coherence time T_c, which is inversely related to the maximum Doppler shift,

$$T_c \propto \frac{1}{f_{D,\max}}. \tag{2.32}$$

Higher mobility therefore results in larger Doppler spread and shorter coherence time, causing the channel to vary more rapidly. These temporal variations are particularly important for channel estimation and CSI-dependent communication techniques, since rapidly varying channels may cause previously acquired channel information to become outdated [15, 45].

Two widely used statistical models for characterizing small-scale fading are Rayleigh and Rician fading. Rayleigh fading is typically used in rich-scattering environments where no dominant direct propagation path exists between transmitter and receiver. Under the Rayleigh fading assumption, the complex channel coefficient is commonly modeled as

$$h \sim \mathcal{CN}(0, \sigma_h^2), \tag{2.33}$$

so that the channel envelope $r = |h|$ follows a Rayleigh distribution with probability density function

$$f_r(r) = \frac{2r}{\sigma_h^2} \exp\left(-\frac{r^2}{\sigma_h^2}\right), \qquad r \geq 0, \tag{2.34}$$

where $\sigma_h^2 = \mathbb{E}[|h|^2]$ denotes the average channel power.

In contrast, Rician fading models scenarios in which a dominant Line-of-Sight (LOS) or strong specular component coexists with scattered multipath components [44]. The choice of fading model significantly influences channel behavior and expected communication performance.

For Rician fading, the relative strength of the dominant component is commonly characterized by the Rician K-factor,

$$K = \frac{P_{\text{dom}}}{P_{\text{scat}}}, \tag{2.35}$$

where P_{dom} denotes the average power of the dominant LOS or specular component and P_{scat} represents the total average power of the scattered multipath components.

The corresponding value in decibels is given by

$$K_{\text{dB}} = 10 \log_{10}(K). \tag{2.36}$$

While Rayleigh and Rician models characterize the statistical behavior of individual channel coefficients, MIMO performance also depends critically on the statistical relationships among the different antenna channels. For MIMO systems, small-scale fading characteristics alone are not sufficient to determine performance. Equally important is the degree of spatial correlation among antenna channels. Spatial correlation describes the statistical dependence between

signals observed at different antennas and plays a central role in determining the effective rank and spatial degrees of freedom of the MIMO channel [13, 15].

A common representation of spatial correlation is provided by channel covariance matrices. For example, the receive-side covariance matrix can be expressed as

$$\mathbf{R}_r = \frac{1}{N_t}\mathbb{E}\left[\mathbf{H}\mathbf{H}^H\right], \tag{2.37}$$

where the normalization by N_t accounts for the number of transmit dimensions. Similarly, the transmit-side covariance matrix can be represented as

$$\mathbf{R}_t = \frac{1}{N_r}\mathbb{E}\left[\mathbf{H}^H\mathbf{H}\right]. \tag{2.38}$$

High spatial correlation generally reduces the number of effectively independent spatial channels, which may reduce achievable diversity benefits and significantly limit spatial multiplexing performance. In contrast, low correlation improves channel independence and enables more efficient exploitation of spatial resources. Spatial correlation is influenced by several practical factors, including antenna spacing, antenna geometry, polarization characteristics and the surrounding propagation environment [15].

Consequently, representative MIMO system analysis requires accurate characterization of small-scale fading across the temporal, frequency and spatial domains. Multipath delay dispersion determines frequency-selective behavior, Doppler effects determine temporal channel variability, and spatial correlation governs the degree of independence among antenna channels. Together, these factors strongly influence channel rank, diversity gain, CSI accuracy and achievable MIMO performance, making them fundamental components of realistic wireless channel modeling [15, 17].

2.2.4 Realistic Channel Modeling for MIMO Systems

The increasing complexity of wireless communication systems has driven the development of progressively more sophisticated channel modeling frameworks capable of capturing realistic propagation behavior [15]. Unlike simplified analytical models, realistic channel models aim to represent the combined effects of large-scale attenuation, small-scale fading, spatial correlation, antenna characteristics and user-dependent propagation conditions. Such models are particularly important for MIMO systems, where channel structure directly influences achievable diversity gain, spatial multiplexing efficiency and overall system performance.

Several important channel modeling frameworks have been developed over the years for wireless system evaluation. Early standardized modeling efforts, including COST 207 and COST 259, provided important foundations for the characterization of mobile radio propagation [46,47]. COST 207 established scenario-dependent multipath channel descriptions for cellular environments, while COST 259 extended this perspective toward more detailed spatial and directional channel characterization. These models introduced propagation characterization and enabled more realistic analysis of large-scale and small-scale fading effects in practical

wireless environments.

Subsequent frameworks, such as the WINNER channel models, further improved realism by introducing geometry-based stochastic modeling with more detailed scenario-specific propagation characterization [20]. By incorporating parameters such as multipath delays, angles of departure and arrival, polarization and spatial channel characteristics, these models enabled more representative evaluation of multi-antenna systems across heterogeneous deployment environments.

In geometry-based stochastic channel models, propagation is represented through groups of multipath components associated with parameters such as delays, powers and angles of departure and arrival. Rather than modeling each channel coefficient independently, the channel matrix is generated from a common spatial propagation structure, allowing correlations among antenna elements and links to emerge from the underlying geometry and propagation characteristics. A generic time- and frequency-dependent multipath representation underlying such channel models can be expressed as [15]

$$\mathbf{H}(t, f) = \sum_{\ell=1}^{L} \mathbf{H}_\ell e^{-j2\pi f \tau_\ell} e^{j2\pi \nu_\ell t}, \tag{2.39}$$

where L denotes the number of multipath components, $\mathbf{H}_\ell$ represents the spatial MIMO channel contribution of the ℓ-th component, τ_ℓ denotes its propagation delay and ν_ℓ represents the corresponding Doppler shift. This representation illustrates how the overall MIMO channel results from the superposition of multiple propagation components with distinct spatial, temporal and frequency-dependent characteristics. In standardized geometry-based stochastic models, these components are further organized into clusters and parameterized according to the considered propagation scenario.

More recently, channel modeling has been extensively standardized by the Third Generation Partnership Project (3GPP), which has developed comprehensive channel models for modern wireless communication systems. In particular, 3GPP TR 36.873 introduced three-dimensional channel modeling for LTE-based systems, extending conventional two-dimensional channel representations by incorporating elevation-domain propagation in addition to azimuth-domain characteristics [16]. This enabled more realistic modeling of base-station height, vertical beamforming and advanced multi-antenna deployments such as full-dimension MIMO (FD-MIMO).

Building upon this foundation, 3GPP TR 38.901 further extended standardized channel modeling for 5G and beyond wireless systems, supporting broader frequency ranges, more diverse deployment scenarios and increasingly complex antenna-array configurations [17].

These standardized channel models support diverse deployment scenarios, including urban microcell (UMi), urban macrocell (UMa), rural macrocell (RMa) and indoor environments under both LOS and NLOS conditions. They provide realistic representation of spatial consistency, polarization effects, antenna-array characteristics and user-dependent channel variability [16, 17].

As a result, these models have become essential tools for accurate MIMO system evaluation and form the basis of many modern simulation frameworks used for realistic wireless performance analysis [17, 20].

2.2.5 Simulation Frameworks for Realistic MIMO Evaluation

Accurate evaluation of modern MIMO communication systems requires simulation frameworks capable of capturing both wireless channel behavior and relevant communication-system operating characteristics [15]. Depending on the objective and level of abstraction, wireless system evaluation is commonly performed using either link-level or system-level simulation approaches.

Link-level simulation focuses on the detailed physical-layer behavior of an individual communication link between transmitter and receiver. In such frameworks, the relevant signal-processing chain is explicitly modeled, including signal generation, modulation, channel effects, channel estimation, detection, equalization and decoding. This level of analysis enables detailed investigation of physical-layer mechanisms and is particularly useful for studying receiver behavior, signal detection performance and the impact of practical impairments such as channel estimation errors or interference. Link-level simulation therefore plays an important role when the objective is to analyze communication behavior at the signal-processing level [1].

System-level simulation adopts a broader perspective by focusing on the behavior of wireless communication systems under realistic deployment conditions. Rather than explicitly modeling every physical-layer operation, system-level frameworks employ suitable abstraction mechanisms to represent link performance while incorporating realistic propagation behavior, user distributions, interference conditions and network interactions. This approach enables the efficient analysis of large-scale wireless scenarios and provides insight into how propagation conditions, antenna configurations and spatial user characteristics influence overall system performance [17].

Both simulation levels are employed in this thesis according to the objective of each investigation. Link-level analysis is used when detailed physical-layer behavior must be explicitly examined, particularly for signal detection under imperfect CSI and cooperative MIMO transmission. System-level simulation, in contrast, is employed for propagation-aware investigations requiring realistic deployment conditions, spatial user distributions and standardized channel modeling.

The main system-level simulation platform employed in this work is the Vienna LTE-A System-Level Simulator v2.0 (Q3), developed by the Vienna University of Technology [48]. The framework was selected because it combines standardized propagation modeling with flexible configuration of deployment and antenna parameters, while maintaining the computational efficiency required for extensive system-level investigations.

A major advantage of the Vienna framework is its ability to support system-level evaluation under a wide range of propagation and deployment conditions. Its flexible simulation structure

enables the investigation of MIMO performance across different channel conditions, antenna configurations and user scenarios, making it particularly suitable for propagation-aware system-level studies [48].

The Vienna LTE-A System-Level Simulator therefore provides the system-level simulation basis for the propagation-aware MIMO investigations presented in the following chapters, while additional models and algorithms are introduced where required to examine imperfect CSI, energy-aware operation and adaptive transmission strategies.

2.3 Channel State Information and Channel Uncertainty

2.3.1 CSI in MIMO Communications

Channel State Information (CSI) refers to the available knowledge of the wireless channel between the transmitter and the receiver [1, 11]. In MIMO communication systems, the physical channel is represented by the channel matrix $\mathbf{H} \in \mathbb{C}^{N_r \times N_t}$, whose entries characterize signal propagation across the transmit–receive antenna pairs. Accurate knowledge of this matrix is fundamental for efficient MIMO operation because it enables communication systems to exploit the spatial characteristics of the wireless channel.

The physical channel matrix $\mathbf{H}$ reflects the combined influence of the propagation mechanisms discussed in the preceding sections, including path loss, shadowing, multipath fading, Doppler effects, LOS/NLOS conditions and spatial correlation. The physical channel and the available CSI should therefore be distinguished: propagation conditions determine the actual channel $\mathbf{H}$, whereas channel estimation and related acquisition mechanisms determine how accurately this channel is known to the communication system. When the channel is estimated rather than perfectly known, the available estimate is commonly denoted by $\hat{\mathbf{H}}$. Consequently, even a complex or strongly varying propagation channel may, in principle, be perfectly known, whereas estimation errors, noise, limited pilot resources or channel aging may cause the available CSI to deviate from the true channel.

At the receiver, CSI plays a central role in signal detection and equalization. Accurate channel knowledge enables reliable separation of simultaneously transmitted data streams, compensation for channel distortions and mitigation of inter-stream interference. This is particularly important in spatial multiplexing MIMO systems, where multiple parallel data streams must be detected under challenging channel conditions [13].

At the transmitter, CSI supports transmission optimization through techniques such as precoding, power allocation and adaptive transmission strategies. By exploiting channel knowledge, the transmitter can dynamically adjust communication parameters in order to improve reliability, throughput and overall system efficiency. In adaptive MIMO systems, CSI may further guide decisions related to antenna configuration, transmission mode selection and resource allocation [23].

Theoretical analyses of MIMO communication systems often assume perfect CSI, corresponding to exact knowledge of the relevant channel state at the receiver, the transmitter

or both, depending on the considered system model. Perfect CSI provides an important performance benchmark by isolating the effects of channel uncertainty and enabling the theoretical capabilities of channel-dependent detection, precoding and adaptation mechanisms to be evaluated [11].

In practical wireless systems, however, perfect channel knowledge is rarely available. CSI must typically be acquired through channel estimation procedures based on pilot or reference signals and may subsequently be affected by estimation inaccuracies, feedback limitations, transmission delays and channel variations. As a result, the channel information available for communication decisions inevitably contains uncertainty and deviates from the true channel state [21, 22].

The dominant source of CSI uncertainty is channel estimation error. Since channel estimation is typically performed using pilot or reference signals transmitted over noisy wireless channels, the estimated channel inevitably contains errors. The accuracy of channel estimation therefore depends strongly on signal-to-noise ratio, pilot quality and estimation methodology [21].

Another important source of uncertainty arises from pilot limitations. In practical communication systems, pilot resources are constrained by bandwidth, latency and signaling overhead considerations. Limited pilot density or insufficient training duration may reduce channel estimation accuracy, particularly in systems with large antenna dimensions or rapidly varying channel conditions [22].

CSI uncertainty may also arise from feedback delay and channel aging effects. In systems where channel information must be estimated at the receiver and communicated back to the transmitter, delays introduced by feedback signaling may cause the available CSI to become outdated before transmission decisions are applied. This effect becomes particularly severe in high-mobility scenarios or rapidly changing wireless environments, where increased temporal channel variability reduces channel coherence time and makes accurate CSI maintenance increasingly difficult [23].

Finally, hardware impairments such as oscillator instability, synchronization errors, phase noise and non-ideal radio-frequency components may introduce additional distortions that degrade channel estimation quality. These practical non-idealities further contribute to CSI uncertainty and may significantly affect MIMO system performance under realistic operating conditions [15].

In the context of this thesis, the primary form of CSI impairment considered is channel estimation uncertainty, which introduces deviations between the estimated channel and the true propagation channel. Such deviations directly affect signal detection, equalization and adaptive transmission decisions, making CSI uncertainty a central factor in the performance analyses presented in the following chapters. The mathematical models used to represent this uncertainty are introduced in the following subsection.

2.3.2 Modeling CSI Imperfections

In order to analyze the impact of channel uncertainty on wireless communication performance, CSI imperfections must be represented through appropriate mathematical models. Such models provide a systematic framework for characterizing deviations between the estimated channel and the true propagation channel, enabling quantitative evaluation of performance degradation under imperfect CSI conditions [15, 22].

A widely adopted approach is the additive channel estimation error model, in which the estimated channel matrix is expressed as [22]

$$\hat{\mathbf{H}} = \mathbf{H} + \mathbf{E} \tag{2.40}$$

where $\mathbf{H}$ denotes the true channel matrix, $\hat{\mathbf{H}}$ represents the estimated channel available to the communication system and $\mathbf{E}$ is the channel estimation error matrix. In this thesis, this formulation is referred to as Channel Estimation Error Model I *(CEEM-I)*.

Under CEEM-I, the error matrix represents the uncertainty between the true and estimated channel matrices. The entries of $\mathbf{E}$ are commonly modeled as independent zero-mean complex Gaussian random variables:

$$e_{ij} \sim \mathcal{CN}(0, \sigma_e^2) \tag{2.41}$$

where σ_e^2 denotes the channel estimation error variance.

An alternative CSI uncertainty formulation employed in this thesis retains the additive error structure but allows the estimation error variance to depend on the effective training quality. The estimated channel is expressed as

$$\hat{\mathbf{H}} = \mathbf{H} + \mathbf{E}, \tag{2.42}$$

where the entries of the estimation error matrix are modeled as

$$e_{ij} \sim \mathcal{CN}(0, \sigma_{e,\mathrm{II}}^2). \tag{2.43}$$

The corresponding estimation error variance is given by

$$\sigma_{e,\mathrm{II}}^2 = \frac{1}{1 + L_p \gamma_s}, \tag{2.44}$$

where L_p denotes the effective pilot or training length and $\gamma_s = E_s/N_0$ represents the symbol-level signal-to-noise ratio. In this thesis, this formulation is referred to as Channel Estimation Error Model II *(CEEM-II)*.

Unlike CEEM-I, where the estimation error variance is externally specified and remains fixed for a given simulation scenario, CEEM-II relates the CSI uncertainty to the effective training quality. Consequently, increasing the SNR or the pilot length reduces the channel estimation error variance and improves CSI accuracy. The impact of imperfect CSI can be

illustrated using the MIMO input–output relation given in (2.1), where $\mathbf{x}$ denotes the transmitted signal vector, $\mathbf{y}$ is the received signal vector, and $\mathbf{n}$ represents additive noise. Substituting the additive CSI error model yields

$$\mathbf{H} = \hat{\mathbf{H}} - \mathbf{E} \tag{2.45}$$

and therefore

$$\mathbf{y} = (\hat{\mathbf{H}} - \mathbf{E})\mathbf{x} + \mathbf{n} \tag{2.46}$$

which can be rewritten as

$$\mathbf{y} = \hat{\mathbf{H}}\mathbf{x} - \mathbf{E}\mathbf{x} + \mathbf{n}. \tag{2.47}$$

This expression clearly shows that imperfect CSI introduces an additional interference term, $\mathbf{Ex}$, which acts as residual interference during signal detection. The received signal therefore consists of three components: the desired signal term based on the estimated channel, $\hat{\mathbf{H}}\mathbf{x}$, the residual interference term caused by CSI uncertainty, $\mathbf{Ex}$, and the additive noise term, $\mathbf{n}$. As CSI uncertainty increases, the residual interference becomes more significant, reducing detection accuracy and progressively degrading communication performance [22].

A key parameter used throughout this thesis to quantify CSI uncertainty is the channel estimation error variance, σ_e^2. Smaller values of σ_e^2 correspond to more accurate channel knowledge, with $\sigma_e^2 = 0$ representing perfect CSI, whereas increasing values indicate progressively stronger CSI uncertainty and degraded channel knowledge.

The CEEM-I and CEEM-II formulations provide complementary models for representing CSI uncertainty and form the basis for the imperfect CSI analyses developed throughout this thesis.

2.3.3 Impact of Imperfect CSI on MIMO Performance

Imperfect channel state information can significantly degrade the performance of MIMO communication systems by reducing the effectiveness of channel-dependent transmission and signal-processing techniques [15, 22]. Since many advanced MIMO strategies rely heavily on accurate channel knowledge, CSI uncertainty directly affects communication reliability, achievable throughput and overall system robustness.

In diversity-oriented transmission schemes, imperfect CSI reduces the effectiveness of diversity combining and signal recovery mechanisms. As channel estimation accuracy deteriorates, inaccurate weighting or processing of the received signal branches may prevent the receiver from fully exploiting the available diversity benefits, resulting in degraded error performance and reduced communication reliability [1].

Spatial multiplexing techniques are generally highly sensitive to CSI uncertainty. Since multiplexing relies on accurate channel knowledge to separate simultaneously transmitted data streams, estimation errors may significantly degrade signal detection performance. Inaccurate

CSI leads to imperfect interference suppression and increased residual inter-stream interference, thereby limiting the throughput gains achievable through spatial multiplexing [11].

One of the most important consequences of imperfect CSI is the presence of residual interference. As shown in the previous subsection, under the additive error model the mismatch between the true and estimated channel introduces the residual term $-\mathbf{Ex}$. This term cannot be accounted for perfectly by a receiver operating on the basis of the estimated channel and therefore contributes to degraded signal detection and increased error probability.

When channel estimation errors remain significant as the signal-to-noise ratio increases, performance degradation may become particularly pronounced at moderate-to-high SNR. In such conditions, the residual impairment associated with CSI uncertainty may become dominant relative to thermal noise, potentially leading to error-floor behavior in which further increases in transmit SNR provide progressively smaller performance improvements [22].

These observations highlight that CSI uncertainty fundamentally alters MIMO system behavior and must be explicitly considered in realistic performance evaluation and communication system design. The resulting performance degradation becomes particularly important in modern MIMO systems employing spatial multiplexing, cooperative transmission and adaptive operation, all of which strongly depend on reliable channel knowledge.

2.4 Reliability and Energy Efficiency in Wireless Systems

2.4.1 Reliability Metrics in Wireless Communications

Communication reliability is a fundamental performance objective in wireless communication systems and reflects the ability of a communication link to successfully deliver information with acceptable error performance under varying channel conditions [1, 15]. In practical wireless environments, reliability is strongly influenced by fading, interference, channel uncertainty and dynamic propagation conditions.

The reliability of wireless systems is commonly evaluated using several key performance metrics, among which Bit Error Rate (BER), Packet Error Rate (PER) and outage probability are the most widely used. BER measures the probability that a transmitted bit is incorrectly detected at the receiver and provides direct insight into the physical-layer error performance of modulation, coding and detection schemes. Lower BER values indicate higher communication reliability [44].

BER is formally defined as the probability of incorrect bit detection,

$$BER = P(\hat{b} \neq b), \tag{2.48}$$

where b and $\hat{b}$ denote the transmitted and detected bits, respectively. In simulation-based performance evaluation, BER is commonly estimated as

$$\widehat{BER} = \frac{N_{\text{error}}}{N_{\text{total}}}, \tag{2.49}$$

where N_{error} denotes the number of incorrectly detected bits and N_{total} represents the total number of transmitted bits. Packet Error Rate (PER) extends reliability evaluation to the packet level by measuring the probability that a transmitted packet is unsuccessfully received due to one or more bit errors. PER is particularly relevant in practical wireless systems where communication is typically packet-based. Even relatively small BER values may lead to significant packet failure probabilities for sufficiently large packet lengths [29]. Assuming statistically independent bit errors within a packet, PER can be expressed as

$$PER = 1 - (1 - BER)^L \tag{2.50}$$

where L denotes the packet length in bits.

Outage probability provides a system-level reliability metric by quantifying the probability that the communication system fails to satisfy a predefined performance requirement, such as a minimum signal-to-noise ratio, data rate or quality-of-service threshold. Outage analysis is particularly useful under severe fading or highly variable channel conditions [39]. A common outage definition is

$$P_{\text{out}} = P\left(R_{\text{inst}} < R_{\text{th}}\right), \tag{2.51}$$

where R_{inst} denotes the instantaneous achievable rate and R_{th} represents the minimum required rate threshold.

These reliability metrics provide complementary perspectives on wireless system performance. BER characterizes physical-layer detection accuracy, PER reflects packet-level communication success and outage probability captures system-level reliability under practical operating constraints. Together, these metrics provide a fundamental framework for evaluating communication robustness throughout this thesis.

These reliability measures are strongly influenced by channel quality indicators such as SNR and SINR. In general, deteriorating channel conditions reduce detection accuracy, leading to higher BER, increased packet failure probability and higher outage probability. In practical wireless systems, such reliability degradation often results in more frequent retransmissions, directly increasing communication latency and energy consumption. Consequently, communication reliability is closely linked to energy efficiency, particularly in systems operating under strict energy constraints [30].

2.4.2 Energy Consumption and Retransmission Cost in Wireless Systems

Communication reliability and energy consumption are closely interconnected in practical wireless systems. Transmission failures caused by fading, interference, channel uncertainty or adverse propagation conditions often lead to retransmissions, increasing the total resources required for successful data delivery. Mechanisms such as Automatic Repeat Request (ARQ) and Hybrid Automatic Repeat Request (HARQ) improve communication reliability by enabling retransmission of unsuccessfully received packets, but at the cost of increased latency, channel

occupancy and energy expenditure [27, 29].

As packet error rates increase, retransmissions become more frequent, resulting in higher energy consumption per successfully delivered packet. Accurate evaluation of wireless energy efficiency therefore requires realistic modeling of total energy consumption beyond transmission power alone. Practical wireless systems consume energy through multiple components, including signal transmission, circuit operation, signal processing and hardware-related overhead [30, 33].

A general conceptual decomposition of communication-related energy consumption may be expressed as

$$E_{\text{total}} = E_{\text{tx}} + E_{\text{circuit}} + E_{\text{proc}} + E_{\text{overhead}} \tag{2.52}$$

where E_{tx} denotes transmission energy, E_{circuit} represents circuit-related energy consumption, E_{proc} corresponds to signal-processing energy and E_{overhead} captures additional hardware-related overhead.

Transmission energy, E_{tx}, represents the energy directly consumed for wireless signal transmission over the communication channel and depends primarily on transmission power, transmission duration and communication distance. This component is strongly influenced by propagation conditions and required communication reliability, since poor channel conditions or stringent reliability requirements often necessitate higher transmission power or repeated transmissions.

Circuit energy, E_{circuit}, accounts for energy consumed by the radio-frequency hardware required for communication operation, including power amplifiers, mixers, oscillators, filters, analog-to-digital converters and digital-to-analog converters. Unlike transmission energy, circuit-related consumption may remain significant even when transmission power is relatively low, particularly in systems employing multiple active radio chains [32].

Processing energy, E_{proc}, captures the computational cost associated with baseband signal processing operations such as modulation, coding, decoding, channel estimation, signal detection and data recovery. This component becomes increasingly important in advanced communication systems employing complex signal-processing algorithms or sophisticated detection schemes.

The overhead term, E_{overhead}, represents additional energy costs associated with system operation, including hardware activation, control signaling, pilot transmission and protocol-related processing. Depending on system architecture and communication strategy, this overhead may become non-negligible and substantially affect overall energy efficiency.

In advanced wireless systems such as MIMO networks, realistic energy evaluation becomes particularly important because communication performance improvements are often achieved through increased system complexity. The use of multiple antennas, diversity schemes, spatial multiplexing and adaptive transmission strategies may significantly improve communication reliability or throughput, but these gains are often accompanied by increased circuit energy consumption, additional hardware activation and higher signal-processing complexity [13].

For example, activating additional transmit or receive antennas may provide additional spatial diversity opportunities and reduce retransmission requirements, but it also increases RF-chain power consumption and processing complexity. Similarly, more sophisticated detection algorithms or adaptive transmission strategies may improve performance under challenging channel conditions while introducing additional computational cost. As a result, performance gains achieved through advanced MIMO techniques do not necessarily translate directly into improved energy efficiency once practical implementation costs are taken into account [30,32].

Consequently, realistic energy evaluation must jointly consider communication reliability, retransmission cost and implementation complexity, forming the foundation for analyzing reliability–energy trade-offs in practical wireless systems.

2.4.3 Reliability–Energy Trade-offs in MIMO Communications

Reliability and energy efficiency are fundamentally interconnected in MIMO communication systems. Improving communication reliability often reduces transmission failures and retransmissions, but usually requires additional resource expenditure in the form of higher transmission power, increased spatial diversity, more active antennas or more sophisticated signal-processing algorithms. As a result, optimizing MIMO system performance requires balancing these competing objectives [30, 32].

A useful metric for evaluating this trade-off is the average energy required for successful packet delivery. Assuming independent transmission attempts and a constant packet error rate across retransmissions, the expected number of transmission attempts required for successful packet delivery is

$$\mathbb{E}[N_{\text{attempts}}] = \frac{1}{1 - PER}. \tag{2.53}$$

Consequently, the expected energy required for successful packet delivery can be expressed as [31]

$$E_{\text{succ}} = \frac{E_{\text{total}}}{1 - PER}, \tag{2.54}$$

where E_{total} denotes the total energy consumed per transmission attempt and PER denotes the packet error rate. This formulation captures the fact that lower communication reliability increases the expected number of transmission attempts required for successful packet delivery, thereby increasing the expected total energy expenditure.

In the adaptive MIMO analyses developed later in this thesis, a mode-dependent formulation is adopted in order to explicitly account for the variation of hardware and processing costs across different transmission configurations. For a transmission mode $m \in \mathcal{M}$, the total energy consumed per transmission attempt is expressed as

$$E_{\text{total},m} = E_{\text{tx}} + \alpha_m + \beta_m, \tag{2.55}$$

where α_m represents the mode-dependent hardware or circuit-related energy overhead and

β_m captures the mode-dependent signal-processing or complexity-related energy cost.

The corresponding energy required for successful packet delivery is therefore given by

$$E_{\text{succ},m} = \frac{E_{\text{total},m}}{1 - PER_m}, \tag{2.56}$$

where PER_m denotes the packet error rate associated with transmission mode m.

This trade-off becomes particularly important in MIMO systems employing multiple transmission strategies. Diversity-oriented configurations typically improve communication reliability by reducing packet errors and retransmissions, but often require additional hardware activation and increased signal-processing complexity. In contrast, multiplexing-oriented transmission strategies improve throughput and spectral efficiency but may become more sensitive to channel conditions, interference and CSI uncertainty [14].

Consequently, the communication strategy that achieves the highest reliability does not necessarily provide the best energy efficiency. Under some operating conditions, highly reliable but complex MIMO configurations may consume more energy than simpler transmission schemes with moderately lower reliability. Conversely, low-complexity transmission strategies may suffer from poor reliability and excessive retransmission cost. The optimal operating point therefore depends strongly on channel conditions, reliability requirements, CSI quality, hardware constraints and overall system objectives.

These observations highlight the importance of adaptive transmission strategies capable of dynamically balancing reliability and energy consumption. Rather than relying on fixed communication configurations, MIMO systems operating under varying conditions increasingly require intelligent mode selection mechanisms that adapt transmission strategy according to prevailing operating conditions. Such reliability-aware and energy-aware adaptation forms a central component of the adaptive MIMO frameworks investigated in this thesis.

2.4.4 Energy-Constrained Wireless Systems: IoT and LPWAN

The reliability–energy trade-offs discussed in the previous sections become particularly important in energy-constrained wireless systems, such as Internet of Things (IoT) networks and Low-Power Wide-Area Network (LPWAN) deployments [6, 7]. In these systems, communication performance is constrained not only by channel conditions and reliability requirements but also by strict energy limitations imposed by battery-powered operation and long device lifetime requirements.

IoT systems typically consist of large numbers of distributed devices performing sensing, monitoring or control tasks under limited power and hardware resources. In such environments, communication reliability remains essential for ensuring accurate data delivery, while energy efficiency directly affects device lifetime and long-term system viability. As a result, communication design must carefully balance reliability, resource utilization and energy expenditure [6].

LPWAN technologies were developed to support long-range communication under stringent

power constraints, enabling wide-area connectivity for large-scale IoT deployments. These systems typically prioritize low power consumption, extended coverage and low-cost device operation, often at the expense of reduced data rate and increased transmission latency [5, 7].

Among LPWAN technologies, LoRa has emerged as one of the most widely adopted solutions for low-power wide-area communication. By employing chirp spread spectrum modulation and configurable communication parameters such as spreading factor, bandwidth and coding rate, LoRa enables flexible trade-offs among communication range, reliability, data rate and energy consumption [5].

From a performance-characterization perspective, LoRa communication differs substantially from conventional broadband MIMO operation. LoRa links often operate under low-SNR and long-range conditions, where spreading factor, bandwidth, coding rate and channel impairments strongly affect link reliability, packet reception and achievable throughput. These characteristics provide a useful energy-constrained communication context for investigating the broader reliability–energy principles considered in this thesis and for assessing how diversity-oriented communication strategies behave under stringent link and resource constraints.

Despite their energy-efficient design, IoT and LPWAN systems remain highly sensitive to reliability–energy trade-offs. Long communication distances, low signal-to-noise ratios, retransmissions and hardware limitations may significantly affect both communication robustness and device lifetime. In particular, mechanisms that improve communication reliability often increase transmission duration and energy expenditure, while aggressive energy-saving strategies may reduce communication robustness [7].

These characteristics further highlight the importance of adaptive and energy-aware communication strategies capable of maintaining reliable operation under strict resource constraints. Such challenges are directly relevant to the analyses presented later in this thesis, particularly in the context of energy-aware communication design under realistic operating conditions.

2.4.5 Adaptive MIMO Operation and Mode Selection

Adaptive MIMO operation is motivated by the strong dependence of communication performance on channel conditions, CSI quality, reliability requirements and energy constraints [1, 15]. Under practical wireless operating conditions, fixed transmission configurations rarely provide optimal performance across all scenarios.

Adaptive communication addresses this challenge by enabling wireless systems to dynamically adjust transmission strategies according to prevailing channel and system conditions. Rather than relying on a fixed communication configuration, adaptive systems continuously evaluate relevant parameters and select transmission strategies that best satisfy the desired performance objectives. This capability enables more efficient and robust operation across diverse wireless environments [34].

In MIMO systems, adaptation may involve switching among different transmission strategies, including diversity-oriented transmission, spatial multiplexing, antenna-configuration

adaptation and cooperative communication modes. Diversity-oriented modes prioritize communication reliability and robustness, whereas multiplexing-oriented modes focus on maximizing spectral efficiency and throughput. Cooperative modes may further improve reliability and coverage under challenging propagation conditions. The most suitable transmission strategy depends strongly on channel conditions, CSI quality, reliability requirements and energy constraints [13].

The mode selection problem may generally be formulated as

$$m^* = \arg \min_{m \in \mathcal{M}} J(m), \tag{2.57}$$

where $\mathcal{M}$ denotes the set of candidate transmission modes and $J(m)$ represents a mode-dependent cost function defined according to the desired optimization objective. Depending on the considered system requirements, the cost function may directly represent quantities to be minimized, such as BER, outage probability or energy consumption. Performance objectives that are naturally maximized, such as throughput, can equivalently be incorporated through an appropriately defined decreasing cost function, for example $J(m) = -R_m$, where R_m denotes the achievable throughput of mode m. Adaptive mode selection may therefore be channel-aware, reliability-aware or energy-aware. Channel-aware adaptation exploits channel quality and propagation characteristics to improve communication performance. Reliability-aware adaptation prioritizes robust communication under uncertain channel conditions, while energy-aware adaptation explicitly accounts for transmission energy, hardware activation cost and signal-processing complexity [30].

Such adaptive frameworks enable MIMO systems to dynamically balance communication reliability, spectral efficiency, implementation complexity and energy consumption according to prevailing operating conditions. In this dissertation, this perspective is extended beyond conventional channel-aware adaptation by jointly considering communication reliability, energy consumption and implementation-related costs. Adaptive transmission is therefore treated as a decision process in which the preferred operating mode is selected according to both communication performance and resource requirements under the prevailing system conditions.

2.5 Cooperative MIMO Communications

2.5.1 Fundamentals of Cooperative Communications

Cooperative communication has emerged as an important transmission paradigm for improving wireless communication reliability, coverage and robustness under challenging operating conditions [39, 40]. Unlike conventional point-to-point communication, where data transmission occurs directly between a source and a destination, cooperative communication enables intermediate wireless nodes to assist in information delivery by participating in the transmission process.

The fundamental principle of cooperative communication is based on relay-assisted trans-

mission. Instead of relying solely on the direct communication path, additional transmission paths are established through cooperating nodes that receive, process and forward information toward the destination. These additional communication paths provide alternative routes for signal delivery and can improve communication robustness under adverse channel conditions [39].

A key advantage of cooperative communication lies in its ability to provide distributed spatial diversity. In conventional MIMO systems, spatial diversity is achieved through multiple antennas located at the transmitter, receiver or both. Cooperative communication extends the diversity principle by exploiting spatially separated wireless nodes and independently or weakly correlated propagation paths. Through relay-assisted transmission, distributed nodes can therefore create additional diversity opportunities even when individual devices have limited antenna resources. As a result, cooperative communication can improve communication reliability and coverage without requiring all antenna resources to be physically co-located [40].

This concept is illustrated in Figure 2.2, where conventional direct transmission is compared with cooperative relay-assisted communication. In the direct case, information reaches the destination through a single communication path. In the cooperative case, the destination can benefit from both the direct source–destination path and the relay-assisted source–relay–destination path, thereby exploiting additional path diversity and improving robustness under adverse channel conditions.

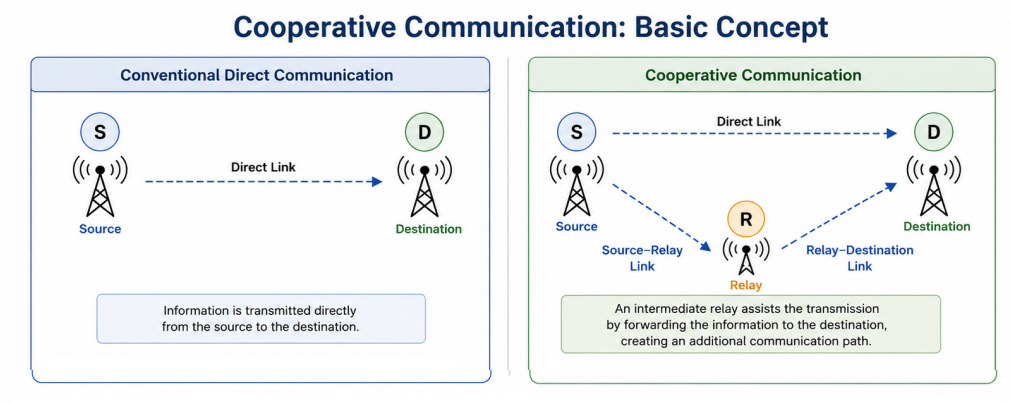


Figure 2.2. Basic concept of cooperative communication.

The motivation for cooperative communication arises from the limitations of direct wireless transmission in realistic propagation environments. Wireless links may suffer from fading, shadowing, interference and unfavorable propagation conditions, all of which may degrade communication reliability and coverage. Under such conditions, relay-assisted communication can provide additional transmission robustness and improve end-to-end communication performance [1].

These characteristics have made cooperative communication an important research area in modern wireless systems, particularly in communication scenarios where reliability, coverage enhancement and robustness under practical channel conditions are critical design objectives. Such considerations are especially relevant in cooperative MIMO systems, where relay-assisted

transmission can significantly influence performance under realistic propagation conditions and imperfect channel knowledge [39, 41].

2.5.2 Decode-and-Forward Relaying

Among the various cooperative communication protocols proposed in the literature, Decode-and-Forward (DF) relaying has attracted significant attention due to its conceptual simplicity and practical implementation characteristics [39, 41]. In DF cooperative systems, an intermediate relay node assists communication by receiving, decoding and subsequently retransmitting the detected information toward the destination.

DF relaying typically operates using a two-phase transmission protocol. During the first phase, the source transmits information simultaneously toward both the relay and the destination through the source–relay and source–destination communication links. During the second phase, the relay forwards the decoded information toward the destination, thereby providing an additional relay-assisted communication path [39].

This two-phase DF relaying operation is illustrated in Figure 2.3. In Phase 1, the source broadcasts the transmitted signal to both the relay and the destination. The relay attempts to decode the received information, while the destination simultaneously receives the direct transmission. In Phase 2, the relay forwards the decoded signal to the destination, allowing the destination to exploit both direct and relay-assisted transmissions for improved communication reliability.

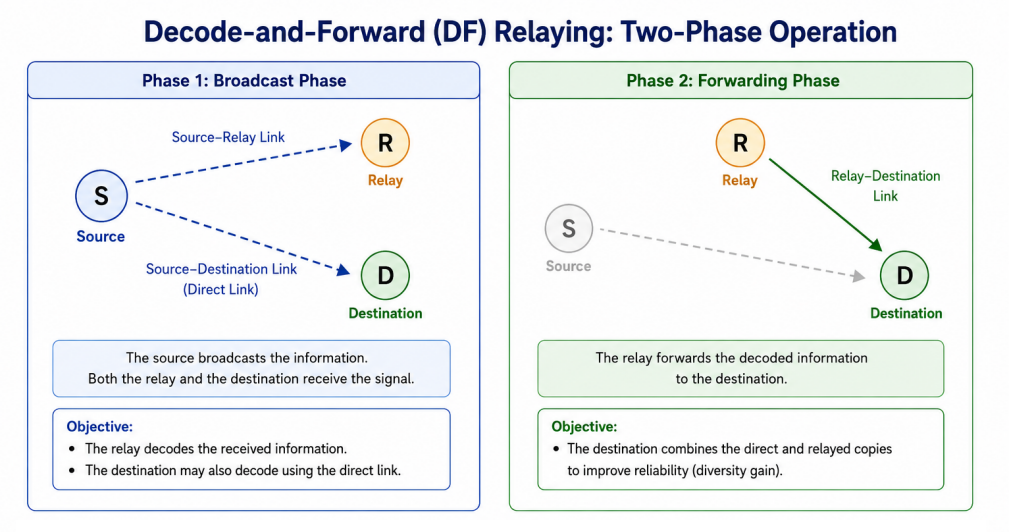


Figure 2.3. Two-phase Decode-and-Forward cooperative relaying

.

During the first phase, the source transmission is received by both the relay and the destination. The corresponding received signals can be expressed as

$$\mathbf{y}_{SR} = \mathbf{H}_{SR}\mathbf{x} + \mathbf{n}_{SR}, \tag{2.58}$$

and

$$\mathbf{y}_{SD} = \mathbf{H}_{SD}\mathbf{x} + \mathbf{n}_{SD}, \tag{2.59}$$

where $\mathbf{H}_{SR}$ and $\mathbf{H}_{SD}$ denote the source–relay and source–destination channel matrices, respectively, while $\mathbf{n}_{SR}$ and $\mathbf{n}_{SD}$ represent the corresponding additive noise vectors. The relay processes its received observation in order to recover the transmitted information, while the destination retains the direct-link observation for subsequent detection or combining.

During the second phase, provided that relay participation is enabled, the relay retransmits a regenerated version of the decoded information toward the destination. The received signal over the relay–destination link can be expressed as

$$\mathbf{y}_{RD} = \mathbf{H}_{RD}\mathbf{x}_R + \mathbf{n}_{RD}, \tag{2.60}$$

where $\mathbf{x}_R$ denotes the regenerated transmit signal produced at the relay after detection, decoding and, where applicable, re-encoding and modulation, $\mathbf{H}_{RD}$ represents the relay–destination channel matrix and $\mathbf{n}_{RD}$ denotes the corresponding additive noise vector.

The destination then combines information received from the direct source–destination path and the relay-assisted path in order to improve overall communication reliability. The main advantage of DF relaying lies in its ability to improve communication robustness by providing an additional independently faded communication path. Under favorable channel conditions, DF cooperation can significantly improve diversity gain, enhance reception reliability and extend communication coverage [40].

Despite these advantages, the effectiveness of DF relaying depends strongly on relay reliability and channel conditions. If the relay incorrectly decodes the received signal, error propagation may occur during retransmission, potentially degrading overall system performance. Furthermore, practical impairments such as imperfect channel state information and unreliable relay operation may substantially reduce the expected benefits of cooperative transmission [39].

Consequently, while DF relaying provides a powerful mechanism for enhancing communication reliability, its performance depends strongly on relay quality, channel conditions and protocol operation [39, 41].

2.5.3 Benefits and Limitations of Cooperative MIMO

Cooperative MIMO communication offers several important advantages for wireless systems operating under challenging propagation conditions. By combining direct and relay-assisted transmission paths, cooperative communication can improve communication reliability, enhance robustness against fading and provide performance gains beyond conventional direct transmission [40, 41].

One of the most important benefits of cooperative MIMO is diversity gain. Through relay-assisted transmission, the destination receives multiple independently faded versions of the transmitted signal through distinct communication paths. This additional spatial diversity re-

duces sensitivity to channel fading and improves overall signal detection reliability, particularly in adverse wireless environments [39].

Another significant advantage is coverage extension. In scenarios where direct communication between source and destination is weak or unreliable due to distance, shadowing or severe propagation loss, relay-assisted transmission can provide an alternative communication path that improves signal quality and extends effective communication range. This characteristic makes cooperative communication particularly attractive in wireless systems requiring robust coverage under non-ideal propagation conditions [41].

Despite these advantages, cooperative MIMO systems also exhibit important practical limitations. The effectiveness of cooperative transmission depends strongly on relay quality, channel conditions and protocol operation. If relay reception or decoding performance is poor, the expected cooperation gain may be significantly reduced. In particular, decoding errors at the relay may propagate through retransmission and degrade the quality of the signal received at the destination [39].

Cooperative MIMO performance is also highly sensitive to channel state information accuracy. Since cooperative transmission relies on multiple communication links, channel estimation uncertainty may affect signal detection, combining efficiency and relay operation across all transmission paths. Imperfect CSI can introduce residual interference, reduce effective diversity gain and significantly degrade overall communication performance.

For the BER-based performance comparisons considered in this thesis, the benefit of cooperative transmission relative to direct transmission can be quantified through the difference

$$G_{\text{coop}}^{(\text{BER})} = BER_{\text{direct}} - BER_{\text{coop}}, \tag{2.61}$$

where BER_{direct} and BER_{coop} denote the bit error rates achieved under direct and cooperative transmission, respectively. Under this definition, $G_{\text{coop}}^{(\text{BER})} > 0$ indicates that cooperation improves BER performance, $G_{\text{coop}}^{(\text{BER})} = 0$ indicates equivalent BER performance, and $G_{\text{coop}}^{(\text{BER})} < 0$ indicates that cooperative transmission performs worse than direct transmission.

These limitations highlight that cooperative transmission is not inherently beneficial under all operating conditions. Under unfavorable propagation, relay or CSI conditions, cooperative transmission may even underperform direct communication. The practical effectiveness of cooperative MIMO depends strongly on propagation conditions, relay reliability and CSI quality. Consequently, reliable cooperative communication often requires adaptive and reliability-aware transmission strategies capable of accounting for practical wireless impairments.

2.5.4 Practical Considerations for Cooperative Operation

Although cooperative communication has traditionally been introduced as a diversity-enhancing transmission strategy, its practical effectiveness depends on several underlying assumptions. In realistic wireless systems, cooperation involves additional communication links, relay processing and channel estimation procedures, each introducing potential performance limitations. Consequently, the overall benefit of cooperation depends not only on the availability of a relay,

but also on channel quality, CSI accuracy and relay reliability.

Relay participation also introduces additional communication and implementation costs. In half-duplex cooperative systems, relay-assisted transmission typically requires an additional transmission phase, increasing communication latency and consuming additional time–frequency resources. Relay reception, signal processing, channel estimation and retransmission may further increase energy consumption and implementation complexity. Cooperation is therefore beneficial only when the resulting reliability or coverage improvement justifies these additional costs.

An important practical consideration is consequently whether the relay should participate in every transmission. Selective or conditional relaying strategies address this issue by allowing relay activation to depend on available channel-quality or reliability information. When the source–relay link is sufficiently reliable, relay participation may provide useful additional information at the destination. Conversely, forwarding unreliable information may propagate decoding errors and reduce or even reverse the expected cooperation benefit.

A generic relay activation rule can be expressed as

$$a_R = \begin{cases} 1, & \gamma_{SR} \geq \gamma_{\text{th}}, \\ 0, & \gamma_{SR} < \gamma_{\text{th}}, \end{cases} \tag{2.62}$$

where a_R denotes the relay activation state, γ_{SR} represents a suitable source–relay link-quality metric and γ_{th} is the corresponding activation threshold.

These observations indicate that cooperative transmission should be regarded as a conditional communication strategy whose effectiveness depends on the prevailing operating conditions. Rather than assuming that relay participation is always beneficial, practical cooperative systems may employ activation or selection mechanisms that account for channel quality, CSI accuracy and relay reliability. The resulting decision of whether and when cooperation should be activated provides the theoretical basis for the adaptive cooperative communication investigations developed later in this dissertation.

2.6 Chapter Summary

This chapter established the theoretical foundations required for the analysis of MIMO communication systems under realistic and non-ideal operating conditions. The fundamental principles of MIMO transmission were introduced through the concepts of spatial diversity, spatial multiplexing, channel rank and spatial degrees of freedom, together with the inherent trade-off between reliability and spectral efficiency. Particular attention was then given to realistic wireless propagation, including large- and small-scale effects, spatial correlation and standardized channel modeling frameworks. These concepts demonstrate that the performance benefits theoretically available from multiple antennas depend strongly on the underlying propagation environment and the resulting spatial structure of the MIMO channel.

Building upon this channel perspective, the chapter examined the role of Channel State In-

formation and the consequences of imperfect channel knowledge. The distinction between the physical channel and its estimated representation is particularly important in MIMO systems, since CSI uncertainty directly affects detection, combining and other channel-dependent operations. The resulting degradation in communication reliability was further connected to packet errors, retransmission requirements and energy expenditure. This relationship highlights that reliability and energy efficiency cannot always be considered independently: transmission strategies that improve robustness may require additional hardware and processing resources, whereas less complex configurations may incur higher retransmission costs when reliability deteriorates.

These interactions provide the motivation for adaptive and cooperative communication strategies. Adaptive MIMO operation enables the transmission configuration to respond to channel conditions, CSI quality, reliability requirements and energy constraints, rather than relying on a fixed operating mode. Similarly, cooperative communication introduces additional opportunities for diversity and coverage enhancement, while also demonstrating that relay participation is beneficial only when the underlying link and CSI conditions are sufficiently reliable.

The theoretical framework developed throughout this chapter therefore provides a common basis for the investigations presented in the following chapters, where the effects of realistic propagation and imperfect CSI are examined together with cooperative and adaptive transmission strategies, with particular emphasis on communication reliability, energy efficiency and implementation-related constraints.

3 State of the Art and Research Gaps

This chapter provides a critical review of the existing literature in the main research areas related to this thesis. Its purpose is not merely to summarize prior studies, but to examine how the relevant research directions have evolved, the assumptions underlying existing approaches and the limitations that remain unresolved in the analysis of MIMO communication systems under realistic operating conditions.

As established in the preceding chapters, the performance of MIMO systems is shaped by the interaction of realistic propagation conditions, imperfect channel state information, communication reliability requirements, energy constraints and adaptive transmission mechanisms. These considerations define the broader research context of the thesis and motivate the four research directions introduced in Chapter 1. The purpose of the present chapter is therefore to examine how these directions have been addressed in the existing literature, how the corresponding research has evolved and which limitations remain relevant to the objectives of this thesis.

The literature review presented in this chapter is organized around four interconnected research directions that reflect the scientific progression of the thesis: realistic MIMO system characterization under non-ideal propagation conditions; reliability–energy trade-offs in MIMO and energy-constrained wireless communication systems; adaptive energy-aware MIMO operation; and cooperative relay-assisted MIMO communication under practical constraints.

For each research direction, the review considers the evolution of existing approaches, their underlying modeling assumptions, the performance criteria employed and the practical system constraints incorporated into the analysis. Particular attention is given to how existing studies address realistic operating conditions and to the extent to which their assumptions and methodological choices allow MIMO behavior to be interpreted across different propagation, reliability, energy, adaptive and cooperative communication scenarios.

The findings emerging from these four research directions are brought together in the final section of the chapter, where the remaining research gaps are identified and the position of this thesis with respect to the existing literature is established. In this way, the chapter provides the literature-based foundation for the characterization, reliability–energy, adaptive and cooperative communication analyses developed in the subsequent chapters.

3.1 Literature Review on Realistic MIMO System Characterization

Existing literature on MIMO system performance evaluation has progressively evolved from simplified analytical models toward increasingly realistic channel modeling and system-level characterization frameworks [11, 49, 50]. Early studies primarily relied on idealized propa-

gation assumptions, including independent and identically distributed Rayleigh fading, statistically homogeneous propagation environments and simplified antenna configurations. Such assumptions enabled tractable analysis and provided important theoretical insights into MIMO capacity, diversity gain and spatial multiplexing performance [51]. However, their ability to accurately represent practical wireless deployments remains limited, particularly when deployment-dependent propagation effects, antenna characteristics and user distributions are expected to influence system behavior.

Subsequent research introduced more advanced channel modeling frameworks incorporating large-scale and small-scale propagation effects, including path loss, shadowing, spatial correlation and multipath propagation [15]. This transition led to the adoption of geometry-based and standardized channel models, such as the Spatial Channel Model (SCM), WINNER and later the 3GPP channel modeling frameworks [20]. In particular, 3GPP TR 36.873 and TR 38.901 have become widely adopted for realistic MIMO performance evaluation, as they provide comprehensive representations of practical propagation conditions, including LOS/NLOS transitions, three-dimensional propagation effects, polarization behavior and cluster-based multipath characteristics [16, 17, 52].

In parallel, advanced system-level simulation frameworks have enabled large-scale performance evaluation under standardized channel assumptions [53]. These frameworks support the systematic analysis of key communication metrics, including signal-to-interference-plus-noise ratio (SINR), spectral efficiency and throughput across diverse deployment scenarios [52, 54]. As a result, a substantial body of literature has focused on evaluating MIMO system behavior under increasingly realistic channel and deployment conditions [55, 56]. This evolution has significantly improved the realism of MIMO performance assessment and has provided valuable insight into the behavior of wireless systems beyond idealized analytical assumptions.

This need for realistic characterization is not limited to conventional broadband cellular MIMO deployments. The same fundamental question also arises in low-power and long-range wireless links, where the achievable benefits of MIMO techniques must be examined under substantially different operating conditions. In LoRa-type and LPWAN communication scenarios, performance is strongly shaped by low received signal levels, spreading-factor-dependent operation, long-range propagation and increased sensitivity to channel impairments [6, 7, 57, 58]. Under such conditions, the practical behavior of diversity-oriented and multiplexing-oriented MIMO schemes cannot be inferred directly from conventional broadband MIMO results. Although LoRa-based systems have been widely studied in terms of coverage, connectivity and link reliability, comparatively limited attention has been devoted to the characterization of diversity-oriented and spatial-multiplexing MIMO behavior under LoRa-type operating conditions [59, 60]. In particular, the combined effects of low-SNR operation, long-range propagation and imperfect CSI on the relative performance of alternative MIMO configurations remain insufficiently explored [59, 61].

Despite these advances, important limitations remain in the existing literature. A substantial part of prior work evaluates MIMO performance under predefined deployment and

antenna assumptions, often focusing on aggregate performance metrics such as SINR, spectral efficiency and throughput [52, 54]. While such studies provide valuable performance benchmarks, they may offer limited insight into the deployment-dependent mechanisms responsible for the observed behavior. Recent findings indicate that factors such as antenna configuration, polarization characteristics and heterogeneous user distributions can substantially affect practical MIMO performance [62–64]. However, these effects are not always systematically isolated and interpreted in conventional system-level performance evaluations.

Recent studies increasingly acknowledge that deployment-related structural characteristics may significantly influence MIMO performance [62,65–68]. Factors such as antenna geometry, antenna spacing, polarization behavior and user distribution directly affect channel correlation, spatial diversity and effective channel rank, thereby influencing achievable SINR, spectral efficiency, throughput and multiplexing capability [56,63,69,70]. However, while these factors have been individually investigated in different contexts, their role is often examined under specific configurations or performance objectives. Consequently, limited attention has been devoted to systematically characterizing how multiple deployment-related factors jointly shape MIMO behavior under realistic propagation conditions. In particular, the combined influence of antenna geometry, polarization behavior, propagation asymmetry and heterogeneous user distribution remains insufficiently characterized.

This limitation directly motivates the first research direction of this thesis. Rather than treating deployment-related structural characteristics primarily as fixed modeling assumptions, the present work examines their influence explicitly under realistic propagation conditions, with particular emphasis on antenna geometry, polarization behavior, propagation asymmetry and user distribution. Using standardized 3GPP-based channel models and advanced system-level simulation frameworks [52, 56, 62], the analysis investigates how these factors affect channel and system behavior across heterogeneous operating conditions. The objective is therefore not only to quantify conventional performance metrics, but also to identify and interpret the mechanisms through which realistic structural and propagation characteristics shape MIMO performance under realistic operating conditions. In this way, the first research direction establishes the characterization foundation required for the subsequent reliability–energy, adaptive operation and cooperative communication analyses developed throughout the thesis.

The characterization perspective developed in this research direction also highlights that system behavior cannot be assessed independently of reliability and resource constraints. This becomes particularly important in energy-constrained communication environments, where propagation conditions and link impairments directly influence packet delivery, retransmission requirements and energy expenditure. These considerations provide the transition to the following research direction, which examines reliability–energy trade-offs in MIMO and energy-constrained wireless communication systems.

3.2 Literature Review on Reliability–Energy Trade-offs in MIMO and Energy-Constrained Wireless Systems

Reliability–energy trade-offs in wireless communications can be approached from multiple perspectives depending on system architecture, performance objectives and operating constraints [30, 32, 71]. Within the broader literature on reliability–energy trade-offs, three research directions are particularly relevant to the scope of this thesis: retransmission-aware energy modeling [72], energy-efficient MIMO communication design [32, 69] and energy-aware communication strategies for energy-constrained wireless systems such as IoT and LPWAN networks [6, 7, 57].

Early research on wireless energy efficiency established that minimizing transmission power alone does not necessarily minimize the total energy required for communication [32, 73, 74]. In particular, studies incorporating both transmission and circuit energy demonstrated that the relative contribution of these components depends strongly on transmission parameters and operating conditions [31, 73, 74]. Subsequent work further formalized energy-efficiency optimization by jointly considering achievable communication performance, resource-allocation requirements and practical power consumption, including transmit-independent circuit power [30, 31, 71, 75]. Together, these studies provide a fundamental theoretical basis for more comprehensive energy models that account for implementation-related costs beyond radiated transmission energy.

Subsequent research extended this perspective by developing more comprehensive energy models that incorporate retransmission behavior, practical propagation conditions and implementation-related energy costs [30, 72, 76]. Under such models, energy efficiency depends not only on the energy expended during an individual transmission attempt, but also on the probability of successful packet delivery and the additional resources required when transmission fails [72]. At the same time, hardware activation, circuit power consumption and signal-processing requirements introduce energy costs that may remain significant even when radiated transmission power is relatively low [69, 77]. These considerations broadened energy-efficiency analysis from transmission-oriented optimization toward a more complete evaluation of the energy required for reliable communication.

A substantial body of literature has also focused on energy-efficient MIMO communication design, where multiple transmission strategies introduce additional performance and energy trade-offs [32, 69, 77]. Existing studies have investigated the energy-efficiency implications of diversity-oriented transmission, spatial multiplexing and adaptive antenna configurations, showing that MIMO techniques can improve communication reliability, throughput and spectral efficiency under different operating conditions [76, 78–80]. However, the resulting energy-performance trade-offs remain highly dependent on system configuration, channel conditions and implementation assumptions.

More recent studies increasingly recognize that practical MIMO energy-efficiency analysis must account for implementation-related costs in addition to radiated transmission energy,

including hardware activation, circuit power consumption and signal-processing complexity [69, 76, 81]. This consideration is particularly important for diversity-oriented transmission, where activating additional antennas or employing more complex processing may improve communication reliability and reduce retransmission requirements, while simultaneously increasing the energy consumed per transmission attempt [32, 72, 82, 83]. Consequently, the MIMO configuration providing the highest reliability does not necessarily provide the highest practical energy efficiency, especially when the additional energy cost of hardware and processing becomes significant [77].

Beyond conventional MIMO systems, similar reliability–energy trade-offs have also attracted significant attention in energy-constrained wireless systems, particularly in IoT and LPWAN networks [6, 7]. Existing studies have shown that limited power budgets, long device lifetime requirements and strict energy-efficiency constraints make communication reliability and energy consumption strongly interconnected in such environments [84, 85]. Among LPWAN technologies, LoRa has emerged as an important platform for studying these trade-offs, with existing literature highlighting the strong coupling between communication reliability, transmission duration and energy consumption through parameters such as spreading factor, bandwidth and coding rate [57, 58, 86, 87]. These trade-offs become even more challenging under long communication distances, low received signal levels and practical channel impairments [59, 61, 88].

Despite significant progress in energy-efficient wireless communication design, important limitations remain in the existing literature. Existing studies have extensively investigated individual aspects of the reliability–energy relationship, including retransmission behavior, propagation conditions, hardware-related energy overhead and practical channel impairments [30, 76, 85, 86]. However, these factors are frequently examined within different system models, communication scenarios or optimization objectives, making their combined influence on practical energy efficiency more difficult to characterize. Consequently, the joint interaction among realistic propagation conditions, communication reliability, retransmission behavior, implementation-related energy costs and channel impairments remains insufficiently characterized, particularly across MIMO and energy-constrained wireless communication environments [59, 69, 77].

This limitation directly motivates the second research direction of this thesis. The present work contributes to addressing this gap through a systematic investigation of reliability–energy trade-offs in MIMO systems under realistic and non-ideal operating conditions, jointly considering propagation behavior, communication reliability, retransmission cost and implementation-related energy expenditure. Particular emphasis is placed on identifying the operating conditions under which improved communication reliability enhances energy efficiency, as well as conditions where additional reliability gains may introduce disproportionate energy cost or even reduce overall energy efficiency. The analysis is further extended to energy-constrained IoT and LPWAN communication environments, with particular emphasis on LoRa-based systems under practical channel impairments. Through this perspective, the thesis examines how

communication reliability and practical energy efficiency interact across different wireless operating conditions and system configurations.

3.3 Literature Review on Adaptive Energy-Aware MIMO Operation

The strong dependence of MIMO performance on channel conditions, propagation characteristics, CSI quality and system requirements has motivated extensive research on adaptive transmission strategies capable of adjusting system operation to changing wireless conditions [1, 89]. Rather than relying on a fixed transmission configuration, adaptive MIMO approaches seek to exploit variations in channel and system conditions by dynamically selecting transmission parameters or operating modes according to the desired performance objectives. As energy consumption has become an increasingly important design constraint, particularly in systems employing multiple active antennas and RF chains, adaptive MIMO research has progressively expanded beyond conventional channel-aware adaptation to incorporate energy-efficiency and reliability considerations [69, 78]. Within this broader perspective, adaptive operation provides a mechanism for balancing communication performance, reliability and energy expenditure according to prevailing operating conditions.

Building on this motivation, a substantial body of research has investigated adaptive MIMO mechanisms for dynamically adjusting system operation according to changing channel and system conditions [89–91]. Existing approaches include antenna-selection strategies, adaptive diversity and multiplexing configurations, RF-chain activation policies and energy-aware transmission mechanisms [78, 92–94]. Through such mechanisms, MIMO systems can adapt the number of active antennas, transmission configuration or resource utilization according to prevailing operating conditions and performance requirements. Existing studies have demonstrated that adaptive operation can provide significant performance and energy-efficiency benefits compared with fixed transmission configurations, although the resulting gains depend strongly on the adopted adaptation criterion, channel conditions and system constraints [78, 89, 92, 93].

Despite these advances, important limitations remain in the existing literature. Many adaptive MIMO approaches are formulated around specific optimization objectives, such as throughput, communication reliability or energy efficiency, with transmission decisions optimized according to the corresponding performance criterion [89, 90, 95]. While such approaches provide valuable insight into the performance benefits of adaptive transmission, their primary emphasis is typically placed on identifying the preferred transmission strategy or optimizing a target performance metric under given operating conditions. Comparatively less attention has been devoted to characterizing how the resulting adaptive decisions evolve across broader operating conditions, particularly when realistic propagation variability, CSI uncertainty and practical implementation constraints are jointly considered [90, 91, 96].

This challenge becomes particularly important in MIMO systems, where adaptive trans-

mission decisions depend on the interaction among communication reliability, retransmission behavior, hardware activation cost, signal-processing complexity and CSI quality [76, 90, 96]. Higher-order diversity configurations may improve communication robustness and reduce the likelihood of unsuccessful packet delivery under challenging channel conditions, but these benefits may require additional active RF chains, hardware resources and signal-processing effort [77, 78]. Conversely, simpler transmission configurations may provide greater energy efficiency when channel conditions are sufficiently favorable and additional diversity resources offer limited reliability benefit. Consequently, the energy-efficient transmission mode may vary across operating conditions as the relative contributions of reliability, retransmission cost and implementation-related energy expenditure change. CSI uncertainty further complicates this decision process by affecting the estimated performance and reliability of candidate transmission configurations [96, 97].

More specifically, the structural behavior of adaptive MIMO policies across broader operating conditions remains less extensively characterized. Existing studies have investigated mode-switching strategies, switching thresholds and operating regions for specific MIMO configurations and performance objectives, including adaptation between diversity and spatial-multiplexing modes [98, 99]. Such approaches provide valuable insight into when particular transmission modes become preferable under changing channel conditions. However, comparatively limited attention has been devoted to systematically characterizing the broader structure of energy-aware MIMO selection policies when reliability, retransmission cost, implementation-related energy expenditure and CSI uncertainty jointly influence the selection decision. In particular, the organization of energy-aware operating regions across multiple candidate MIMO configurations, the transition relationships between neighboring modes and the stability of the resulting selection policy under imperfect CSI remain insufficiently explored.

This limitation directly motivates the third research direction of this thesis. The present work develops an adaptive energy-aware MIMO framework for operation under realistic propagation conditions and imperfect CSI. The proposed framework dynamically selects the energy-efficient transmission configuration by jointly accounting for communication reliability, retransmission burden, hardware-related energy cost and signal-processing complexity. Beyond identifying the preferred transmission mode, the analysis examines the structure of adaptive operating behavior through operating-region characterization, transition analysis and stability evaluation across different operating conditions and CSI uncertainty levels. In this way, adaptive mode selection is considered not only as an optimization problem, but also as a structured operating policy whose organization, transitions and stability provide additional insight into energy-aware MIMO operation.

3.4 Literature Review on Cooperative MIMO Communications under Realistic Operating Conditions

The preceding research directions in this thesis progressively move from understanding MIMO behavior under realistic propagation conditions to examining the reliability–energy trade-offs that emerge from this behavior and the adaptive mechanisms that can respond to changing operating conditions. Together, these perspectives highlight that MIMO design involves not only characterizing system performance, but also determining how available transmission resources should be employed as channel conditions, reliability requirements and implementation constraints change. A further dimension of this problem arises when the available transmission resources are extended beyond the source and destination themselves. Cooperative communication introduces additional nodes into the transmission process, creating new opportunities for spatial diversity and reliability enhancement, while also making system performance dependent on the quality and operation of the cooperative links [39, 41].

Within cooperative MIMO architectures, spatially distributed nodes can coordinate their transmissions to provide the destination with multiple signal observations without requiring all antenna elements to be physically collocated [100, 101]. Relay-assisted transmission represents one of the principal mechanisms for realizing such cooperation, whereby an intermediate node receives information from the source and assists its delivery to the destination through an additional communication path. This distributed use of spatial resources can provide diversity benefits and improve communication robustness, particularly when the direct source–destination link is affected by unfavorable propagation conditions [39, 41].

Among the various relay-assisted communication strategies investigated in the literature, Decode-and-Forward (DF) relaying has received significant attention as a practical approach for exploiting distributed spatial diversity [39, 102]. In DF systems, successful relay decoding enables the destination to exploit an additional independently faded communication path, which can improve reception robustness, extend coverage and enhance link reliability under favorable operating conditions [39, 103]. These potential benefits have motivated extensive investigation of DF cooperation, particularly in scenarios where the direct source–destination link is affected by fading, path loss or limited coverage.

More recent research has extended cooperative communication concepts toward collaborative and virtual MIMO architectures, in which nearby terminals or spatially distributed nodes cooperate to emulate larger antenna arrays and exploit distributed spatial resources [104, 105]. Such architectures have attracted increasing attention in next-generation wireless systems due to their potential to enhance spatial diversity, coverage and spectral efficiency [106, 107]. Much of this literature focuses on the performance gains achievable through cooperation and on the design mechanisms required to realize these gains. Comparatively less emphasis has been placed on characterizing the operating conditions under which the expected benefits of cooperation may diminish or, under sufficiently unfavorable conditions, give rise to performance degradation.

Despite these advantages, important limitations remain in the existing literature. Several cooperative relaying studies evaluate the potential benefits of relay-assisted transmission under idealized or favorable channel-knowledge assumptions, including perfect CSI at the relay and/or destination [108–110]. While such assumptions facilitate the analysis of cooperative diversity gains and provide valuable insight into the performance potential of relay-assisted transmission, they may not fully capture the behavior of cooperative systems when channel estimation uncertainty becomes significant. Moreover, practical DF operation introduces an additional dependency on successful relay decoding, since decoding errors at the relay may affect the signal subsequently forwarded to the destination [92]. Consequently, the performance benefits associated with cooperation under ideal or favorable operating assumptions cannot necessarily be assumed to persist when channel estimation uncertainty and relay decoding imperfections are taken into account.

Under realistic operating conditions, however, cooperative transmission introduces additional system complexity and new sources of uncertainty. In particular, channel estimation errors may significantly degrade cooperative communication performance, while unreliable relay decoding may introduce error propagation through the relay-assisted communication path [103, 111, 112]. These impairments can substantially reduce the performance gains expected from cooperative transmission, particularly when channel uncertainty affects both signal detection and relay operation. Consequently, the effectiveness of cooperative communication becomes strongly dependent on the prevailing operating conditions, including channel quality, relay decoding reliability and CSI accuracy.

Although imperfect CSI, relay decoding errors and selective relay operation have been investigated in cooperative communication systems [103, 111, 113], comparatively less attention has been devoted to characterizing their combined effect on the relative performance of cooperative and direct MIMO transmission. Existing studies provide important insight into performance degradation caused by channel estimation uncertainty and relay error propagation, as well as mechanisms for limiting unreliable relay participation. However, the SNR-dependent operating conditions under which the combined influence of CSI uncertainty and imperfect relay decoding eliminates the expected cooperation gain are less extensively characterized. In particular, the transition from beneficial to detrimental cooperation, where relay-assisted MIMO transmission underperforms the corresponding direct MIMO link, remains insufficiently explored when CSI uncertainty and relay decoding reliability are jointly considered.

This limitation directly motivates the fourth research direction of this thesis. The present work investigates cooperative relay-assisted MIMO systems under realistic operating conditions, with particular emphasis on imperfect CSI and relay decoding reliability. The analysis identifies harmful cooperation operating regions in which cooperative transmission underperforms direct MIMO communication under the combined influence of channel uncertainty and relay error propagation. To address this behavior, a reliability-aware relay activation mechanism is developed, enabling adaptive relay participation according to prevailing communica-

tion conditions and reducing performance degradation associated with harmful cooperation. In this way, the cooperative communication analysis extends the characterization-driven and operating-condition-aware perspective of the thesis to relay-assisted MIMO operation under practical wireless impairments.

3.5 Research Gaps and Thesis Positioning

The literature reviewed in the preceding sections demonstrates the significant progress achieved in MIMO communications over the past decades. Extensive research has established the theoretical foundations of diversity, spatial multiplexing, adaptive transmission and cooperative communication, while increasingly realistic channel models and system-level simulation frameworks have improved the ability to evaluate wireless systems under representative operating conditions. Nevertheless, the reviewed literature also reveals that important aspects of MIMO behavior remain incompletely understood, particularly when realistic propagation conditions, imperfect channel state information, communication reliability, energy consumption and implementation constraints are considered from an integrated system perspective.

The first major research gap concerns the realistic characterization of MIMO system behavior under non-ideal wireless propagation conditions. Although standardized channel models and advanced simulation platforms have significantly improved the realism of performance evaluation, the combined system-level influence of deployment-dependent factors such as antenna geometry, polarization characteristics, propagation asymmetries and non-uniform user distributions remains less systematically characterized. In particular, existing studies often evaluate MIMO performance under realistic channel models without explicitly examining and interpreting how the interaction among these deployment-dependent factors shapes key performance metrics such as SINR, spectral efficiency and throughput. As a result, important limitations remain in understanding how deployment-dependent structural characteristics shape MIMO system behavior under realistic propagation conditions.

The second major research gap concerns the interaction between communication reliability and energy efficiency in wireless systems. While reliability enhancement and energy-efficient communication have both received substantial research attention, retransmission behavior, hardware-related energy overhead, signal-processing complexity and realistic channel impairments are frequently examined within different system models, communication scenarios or optimization objectives. Consequently, their combined influence on practical reliability–energy behavior remains insufficiently characterized across heterogeneous operating conditions, providing limited insight into the conditions under which higher-order diversity schemes offer meaningful energy benefits and those under which simpler transmission configurations remain more energy-efficient. These challenges become even more critical in energy-constrained IoT and LPWAN environments, where communication reliability and energy consumption are tightly coupled under strict resource limitations and practical channel impairments.

The third major research gap concerns adaptive MIMO operation under realistic system

constraints. Although adaptive transmission strategies have been widely investigated as an effective mechanism for improving communication performance, much of the existing literature formulates adaptation around specific performance objectives, such as throughput, reliability, spectral efficiency or energy efficiency, and evaluates the resulting transmission decisions under predefined system and operating assumptions. Comparatively limited attention has been devoted to adaptive frameworks that explicitly account for retransmission-aware operation, hardware-related implementation cost, processing complexity and imperfect CSI within a unified decision process. Furthermore, the structural behavior of adaptive mode-selection decisions, including operating-region formation, transition behavior between neighboring transmission modes and stability under CSI uncertainty, remains insufficiently characterized. This limits the understanding of adaptive operation not only as an optimization outcome, but also as an interpretable and structured system behavior under realistic wireless conditions.

The fourth major research gap concerns cooperative MIMO communication under practical operating conditions. Cooperative transmission has been extensively studied as a mechanism for improving communication reliability, extending coverage and exploiting distributed spatial diversity. At the same time, prior research has demonstrated that imperfect CSI, relay decoding errors and unreliable relay participation can degrade cooperative performance, while selective relaying mechanisms have been developed to limit the impact of unreliable cooperation. However, comparatively less attention has been devoted to characterizing the relative performance of cooperative and direct MIMO transmission when CSI uncertainty and relay decoding reliability are jointly considered. In particular, the SNR-dependent transition from beneficial to detrimental cooperation under different levels of CSI uncertainty and relay decoding reliability, where relay-assisted transmission underperforms the corresponding direct MIMO link, remains insufficiently characterized.

Although the four research gaps concern different aspects of MIMO communication, they share a common underlying challenge: understanding how system behavior changes when realistic propagation conditions, reliability requirements, energy constraints, channel uncertainty and available transmission resources are considered explicitly. Across the reviewed literature, these aspects are typically addressed within different research frameworks and according to different system objectives. This creates a need for a more coherent perspective that connects realistic system characterization with reliability–energy behavior, adaptive transmission decisions and the performance of cooperative communication under practical impairments.

This thesis is positioned at the intersection of these research gaps. Rather than addressing realistic propagation, energy efficiency, adaptive operation and cooperative communication as independent problems, the thesis adopts a characterization-driven perspective in which system behavior is first analyzed under realistic operating conditions and then used to guide optimization and adaptive transmission design. In this sense, realistic system characterization is not treated merely as a performance evaluation tool, but as the foundation for identifying performance-limiting mechanisms, interpreting reliability–energy trade-offs and developing robust transmission strategies under the considered wireless impairments.

More specifically, the thesis addresses the identified gaps through four complementary research directions: realistic MIMO system characterization under standardized 3GPP channel models and realistic deployment conditions, systematic analysis of reliability–energy trade-offs under retransmission-aware and implementation-aware assumptions, adaptive energy-aware MIMO framework design with operating-region, transition and stability characterization and cooperative relay-assisted MIMO analysis under imperfect CSI and relay reliability limitations.

Overall, the literature review highlights the importance of understanding MIMO system behavior across realistic and varying operating conditions rather than considering individual performance aspects in isolation. Building on the identified research gaps, this thesis establishes a unified characterization-driven framework that connects realistic system behavior with reliability–energy analysis, adaptive transmission decisions and cooperative communication under the considered non-ideal conditions. This framework provides the common methodological perspective through which the research developed in the subsequent chapters is organized and interpreted.

4 MIMO Performance Characterization Under Realistic Wireless Conditions

The preceding chapters established that the performance of MIMO communication systems depends strongly on both the characteristics of the wireless environment and the operating conditions under which communication takes place. While idealized channel assumptions provide valuable theoretical insight into the potential gains of MIMO systems, wireless systems operate under non-ideal conditions where propagation asymmetries, channel uncertainty and system-level constraints may significantly alter achievable performance. In particular, factors such as antenna geometry, polarization behavior, user distribution, operating signal-to-noise ratio and channel state information quality directly influence the effective structure of the MIMO channel and consequently affect key communication metrics, including signal-to-interference-plus-noise ratio (SINR), spectral efficiency, throughput and communication reliability [1, 15].

Within the broader context of this thesis, the characterization of MIMO behavior under realistic conditions constitutes a necessary foundation for the optimization-oriented analyses presented in the subsequent chapters. Before investigating energy-efficiency trade-offs, adaptive transmission mechanisms and cooperative communication strategies, it is first essential to understand how realistic wireless conditions influence the achievable gains and limitations of MIMO systems. This characterization stage therefore addresses the first central research question of the thesis: how MIMO systems behave under realistic wireless operating conditions.

To provide a comprehensive characterization framework, this chapter examines MIMO system performance through two complementary analysis dimensions. The first dimension focuses on propagation-driven characterization in conventional broadband wireless systems, where realistic deployment conditions introduce spatial asymmetries, heterogeneous user distributions and environment-dependent propagation effects. The second dimension focuses on constraint-driven characterization in low-power wireless communication systems, where low-SNR operation, limited energy resources and channel uncertainty impose strict constraints on the feasibility of MIMO techniques. Together, these two perspectives provide a broader understanding of MIMO behavior across fundamentally different wireless operating regimes.

The first part of this chapter investigates MIMO performance under realistic propagation conditions using standardized 3GPP channel models and the Vienna System-Level Simulator [17, 49]. A structured system-level simulation framework is employed to evaluate the impact of deployment parameters, including transmit power, carrier frequency, propagation K-factor, antenna polarization, MIMO antenna configuration, user mobility, user density and cell size. Particular emphasis is placed on understanding how realistic propagation asymmetries influence system-level performance metrics such as SINR, spectral efficiency and throughput.

The second part of this chapter extends the characterization analysis to low-power communication environments inspired by LoRa-type operating conditions, providing a highly

constrained scenario in which the behavior of MIMO transmission strategies can be investigated. In this context, the analysis focuses on diversity-oriented and multiplexing-oriented MIMO schemes under low-SNR conditions and imperfect channel state information. Particular emphasis is placed on identifying the operating conditions under which the use of multiple-antenna techniques can provide performance benefits in communication scenarios characterized by strict power constraints, demanding reliability requirements and increased sensitivity to channel uncertainty.

Beyond quantifying performance variations, this chapter examines the mechanisms through which wireless propagation characteristics and implementation-related operating constraints affect MIMO system behavior. Particular emphasis is placed on understanding how channel conditions, environmental characteristics and system limitations jointly determine the achievable benefits of MIMO techniques. The findings presented in this chapter establish the characterization foundation for the subsequent analyses developed throughout the thesis, where reliability–energy trade-offs, adaptive transmission strategies and cooperative communication mechanisms are systematically investigated under increasingly complex operating conditions.

4.1 Broadband MIMO Characterization Under Realistic Propagation Conditions

4.1.1 Broadband MIMO Simulation Framework

This subsection presents the simulation scenario and the main system assumptions adopted for the propagation-driven characterization of broadband MIMO systems under realistic wireless conditions. The selected configuration is designed to provide a representative urban deployment environment while enabling systematic investigation of deployment-dependent factors that influence MIMO system performance. The main simulation parameters used throughout this chapter are summarized in Table 4.1.

The analysis is performed using the Vienna LTE-A Downlink System-Level Simulator v2.0 (Q3), a widely adopted MATLAB-based platform for realistic system-level evaluation of cellular MIMO networks [48, 53]. The system-level implementation is particularly suitable for this part of the analysis, as it enables accurate modeling of propagation-dependent behavior, inter-cell interference and user distribution effects under realistic deployment conditions.

The simulation setup follows the standardized 3GPP Urban Microcell (UMi) Street Canyon deployment scenario, which provides a realistic representation of dense urban wireless environments characterized by strong propagation variability, heterogeneous user placement and complex line-of-sight (LOS) and non-line-of-sight (NLOS) transitions [16, 17]. Such environments are particularly suitable for studying broadband MIMO behavior, since system performance becomes highly sensitive to propagation asymmetries, spatial channel characteristics and user distribution.

The considered wireless environment operates at a carrier frequency of 28 GHz with a

Table 4.1. Main simulation parameters used for broadband MIMO characterization under realistic propagation conditions.

Parameter	Value
General Simulation Parameters	
Simulation Platform	Vienna LTE-A SLS v2.0 (Q3 2018)
Deployment Scenario	3GPP UMi Street Canyon
Carrier Frequency	28 GHz
Bandwidth	10 MHz
Subcarrier Spacing	60 kHz
Simulation Duration	10 TTIs
TTI Duration	1 ms
Transmit Power	47 dBm
Polarization Configuration	Single / Dual
Indoor User Percentage	80%
User Density	2500 users/km^2
Users per Cell	75
UMi Deployment Parameters	
BS Height	10 m
UE Height	1.5 m
Building Floor Height	3 m
Baseline User Velocity	0 m/s
MIMO Configuration	
BS Antennas	4
UE Antennas	2

system bandwidth of 10 MHz. The choice of millimeter-wave operation introduces more challenging propagation conditions compared to conventional sub-6 GHz systems, including increased path loss, stronger blockage sensitivity and higher dependence on LOS conditions. These characteristics make the considered scenario particularly relevant for investigating realistic propagation effects and their impact on MIMO system performance [45].

A multi-user downlink communication scenario is considered throughout the analysis. The baseline MIMO configuration consists of four transmit antennas at the base station and two receive antennas at the user equipment, corresponding to a 4×2 MIMO system. This configuration provides a suitable balance between spatial diversity and spatial multiplexing capability, enabling meaningful evaluation of MIMO performance under realistic deployment conditions. In addition, both single-polarized and dual-polarized antenna configurations are examined in order to systematically analyze the influence of polarization behavior on system-level performance.

User deployment follows a heterogeneous spatial distribution including both indoor and outdoor users. In particular, 80% of users are assumed to be located indoors, while the remaining users are placed outdoors. This assumption reflects realistic urban deployment conditions, where indoor users typically constitute a significant portion of total network traffic. More importantly, such heterogeneous user placement introduces propagation asymmetries due to differences in penetration loss, blockage conditions and effective channel quality, making it particularly relevant for the objectives of this chapter.

The considered user density is 2500 users/km^2, corresponding to approximately 75 users per cell. This configuration enables realistic modeling of multi-user communication conditions, including inter-user variability and resource-allocation effects. Additional deployment parameters, including antenna height, user height, mobility assumptions and cell dimensions, are selected according to the standardized 3GPP scenario configuration.

Performance Evaluation Metrics

The performance analysis presented in this chapter is based on three key system-level performance metrics: signal-to-interference-plus-noise ratio (SINR), spectral efficiency and throughput. These metrics are selected because they provide complementary insight into MIMO system behavior under realistic wireless propagation conditions and enable quantitative evaluation of deployment-dependent performance variations [1, 15].

The signal-to-interference-plus-noise ratio (SINR) is used as the primary indicator of received signal quality, reflecting the combined impact of useful signal power, interference and noise. In the considered multi-cell wireless environment, SINR is strongly influenced by large-scale and small-scale propagation effects, antenna geometry, spatial channel characteristics, polarization configuration and inter-cell interference. As a result, it provides a direct indicator of how deployment-dependent asymmetries affect link quality and overall communication performance. SINR is defined as

$$\mathrm{SINR} = \frac{P_{\mathrm{signal}}}{P_{\mathrm{interference}} + P_{\mathrm{noise}}} \tag{4.1}$$

where P_{signal} denotes the received signal power, $P_{\mathrm{interference}}$ represents the total interference power and P_{noise} is the noise power. Within the employed LTE-A system-level simulation framework, link quality is evaluated from post-equalization SINR values, with effective SINR processing performed through Mutual Information Effective SINR Mapping (MIESM).

Spectral efficiency is used to evaluate how efficiently the available spectral resources are utilized under different deployment conditions. It reflects the amount of information that can be successfully supported per unit bandwidth and therefore serves as a key indicator of communication efficiency. In the employed LTE-A system-level simulation framework, spectral efficiency is evaluated within the link-to-system abstraction of the simulator rather than directly through the idealized Shannon capacity expression. Post-equalization SINR values are mapped to effective link quality through MIESM, while channel-quality information is derived using link-level BLER curves and the corresponding CQI mapping. Consequently, the

resulting spectral-efficiency values reflect the transmission and link-adaptation mechanisms represented within the LTE-A simulation framework, providing a system-level measure of spectral utilization under different propagation and deployment conditions.

Throughput represents the effective data rate successfully delivered to users and serves as a system-level performance metric in this chapter. Unlike SINR and spectral efficiency, which primarily characterize signal quality and spectral utilization, throughput reflects the effective communication performance achieved by the simulated users. Within the LTE-A system-level framework, the resulting user throughput incorporates the effects of link quality, resource allocation, scheduling and transmission success, thereby capturing how physical-layer channel conditions translate into effective delivered data rates. This makes throughput an effective indicator of overall system performance under realistic deployment conditions.

Together, these metrics provide a comprehensive framework for evaluating MIMO system behavior. More specifically, SINR reflects physical-layer communication quality, spectral efficiency captures spectral utilization and throughput represents effective user-level performance. Their combined analysis enables systematic investigation of how antenna geometry, polarization characteristics and user-distribution asymmetries influence MIMO performance under realistic wireless propagation conditions.

4.1.2 Initial Sensitivity Analysis of Key System and Channel Parameters

Before investigating the impact of deployment-dependent factors such as antenna geometry, polarization characteristics and user-distribution asymmetries on MIMO system performance, the sensitivity of the adopted simulation framework is first examined through controlled variations of fundamental system and propagation parameters. The objective of this section is to assess how the considered simulation environment responds to variations in parameters with well-established physical significance and to establish a baseline for interpreting the more detailed characterization analyses that follow.

Three key parameters are considered: transmit power, carrier frequency and propagation K-factor. These parameters are selected because they capture distinct aspects of system and propagation behavior that directly influence MIMO performance. Transmit power determines the available signal level, carrier frequency affects propagation characteristics, while the K-factor controls the relative contribution of deterministic and scattered channel components. Their impact is evaluated using the system-level performance metrics introduced in the previous section, namely signal-to-interference-plus-noise ratio (SINR), spectral efficiency and throughput.

Impact of Transmit Power

Transmit power directly affects the received signal level and therefore represents a fundamental system parameter influencing wireless communication performance [1]. Increasing transmit power generally improves the received signal strength; however, in a multi-cell environment, the resulting SINR improvement also depends on the corresponding interference

conditions.

From a theoretical perspective, higher transmit power is generally expected to provide greater benefit when system performance is limited by noise or insufficient received signal strength. In interference-limited conditions, however, increasing transmit power may provide smaller SINR gains because the interference generated by neighboring cells may increase simultaneously. The resulting impact on spectral efficiency and throughput therefore depends not only on received signal strength, but also on interference conditions and the link-adaptation and resource-allocation mechanisms represented by the system-level simulator.

The simulation results shown in Figure 4.1 and Figure 4.2 illustrate that the impact of transmit power is not uniform across the considered performance metrics. For average UE throughput, the CDFs exhibit substantial overlap and crossing, while the 10 W configuration shows a more favorable distribution over a considerable part of the user population. Increasing the transmit power to 30 W and 50 W therefore does not result in a systematic improvement in average UE throughput.

A similar behavior is observed for spectral efficiency. Although higher transmit power can improve spectral utilization, the distributions are not uniformly ordered across the entire range. The substantial overlap and crossing of the CDF curves indicate that increasing transmit power does not produce a uniform improvement in spectral efficiency under the considered multi-cell operating conditions.

Overall, the results confirm the expected sensitivity of system performance to transmit power, while also showing that the resulting gains are not uniform across the simulated user population. The substantial overlap between the higher-power configurations indicates that increasing transmit power does not produce proportional improvements in spectral efficiency and throughput across all operating conditions. These observations are consistent with the expected behavior of a multi-cell system-level environment, where performance is jointly determined by received signal strength, interference conditions and the underlying link-adaptation and resource-allocation mechanisms.

Impact of Carrier Frequency

Carrier frequency is an important parameter in wireless communication systems because propagation characteristics and path loss generally exhibit frequency-dependent behavior [1, 45]. Consequently, variations in carrier frequency can modify the propagation conditions experienced by wireless links and influence the resulting system-level performance.

From a theoretical perspective, increasing carrier frequency can lead to increased propagation loss under otherwise comparable conditions. In realistic multi-cell environments, however, the resulting system-level performance is not determined by frequency-dependent path loss alone. User location, propagation geometry, interference conditions and the frequency-dependent characteristics incorporated into the adopted channel model jointly determine the effective link conditions experienced by individual users.

The simulation results shown in Figure 4.3 and Figure 4.4 illustrate this behavior. Variations

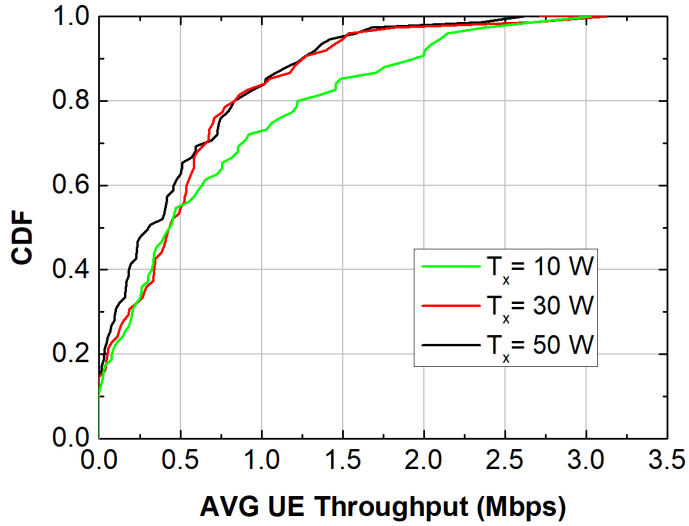


Figure 4.1. Impact of transmit power on average UE throughput.

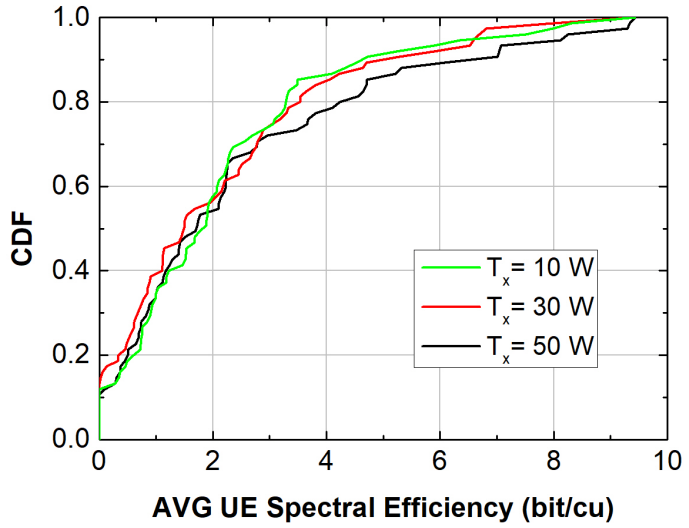


Figure 4.2. Impact of transmit power on average UE spectral efficiency.

in carrier frequency modify both the throughput and spectral-efficiency distributions, but the three configurations exhibit substantial overlap and repeated crossings across the user population. Therefore, increasing the carrier frequency from 2.4 to 3.5 and 5.8 GHz does not result in a uniform degradation of system performance across all simulated users.

A similar behavior is observed for spectral efficiency, where differences among the three carrier-frequency configurations depend on the considered region of the CDF rather than following a strictly monotonic ordering. These results indicate that, within the examined frequency range and simulation conditions, the influence of carrier frequency is strongly dependent on the overall propagation and interference environment experienced by each user.

Overall, the results confirm that the simulation framework responds to variations in carrier

frequency while demonstrating that their system-level impact cannot be interpreted solely through the expected increase in propagation loss with frequency. Instead, the resulting throughput and spectral-efficiency distributions reflect the combined influence of frequency-dependent propagation characteristics and the heterogeneous operating conditions represented by the multi-cell simulation environment.

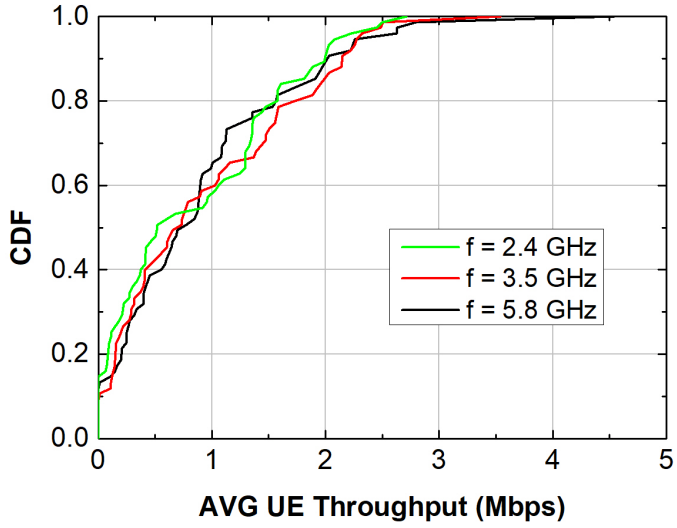


Figure 4.3. Impact of carrier frequency on average UE throughput.

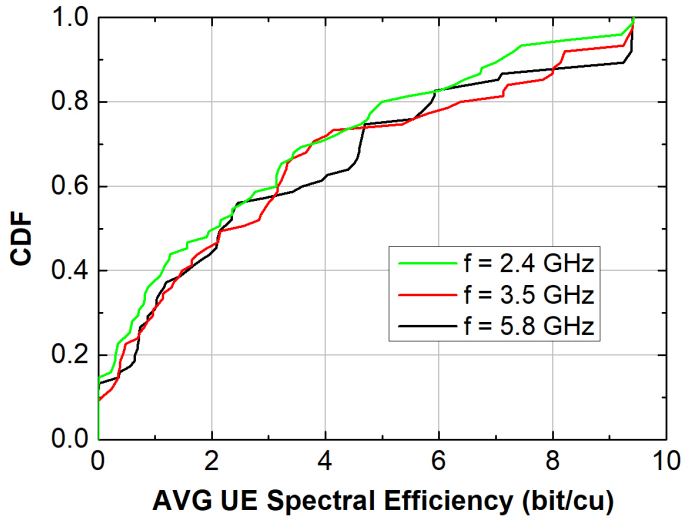


Figure 4.4. Impact of carrier frequency on average UE spectral efficiency.

Impact of Propagation K-Factor

The propagation K-factor characterizes the relative strength of the dominant deterministic component compared with the scattered multipath components in a Rician wireless channel

[15]. Increasing the K-factor therefore corresponds to stronger dominance of the deterministic component and reduced fading variability, whereas lower K-factor values indicate a greater relative contribution from scattered multipath propagation.

From a MIMO perspective, however, a higher K-factor does not necessarily imply uniformly improved system performance. Although stronger deterministic propagation can reduce fading severity and increase channel stability, the scattered multipath components contribute to the spatial richness of the channel. Consequently, the resulting MIMO performance depends on the interaction between the deterministic and scattered channel components, antenna configuration and the spatial characteristics of the propagation environment.

The simulation results shown in Figure 4.5 and Figure 4.6 illustrate this non-uniform behavior. Changes in the K-factor modify both the throughput and spectral-efficiency distributions, but the corresponding CDFs exhibit substantial overlap and several crossings. No configuration therefore provides a uniform performance advantage across the entire simulated user population.

For average UE throughput, the differences among the K-factor configurations depend on the considered region of the distribution, with the lower K-factor configuration exhibiting a more extended upper-performance tail. A similar dependence is observed for spectral efficiency, where increasing the K-factor does not produce a monotonic shift toward higher values. These results indicate that reduced fading variability alone does not determine the resulting MIMO performance.

Overall, the results confirm the sensitivity of the simulation framework to changes in the propagation K-factor while highlighting the importance of the underlying spatial channel structure. The balance between deterministic and scattered propagation components influences MIMO performance in a manner that depends on the operating conditions experienced by individual users, rather than producing a uniform performance improvement as the K-factor increases.

The initial sensitivity analysis demonstrates that the adopted simulation framework responds consistently to controlled variations in fundamental system and propagation parameters. Changes in transmit power, carrier frequency and propagation K-factor produce observable variations in the throughput and spectral-efficiency distributions, while the resulting performance differences are not necessarily uniform across the simulated user population. This behavior reflects the system-level nature of the considered environment, where the influence of individual parameters is combined with heterogeneous propagation, interference and spatial channel conditions.

These observations provide a baseline consistency assessment of the adopted simulation environment and demonstrate its sensitivity to fundamental system and propagation characteristics. At the same time, the non-uniform behavior observed across the corresponding performance distributions highlights the importance of examining MIMO performance beyond isolated parameter trends and motivates a more detailed characterization of deployment-dependent effects.

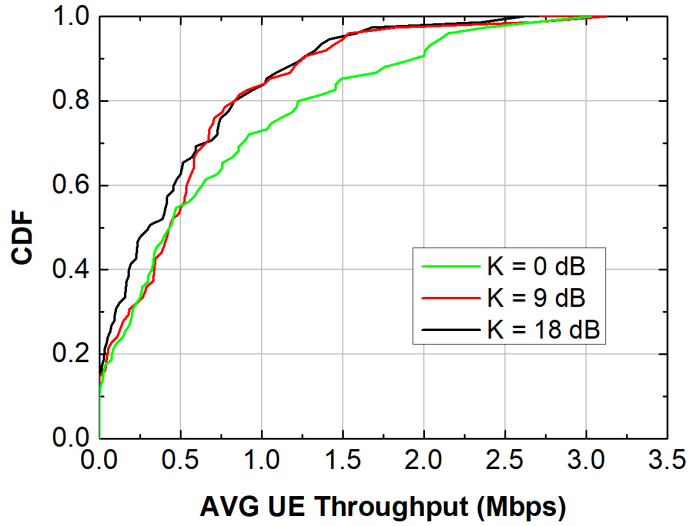


Figure 4.5. Impact of propagation K-factor on average UE throughput.

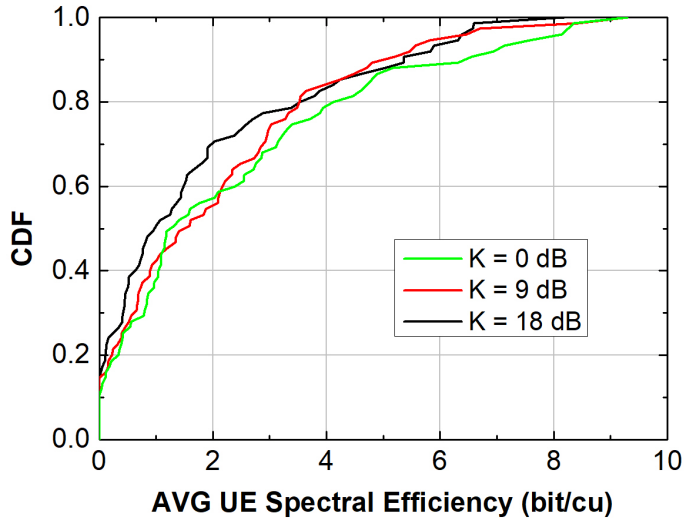


Figure 4.6. Impact of propagation K-factor on average UE spectral efficiency.

4.1.3 Performance Under Realistic Propagation Conditions

Following the baseline sensitivity analysis, this subsection proceeds to the main characterization of broadband MIMO performance under realistic propagation and deployment conditions. The objective is to examine how system, deployment and environmental parameters influence the achievable throughput, spectral efficiency and SINR behavior of MIMO systems. In particular, the analysis considers a set of representative configuration dimensions, including transmit power and antenna polarization, antenna geometry, user mobility, indoor–outdoor user distribution, indoor propagation conditions, user density and cell radius. Collectively, these parameters capture different aspects of the propagation environment, spatial channel structure, deployment geometry and network operating conditions. The following analysis

therefore aims not only to quantify the resulting performance variations, but also to interpret the mechanisms through which realistic propagation and deployment characteristics shape MIMO behavior.

Impact of Transmit Power and Antenna Polarization

Following the initial sensitivity analysis, the analysis is extended to investigate the joint impact of transmit power and antenna polarization on MIMO system performance. The objective is to determine whether increasing transmit power and modifying the polarization configuration lead to consistent improvements in the main performance indicators, namely average UE throughput, average UE spectral efficiency and UE SINR. Transmit-power values are expressed in dBm throughout the analysis; accordingly, the "dB" notation retained in the legends of the simulation-generated figures should be interpreted as dBm.

Table 4.2 summarizes the obtained results. As expected, increasing transmit power can improve the achievable performance, since higher radiated power generally enhances the received signal level and may improve the effective SINR experienced by users. However, the results reveal two important non-ideal behaviors. First, the performance improvement with increasing transmit power is not strictly monotonic across all configurations. Second, dual-polarized operation does not consistently outperform single-polarized operation, despite its theoretical potential for polarization diversity and additional spatial degrees of freedom.

Table 4.2. Channel performance under varying transmit power and antenna polarization configurations.

Channel Specifications	Average Cell Throughput (Mbps)	Avg UE Spectral Efficiency (bit/cu)
Power Tx = 47 dBm, Pol = 1	28.01	3.93
Power Tx = 50 dBm, Pol = 1	26.71	3.46
Power Tx = 53 dBm, Pol = 1	33.01	4.76
Power Tx = 47 dBm, Pol = 2	23.62	3.04
Power Tx = 50 dBm, Pol = 2	24.47	3.40
Power Tx = 53 dBm, Pol = 2	25.19	3.20

Pol = 1: Single polarization, Pol = 2: Dual polarization.

This behavior indicates that the effect of polarization cannot be interpreted independently of the propagation environment and antenna configuration. Although dual-polarized antennas can, in principle, exploit two orthogonal polarization components and provide additional degrees of freedom through polarization diversity and polarization multiplexing, the resulting performance gain depends strongly on the correlation between polarization branches, the angular distribution of multipath components and the alignment between transmitting and receiving antenna elements [62,63]. Under realistic urban propagation conditions, polarization

mismatch, spatial imbalance and heterogeneous propagation characteristics may limit the expected benefits of dual polarization [17, 66].

The CDF curves in Figures 4.7–4.9 provide additional insight into the observed performance behavior. The throughput and spectral efficiency distributions show that single-polarized configurations may outperform dual-polarized configurations in this specific deployment setting, particularly at higher transmit power levels. More importantly, the SINR distributions remain concentrated within a relatively narrow range across the examined configurations, suggesting that variations in transmit power and polarization do not translate into correspondingly large shifts in the resulting SINR distribution. Therefore, the results demonstrate that increasing transmit power does not automatically translate into proportional performance gains and that polarization-related benefits depend strongly on the effective channel structure.

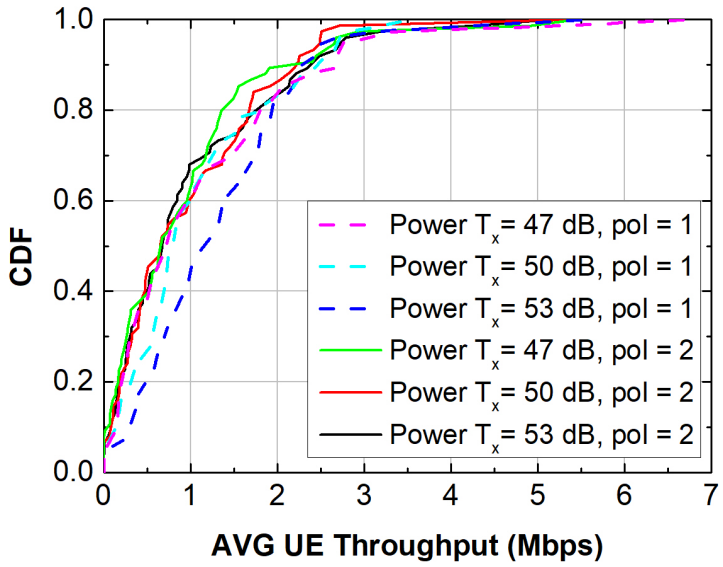


Figure 4.7. CDF of average UE throughput for different transmit power and antenna polarization configurations.

From a broader MIMO characterization perspective, these findings highlight that antenna polarization should not be treated as an isolated hardware feature, but rather as a parameter that interacts strongly with propagation characteristics and channel geometry. Under realistic 3GPP deployment conditions, polarization may either improve or degrade effective MIMO performance depending on the surrounding propagation environment and the resulting channel structure. Overall, these results indicate that MIMO performance under realistic propagation conditions is governed by complex interactions between antenna configuration and channel characteristics rather than by isolated parameter variations.

Impact of Antenna Geometry and Polarization

This section extends the analysis to investigate the combined impact of antenna geometry and antenna polarization on MIMO system performance under realistic propagation conditions. In multi-user MIMO deployments, antenna-related design choices directly influence

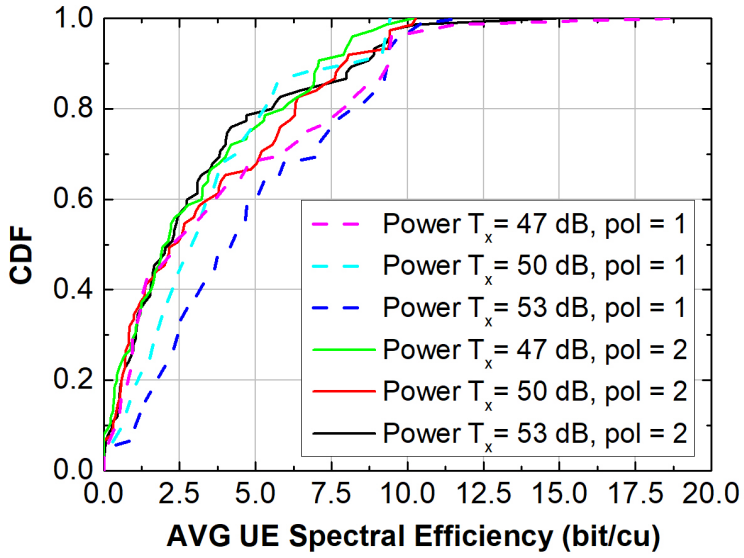


Figure 4.8. CDF of average UE spectral efficiency for different transmit power and antenna polarization configurations.

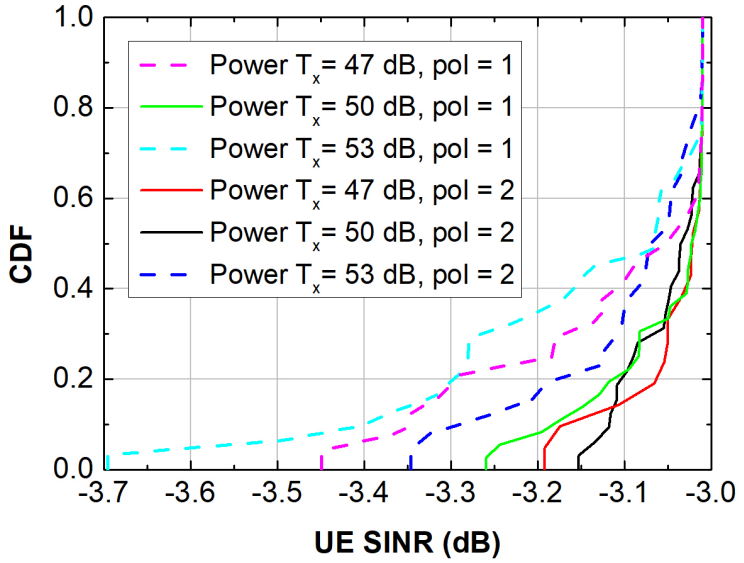


Figure 4.9. CDF of UE SINR for different transmit power and antenna polarization configurations.

channel rank, spatial correlation and multiplexing capability, thereby affecting the achievable throughput and spectral efficiency [15, 69]. In contrast to the previous experiment, where transmit power and polarization were jointly varied, the present analysis focuses on the effect of increasing the number of antenna elements while simultaneously examining the role of single and dual polarization. The objective is to determine how antenna-related characteristics shape the spatial properties of the wireless channel and influence the main performance metrics, namely average UE throughput, average UE spectral efficiency and UE SINR.

Table 4.3 summarizes the obtained results. The performance improvement with increasing antenna dimensions is clearly visible. For single-polarized configurations, the average cell throughput increases from 14.46 Mbps for the 2×1 configuration to 20.35 Mbps for the 4×2 configuration, while the average UE spectral efficiency improves from 2.02 to 2.96 bit/cu. Similar behavior is observed for dual-polarized configurations, where the highest performance is achieved for the 4×2 MIMO system, reaching 22.32 Mbps average cell throughput and 3.03 bit/cu spectral efficiency.

Table 4.3. Channel performance under varying antenna configurations and polarization settings.

Channel Specifications	**Average Cell Throughput (Mbps)**	**Avg UE Spectral Efficiency (bit/cu)**
MIMO 2×1, Pol = 1	14.46	2.02
MIMO 2×2, Pol = 1	19.05	2.54
MIMO 4×2, Pol = 1	20.35	2.96
MIMO 2×1, Pol = 2	16.54	2.30
MIMO 2×2, Pol = 2	20.08	2.72
MIMO 4×2, Pol = 2	22.32	3.03

Pol = 1: Single polarization, Pol = 2: Dual polarization.

An important observation is that dual polarization consistently outperforms the corresponding single-polarized configurations across all examined antenna setups. This finding suggests that performance improvements are not driven solely by antenna scaling, but also by the effective exploitation of polarization diversity. From a theoretical perspective, dual-polarized antennas can exploit orthogonal polarization components to provide polarization diversity and additional spatial degrees of freedom, although the extent of these benefits depends on the effective propagation and channel conditions [62, 63].

The CDF curves in Figures 4.10, 4.11, and 4.12 provide a more detailed view of the observed performance behavior. The throughput and spectral-efficiency distributions exhibit substantial overlap and crossing among the examined configurations, indicating that the average improvements reported in Table 4.3 do not correspond to uniform performance gains across the entire distribution. Nevertheless, the larger antenna configurations and dual-polarized operation generally provide favorable average throughput and spectral-efficiency performance.

The SINR distributions are also closely spaced and exhibit considerable overlap, suggesting that the observed throughput and spectral-efficiency differences cannot be attributed to a uniform improvement in SINR across all examined configurations.

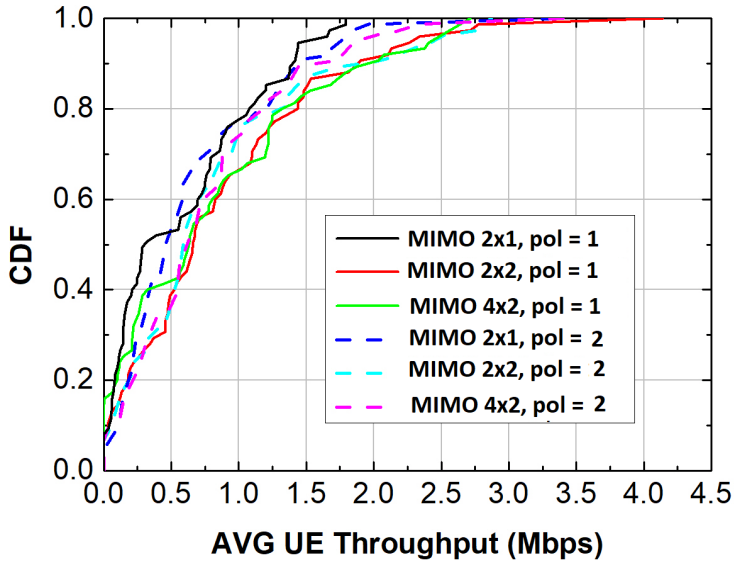


Figure 4.10. CDF of average UE throughput for different antenna configurations and polarization settings.

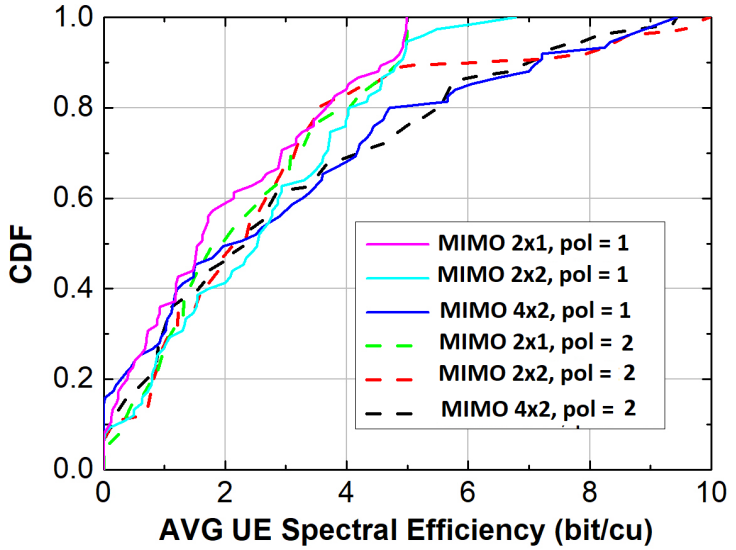


Figure 4.11. CDF of average UE spectral efficiency for different antenna configurations and polarization settings.

These results highlight the important role of antenna configuration and polarization in MIMO system performance. Increasing the antenna dimensions is associated with higher average throughput and spectral efficiency across the examined configurations, while dual-polarized operation provides an additional average performance benefit for each corresponding

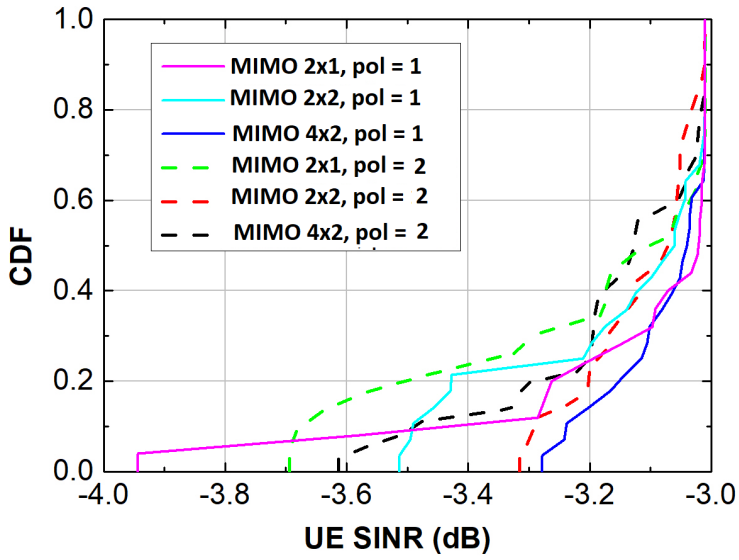


Figure 4.12. CDF of UE SINR for different antenna configurations and polarization settings.

antenna setup. At the same time, the substantial overlap among the CDF distributions demonstrates that these gains are not uniformly experienced across all operating conditions. From a broader characterization perspective, the findings therefore indicate that the performance impact of antenna scaling and polarization emerges from their interaction with the effective propagation and spatial channel conditions rather than from antenna configuration alone.

Impact of User Mobility and Indoor User Fraction

This section extends the analysis to investigate the combined impact of user mobility and indoor-outdoor user distribution on MIMO system performance under realistic urban propagation conditions. Unlike the previous simulations, which focused primarily on antenna-related parameters, the present analysis introduces user dynamics as an additional source of channel variability. The objective is to evaluate how mobility-induced channel variations and heterogeneous user distributions affect average UE throughput, average UE spectral efficiency and UE SINR.

Table 4.4 summarizes the obtained results. A clear performance degradation is observed as user mobility increases, while variations in indoor-user fraction produce comparatively smaller performance changes under the considered low-penetration scenario. For instance, in the 50% indoor-user scenario, average cell throughput drops from 15.60 Mbps at 0.3 m/s to 7.76 Mbps at 1.2 m/s, corresponding to an almost 50% reduction. A similar trend is observed in spectral efficiency, which decreases from 2.42 to 1.09 bit/cu. This behavior indicates that, within the examined operating conditions, user mobility has a substantially stronger influence on system performance than the considered variations in indoor-user fraction.

From a propagation perspective, increasing user velocity reduces channel coherence time and increases Doppler spread, leading to faster temporal variations of the wireless channel

Table 4.4. Channel performance under varying indoor-user fractions and user mobility levels.

Channel Specifications	Average Cell Throughput (Mbps)	Avg UE Spectral Efficiency (bit/cu)
Indoor fraction 50%, velocity = 0.3 m/s	15.60	2.42
Indoor fraction 50%, velocity = 0.8 m/s	10.92	1.67
Indoor fraction 50%, velocity = 1.2 m/s	7.76	1.09
Indoor fraction 80%, velocity = 0.3 m/s	16.80	2.67
Indoor fraction 80%, velocity = 0.8 m/s	10.12	1.49
Indoor fraction 80%, velocity = 1.2 m/s	7.84	1.67
Only indoor users, velocity = 0.3 m/s	18.23	2.58
Only indoor users, velocity = 1.2 m/s	10.21	1.61
Only outdoor users, velocity = 1.2 m/s	8.56	1.13
Only outdoor users, velocity = 3 m/s	6.28	0.92
Only outdoor users, velocity = 6 m/s	5.17	0.70

[1, 15]. Such variations can make the instantaneous channel conditions less stable and may affect the ability of the communication system to maintain favorable transmission conditions. The observed reductions in throughput and spectral efficiency are consistent with the increased temporal variability associated with higher user mobility.

The CDF curves in Figures 4.13, 4.14 and 4.15 provide further insight into the combined influence of mobility and indoor-user distribution. The throughput and spectral-efficiency distributions generally indicate lower performance as mobility increases when comparable indoor-user conditions are considered, although substantial overlap and crossing are observed among the different configurations. The SINR distributions also exhibit considerable overlap, without a uniform ordering across all mobility and indoor-user settings. These results indicate that the pronounced reductions observed in the average throughput and spectral-efficiency values do not correspond to an equally uniform shift in the SINR distribution.

An important observation is that, under the considered low-penetration scenario, changes in user mobility have a significantly stronger impact on performance than variations in indoor-user density. For a fixed mobility profile, increasing the indoor fraction from 50% to 80% generally results in smaller and less systematic performance variations than those observed when user mobility is increased. For example, at 0.3 m/s, the average cell throughput increases slightly from 15.60 Mbps to 16.80 Mbps. In contrast, for a fixed indoor fraction of 50%, increasing user speed from 0.3 m/s to 1.2 m/s reduces throughput from 15.60 Mbps to 7.76 Mbps. This substantial degradation confirms that mobility-induced channel dynamics dominate over user-distribution effects in determining overall MIMO performance under low-penetration conditions.

In contrast to the clear mobility-related trend, the impact of the indoor-user fraction is less systematic. For comparable mobility levels, increasing the proportion of indoor users does not

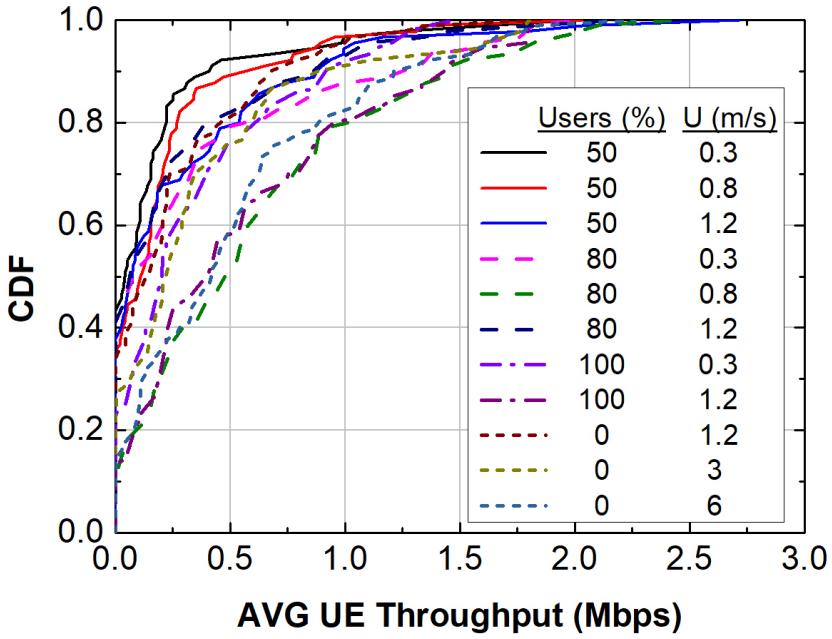


Figure 4.13. CDF of average UE throughput for different indoor-user fractions and user mobility levels.

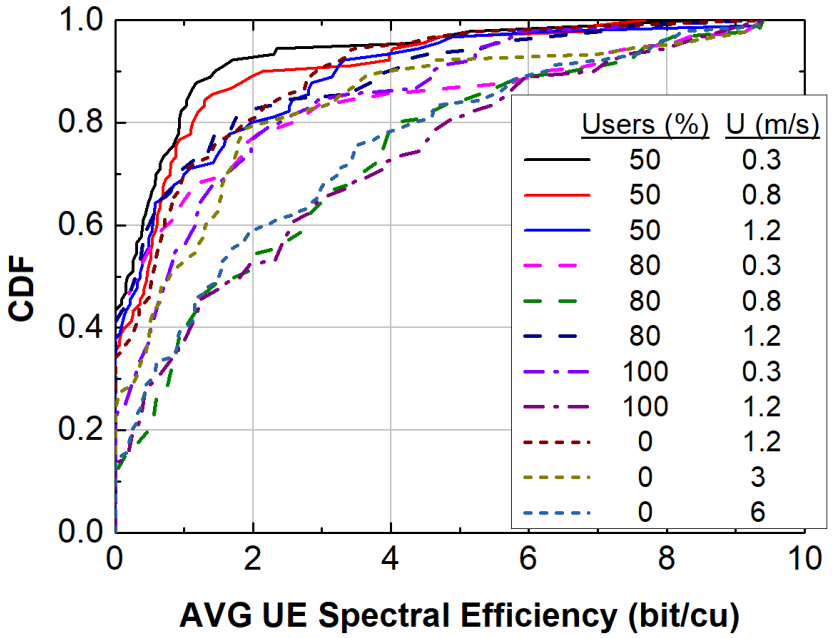


Figure 4.14. CDF of average UE spectral efficiency for different indoor-user fractions and user mobility levels.

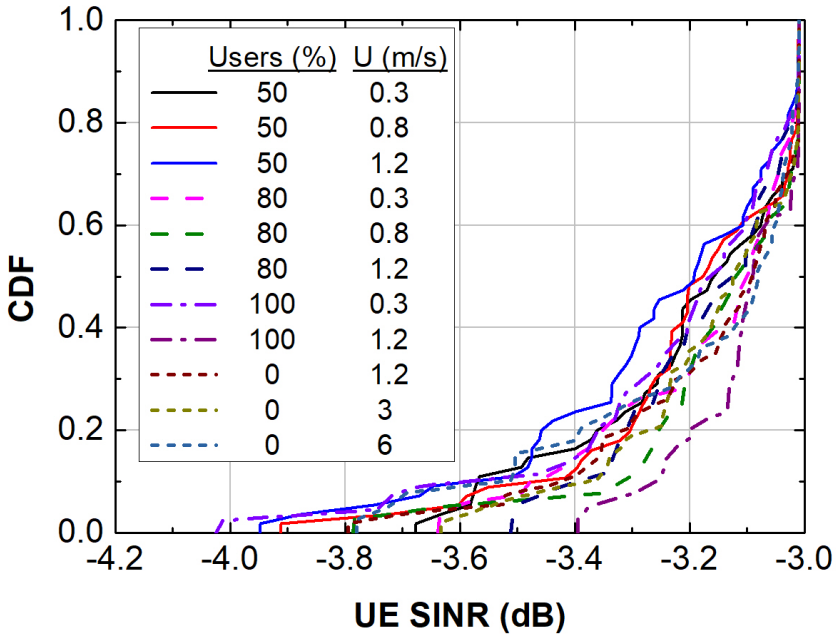


Figure 4.15. CDF of UE SINR for different indoor-user fractions and user mobility levels.

lead to a monotonic degradation or improvement in throughput and spectral efficiency. Instead, the resulting performance depends on the specific mobility level and propagation conditions represented by the considered low-penetration scenario. This indicates that indoor-user fraction acts as a secondary but configuration-dependent factor, whose influence becomes apparent through its interaction with user mobility and the underlying propagation environment.

These results highlight the important role of user mobility in realistic MIMO system characterization. Across the examined configurations, increasing mobility is associated with substantial reductions in average throughput and spectral efficiency, whereas variations in indoor-user fraction produce comparatively smaller and less systematic performance changes. At the same time, the overlapping SINR distributions demonstrate that these performance differences cannot be explained by a uniform shift in received signal quality alone. Overall, the findings show that temporal channel variation and heterogeneous user placement can influence MIMO performance in different ways, further emphasizing the need to characterize system behavior across multiple realistic operating conditions.

Impact of Indoor User Fraction in the Indoor Office Scenario

This section extends the analysis to investigate MIMO system performance under the 3GPP TR 38.901 indoor office scenario. In contrast to the previous simulation, which considered an urban microcell environment with mixed indoor and outdoor users, the present analysis adopts the indoor office configuration of the Vienna LTE-A system-level simulator and performs a controlled variation of the indoor-user fraction in order to examine its influence on system performance.

The considered configuration follows the 3GPP TR 38.901 indoor office model implemented in the simulator. The indoor office geometry is characterized by an inter-site distance of 20 m, with transmitter and UE heights of 3 m and 1 m, respectively. Users are assumed to move at 0.3 m/s, representing low-mobility indoor operation. Although the default indoor office configuration assumes an indoor-user fraction of 100%, the present analysis varies this parameter between 25%, 50%, 75% and 100% as a controlled sensitivity experiment.

The objective is to evaluate how variations in the indoor-user fraction influence the main performance metrics, namely average UE throughput, average UE spectral efficiency and UE SINR, within the adopted indoor office simulation framework.

Table 4.5 summarizes the obtained results. The indoor-user fraction does not produce a monotonic performance trend. The highest average throughput is obtained for the intermediate indoor-user fractions, with 50% indoor users reaching 6.83 Mbps and 75% indoor users reaching 6.61 Mbps, whereas the 25% and 100% cases both reach 4.64 Mbps. A similar non-monotonic behavior is observed for spectral efficiency, which reaches its highest value of 0.98 bit/cu for the 50% configuration.

Table 4.5. Channel performance under varying indoor-user fractions in the indoor office propagation model.

Channel Specifications	**Average Cell Throughput (Mbps)**	**Avg UE Spectral Efficiency (bit/cu)**
Indoor fraction 25%, velocity = 0.3 m/s	4.64	0.78
Indoor fraction 50%, velocity = 0.3 m/s	6.83	0.98
Indoor fraction 75%, velocity = 0.3 m/s	6.61	0.91
Indoor fraction 100%, velocity = 0.3 m/s	4.64	0.69

An important observation is that the indoor-user fraction does not produce a uniform or monotonic performance response under the considered indoor office conditions. Intermediate fractions of 50% and 75% provide the highest average throughput and spectral efficiency, whereas lower performance is observed for both the 25% and 100% cases. This indicates that the influence of the indoor-user fraction cannot be interpreted through the fraction value alone, but depends on the resulting user locations and the propagation conditions experienced across the simulated deployment. The indoor-user fraction should therefore be interpreted as a deployment-dependent parameter whose impact emerges through the spatial distribution of users and their corresponding channel conditions.

The CDF curves in Figures 4.16, 4.17, and 4.18 provide a more detailed view of this behavior. The throughput and spectral-efficiency distributions exhibit substantial overlap across the examined indoor-user fractions, indicating that the average differences reported in Table 4.5 do not correspond to a uniform performance ordering across the entire user population. Similarly, the SINR distributions remain relatively close and exhibit considerable overlap, showing that changes in indoor-user fraction do not produce a uniform shift in received

link quality. These results further support the observation that the influence of indoor-user fraction is non-monotonic and depends on the effective propagation conditions experienced across the deployment.

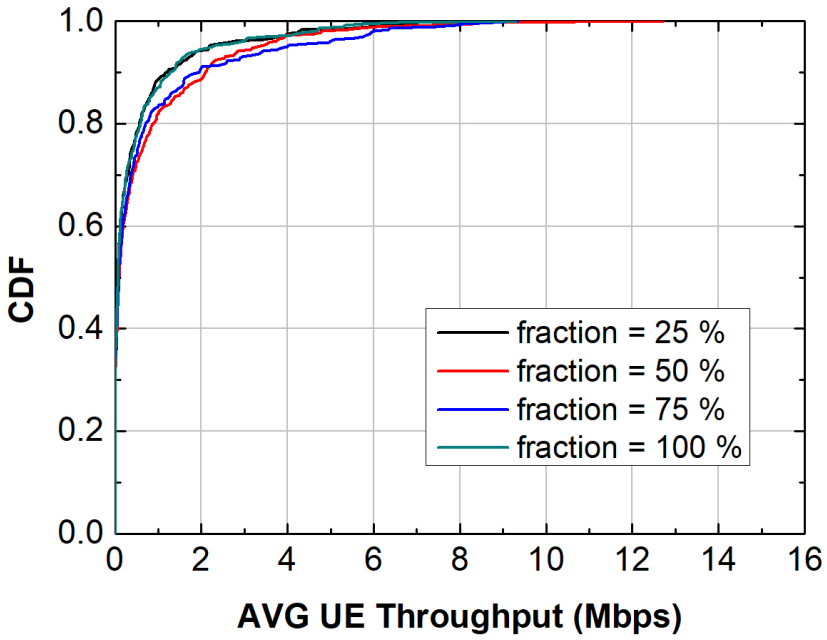


Figure 4.16. CDF of average UE throughput for different indoor-user fractions in the indoor office model.

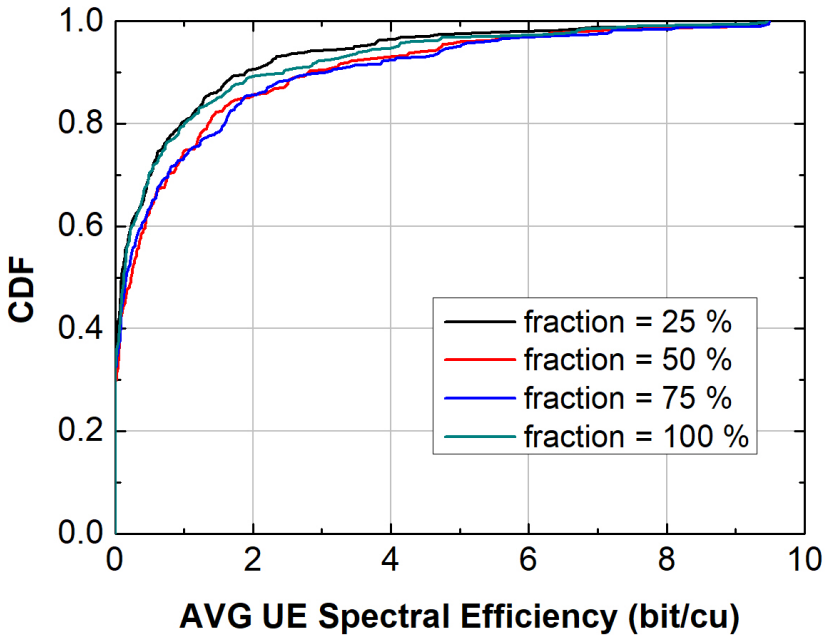


Figure 4.17. CDF of average UE spectral efficiency for different indoor-user fractions in the indoor office model.

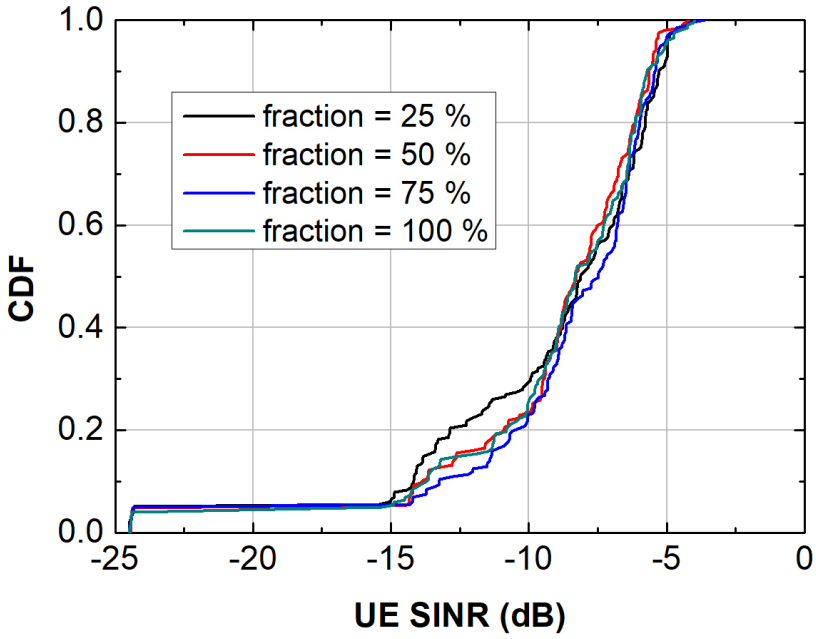


Figure 4.18. CDF of UE SINR for different indoor-user fractions in the indoor office model.

These results highlight the importance of user distribution in MIMO system analysis. Within the controlled indoor office experiment, changes in the indoor-user fraction modify the average throughput and spectral-efficiency performance, but the corresponding CDFs show that these effects are not uniformly experienced across the simulated user population. The closely spaced SINR distributions further indicate that the observed performance differences cannot be attributed to a uniform change in received link quality alone. Together with the preceding results on antenna configuration, polarization and user mobility, these findings reinforce the broader observation that MIMO performance depends strongly on the interaction between user distribution, propagation conditions and spatial channel characteristics.

Impact of User Density

This section investigates the impact of user density on MIMO system performance under realistic urban microcell propagation conditions. Unlike the previous simulations, which focused on propagation asymmetries caused by mobility, indoor penetration and antenna-related parameters, the present analysis examines how increasing the number of active users affects average UE throughput, average UE spectral efficiency and UE SINR. The objective is to evaluate how user density influences resource allocation, scheduling behavior and the range of channel conditions represented within multi-user MIMO deployments.

To capture both conventional and extreme operating conditions, the number of users is progressively increased from low-load to highly congested scenarios.

The CDF curves in Figures 4.19, 4.20, and 4.21 reveal a strong dependence of system behavior on the number of active users. However, the resulting distributions do not exhibit a simple or uniform ordering across the examined loading conditions. Instead, the effect of

increasing user density differs across throughput, spectral efficiency and SINR, indicating that network loading interacts with the underlying resource-allocation and propagation conditions represented by the system-level simulation.

Figure 4.19 shows that user density has a pronounced effect on the shape and spread of the throughput distribution. Several low-to-moderate loading configurations exhibit substantial overlap, whereas the highest loading cases produce markedly different distributions, particularly in the upper throughput range. The 1000-user configuration exhibits the broadest distribution and substantially higher throughput values for part of the evaluated population. This behavior should not be interpreted as a general throughput improvement caused by higher user density. In the adopted simulation framework, users are randomly distributed within each sector, while proportional-fair scheduling allocates resources according to both instantaneous transmission efficiency and previously achieved throughput. Increasing the user population therefore enlarges both the range of sampled channel conditions and the scheduling candidate pool, allowing favorable channel realizations to be exploited for a subset of users. Consequently, increasing user density modifies the shape and variability of the throughput distribution rather than producing a uniform performance shift.

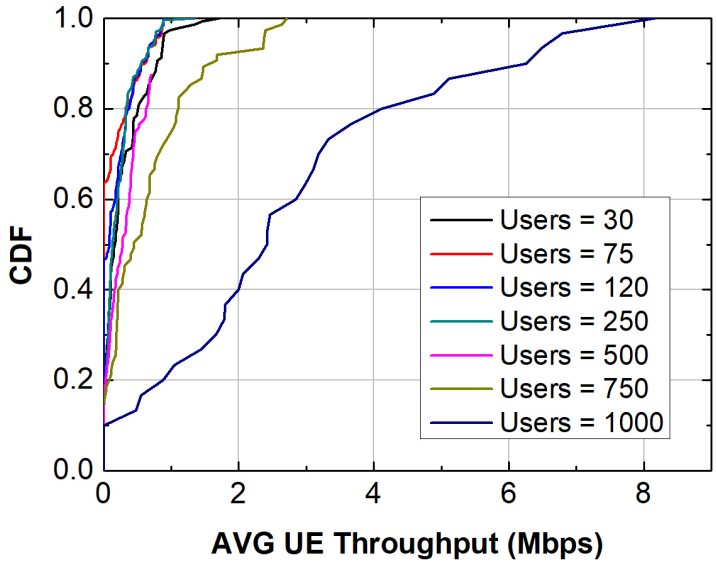


Figure 4.19. CDF of average UE throughput for different user densities.

Figure 4.20 shows a similarly complex behavior for spectral efficiency. The CDF curves exhibit substantial overlap and multiple crossings, demonstrating that no single user-density configuration provides uniformly superior spectral efficiency across the entire distribution. Nevertheless, the distribution changes considerably as the number of active users increases, particularly for the higher loading conditions. This behavior indicates that network loading affects different operating points of the system differently rather than producing a uniform gain or degradation in spectral utilization.

The SINR distributions shown in Figure 4.21 further illustrate the sensitivity of system

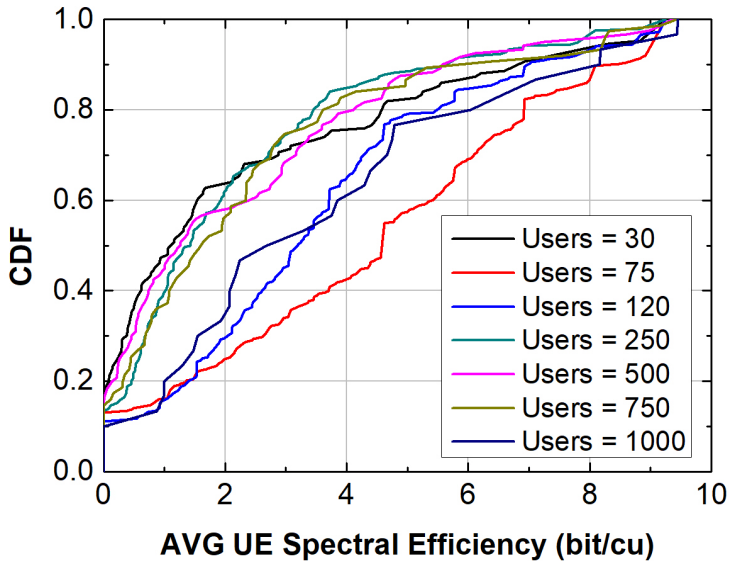


Figure 4.20. CDF of average UE spectral efficiency for different user densities.

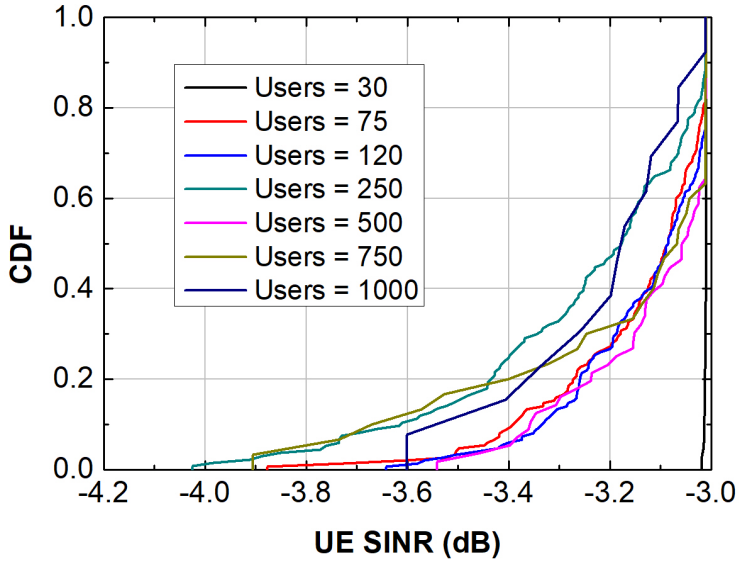


Figure 4.21. CDF of UE SINR for different user densities.

behavior to network loading. The 30-user configuration exhibits a highly concentrated SINR distribution, whereas increasing the number of users generally produces broader distributions over the examined SINR range. However, the curves substantially overlap and their ordering varies across the distribution. Therefore, the effect of user density is more appropriately interpreted as a change in the distribution and variability of the experienced SINR rather than as a uniform improvement or degradation in link quality. The broader SINR distributions at higher user densities are also consistent with the larger set of randomly distributed user locations, which represents a wider range of propagation and link conditions within the simulated cells.

Taken together, these results demonstrate that user density constitutes an important system-level dimension of MIMO performance. Changes in the number of active users affect not only the observed performance levels but also the shape and variability of the corresponding distributions. The absence of a consistent ordering across throughput, spectral efficiency and SINR indicates that network loading cannot be characterized through a single performance metric or a simple increasing or decreasing relationship. Instead, its influence emerges from the interaction between the size and spatial distribution of the user population, the resulting diversity of channel conditions and the resource-allocation decisions of the proportional-fair scheduler. These observations complement the preceding antenna-, mobility- and propagation-related analyses and contribute to the broader characterization of MIMO behavior under realistic deployment conditions.

Impact of Deployment Scale

This section investigates the impact of deployment scale on MIMO system performance under realistic urban microcell propagation conditions. While the previous simulations focused on user-related and network-loading effects, the present analysis examines how the spatial scale of the deployment influences wireless channel behavior. The objective is to evaluate how increasing the deployment scale affects average UE throughput, average UE spectral efficiency and UE SINR through changes in propagation conditions, user distribution and spatial channel characteristics.

The considered deployment-scale values range from 50 m to 200 m, representing different deployment scales within the urban microcell (UMi) scenario [16,17]. In addition, an extended case with a cell radius of 500 m is included to investigate system behavior beyond the primary range considered in the analysis.

The CDF curves in Figures 4.22, 4.23 and 4.24 reveal a clear dependence of system performance on cell radius. However, the observed variations do not follow a uniformly monotonic trend across the considered performance metrics, indicating that the effect of cell radius depends on the combined propagation and interference conditions of the system-level environment.

Figure 4.22 shows that the 50 m configuration exhibits a distinct throughput distribution, with a substantial fraction of users concentrated at relatively low throughput values. In contrast, the distributions corresponding to 100, 200 and 500 m show considerable overlap, with no consistent ordering over the entire CDF range. This indicates that increasing the cell radius does not result in a proportional or uniformly monotonic change in user throughput under the considered system-level conditions.

A similar behavior is observed in Figure 4.23. The 50 m configuration exhibits a distinct spectral-efficiency distribution, while the curves corresponding to 100, 200 and 500 m remain relatively close and intersect at several points. Therefore, the relationship between cell radius and spectral efficiency does not follow a simple monotonic trend, but rather reflects the combined influence of propagation conditions, interference and user distribution.

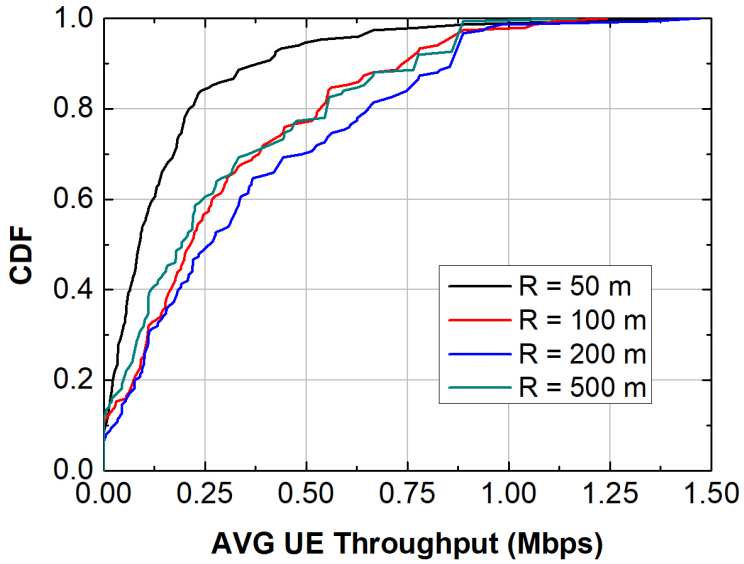


Figure 4.22. CDF of average UE throughput for different cell radius values.

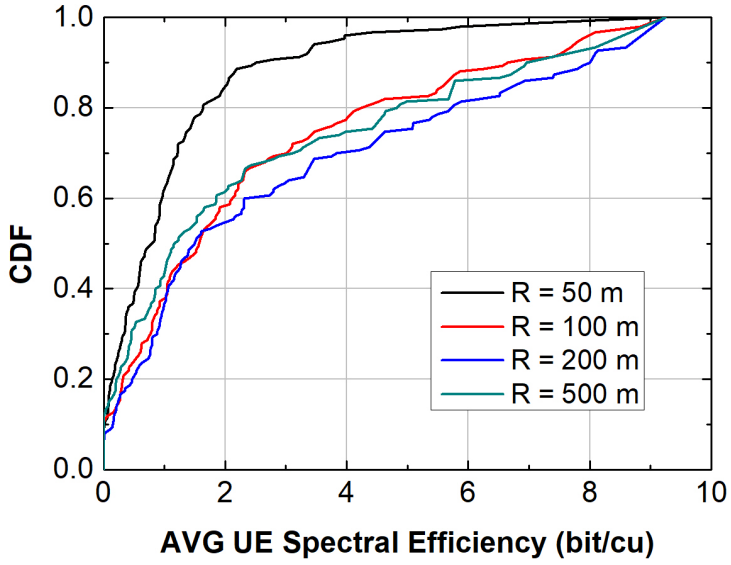


Figure 4.23. CDF of average UE spectral efficiency for different cell radius values.

The SINR distributions shown in Figure 4.24 provide further insight into this behavior. The 50 m configuration exhibits a considerably broader SINR distribution, extending toward substantially lower values, whereas the distributions corresponding to 100, 200 and 500 m are more strongly concentrated within a narrower SINR range. This result indicates that the effect of cell radius on SINR cannot be attributed solely to distance-dependent path loss, but also reflects changes in the interference conditions and spatial geometry of the system-level environment. The broader SINR distribution observed for the 50 m configuration is consistent with stronger spatial variability in the balance between serving and interfering links under the more compact deployment geometry.

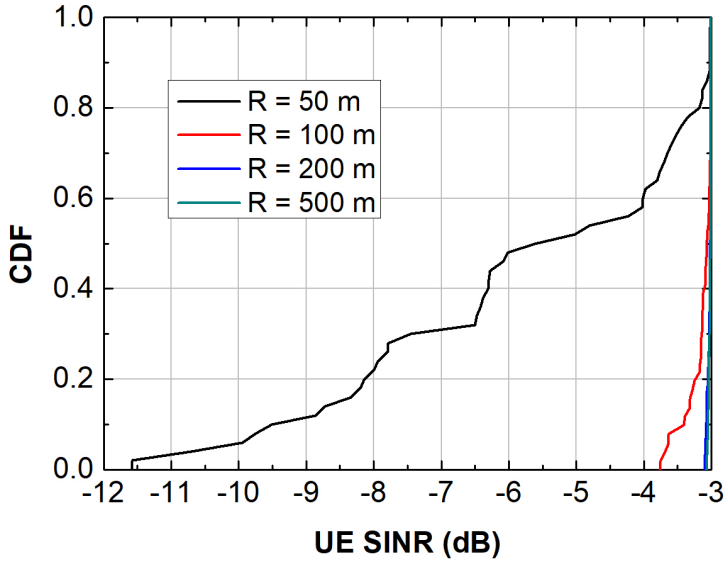


Figure 4.24. CDF of UE SINR for different cell radius values.

Table 4.6. Average performance for different cell radius values.

Cell Radius (m)	Average Cell Throughput (Mbps)	Avg. UE Spectral Efficiency (bit/cu)
50	14.36	2.32
100	14.45	2.52
200	12.44	2.12
500	7.91	1.31

The average performance values in Table 4.6 provide additional insight into the trends observed in the CDFs. Average cell throughput remains nearly unchanged between 50 and 100 m, with values of 14.36 and 14.45 Mbps, respectively, while average UE spectral efficiency slightly increases from 2.32 to 2.52 bit/cu. Beyond 100 m, however, both metrics decrease substantially, reaching 12.44 Mbps and 2.12 bit/cu at 200 m and 7.91 Mbps and 1.31 bit/cu at 500 m. Compared with the 100 m configuration, the 500 m case corresponds to an approximately 45% reduction in average cell throughput and a 48% reduction in average

UE spectral efficiency. Thus, although the CDFs do not exhibit a uniformly monotonic ordering across the entire distribution, the average values reveal a clear degradation in overall performance as the deployment scale extends beyond the smaller-radius configurations.

An important observation is that deployment scale modifies the spatial characteristics of the system-level environment and the resulting variability in user performance. The differences observed across the considered configurations indicate that deployment geometry affects the balance between serving and interfering links, leading to distinct performance distributions across the cell. Therefore, the influence of cell radius should be interpreted as a combined propagation and interference effect rather than solely as a consequence of increasing user-to-base-station distance.

More importantly, the results show that the effect of cell radius cannot be characterized by a single performance trend across the considered metrics. Although changes in deployment scale produce noticeable variations in throughput, spectral efficiency and SINR, these variations are not consistently ordered with increasing cell radius. This behavior highlights the importance of considering the interaction between propagation, interference and network geometry when evaluating MIMO performance at the system level.

Overall, these findings demonstrate that deployment scale constitutes an important factor in MIMO performance characterization, influencing the resulting throughput, spectral-efficiency and SINR distributions through the combined effects of propagation conditions, interference and network geometry. The observed non-monotonic behavior further emphasizes the importance of system-level evaluation when assessing MIMO performance under realistic deployment conditions.

4.1.4 Cross-Scenario Insights for Broadband MIMO Systems

This section synthesizes the main findings of the systematic simulation-based analysis of the factors affecting MIMO system performance under realistic propagation conditions. The objective is not only to compare performance variations in terms of average UE throughput, average UE spectral efficiency and UE SINR, but also to identify recurring cross-scenario patterns that are not evident from the individual simulations alone. Particular attention is therefore given to the distribution and variability of user performance and to the extent to which the observed behavior remains consistent across different system, propagation and deployment conditions.

The analysis covered a broad range of system, propagation and deployment parameters, including transmit power, configuration, polarization, user mobility, indoor–outdoor user distribution, user density and deployment scale, enabling MIMO behavior to be examined across heterogeneous operating conditions. Across the preceding simulations, a recurring observation was that average performance values alone were not always sufficient to describe the resulting system behavior. In several cases, configurations with comparable average throughput or spectral efficiency exhibited substantially different performance distributions, while the corresponding CDFs showed considerable overlap and crossing. These observations demonstrate

the importance of considering both average and distributional performance when characterizing MIMO behavior under realistic operating conditions.

Based on these observations, the cross-scenario analysis reveals that broadband MIMO performance under realistic propagation conditions is governed by a set of interacting mechanisms rather than by isolated system parameters. Although each simulation examined a different factor, the overall results consistently point to several common characterization insights that help explain the observed MIMO behavior.

Insight 1: Spatial dimensionality governs achievable MIMO gains. The first major insight is that the achievable performance gains of broadband MIMO systems are strongly influenced by spatial dimensionality, which is primarily determined by antenna geometry, antenna scaling and polarization configuration. Increasing the number of antenna elements generally improved throughput and spectral efficiency by providing additional spatial degrees of freedom and supporting more effective spatial multiplexing. However, the benefits of dual-polarized operation were configuration-dependent and were not consistently observed across all examined scenarios. This indicates that the potential gains associated with additional spatial dimensions cannot be attributed to antenna scaling or polarization alone, but depend strongly on their interaction with the underlying channel structure and propagation conditions.

Insight 2: Propagation and deployment conditions shape MIMO performance. The second major insight is that MIMO performance is strongly influenced by the spatial distribution of users and the geometry of the deployment. Variations in indoor–outdoor user distribution and deployment scale produced noticeable changes in throughput, spectral efficiency and SINR, but these changes did not follow a simple or uniformly monotonic trend across the examined conditions. In particular, increasing the indoor-user fraction did not consistently improve or degrade performance, while changes in deployment scale affected both average performance and the corresponding user-level distributions. These results demonstrate that MIMO performance depends not only on the selected system configuration, but also on where users are located and on the spatial conditions under which communication takes place.

Insight 3: User dynamics and network loading strongly influence MIMO performance. The third major insight is that MIMO performance is strongly influenced by user dynamics and network loading. Increasing user mobility generally resulted in substantial reductions in throughput and spectral efficiency under comparable user-distribution conditions, reflecting the increased temporal variability of the wireless channel. In contrast, increasing user density primarily modified the shape and spread of the throughput, spectral-efficiency and SINR distributions, without producing a consistent monotonic performance trend across the examined loading conditions. These results demonstrate that user mobility and network loading affect MIMO performance through different mechanisms and should therefore be considered explicitly when characterizing system behavior under realistic operating conditions.

Table 4.7. Summary of the main findings for simulations related to system-level parameters (Simulations 1–5).

Sim	Parameter(s) Varied	Main Findings	System-Level Implications
1	Transmit Power (10–50 W)	Higher transmit power generally improved performance, although the observed gains were not uniformly monotonic across the examined operating conditions.	Transmit-power optimization is important, since increasing radiated power does not necessarily produce proportional performance gains under realistic system-level conditions.
2	Carrier Frequency (2.4–5.8 GHz)	Increasing carrier frequency was associated with lower average performance, although the corresponding throughput and spectral-efficiency distributions exhibited substantial overlap and no uniform degradation across the simulated user population.	Carrier-frequency selection should account for frequency-dependent propagation characteristics and their interaction with the deployment environment.
3	K-factor (0–18 dB)	Variations in the Rician K-factor modified the resulting performance by changing the balance between dominant LOS and scattered propagation components, with the observed response depending on the considered operating conditions.	The influence of LOS dominance on MIMO performance should be evaluated together with the underlying spatial and propagation characteristics rather than through the K-factor alone.
4	Transmit Power + Polarization	Transmit power variations produced non-monotonic performance trends, while polarization effects depended strongly on the effective channel structure.	Power control and polarization design should be jointly optimized, since higher transmit power or dual polarization do not automatically guarantee proportional performance gains.
5	Number of Antenna Elements + Polarization	Increasing antenna dimensions and dual-polarized operation were associated with higher average throughput and spectral efficiency, although the corresponding CDFs exhibited substantial overlap across configurations.	Antenna scaling and polarization provide important spatial design dimensions, but their performance benefits depend on their interaction with the effective propagation and channel conditions.

Insight 4: Broadband MIMO performance is inherently configuration- and operating-condition-dependent. The final major insight is that broadband MIMO performance cannot be characterized through simple or universally monotonic relationships with individual system parameters. Across the examined characterization scenarios, antenna configuration, polarization, user distribution, mobility, network loading and deployment geometry produced performance changes that varied across metrics and operating conditions. In several cases, the corresponding throughput, spectral-efficiency and SINR distributions overlapped or crossed, while improvements observed in one performance metric were not necessarily accompanied by equivalent improvements in others. These results demonstrate that MIMO performance emerges from the interaction between system configuration, user dynamics, propagation conditions and deployment characteristics rather than from isolated parameter variations.

For clarity, the main findings of all simulation scenarios are summarized in Tables 4.7 and 4.8. The tables consolidate the dominant parameters examined in each simulation, their observed impact on MIMO performance and the associated implications for realistic wireless system design.

Taken together, the broadband MIMO analysis reveals that performance under realistic

Table 4.8. Summary of the main findings for simulations related to deployment and environmental parameters (Simulations 6–9).

Sim	Parameter(s) Varied	Main Findings	System-Level Implications
6	User Mobility + Indoor Fraction	Higher mobility was associated with substantial reductions in average throughput and spectral efficiency, while variations in indoor-user fraction produced smaller and less systematic performance changes under the considered low-penetration conditions.	Mobility and user-distribution characteristics should be jointly considered when evaluating MIMO performance, since temporal channel dynamics can substantially affect the achievable performance.
7	Indoor Deployment Model	Indoor-user fraction produced non-monotonic performance behavior, with the intermediate 50% and 75% configurations achieving higher average throughput and spectral efficiency than the 25% and 100% cases.	The impact of indoor-user distribution is deployment-dependent and should be evaluated together with the underlying propagation conditions rather than interpreted through indoor-user fraction alone.
8	Number of Users	Increasing user density produced substantial changes in the shape and variability of the throughput, spectral-efficiency and SINR distributions, without a consistent monotonic ordering across the examined loading conditions.	Network load should be evaluated across multiple performance metrics and distributional characteristics, since user density does not produce a uniform performance response under realistic system-level conditions.
9	Deployment Scale	Changes in deployment scale produced non-uniform distributional changes, while the average metrics revealed clear performance degradation beyond the smaller-scale configurations, with the 500 m case showing approximately 45% lower average cell throughput and 48% lower average UE spectral efficiency than the 100 m configuration.	Deployment scale should be evaluated through both average and distributional performance metrics, since changes in deployment geometry affect MIMO behavior through the combined propagation and interference environment.

system-level propagation conditions cannot be described through simple, universally valid relationships between individual system parameters and conventional performance metrics. Across the examined characterization scenarios, parameter variations often produced non-uniform responses, overlapping or crossing performance distributions and different sensitivities across throughput, spectral efficiency and SINR. The main findings emerging from the cross-scenario analysis can therefore be summarized as follows:

- **Realistic MIMO performance is inherently context-dependent.** The examined antenna, user, mobility, network-loading and deployment conditions did not produce universally valid or consistently monotonic performance trends. Consequently, the suitability of a MIMO configuration cannot be determined independently of the operating environment.

- **Conventional average metrics provide only a partial characterization of system behavior.** The observed differences between average performance values and user-level distributions demonstrate that mean throughput or spectral efficiency alone may conceal important differences across the simulated user population. A meaningful characterization therefore requires the joint examination of multiple metrics and their corresponding distributions.

- **Characterization is a prerequisite for informed MIMO configuration and adap-**

tation. Since the relative benefit of different configurations changes with propagation, mobility, network load and deployment conditions, configuration decisions require knowledge of the current operating regime. The results therefore provide a direct motivation for moving from static MIMO operation toward characterization-driven and adaptive transmission strategies.

These findings establish the central outcome of the broadband analysis: MIMO behavior is shaped jointly by system configuration, user dynamics, network loading and deployment conditions. Such characterization is not merely descriptive; it provides the information required to determine when a particular MIMO configuration is beneficial, when its expected gains diminish, and when changing operating conditions may justify a different transmission strategy. In this sense, the characterization developed in this chapter provides the necessary foundation for moving from static MIMO configuration toward operating-condition-aware and ultimately adaptive MIMO operation.

While the preceding analysis provides a comprehensive characterization of broadband MIMO systems under realistic propagation conditions, wireless communication systems may operate under fundamentally different resource and reliability constraints. In particular, low-power wireless environments introduce strict limitations in terms of energy availability, operating SNR and communication reliability. Under such conditions, the relative importance of spatial diversity, multiplexing capability and implementation complexity may differ substantially from that observed in conventional broadband MIMO systems.

Motivated by this observation, the following section extends the characterization analysis to low-power LoRa-type communication systems. The objective is to investigate how severe energy, SNR and reliability constraints influence the behavior of MIMO techniques and, in particular, whether the performance trends and spatial benefits identified in broadband systems remain valid when communication operates under highly constrained conditions. This comparison provides a broader basis for identifying which MIMO characteristics remain beneficial across fundamentally different wireless operating regimes.

4.2 LoRa-Type MIMO Characterization Under Constrained Operating Conditions

The preceding section focused on broadband MIMO systems operating under realistic 3GPP propagation conditions and demonstrated that MIMO performance is governed by multiple interacting factors, including antenna configuration, channel dynamics, propagation heterogeneity and network load. The analysis revealed non-monotonic and configuration-dependent behavior across several operating conditions, while average performance metrics alone were not always sufficient to capture the observed performance variability. These findings highlighted the importance of systematic, multi-dimensional characterization for understanding MIMO behavior under realistic broadband operating conditions. However, realistic wireless operation is not determined solely by propagation conditions. In many communication scenarios, system behavior is also strongly constrained by strict operating limitations related to energy availability, communication range, bandwidth and hardware complexity. These constraints introduce fundamentally different design requirements and may significantly alter the achievable gains and role of MIMO techniques.

To investigate this complementary dimension of realistic MIMO operation, the analysis is extended to low-power wide-area network (LPWAN) environments using LoRa-type communication systems as a representative constrained wireless framework. Unlike conventional broadband systems, where MIMO techniques are typically employed to maximize throughput and spectral efficiency, LPWAN systems operate under fundamentally different priorities, where communication reliability, energy efficiency and coverage robustness are often more critical than throughput maximization.

As a result, the role of MIMO changes significantly under constrained operating conditions. Spatial diversity techniques may improve communication reliability and coverage robustness by mitigating severe channel impairments, whereas spatial multiplexing may offer more limited performance benefits due to low-SNR operation, narrow bandwidth and strict energy constraints. Consequently, MIMO techniques that perform efficiently in broadband systems may behave substantially differently in LPWAN environments.

Despite increasing interest in LoRa and LPWAN systems, the role of MIMO under such constrained operating conditions remains insufficiently understood. Existing studies primarily focus on isolated aspects such as coverage improvement, gateway diversity or specific detection schemes, while systematic comparisons between diversity-oriented and spatial multiplexing approaches remain limited. Furthermore, the combined impact of antenna configuration, low-SNR operation and CSI uncertainty has not been comprehensively analyzed within a unified evaluation framework.

The main objective of this section is therefore to systematically characterize the feasibility, limitations and performance trade-offs of MIMO techniques in LoRa-type wireless systems. The analysis examines both diversity-oriented and spatial multiplexing configurations under constrained operating conditions and imperfect channel state information, with particular

emphasis on reliability, robustness and operating limits.

The analysis begins with system-level coverage characterization under large-scale propagation effects. It then proceeds to link-level evaluation of diversity-oriented MIMO schemes under perfect and imperfect CSI conditions, followed by a comparative assessment of spatial multiplexing performance using throughput-oriented metrics. Through this progressively structured analysis, the section aims to provide a comprehensive characterization of how severe operating constraints reshape the achievable gains and limitations of MIMO techniques in LPWAN environments.

4.2.1 Simulation Methodology and System Assumptions

This subsection presents the simulation framework adopted for the characterization of MIMO techniques under constrained LoRa-type operating conditions. The objective is to establish a consistent evaluation environment for characterizing coverage behavior, diversity-oriented MIMO schemes and spatial multiplexing configurations under low-SNR operation and imperfect channel state information.

The simulation framework combines the Vienna LTE-A System-Level Simulator v2.0 (Q3 release) with dedicated Monte Carlo link-level routines developed for the considered MIMO and LoRa-type evaluations. The Vienna framework provides the basis for system-level propagation and coverage characterization, while the link-level routines enable controlled evaluation of antenna configurations, receiver processing, channel-estimation uncertainty and error-performance metrics. This combined methodology is particularly important for the present analysis, where different MIMO configurations and CSI conditions must be compared under consistent propagation, power-normalization and receiver-processing assumptions.

To support the considered LPWAN-oriented analysis, the simulation framework is extended with LoRa-type physical-layer abstractions. The objective is not to reproduce the complete LoRa chirp spread spectrum waveform or the full LoRaWAN protocol stack, but to capture the operating characteristics that are relevant to the present MIMO investigation. The link-level MIMO evaluation employs a QPSK-based baseband abstraction, while spreading-factor effects are represented through the corresponding effective-SNR adjustments adopted in the simulation framework. The resulting analysis should therefore be interpreted as a system-level and link-level characterization of MIMO behavior under LoRa-type constrained operating conditions rather than as a waveform-level implementation of the LoRa physical layer.

The considered MIMO transmission modes are evaluated using the linear baseband MIMO signal model introduced in Chapter 2. Diversity-oriented configurations are examined through space–time block coding, while spatial multiplexing configurations are evaluated using linear ZF and MMSE receiver processing. For fair comparison across antenna configurations and transmission modes, the transmitted signals are normalized such that the total transmit power per channel use remains constant. This common modeling and power-normalization structure enables direct comparison between diversity- and multiplexing-oriented mechanisms under consistent channel and receiver-processing assumptions.

Channel state information uncertainty is incorporated using the CSI error modeling framework introduced in Chapter 2. Perfect CSI is considered as a reference case, while imperfect CSI is represented using both CEEM-I, with externally specified fixed estimation-error variance and CEEM-II, where the estimation-error variance depends on the effective training quality and operating SNR. This approach allows the sensitivity of diversity and spatial multiplexing schemes to CSI quality to be investigated without introducing estimator-specific assumptions. As a result, the analysis focuses on the impact of CSI uncertainty on MIMO behavior rather than on the design of a particular channel estimation algorithm.

The evaluation methodology follows a progressive structure. First, a coverage-level baseline is established under large-scale propagation effects in order to identify the operating SNR regime and feasibility conditions of the considered LoRa-type deployment. These system-level results provide the operating context for the subsequent link-level analysis. The evaluation then proceeds to diversity-oriented MIMO schemes under perfect and imperfect CSI, followed by spatial-multiplexing configurations evaluated through reliability- and throughput-oriented metrics. This progressive structure enables the transition from propagation-induced operating constraints to the reliability–throughput trade-offs associated with different MIMO transmission strategies.

To ensure reproducibility and fair comparison, the simulation campaign is organized as a series of controlled experiments in which selected parameters are explicitly varied according to the objective of each simulation stage. Across the different experiments, these parameters include antenna configuration, spreading factor, receiver processing and CSI quality. Within each direct comparison, parameters not under investigation are kept unchanged, including the adopted modulation abstraction, transmit-power normalization, noise model and channel assumptions. Monte Carlo averaging is applied in all link-level experiments, with the number of realizations selected according to the requirements of each simulation stage. Consequently, performance differences within each controlled comparison can be associated with the specific transmission mechanism, antenna configuration, receiver strategy or CSI condition being examined.

The main experimental control parameters used in the LoRa-type MIMO characterization are summarized in Table 4.9.

In contrast to the broadband MIMO analysis presented in Section 4.1, where performance evaluation focused primarily on SINR, spectral efficiency and throughput, the constrained operating conditions of LoRa-type systems require a different evaluation perspective. Due to low-SNR operation, constrained communication resources and reliability-oriented communication objectives, performance assessment emphasizes communication robustness, coverage behavior and effective data delivery rather than spectral efficiency alone.

Accordingly, the performance of the considered LoRa-type MIMO configurations is evaluated using four complementary metrics: (i) signal-to-noise ratio (SNR) for coverage characterization and operating region identification, (ii) bit error rate (BER) for link-level reliability evaluation, (iii) packet error rate (PER) for packet-level communication effectiveness and (iv)

Table 4.9. Main simulation parameters used for LoRa-type MIMO characterization under constrained operating conditions.

Category	Description
Simulation framework	Vienna SLS v2.0 (Q3) + custom MATLAB link-level routines
Simulation approach	System-level coverage and Monte Carlo link-level evaluation
Carrier frequency	868 MHz
Reference bandwidth	125 kHz
Link direction	Uplink
Link-level modulation	QPSK baseband abstraction
Spreading-factor range	SF7–SF12
MIMO strategies	STBC diversity and spatial multiplexing
Linear detection	ZF and MMSE (spatial multiplexing)
Channel models	Large-scale propagation / flat i.i.d. Rayleigh fading
CSI conditions	Perfect CSI, CEEM-I and CEEM-II
Power normalization	Constant total transmit power across compared MIMO modes
Monte Carlo evaluation	Independent channel, noise and data realizations
Performance metrics	SNR CDF, BER, PER and normalized goodput

normalized goodput for assessing the trade-off between transmission efficiency and communication reliability.

The SNR is used to characterize the received signal quality under the considered coverage and propagation conditions. At the system level, the receiver noise power is calculated as

$$P_{\text{noise,dBm}} = -174 + 10\log_{10}(B) + NF \tag{4.2}$$

where B is the receiver bandwidth in Hz and NF is the receiver noise figure in dB. The corresponding received SNR is then obtained as

$$\text{SNR}_{\text{dB}} = P_{\text{rx,dBm}} - P_{\text{noise,dBm}} \tag{4.3}$$

In the subsequent link-level Monte Carlo simulations, the SNR axis is represented by the symbol-energy-to-noise-density ratio, E_s/N_0. For a given $\gamma_s = E_s/N_0$ in linear scale, the complex AWGN variance is normalized as

$$\sigma_n^2 = \frac{1}{\gamma_s}, \tag{4.4}$$

under the adopted unit-energy normalization.

The BER quantifies the fraction of incorrectly detected bits and is defined as

$$\text{BER} = \frac{N_{\text{bit,error}}}{N_{\text{bit,total}}}, \tag{4.5}$$

where $N_{\text{bit,error}}$ is the number of erroneous bits and $N_{\text{bit,total}}$ is the total number of transmitted bits.

At the transmission-block level, reliability is characterized through a packet-error metric. Each simulated spatial-multiplexing transmission block is treated as a packet-level error event and is declared erroneous when at least one of its detected bits is incorrect. Accordingly,

$$\text{PER} = \frac{N_{\text{block,error}}}{N_{\text{block,total}}}, \tag{4.6}$$

where $N_{\text{block,error}}$ denotes the number of simulated transmission blocks containing at least one bit error and $N_{\text{block,total}}$ is the total number of transmitted blocks. Thus, the PER reported in the following analysis represents a block-based packet-error abstraction rather than a complete LoRaWAN packet-level PHY simulation.

Finally, effective goodput is used to capture the successfully delivered information rate after transmission-block errors are taken into account. It is defined as

$$G_{\text{eff}} = \eta_{\text{mode}}(1 - \text{PER}), \tag{4.7}$$

where η_{mode} denotes the nominal information rate of the considered transmission mode. For the spatial-multiplexing configurations,

$$\eta_{\text{mode}} = N_s \log_2(M), \tag{4.8}$$

where N_s is the number of simultaneously transmitted spatial streams and M is the modulation order. Under the adopted QPSK abstraction, $\log_2(M) = 2$, yielding

$$G_{\text{eff}} = 2N_s(1 - \text{PER}) \quad \text{bits/channel use.} \tag{4.9}$$

This metric therefore captures the fundamental trade-off between spatial-stream multiplicity and transmission reliability: increasing N_s raises the nominal information rate, but the resulting gain is retained only to the extent that the transmitted blocks are successfully detected.

The analysis therefore begins with a controlled coverage-level evaluation under representative large-scale propagation conditions, considering distance-dependent path loss and log-normal shadowing while excluding small-scale fading and MIMO processing. This separation is intentional: the baseline stage isolates the propagation mechanisms that determine the available link-quality and spreading-factor feasibility conditions before introducing small-scale fading, spatial processing and CSI uncertainty at link level. The resulting operating regime therefore provides the reference context within which the reliability and throughput characteristics of the subsequent diversity and spatial-multiplexing schemes are interpreted.

4.2.2 Baseline Coverage and Operating-Regime Characterization

Before evaluating diversity-oriented and spatial multiplexing MIMO configurations, it is first necessary to characterize the baseline operating conditions of the considered LoRa-type wire-

less environment. In constrained LPWAN systems, communication performance is strongly determined by large-scale propagation effects, coverage limitations and the resulting operating SNR regime. Unlike conventional broadband systems, where MIMO performance is often evaluated under moderate or high-SNR conditions, LoRa-type systems typically operate close to receiver sensitivity limits. As a result, identifying the statistical operating regime becomes a critical prerequisite for meaningful evaluation of MIMO gains.

The objective of this section is to investigate the coverage behavior and operating conditions of the considered LoRa-type deployment under representative large-scale propagation effects. To isolate the impact of large-scale propagation, the analysis is intentionally restricted to distance-dependent path loss and log-normal shadowing, while excluding small-scale fading and multi-antenna transmission. This modeling approach enables the effects of propagation loss, shadowing variability and spreading-factor allocation to be examined without interference from fast-varying channel dynamics.

The adopted baseline configuration reflects typical uplink operation in sub-GHz ISM bands and is summarized in Table 4.10. A single-cell deployment is considered, with uniformly distributed static end devices and SNR-based spreading-factor allocation with a configurable margin. System behavior is primarily evaluated using statistical metrics such as SNR cumulative distribution functions, spreading-factor distributions and coverage maps, providing a representative characterization of the large-scale operating conditions of the considered LPWAN environment.

Table 4.10. Baseline simulation parameters used for coverage and operating-regime characterization.

Parameter	**Value**
Carrier frequency	868 MHz
Bandwidth	125–500 kHz
Transmit power	10–18 dBm
Noise figure	6 dB
Channel model	FSPL + excess loss + log-normal shadowing
Excess propagation loss	30 dB
Shadowing standard deviation (σ)	0–10 dB
Cell radius	Up to 2 km
Number of users	200
UE distribution	Uniform random (static)
Link direction	Uplink
Spreading factors	SF7–SF12
SF allocation	SNR-based with margin
SF margin	0–6 dB
Antenna configuration	SISO
Performance metrics	SNR CDF, SF distribution, coverage maps

To characterize the statistical operating regime of the considered LoRa-type system, the impact of three key baseline parameters is examined: cell radius, shadowing variability and spreading-factor allocation margin. These parameters jointly determine the effective coverage conditions and influence the SNR distribution experienced by end devices across the cell.

For the baseline system-level analysis, the distance-dependent propagation loss is represented by a free-space path-loss term complemented by a fixed excess-loss component used to emulate more demanding urban propagation conditions. The resulting path loss is expressed as

$$PL(d) = 32.45 + 20\log_{10}(f_{\mathrm{MHz}}) + 20\log_{10}(d_{\mathrm{km}}) + L_{\mathrm{excess}}, \tag{4.10}$$

where f_{MHz} is the carrier frequency in MHz, d_{km} is the transmitter–receiver separation in kilometers and L_{excess} denotes the additional propagation-loss term. In the considered baseline simulations, $L_{\mathrm{excess}} = 30$ dB.

Log-normal shadowing is introduced through a zero-mean Gaussian random variable $X_\sigma \sim \mathcal{N}(0, \sigma^2)$, where σ denotes the shadowing standard deviation in dB. Accordingly, the received power at the gateway from a device located at distance d from the gateway is given by

$$P_{\mathrm{rx}}(d) = P_{\mathrm{tx}} + G_{\mathrm{tx}} + G_{\mathrm{rx}} - PL(d) + X_\sigma, \tag{4.11}$$

where P_{tx} denotes the transmit power and G_{tx} and G_{rx} denote the transmitter and receiver antenna gains, respectively.

The receiver noise power and the corresponding received SNR are computed according to (4.2) and (4.3), respectively.

This formulation directly relates cell geometry and shadowing variability to the statistical SNR distribution experienced by the end devices.

Finally, spreading-factor adaptation is implemented through an SNR-based allocation rule. For each device, the selected spreading factor is the lowest spreading factor whose SNR requirement is satisfied after accounting for the specified allocation margin:

$$SF^\star = \min\left\{SF \in \{SF7, \ldots, SF12\} : \mathrm{SNR}_{\mathrm{dB}} \geq \gamma_{SF} + M_{SF}\right\}, \tag{4.12}$$

where γ_{SF} denotes the SNR threshold associated with the receiver sensitivity of the corresponding spreading factor and M_{SF} denotes the spreading-factor allocation margin. The SNR thresholds are obtained from the spreading-factor-specific receiver sensitivities according to

$$\gamma_{SF} = S_{SF} - P_{\mathrm{noise}}, \tag{4.13}$$

where S_{SF} denotes the receiver sensitivity associated with the considered spreading factor. If no spreading factor satisfies the required SNR condition, the corresponding device is classified as being outside the feasible coverage region.

Through this baseline characterization, the combined effects of propagation loss, shadowing variability and spreading-factor allocation are mapped onto the resulting SNR operating

regime, providing the reference conditions for the subsequent evaluation of diversity-oriented and spatial multiplexing MIMO schemes.

Impact of Cell Radius

The impact of cell radius on the operating SNR distribution is illustrated in Figure 4.25. Increasing the cell radius progressively shifts the SNR cumulative distribution toward lower values, reflecting the increased path loss experienced by devices located farther from the gateway. The effect is clearly visible across the examined deployment scales, with the 2 km configuration exhibiting substantially lower SNR values than the 500 m case over most of the user population. This behavior demonstrates that coverage expansion directly shifts a larger fraction of devices toward more challenging low-SNR operating conditions and therefore increases the importance of robust transmission mechanisms.

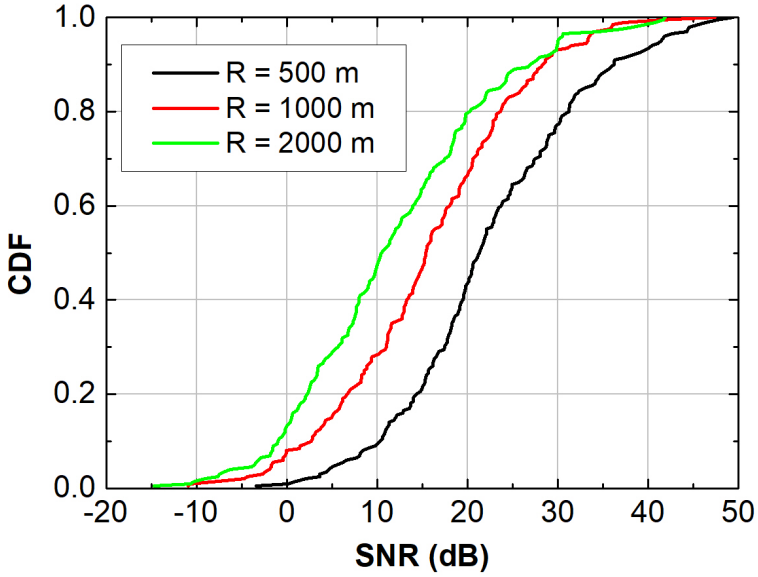


Figure 4.25. CDF of received SNR for different cell radius values.

Impact of Shadowing Variability

In addition to distance-dependent propagation loss, shadowing introduces substantial variability in the operating conditions experienced across the user population. As shown in Figure 4.26, increasing the shadowing standard deviation progressively broadens the SNR distribution. Compared with the deterministic $\sigma = 0$ dB case, larger shadowing values increase the occurrence of both unfavorable low-SNR realizations and favorable high-SNR realizations, producing a substantially wider operating range. From a reliability perspective, the lower-SNR tail is particularly important, since stronger shadowing variability increases the fraction of devices exposed to challenging communication conditions. This result highlights

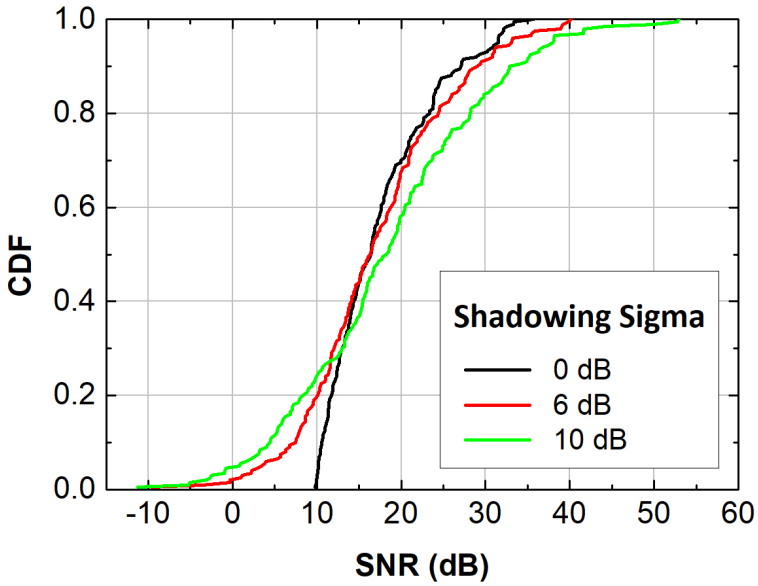


Figure 4.26. CDF of received SNR for different shadowing standard deviation values.

that average SNR alone is insufficient to characterize coverage robustness in heterogeneous LPWAN environments.

Impact of Spreading-Factor Allocation Margin

The effect of the spreading-factor allocation margin is illustrated in Figure 4.27. In contrast to cell radius and shadowing variability, the allocation margin does not directly modify the received SNR, since it is applied after SNR calculation as part of the spreading-factor selection rule. Consequently, the SNR distributions remain broadly similar across the examined margin values, as expected from the adopted model. The role of the margin is instead to impose a more conservative criterion for spreading-factor assignment: increasing M_{SF} requires a larger SNR excess above the corresponding spreading-factor threshold, potentially resulting in the selection of more robust spreading factors or in devices being classified outside the feasible operating region when no spreading factor satisfies the required condition. Therefore, the allocation margin primarily affects adaptation and coverage feasibility rather than the underlying propagation-induced SNR distribution.

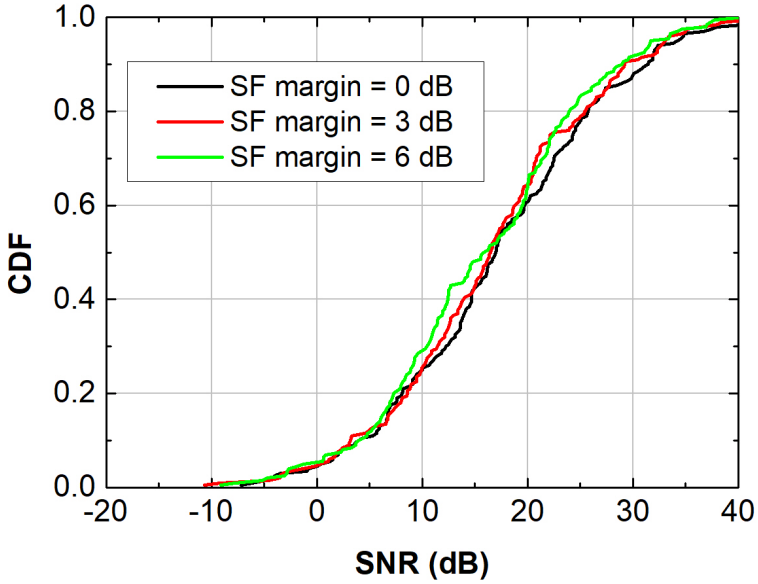


Figure 4.27. CDF of received SNR under different spreading-factor allocation margins.

Overall, the baseline characterization quantifies how deployment scale, shadowing variability and spreading-factor adaptation shape the operating and feasibility conditions of the considered LoRa-type framework. First, increasing the cell radius shifts the received-SNR distribution toward lower values, demonstrating the direct effect of deployment scale and distance-dependent propagation loss on coverage conditions. Second, increasing shadowing variability broadens the SNR distribution and extends the low-SNR tail, showing that environmental heterogeneity affects not only average link conditions but, more importantly, the variability and robustness of coverage across the user population. Third, the spreading-factor allocation margin does not directly alter the underlying SNR distribution; instead, it modifies the adaptation and feasibility conditions by imposing a more conservative criterion for spreading-factor selection. The baseline analysis therefore distinguishes between propagation mechanisms that determine the available link quality and adaptation mechanisms that determine how this link quality can be effectively exploited.

These findings establish the operating context required for the subsequent MIMO characterization. In particular, they demonstrate that the potential benefit of multi-antenna transmission cannot be assessed independently of the underlying propagation and feasibility regime. When operation extends toward low-SNR and highly variable conditions, additional spatial resources may become particularly valuable for improving reliability and robustness, whereas the performance benefit of spatial multiplexing depends on whether the available link quality is sufficient to support multiple simultaneous streams. The baseline characterization therefore defines the conditions under which the following analysis evaluates whether diversity-oriented MIMO can extend reliable operation and whether spatial multiplexing remains practically beneficial under constrained LoRa-type conditions.

4.2.3 Diversity-Oriented MIMO Analysis

Following the baseline operating-regime characterization presented in the previous subsection, the analysis now transitions from system-level coverage evaluation to link-level performance analysis of diversity-oriented MIMO schemes under representative LoRa-type operating conditions. Since constrained LPWAN environments are primarily reliability- and coverage-oriented rather than throughput-driven, spatial diversity constitutes the most natural first MIMO strategy to examine. The objective is therefore to determine whether diversity-oriented transmission can provide meaningful reliability gains within the constrained low-SNR regime identified previously and to assess the extent to which these gains remain robust under imperfect channel state information.

The analysis focuses on space–time block coding (STBC)-based MIMO configurations, which are well aligned with the reliability-oriented operating characteristics of LoRa-type systems. Performance is evaluated in terms of bit error rate (BER) as a function of signal-to-noise ratio (SNR), considering both perfect and imperfect channel state information. Channel uncertainty is modeled using the CSI error framework introduced in Chapter 2 and the CEEM models adopted in the present LoRa-type simulation framework, enabling systematic evaluation of diversity robustness under progressively increasing CSI uncertainty.

The analysis begins under ideal channel conditions assuming perfect CSI, allowing the intrinsic performance gains of spatial diversity to be isolated without the influence of channel estimation errors. The objective at this stage is to establish the baseline performance hierarchy among the considered diversity-oriented MIMO configurations and to identify the relative impact of different antenna arrangements on link reliability.

The BER performance of the examined antenna configurations under perfect CSI is illustrated in Figures 4.28 and 4.29. As expected, all considered configurations exhibit a monotonic BER decrease with increasing SNR, confirming the expected reliability improvement under favorable channel conditions. A clear performance hierarchy emerges across the examined antenna setups, with configurations benefiting from additional receive-side diversity generally exhibiting steeper BER reduction and lower error rates across the considered SNR range.

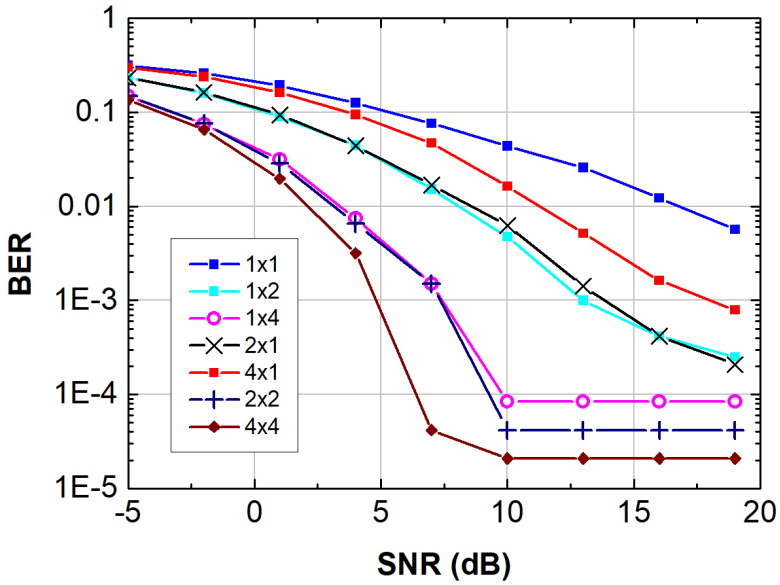


Figure 4.28. BER versus SNR for diversity-oriented MIMO configurations under perfect CSI with SF9.

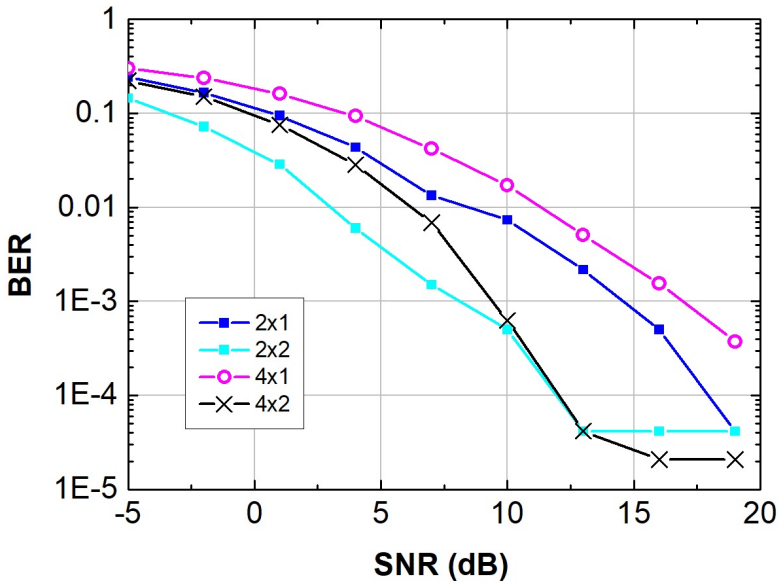


Figure 4.29. BER versus SNR for diversity-oriented MIMO configurations under perfect CSI.

A particularly important observation is the strong role of receive-side diversity in improving link reliability. Configurations employing multiple receive antennas generally achieve lower BER than the corresponding transmit-diversity-oriented configurations. This asymmetry between transmit- and receive-side scaling is also influenced by the adopted constant-total-transmit-power normalization: additional transmit antennas share the available transmit power, whereas additional receive antennas provide further independently faded observations that can be combined at the receiver without dividing the transmitted power among them. Increasing the number of receive antennas therefore provides more effective mitigation of fading and substantially improves BER performance within the adopted simulation framework. These results establish the baseline diversity hierarchy under ideal channel knowledge and provide the reference framework for evaluating the impact of imperfect CSI in the following analysis. After establishing the baseline diversity hierarchy under ideal channel conditions, the analysis proceeds to investigate the robustness of diversity-oriented MIMO schemes under imperfect CSI. The objective is to determine how channel uncertainty affects the achievable diversity gains and to identify the operating conditions under which CSI quality becomes a significant performance-limiting factor. Two complementary CSI error models are considered to represent distinct forms of channel uncertainty: a fixed-error model, in which the estimation-error variance remains independent of SNR and an SNR-dependent model, in which the estimation accuracy improves with the available signal quality and the considered pilot parameter.

Under CEEM-I, imperfect CSI progressively degrades the BER performance of all examined antenna configurations, as illustrated in Figures 4.30, 4.31 and 4.32. At low and moderate SNR values, channel uncertainty initially appears as a performance penalty relative to the perfect-CSI baseline. However, as SNR increases, the effect of the fixed channel-estimation error becomes increasingly dominant. Since the estimation-error variance σ_e^2 remains constant under CEEM-I, increasing the received SNR cannot eliminate the mismatch between the actual and estimated channel coefficients. Consequently, the BER curves progressively deviate from the perfect-CSI reference and, for sufficiently large estimation errors, exhibit clear saturation tendencies and error-floor behavior at high SNR.

The severity of this CSI-induced limitation depends strongly on both the estimation-error variance and the antenna configuration. As shown in Figure 4.30, configurations incorporating receive-side diversity achieve substantially lower BER than their single-receive-antenna counterparts, indicating greater robustness to fixed channel-estimation errors. Figures 4.31 and 4.32 further show that increasing σ_e^2 raises the residual BER level and causes the CSI-limited regime to emerge more prominently as SNR increases. Although receive diversity substantially mitigates this degradation, it does not eliminate the fundamental limitation imposed by an estimation error whose variance remains independent of SNR. These results demonstrate that under CEEM-I, spatial diversity improves robustness to imperfect CSI, while the attainable high-SNR reliability ultimately remains constrained by the quality of the available channel estimate.

Importantly, the relative advantage of higher-diversity antenna configurations is largely

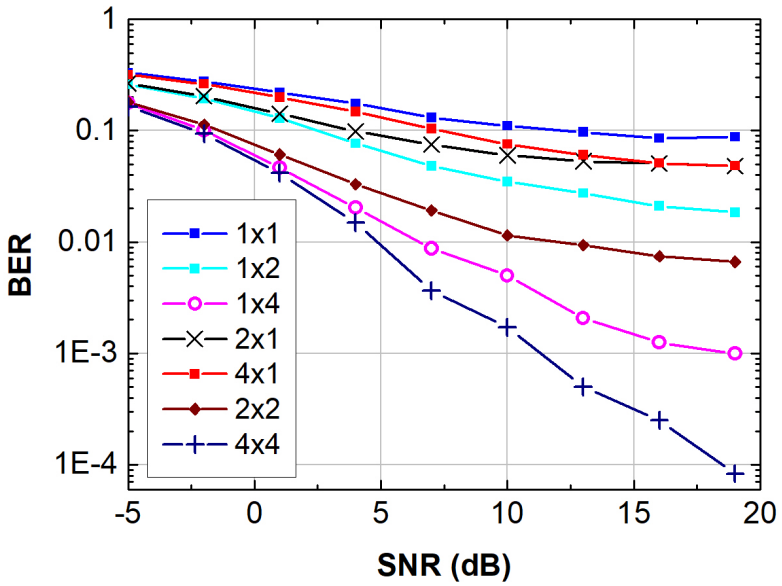


Figure 4.30. BER versus SNR for diversity-oriented MIMO configurations under CEEM-I.

preserved under CEEM-I, indicating that additional spatial diversity remains beneficial even in the presence of CSI uncertainty. However, as the estimation-error variance remains fixed with increasing SNR, the achievable reliability improvement becomes progressively limited by residual CSI uncertainty.

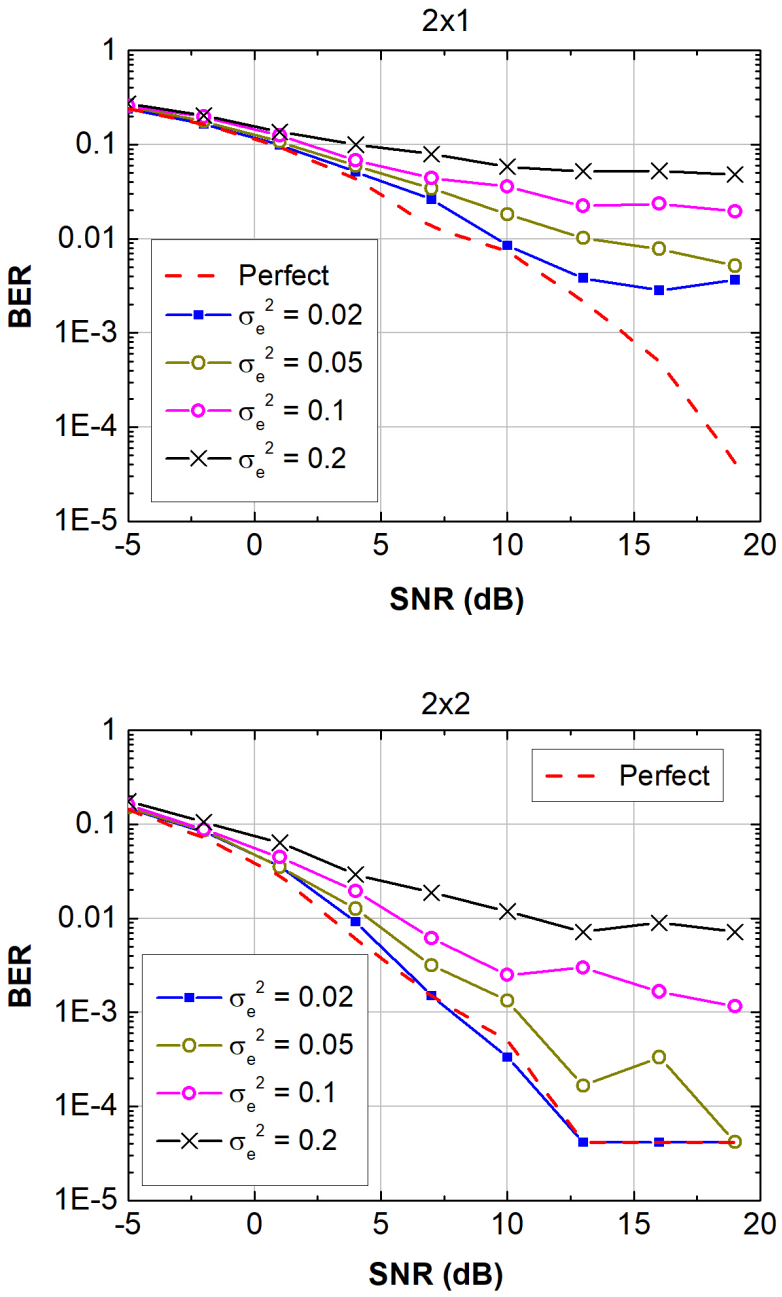


Figure 4.31. BER versus SNR under different CEEM-I uncertainty levels for the 2×1 and 2×2 configurations.

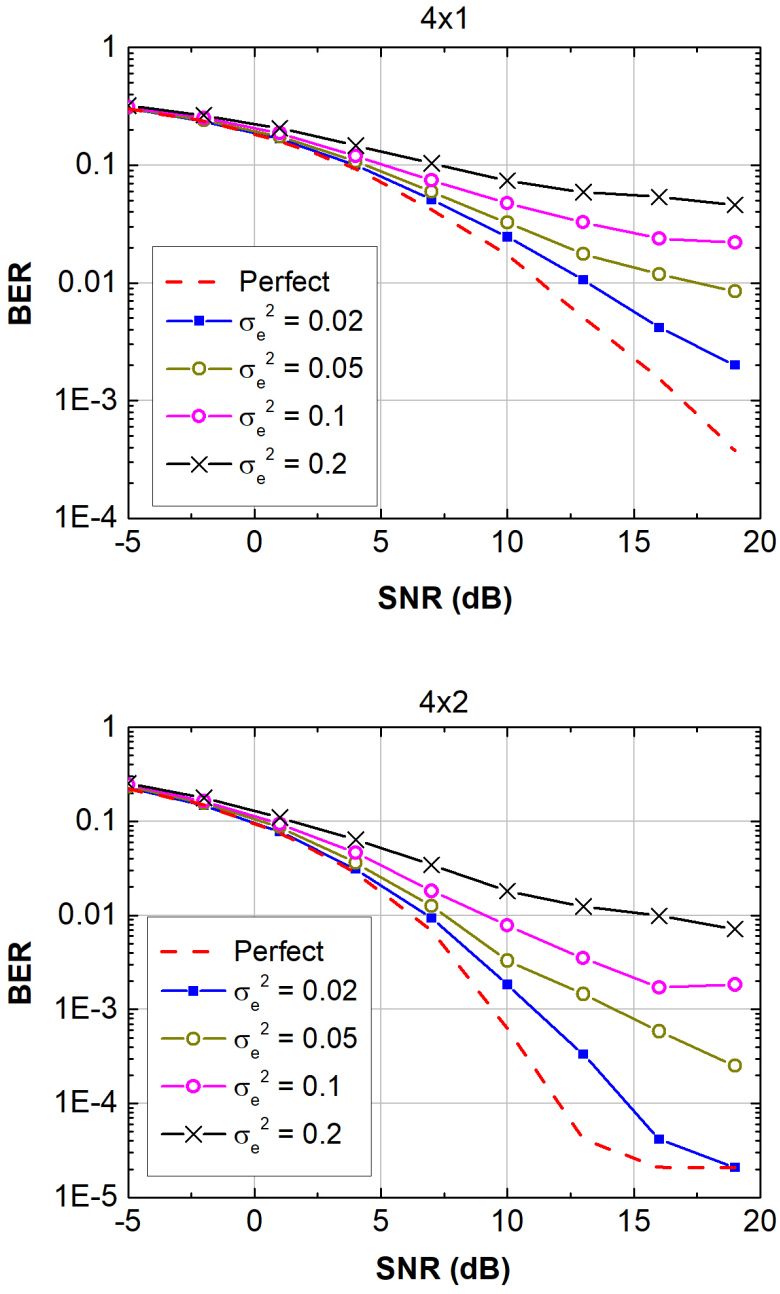


Figure 4.32. BER versus SNR under different CEEM-I uncertainty levels for the 4×1 and 4×2 configurations.

Under CEEM-II, a fundamentally different behavior is observed because the channel-estimation error variance is no longer constant, but decreases with the operating SNR according to $\sigma_e^2 = 1/(1 + L_p\gamma_s)$. Consequently, increasing SNR improves not only the received signal quality but also the accuracy of the channel estimate. As illustrated in Figures 4.33, 4.34, and 4.35, BER therefore continues to decrease as SNR increases, while the performance under imperfect CSI progressively approaches the corresponding perfect-CSI behavior. This contrasts directly with CEEM-I, where the fixed estimation-error variance increasingly limits performance at high SNR.

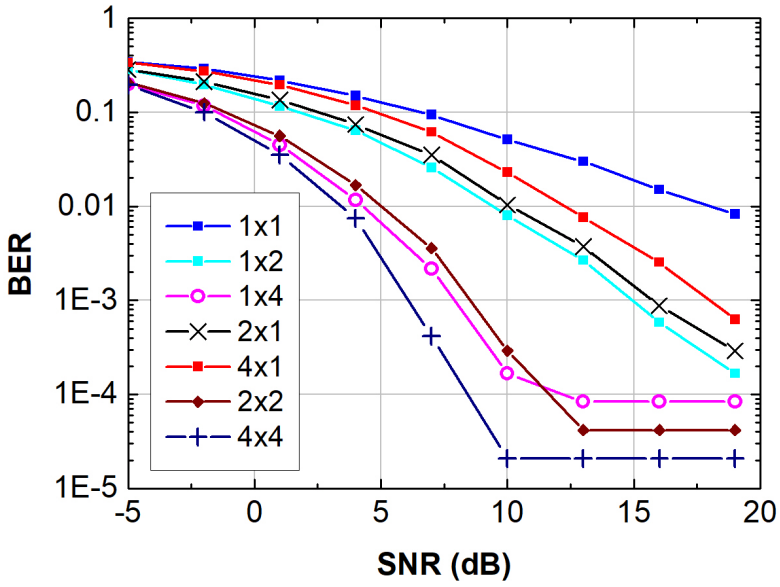


Figure 4.33. BER versus SNR for diversity-oriented MIMO configurations under CEEM-II.

The influence of the pilot parameter L_p is particularly evident in Figures 4.34 and 4.35. Increasing L_p from 2 to 4 and 8 reduces the channel-estimation error variance and generally brings the BER curves closer to the perfect-CSI reference, with the differences becoming progressively less pronounced as SNR increases. At high SNR, some higher-diversity configurations reach the minimum BER observable with the adopted finite Monte Carlo sample size; these points should therefore be interpreted as simulation-resolution limits rather than physical error floors. Overall, the CEEM-II results demonstrate that diversity gains can be largely preserved when CSI quality improves together with SNR, while additional pilot resources accelerate the recovery toward perfect-CSI performance.

Under CEEM-II, the benefit of additional spatial diversity remains clearly observable across the examined antenna configurations. Since the estimation-error variance decreases with increasing SNR, higher-diversity configurations can progressively exploit their spatial combining gains without being subject to the persistent CSI-induced limitation observed under CEEM-I. Taken together, the CEEM-I and CEEM-II results reveal two fundamentally different forms of CSI sensitivity in diversity-oriented LoRa MIMO systems. Under CEEM-I, the estimation-error variance remains fixed independently of SNR.

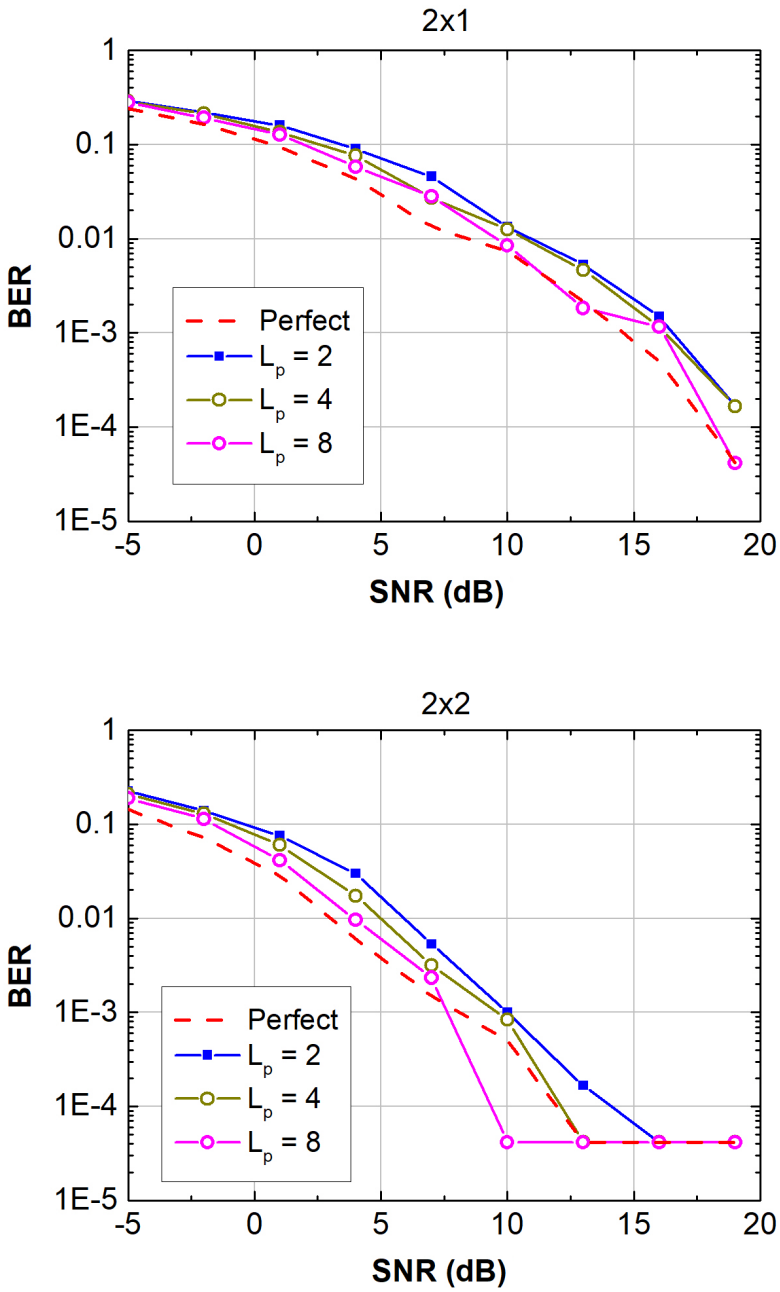


Figure 4.34. BER versus SNR under different CEEM-II uncertainty levels for the 2×1 and 2×2 configurations.

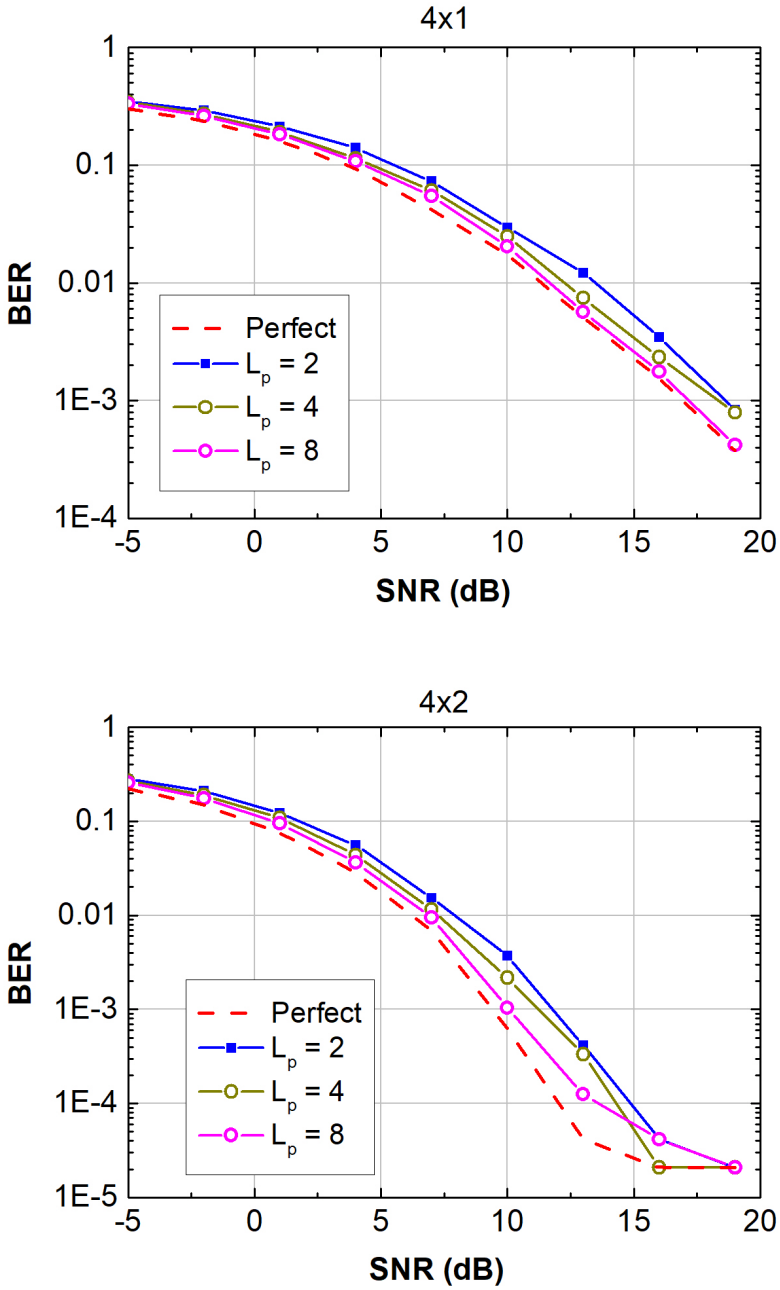


Figure 4.35. BER versus SNR under different CEEM-II uncertainty levels for the 4×1 and 4×2 configurations.

Consequently, as thermal-noise effects diminish with increasing SNR, the residual CSI uncertainty becomes progressively more influential and can limit the achievable BER improvement. In contrast, under CEEM-II, the estimation-error variance decreases with SNR according to the adopted pilot-dependent model. The improvement in received signal quality is therefore accompanied by increasingly accurate channel estimation, allowing the BER performance to progressively approach the corresponding perfect-CSI behavior.

These observations demonstrate that the effectiveness of diversity-oriented MIMO in constrained LoRa-type environments depends not only on the magnitude of CSI uncertainty, but also on how this uncertainty evolves with operating conditions. Spatial diversity remains highly beneficial when channel estimates are sufficiently accurate, while persistent estimation errors, as represented by CEEM-I, can increasingly constrain the achievable gains at higher SNR. Conversely, when estimation quality improves with SNR, as in CEEM-II, a substantial part of the diversity advantage can be recovered. CSI quality and its dependence on the operating SNR therefore constitute key factors governing reliable MIMO operation in low-power wireless systems.

Beyond the BER curve analysis, additional insight can be obtained by examining the SNR requirements needed to satisfy specific target reliability levels. This perspective provides a more practical interpretation of diversity gains by quantifying the effective SNR reduction required to achieve predefined BER targets under different antenna configurations and CSI conditions.

The target-BER analysis confirms the substantial reliability benefits provided by diversity-oriented MIMO configurations. Higher-order diversity schemes require lower SNR values to achieve the same BER target, demonstrating clear SNR savings compared to lower-order or single-antenna configurations. Among the examined setups, configurations with increased receive diversity achieve the largest reductions in required SNR, further reinforcing the dominant role of receive-side diversity in constrained LoRa-type environments.

In addition to antenna diversity, the adopted spreading-factor representation provides further insight into the interaction between LoRa-type transmission parameters and link reliability. Within the considered simulation framework, higher spreading factors are represented through an effective-SNR adjustment that captures the expected processing-gain tendency associated with increased spreading. The resulting BER behavior indicates that this additional robustness can complement the reliability gains obtained through spatial diversity, particularly in low-SNR operating conditions. These results should therefore be interpreted as a system-level assessment of the combined influence of spreading-related processing gain and MIMO diversity within the adopted LoRa-type abstraction, rather than as a full waveform-level characterization of LoRa modulation.

Taken together, the target-BER and spreading-factor analyses provide a practical interpretation of the diversity results. In constrained low-power operating environments, reliable communication depends on the combined interaction between antenna diversity, operating SNR, CSI quality and transmission parameters represented by the spreading factor. Receive-side

diversity emerges as a particularly effective mechanism for reliability enhancement, especially in low-SNR operating regions. At the same time, the contrasting CEEM-I and CEEM-II results demonstrate that the extent to which diversity gains can be exploited depends strongly on the underlying CSI-error behavior: persistent estimation uncertainty can constrain performance, whereas SNR-dependent improvements in channel estimation allow the system to progressively approach the corresponding perfect-CSI behavior.

Overall, these findings characterize diversity-oriented MIMO as an effective reliability-oriented strategy within the considered LoRa-type framework. Spatial diversity can substantially improve communication robustness under constrained operating conditions, while its effectiveness depends on antenna configuration, operating SNR, channel-estimation quality and the adopted transmission parameters. The combined results further demonstrate that CSI uncertainty should not be treated as a single fixed impairment, since its dependence on operating conditions can significantly alter the achievable reliability gains. Similarly, the observed spreading-factor trends should be interpreted within the effective-SNR abstraction adopted in this study, providing an indication of the potential complementary role of spreading and spatial diversity rather than a waveform-level evaluation of LoRa PHY performance.

4.2.4 Spatial Multiplexing Analysis

Having examined diversity-oriented MIMO schemes under constrained LoRa-type operating conditions, the analysis now shifts to spatial multiplexing. Unlike diversity-oriented transmission, which prioritizes communication reliability and robustness, spatial multiplexing aims to increase transmission efficiency by enabling parallel data streams over the same time-frequency resources. This introduces a fundamentally different operating trade-off, where higher throughput potential is achieved at the cost of increased receiver complexity and higher sensitivity to channel impairments.

The objective of this subsection is to evaluate the feasibility of spatial multiplexing in constrained LoRa-type wireless environments and, in particular, to characterize its sensitivity to imperfect channel state information. Although current LoRa and LPWAN deployments primarily rely on single-antenna, reliability-oriented communication, spatial multiplexing remains an important reference case for future infrastructure-assisted or gateway-centric scenarios where increased throughput, parallel transmission capability or gateway-side multi-antenna processing may become desirable.

The analysis focuses on spatial multiplexing with linear Zero-Forcing (ZF) and Minimum Mean Square Error (MMSE) receivers under simulation assumptions and channel models consistent with those adopted in the preceding diversity analysis. This provides a controlled basis for comparing diversity-oriented and multiplexing-oriented MIMO strategies under comparable operating conditions. The evaluation proceeds progressively, beginning with a baseline verification under perfect CSI, followed by analysis under imperfect channel conditions and concluding with throughput-oriented performance evaluation using packet-level and normalized goodput metrics.

Three representative transmission strategies are examined: (i) STBC-based diversity transmission, serving as a reliability-oriented reference, (ii) spatial multiplexing with Zero-Forcing (ZF) detection and (iii) spatial multiplexing with Minimum Mean Square Error (MMSE) detection. System performance is evaluated in terms of BER as a function of SNR for a fixed spreading factor (SF9), consistent with the low-data-rate and low-SNR operating conditions that characterize typical LoRa-type communication.

Perfect-CSI Baseline: Diversity versus Spatial Multiplexing

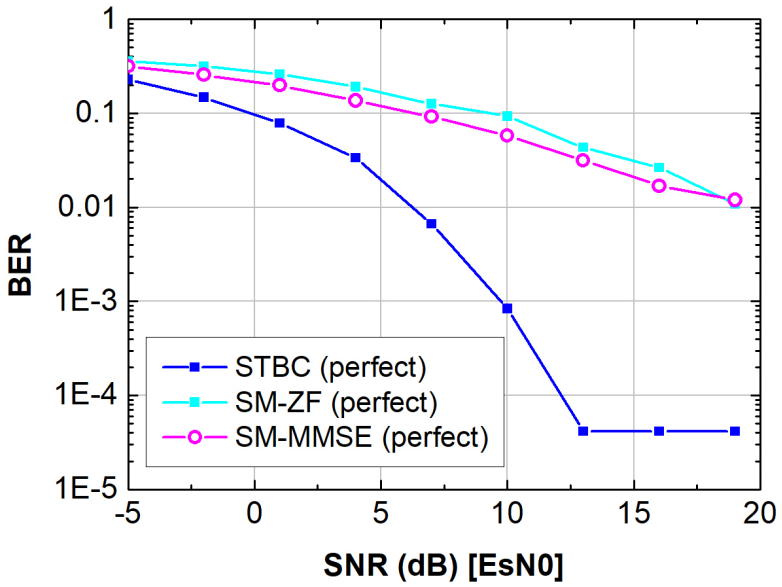


Figure 4.36. BER versus SNR for different transmission mechanisms under perfect CSI.

The resulting BER performance is shown in Figure 4.36. All examined schemes exhibit the expected monotonic BER reduction with increasing SNR. A clear performance hierarchy emerges across the examined transmission mechanisms, with STBC providing the strongest BER performance, particularly in the low-SNR region that is of primary interest for the considered LoRa-type operating framework.

In contrast, spatial multiplexing schemes exhibit noticeably higher BER at low SNR due to the increased detection burden associated with parallel data streams and inter-stream interference suppression. Across the examined SNR range, MMSE provides better BER performance than ZF detection. This behavior is consistent with the operating principles of the two linear detectors, since MMSE explicitly accounts for noise power during detection and therefore reduces the noise-enhancement penalty associated with ZF, particularly when thermal noise remains significant. These results establish the perfect-CSI reference for the subsequent imperfect-CSI analysis and illustrate the expected trade-off between reliability-oriented diversity and throughput-oriented spatial multiplexing. It should be emphasized, however, that the BER comparison alone does not capture the potential benefit of spatial multiplexing, since

its primary objective is not to minimize the error probability but to increase the aggregate transmission capability through parallel spatial streams. The higher BER observed for spatial multiplexing therefore represents a reliability cost that must subsequently be evaluated against the potential gain in effective goodput.

Having established the baseline performance under ideal channel knowledge, the analysis now examines the impact of imperfect CSI on spatial multiplexing performance. The objective is to determine how channel estimation errors affect the reliability of multiplexing-oriented transmission and to assess the relative robustness of ZF and MMSE detection under constrained LoRa-type operating conditions. Channel uncertainty is modeled using the CEEM-I framework introduced previously, enabling controlled evaluation of CSI mismatch effects under fixed estimation error levels.

Particular emphasis is placed on comparing the behavior of spatial multiplexing schemes against the diversity-oriented STBC baseline. This comparison is especially important in constrained low-SNR environments, where the performance penalty associated with imperfect CSI may fundamentally alter the feasibility of throughput-oriented transmission strategies.

Impact of CSI Uncertainty on Spatial Multiplexing

The BER performance under imperfect CSI is presented in Figure 4.37. A clear difference in CSI sensitivity is observed among the examined transmission mechanisms. The STBC scheme, shown in Figure 4.37(c), exhibits relatively graceful performance degradation as channel estimation errors increase, maintaining robust BER behavior even under moderate CSI uncertainty. This observation is fully consistent with the diversity-oriented behavior identified in the previous subsection and further confirms the strong robustness of STBC-based transmission in constrained LoRa-type environments.

In contrast, spatial multiplexing with ZF detection, shown in Figure 4.37(a), exhibits substantially higher sensitivity to CSI imperfections. Increasing the channel-estimation error produces a pronounced BER degradation, since channel inversion based on imperfect CSI introduces residual inter-stream interference in addition to the noise-enhancement behavior inherent to ZF detection. Moreover, because the CEEM-I estimation-error variance remains fixed as SNR increases, the relative influence of channel mismatch becomes progressively more important as thermal-noise effects diminish. Consequently, increasing SNR cannot fully compensate for persistent CSI uncertainty, particularly at the larger examined values of σ_e^2.

MMSE detection, presented in Figure 4.37(b), provides some robustness improvement over ZF, particularly in the low-to-moderate SNR region, where its regularized detection structure limits the noise-enhancement effects associated with direct channel inversion. However, the results also show that this advantage does not remove the fundamental sensitivity of spatial multiplexing to persistent CSI uncertainty. As the CEEM-I estimation-error variance remains independent of SNR, residual channel mismatch increasingly dominates the detection process at higher SNR, leading to pronounced BER limitations for both ZF and MMSE as σ_e^2 increases.

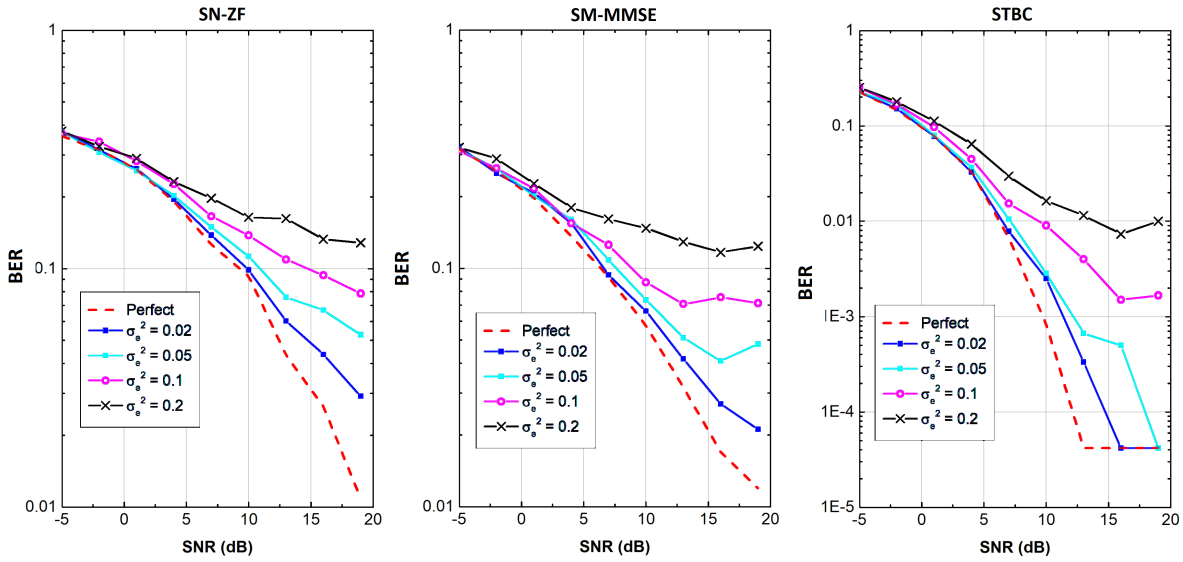


Figure 4.37. BER versus SNR under CEEM-I for different transmission and detection schemes in a 2×2 MIMO configuration: (a) spatial multiplexing with ZF detection, (b) spatial multiplexing with MMSE detection, and (c) STBC transmission.

Overall, the comparison demonstrates that imperfect CSI affects diversity- and multiplexing-

oriented transmission in fundamentally different ways. STBC retains a substantial reliability advantage under CSI uncertainty, whereas spatial multiplexing is considerably more dependent on accurate channel knowledge because stream separation itself relies on the estimated channel matrix. Under CEEM-I, increasing SNR therefore cannot fully recover the multiplexing performance when the CSI error remains fixed, making channel-estimation quality a critical factor in determining whether spatial multiplexing is beneficial.

Impact of Antenna Scaling and Receiver Rank

A quantitative comparison between ZF and MMSE further illustrates this robustness advantage. Table 4.11 reports the relative BER reduction achieved by MMSE with respect to ZF, defined as

$$\Delta_{\mathrm{BER}} = \frac{\mathrm{BER}_{\mathrm{ZF}} - \mathrm{BER}_{\mathrm{MMSE}}}{\mathrm{BER}_{\mathrm{ZF}}} \times 100\%. \tag{4.14}$$

Positive values therefore indicate lower BER for MMSE.

Table 4.11. Relative BER reduction achieved by MMSE compared with ZF under CEEM-I.

SNR (dB)	$\sigma_e^2 = 0.02$	$\sigma_e^2 = 0.20$
4	24.7%	22.2%
10	26.6%	19.0%
16	37.8%	12.0%

Taken together, these results reveal a substantially higher sensitivity of spatial multiplexing to CSI uncertainty compared with diversity-oriented transmission. While MMSE provides a clear robustness advantage over ZF, both multiplexing receivers remain more sensitive to persistent channel-estimation errors than the STBC reference. Under CEEM-I, this sensitivity becomes particularly relevant as SNR increases because the estimation-error variance remains fixed while thermal-noise effects diminish. The achievable reliability of spatial multiplexing therefore becomes increasingly dependent on CSI accuracy rather than on received SNR alone.

These observations reinforce the reliability–throughput trade-off identified throughout this analysis. Diversity-oriented transmission provides greater robustness to CSI mismatch, whereas spatial multiplexing offers increased parallel transmission capability at the cost of greater sensitivity to channel uncertainty. Whether this reliability penalty is justified cannot be determined from BER alone; it must be assessed together with the additional transmission capability provided by multiple spatial streams. This motivates the subsequent scaling and throughput-oriented analyses.

Following the CSI sensitivity analysis, the evaluation now examines how antenna configuration scaling affects the performance of spatial multiplexing in constrained LoRa-type environments. The objective is to determine under which operating conditions spatial multiplexing can provide meaningful system-level benefits and to identify the roles of transmit-side scaling and receiver rank in shaping achievable performance under imperfect CSI.

The scaling analysis focuses exclusively on spatial multiplexing with MMSE detection, since MMSE demonstrated superior robustness compared to ZF in the presence of channel estimation errors. Two complementary scaling dimensions are examined. First, transmit-side scaling is investigated by increasing the number of transmit antennas while keeping the number of receive antennas and consequently the supported number of spatial streams, fixed. Second, receiver-rank scaling is analyzed by varying the number of receive antennas under fixed transmit dimensionality. This enables the effect of additional transmit-side spatial resources to be distinguished from the throughput gains associated with an increased number of supported spatial streams.

The first scaling scenario compares the 2×2, 4×2 and 4×4 configurations under identical CSI conditions. The comparison between 2×2 and 4×2 specifically examines whether additional transmit-side spatial resources provide practical performance benefits when the receiver dimension limits the number of simultaneously supported streams to $N_s = 2$. The 4×4 configuration subsequently represents the full-rank case with $N_s = 4$, allowing the effect of increased multiplexing order to be evaluated.

The BER and PER results shown in Figures 4.38, 4.39, and 4.40 indicate that increasing transmit dimensionality from 2×2 to 4×2 yields only marginal reliability improvements. Although slight BER gains are observed in medium-to-high SNR regions, these improvements do not translate into meaningful packet-level reliability benefits. This behavior confirms that when receiver rank constrains the number of detectable spatial streams, transmit-side scaling alone provides limited performance gains under imperfect CSI.

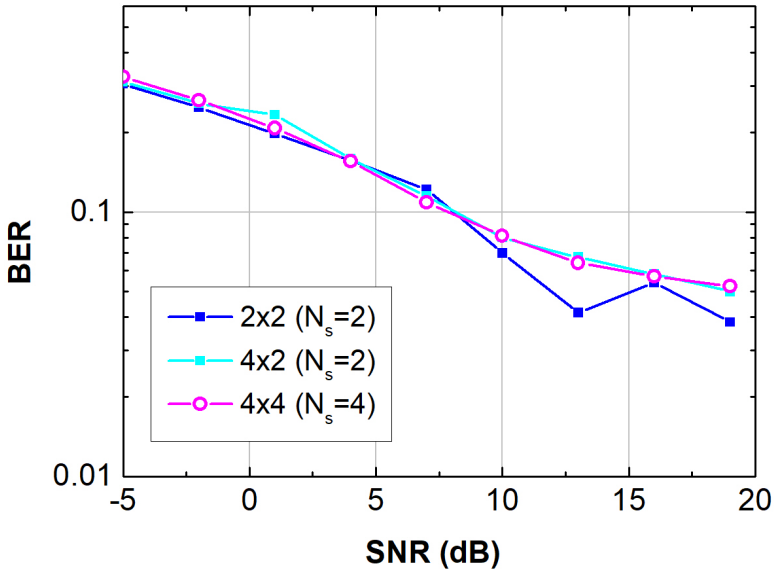


Figure 4.38. BER versus SNR for different antenna configurations using spatial multiplexing with MMSE detection.

A fundamentally different behavior emerges for the 4×4 configuration. While full-rank spatial multiplexing does not improve BER and significantly increases packet error probability

due to the higher multiplexing order and increased detection burden, its behavior changes considerably when evaluated through throughput-oriented metrics. As shown in Figure 4.40, the increased number of parallel spatial streams enables substantially higher normalized goodput in sufficiently favorable operating conditions. This reveals a clear reliability–throughput trade-off: full-rank multiplexing sacrifices reliability in exchange for increased aggregate transmission capability.

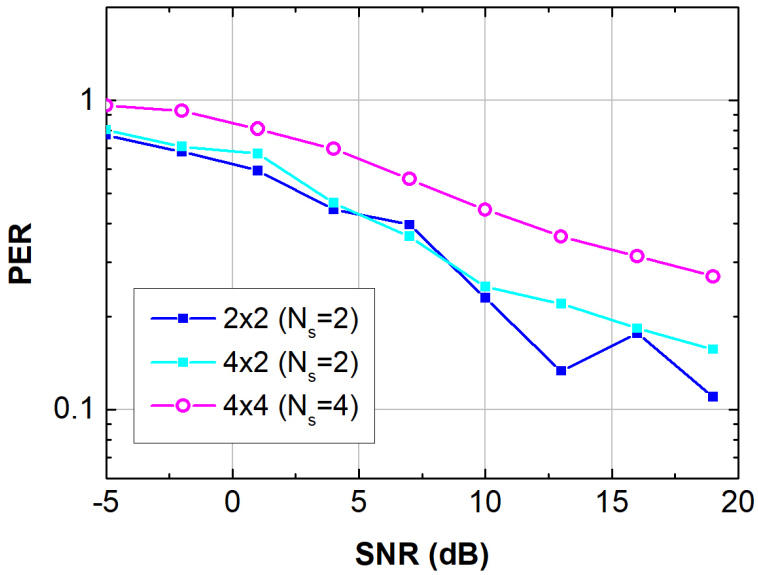


Figure 4.39. PER versus SNR for different antenna configurations using spatial multiplexing with MMSE detection.

The second scaling scenario isolates the impact of receiver rank by fixing transmit dimensionality and varying the number of receive antennas. This analysis reveals a much clearer distinction between reliability-oriented and throughput-oriented performance metrics.

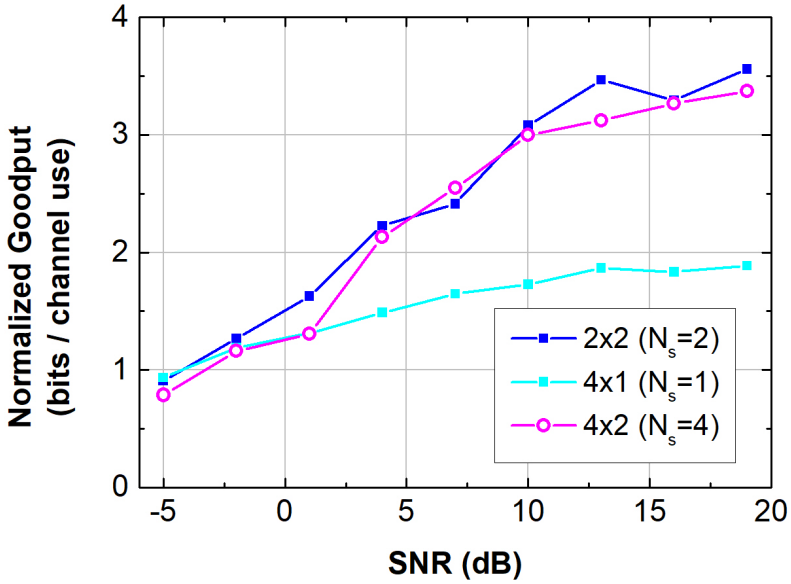


Figure 4.40. Normalized goodput versus SNR for different antenna configurations using spatial multiplexing with MMSE detection.

As shown in Figure 4.41, lower-rank configurations exhibit superior packet-level reliability because fewer spatial streams must be simultaneously separated at the receiver, reducing the impact of inter-stream interference and CSI mismatch. However, their achievable throughput remains fundamentally constrained. In contrast, increasing receiver rank enables the activation of additional spatial streams, resulting in substantially higher normalized goodput at medium and high SNR values, as illustrated in Figure 4.42.

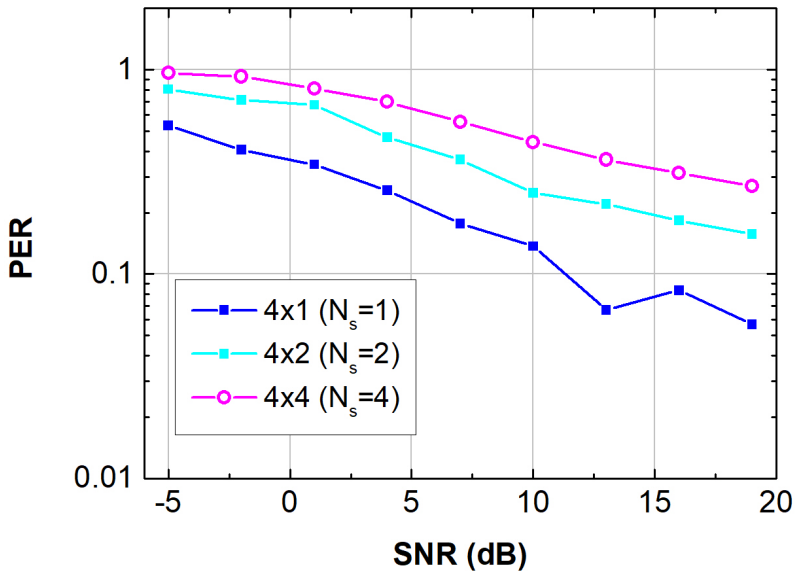


Figure 4.41. PER versus SNR for different receiver-rank configurations using spatial multiplexing with MMSE detection.

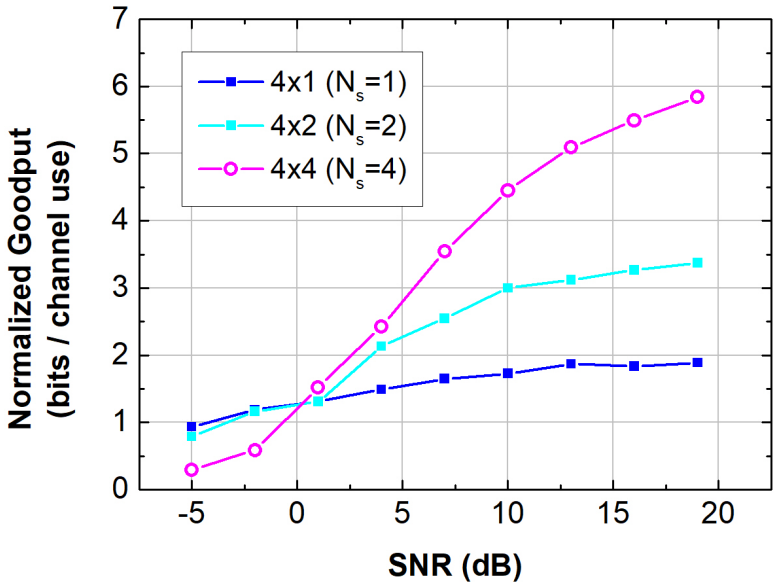


Figure 4.42. Normalized goodput versus SNR for different receiver-rank configurations using spatial multiplexing with MMSE detection.

These results demonstrate that the gains of spatial multiplexing become most evident when performance is evaluated through throughput-oriented metrics rather than BER or PER alone. Increasing the number of supported spatial streams may degrade packet-level reliability while simultaneously increasing effective data delivery when the operating SNR is sufficiently favorable.

Overall, the scaling analysis shows that additional transmit antennas alone provide limited benefit when the receive dimension keeps the number of spatial streams fixed. In contrast, increasing receiver rank can enable a higher multiplexing order and substantially increase normalized goodput, although this gain is accompanied by a reliability penalty. The value of spatial multiplexing is therefore determined by the interaction among receiver rank, operating SNR, CSI quality and the number of simultaneously transmitted streams. Taken together, the BER, PER and goodput results reveal that antenna scaling is beneficial only when it translates into exploitable spatial rank. Increasing the number of transmit antennas while keeping the number of supported streams fixed produces only marginal gains, whereas increasing the receiver dimension enables additional spatial streams and can substantially improve effective data delivery. This improvement, however, is obtained at the expense of packet-level reliability. Consequently, the preferred MIMO configuration changes with the operating objective: low-rank transmission is favored when reliability dominates, whereas higher-rank spatial multiplexing becomes advantageous when channel conditions are sufficiently favorable for the additional streams to compensate for their increased error probability.

These findings characterize spatial multiplexing in the considered LoRa-type framework as a selective, throughput-oriented strategy rather than a universally advantageous MIMO mode. Diversity-oriented transmission remains preferable when reliability is the dominant

requirement or operating conditions are unfavorable, whereas higher-rank spatial multiplexing becomes attractive when sufficient SNR, receiver dimensionality and CSI quality allow the additional spatial streams to produce a net gain in effective data delivery. This strongly condition-dependent behavior provides direct motivation for the adaptive and context-aware MIMO selection examined in the subsequent optimization-oriented analysis.

4.2.5 LoRa Characterization Discussion and Design Implications

This section synthesizes the main findings of the simulation-based characterization of MIMO techniques under constrained LoRa-type operating conditions. The objective is not only to compare the individual performance trends observed in the preceding coverage, diversity and spatial-multiplexing analyses, but also to identify recurring relationships between operating conditions, antenna configuration, CSI quality and transmission objective. Particular attention is therefore given to the conditions under which spatial diversity and spatial multiplexing remain beneficial and to the factors that determine their practical applicability in low-SNR and reliability-constrained wireless environments.

The preceding analysis covered complementary aspects of constrained MIMO operation, beginning with coverage and operating-region characterization and subsequently examining diversity-oriented and multiplexing-oriented transmission under perfect and imperfect CSI. Across these analyses, a recurring observation was that the effectiveness of a given MIMO mechanism could not be determined from antenna dimensionality alone. Instead, the observed performance depended on the interaction between operating SNR, spatial configuration, receiver capability, CSI quality and the underlying communication objective. The resulting behavior can be summarized through four main characterization insights.

Insight 1: Coverage conditions define the feasible MIMO operating region. The coverage analysis demonstrated that the operating SNR of the considered LoRa-type system is strongly shaped by propagation distance, large-scale attenuation and spreading-related operating parameters. As coverage conditions become more demanding, the system progressively moves toward low-SNR operating regions in which communication reliability becomes the dominant design requirement. This has direct implications for MIMO operation, since transmission mechanisms that may be attractive under favorable channel conditions do not necessarily remain effective near the coverage boundary. The value of a MIMO configuration must therefore be evaluated relative to the operating SNR regime in which the link is expected to function rather than independently of the underlying coverage conditions.

Insight 2: Spatial diversity provides the most robust reliability gains under constrained operation. The diversity-oriented analysis showed that spatial diversity remains highly effective under the low-SNR conditions characteristic of the considered LoRa-type framework. STBC-based transmission and configurations providing increased diversity were able to substantially improve BER performance, with receive-side diversity exhibiting particularly strong

reliability benefits. These gains remained observable under imperfect CSI, although their magnitude depended on the underlying channel-estimation conditions. The results therefore indicate that diversity-oriented MIMO is naturally aligned with coverage- and reliability-oriented communication, where the principal objective is to maintain successful data delivery rather than maximize the number of simultaneously transmitted spatial streams.

Insight 3: CSI-error behavior determines whether MIMO gains are constrained or progressively recovered. The comparison between the two CSI error models revealed that MIMO robustness depends not only on the magnitude of channel-estimation uncertainty but also on how this uncertainty evolves with operating SNR. Under CEEM-I, the estimation-error variance remains fixed independently of SNR. Consequently, as thermal-noise effects diminish, persistent CSI mismatch becomes increasingly influential and can constrain the achievable BER improvement. Under CEEM-II, in contrast, the estimation-error variance decreases with SNR according to the adopted pilot-dependent model. Improved received signal quality is therefore accompanied by increasingly accurate channel estimates, allowing performance to progressively approach the corresponding perfect-CSI behavior. This distinction demonstrates that CSI uncertainty should not be treated as a single static impairment when assessing MIMO performance.

Insight 4: Spatial multiplexing provides condition-dependent throughput gains rather than universal reliability improvements. The spatial-multiplexing analysis revealed a fundamentally different operating behavior from diversity-oriented transmission. Spatial multiplexing with ZF and MMSE detection exhibited greater sensitivity to low SNR and CSI uncertainty, with MMSE consistently providing improved robustness relative to ZF. Antenna-scaling results further showed that increasing transmit dimensionality alone provides limited benefit when receiver rank remains constrained. In contrast, when sufficient receiver rank and favorable SNR are available, additional spatial streams can substantially increase normalized goodput even when BER or PER remains less favorable than for diversity-oriented transmission. Spatial multiplexing should therefore be interpreted primarily as a throughput-oriented strategy whose performance benefit depends on the availability of sufficient channel quality, receiver dimensionality and CSI accuracy. The results therefore show that antenna scaling becomes valuable for spatial multiplexing primarily when it translates into exploitable spatial rank and additional parallel streams.

For clarity, the main findings of the LoRa-type characterization are summarized in Table 4.12. The table consolidates the dominant factors examined in the preceding analyses, their observed effects and the corresponding implications for constrained MIMO system design.

Table 4.12. Summary of the main characterization findings for MIMO operation under constrained LoRa-type conditions.

Analysis Dimension	Main Finding	Design Implication
Coverage and operating SNR	Propagation and coverage conditions determine the low-SNR operating region within which MIMO techniques must provide useful performance gains.	MIMO configuration should be selected with explicit consideration of the current link-quality and coverage regime rather than antenna dimensionality alone.
Spatial diversity	Diversity-oriented transmission provides substantial BER improvements under constrained operating conditions, with receive-side diversity providing particularly strong reliability gains.	Spatial diversity is well suited to reliability- and coverage-oriented operation, especially when communication takes place under low-SNR conditions.
CSI uncertainty	Persistent CSI errors under CEEM-I increasingly constrain achievable performance, whereas SNR-dependent estimation improvement under CEEM-II allows performance to progressively approach the corresponding perfect-CSI behavior.	MIMO configuration and receiver design should account not only for CSI-error magnitude but also for the way estimation quality evolves with operating conditions.
ZF versus MMSE	MMSE detection exhibits greater robustness than ZF under low SNR and imperfect CSI, while ZF becomes increasingly vulnerable to noise enhancement and channel mismatch.	MMSE constitutes the more suitable linear detection strategy when spatial multiplexing is employed under constrained and imperfect-CSI conditions.
Transmit-side scaling	Increasing the number of transmit antennas provides limited performance benefit when receiver rank constrains the number of independently detectable spatial streams.	Transmit-side antenna scaling should be accompanied by sufficient receiver dimensionality if additional spatial degrees of freedom are to be effectively exploited.
Receiver rank and multiplexing	Higher receiver rank enables additional spatial streams and substantially greater normalized goodput under sufficiently favorable SNR conditions, despite increased BER or PER.	Higher-rank spatial multiplexing is primarily attractive when throughput gains compensate for the associated reliability penalty.
Spreading-factor representation	Within the adopted effective-SNR abstraction, increased spreading-related processing gain complements spatial diversity by extending reliable operation toward lower-SNR conditions.	Spreading-related robustness and MIMO configuration represent complementary adaptation dimensions, although the observed SF behavior should be interpreted within the adopted LoRa-type abstraction.

Taken together, the LoRa-type MIMO analysis reveals that multi-antenna operation under constrained wireless conditions cannot be characterized through a single universally preferable transmission strategy. The relative effectiveness of diversity and multiplexing changes substantially with operating SNR, CSI quality, antenna configuration, receiver rank and the communication objective. The main findings emerging from the cross-scenario analysis can therefore be summarized as follows:

- **LoRa-type MIMO performance is strongly operating-condition-dependent.** The examined MIMO configurations do not provide uniform benefits across all operating regimes. Diversity-oriented transmission becomes particularly valuable under low-SNR and reliability-constrained conditions, whereas spatial multiplexing becomes attractive primarily when channel quality and receiver capability are sufficient to support multiple spatial streams.

- **Reliability and throughput objectives favor fundamentally different uses of spatial resources.** Spatial diversity exploits antenna resources to improve robustness against channel impairments, while spatial multiplexing uses the available spatial dimensionality to increase aggregate transmission capability. Consequently, the preferred MIMO strategy depends fundamentally on whether the current communication objective prioritizes reliable delivery or increased effective throughput.

- **CSI quality constitutes a central constraint on achievable MIMO gains.** Both diversity and multiplexing performance depend strongly on the accuracy of channel knowledge, but the impact is particularly pronounced for multiplexing-oriented transmission. Moreover, the contrasting CEEM-I and CEEM-II behavior demonstrates that the evolution of estimation quality with SNR can substantially alter the resulting performance regime.

- **Characterization is a prerequisite for informed MIMO configuration and adaptation.** Since the relative benefit of diversity, multiplexing, receiver processing and antenna scaling changes with operating conditions, static MIMO configuration cannot exploit the full range of available spatial transmission opportunities. Effective configuration therefore requires knowledge of the current operating regime and the associated reliability and throughput requirements.

These findings establish the central outcome of the constrained LoRa-type analysis: the preferred use of spatial resources depends fundamentally on the operating regime and communication objective. Under severe coverage or low-SNR conditions, spatial resources are most effectively exploited through diversity to preserve communication reliability. As channel conditions improve and sufficient receiver rank and CSI quality become available, the same spatial resources can instead be exploited through multiplexing to increase effective data delivery. The transition between these operating regimes is therefore not determined by antenna

configuration alone, but by the joint interaction of channel quality, CSI accuracy, receiver capability and transmission objective.

When considered together with the broadband MIMO characterization presented in the preceding section, a common conclusion emerges across fundamentally different wireless operating environments. In broadband systems, MIMO performance was shown to depend strongly on propagation, mobility, antenna configuration, network loading and deployment conditions, with no individual system parameter providing a universally valid indication of the preferred configuration. Similarly, the present LoRa-type analysis demonstrates that under constrained low-power operation, the relative suitability of diversity and multiplexing depends strongly on SNR, CSI quality, receiver rank and reliability requirements. Despite the substantial differences between broadband and constrained wireless systems, both characterization studies therefore point toward the same fundamental design principle: MIMO configuration should be determined according to the prevailing operating conditions rather than through a fixed transmission strategy.

This common behavior provides the conceptual transition from characterization to adaptation. Once the operating regime determines whether additional spatial resources should be used for reliability enhancement, increased throughput or not activated at all, the remaining problem is no longer simply to identify which MIMO configuration performs best in isolation. Instead, it becomes necessary to determine how the transmission configuration should be selected dynamically according to channel conditions, reliability requirements and system constraints. Furthermore, in low-power wireless systems, the activation of additional transmit and receive chains introduces non-negligible hardware, processing and transmission-energy costs. Performance gains must therefore be considered jointly with the energy required to obtain them.

The combined broadband and constrained-system characterization developed in this chapter thus provides the foundation for the optimization-oriented analysis that follows. The subsequent chapters move from static performance characterization toward adaptive and energy-aware MIMO operation, where transmission modes are selected according to the prevailing channel conditions, reliability requirements and implementation costs. In this way, the characterization results obtained here are used not only to explain MIMO behavior under realistic and constrained conditions, but also to motivate the development of operating-condition-aware strategies capable of selecting the appropriate spatial transmission mechanism when its expected benefit justifies its associated cost.

4.3 Summary and Conclusions

This chapter provided a systematic characterization of MIMO system behavior under realistic and constrained wireless operating conditions, addressing the first central research objective of this thesis. The objective was to determine how propagation characteristics, deployment conditions, channel uncertainty and system constraints reshape the achievable gains, limitations

and trade-offs of MIMO communication beyond idealized theoretical assumptions.

The analysis was structured around two complementary characterization dimensions. The first focused on propagation-driven characterization in broadband wireless systems under realistic 3GPP deployment conditions. The results demonstrated that broadband MIMO performance is governed by complex interactions among antenna configuration, polarization, user mobility, propagation heterogeneity, deployment geometry and network load. Across the examined scenarios, spatial dimensionality, propagation heterogeneity and temporal channel stability emerged as important factors governing the resulting SINR, spectral-efficiency and throughput behavior. Importantly, the influence of individual parameters was not uniform across configurations or performance metrics, demonstrating that broadband MIMO behavior cannot be adequately characterized through isolated parameter variations or a single aggregate performance measure.

The second dimension focused on constraint-driven characterization within the considered low-power LoRa-type framework. In this regime, coverage conditions, low-SNR operation, channel-estimation uncertainty and receiver dimensionality substantially altered the role of the available spatial resources. Diversity-oriented transmission provided the most consistent reliability benefits under constrained operating conditions, with receive-side diversity being particularly effective. Spatial multiplexing, in contrast, became attractive primarily from a throughput perspective and only when sufficient operating SNR, receiver rank and CSI quality were available. The analysis further demonstrated that CSI uncertainty cannot be interpreted solely through its instantaneous magnitude, since the way estimation quality evolves with operating SNR can substantially affect the extent to which MIMO gains are preserved or recovered.

Taken together, the two characterization dimensions reveal a common underlying principle despite their substantially different operating environments: MIMO performance is inherently context-dependent. In broadband systems, the effectiveness of a MIMO configuration depends on the interaction between propagation, spatial structure, mobility, deployment conditions and network load. Under constrained LoRa-type operation, the preferred use of spatial resources additionally depends on coverage conditions, operating SNR, CSI quality, receiver rank and whether the communication objective prioritizes reliability or effective throughput. Consequently, antenna dimensionality or nominal spatial capability alone is insufficient to determine the value of a MIMO configuration.

This finding directly addresses the characterization gap identified in Chapter 1. MIMO behavior cannot be adequately represented by isolated idealized scenarios or inferred from a single performance metric, because the value of the available spatial resources changes with the propagation environment, operating regime and communication objective. The contribution of this chapter is therefore not the identification of a universally superior MIMO configuration, but the systematic demonstration of the conditions and mechanisms that determine when different spatial configurations and transmission strategies become beneficial. By connecting realistic operating conditions with their consequences for SINR, spectral efficiency, throughput,

reliability and effective data delivery, the chapter establishes the characterization foundation required for subsequent system design.

At the same time, the results reveal the inherent limitation of characterization alone. Identifying when and why MIMO behavior changes does not determine which transmission strategy should be selected when several competing objectives and implementation costs must be considered simultaneously. In particular, improved reliability or throughput may require additional spatial resources, receiver processing and hardware activation, whose benefits must ultimately be evaluated against their associated energy and implementation costs. The characterization problem therefore naturally leads to a configuration and optimization problem.

Building upon this foundation, the subsequent chapters move from understanding MIMO behavior to determining how spatial resources should be exploited under practical system constraints. The next stage investigates the interaction between communication reliability and energy consumption, including the effects of retransmissions, hardware overhead and non-ideal channel knowledge. These results subsequently support the development of adaptive and energy-aware MIMO strategies in which transmission configurations are selected according to the prevailing operating conditions, reliability requirements and the cost of activating additional spatial resources.

5 Reliability-Aware Energy Optimization in MIMO Systems

This chapter extends the analysis from performance characterization to reliability-aware energy optimization in MIMO systems. While Chapter 4 examined how realistic propagation conditions, antenna configurations and channel impairments influence communication performance, performance characterization alone is insufficient to determine the efficiency of wireless systems. In real-world deployments, improving communication reliability through increased spatial diversity or more robust MIMO configurations may reduce transmission errors, but it simultaneously introduces additional energy costs associated with hardware activation, signal processing and increased system complexity.

As a result, MIMO operation is inherently governed by a fundamental trade-off between communication reliability and energy consumption. Improved reliability reduces packet errors and retransmissions, thereby lowering retransmission-related energy expenditure. However, higher-order diversity schemes and additional active RF chains increase circuit and processing energy requirements. Consequently, the most reliable transmission mode is not necessarily the most energy-efficient one and the energy-optimal MIMO configuration depends on whether the reliability gains achieved under the prevailing channel conditions are sufficient to compensate for the additional hardware and processing energy costs.

To investigate this trade-off, this chapter adopts two complementary perspectives. The first focuses on diversity-based MIMO systems under realistic propagation and deployment conditions and identifies the operating regions in which the reliability benefits of diversity compensate for, or are outweighed by, the additional energy cost of activating more complex MIMO configurations. This analysis establishes the general reliability–energy trade-off governing MIMO operation. The second focuses on MIMO LoRa systems, representing highly energy-constrained LPWAN scenarios in which low-power operation, spreading-factor-dependent transmission characteristics and imperfect CSI further reshape the reliability–energy balance. This complementary analysis examines whether the energy benefits of improved reliability remain sufficient to justify additional MIMO resources under more constrained operating conditions.

The main objective of this chapter is to identify the operating conditions under which different MIMO configurations become energy-optimal while satisfying reliability requirements. Particular emphasis is placed on determining energy-optimal operating regions, transition boundaries and mode-switching behavior across both conventional and constrained wireless environments. Through this analysis, the chapter moves beyond identifying how MIMO systems behave under realistic operating conditions and determines when the reliability benefits of additional spatial resources justify their associated energy cost. The resulting insights establish the optimization foundation for the adaptive transmission strategies developed in the next chapter.

5.1 Energy-Optimal Operating Regions in MIMO Diversity Systems

5.1.1 System Model and Energy Framework

This section investigates the reliability–energy trade-off of diversity-based MIMO systems under realistic propagation conditions and progressively incorporates hardware-related energy constraints. The primary objective is to determine how diversity-induced reliability gains affect the energy required for successful packet delivery and, subsequently, whether these gains remain sufficient to justify the additional implementation cost associated with more complex multi-antenna configurations. Particular emphasis is placed on identifying the operating regions and transition boundaries that govern energy-efficient antenna configuration under varying channel and hardware conditions.

The analysis focuses on four representative diversity-oriented transmission configurations, namely SISO (1×1), SIMO (1×2), Alamouti-based transmit diversity (2×1) and Alamouti-based MIMO diversity (2×2). These configurations enable a systematic comparison between low-complexity and higher-diversity transmission schemes under identical operating conditions.

Consistent with the simulation methodology adopted in Chapter 4, the performance evaluation is carried out within the Vienna LTE-A Downlink System Level Simulator framework, extended to incorporate distance-dependent path loss, spatial correlation and environment-specific propagation characteristics. This enables the evaluation of wireless channels beyond simplified i.i.d. fading assumptions.

The overall evaluation framework follows a progressive two-stage structure. In the first stage, the transmission-energy budget per packet attempt is kept identical across the considered antenna configurations. This isolates the effect of packet reliability and the associated retransmission burden, allowing the intrinsic reliability–energy implications of diversity to be examined without introducing configuration-dependent hardware penalties. In the second stage, circuit and signal-processing energy overheads are explicitly incorporated through configuration-dependent parameters, enabling the resulting operating regions to be evaluated under different hardware-cost regimes.

For each operating point, channel realizations are generated according to the selected propagation scenario, followed by packet transmission and receiver processing based on the considered antenna configuration. Communication reliability is evaluated at packet level through packet error rate estimation, while energy efficiency is assessed using the energy-per-successful-packet metric introduced in Chapter 2.

For each configuration m, the expected energy per successfully delivered packet is expressed as

$$E_{\text{succ}}^{(m)} = \frac{E_{\text{pkt}}^{(m)}}{1 - \text{PER}_m}, \tag{5.1}$$

where $E_{\text{pkt}}^{(m)}$ denotes the energy consumed by a single packet-transmission attempt using configuration m. Assuming independent packet-transmission attempts with constant packet-error probability at each operating point, the expected number of attempts required for successful packet delivery is $1/(1 - \text{PER}_m)$. Accordingly, $E_{\text{succ}}^{(m)}$ represents the expected energy expenditure required to achieve one successful packet delivery under the adopted retransmission abstraction. This formulation directly couples communication reliability with energy expenditure and provides a common metric for comparing the considered MIMO configurations.

In the initial reliability-driven analysis, a common reference transmission-energy budget is assigned to all configurations,

$$E_{\text{pkt}}^{(m)} = E_{\text{tx}}, \qquad \forall m, \tag{5.2}$$

where E_{tx} is expressed in normalized energy units and is kept identical across all antenna configurations.

Under this baseline, the energy per successfully delivered packet becomes

$$E_{\text{succ}}^{(m)} = \frac{E_{\text{tx}}}{1 - \text{PER}_m}. \tag{5.3}$$

so that differences in $E_{\text{succ}}^{(m)}$ arise exclusively from differences in packet reliability. This equal-energy baseline is intentionally adopted to isolate the retransmission-related contribution to the reliability–energy trade-off. Configuration-dependent circuit and processing costs are introduced subsequently in the hardware-aware analysis, where the per-attempt energy model is extended to incorporate the corresponding implementation overhead.

The resulting energy values are therefore interpreted as normalized energy units rather than absolute physical energy consumption. This abstraction enables a controlled evaluation of how packet reliability and the resulting retransmission burden affect energy efficiency without requiring assumptions regarding a specific RF hardware platform.

Table 5.1. Main simulation parameters for energy-efficiency evaluation

Parameter	Value
Simulator	Vienna LTE-A SLS framework
Carrier frequency	2.5 GHz
MIMO configurations	1×1, 1×2, 2×1, 2×2
Nominal reference SNR	10–30 dB
Distance range	5–50 m
Packet length	100 bits
Packets per operating point	2000–5000
Antenna spacing	0.1λ–1.0λ
Propagation environments	Indoor, UMi
Channel conditions	LOS, NLOS
Initial energy baseline	Equal normalized transmit energy
Hardware-aware extension	Configuration-dependent circuit and processing overhead

The simulation campaign focuses on four key operating parameters: transmission distance, operating SNR, antenna spacing and propagation environment. These parameters were selected because they affect the reliability–energy trade-off through complementary physical mechanisms. Transmission distance modifies path loss and effective received signal quality, thereby influencing packet reliability and retransmission probability. Operating SNR controls the available link-quality margin and consequently shifts the conditions under which reliability improvements translate into energy savings. Antenna spacing influences spatial correlation and the achievable diversity benefit, while the propagation environment determines the large-scale and small-scale channel characteristics under LOS and NLOS conditions.

The analysis first examines these propagation- and reliability-driven effects under the common transmission-energy baseline, thereby identifying how channel conditions alone reshape the retransmission-related energy cost of the considered configurations. Hardware-related energy overhead is then introduced explicitly to determine whether the resulting reliability gains remain sufficient to compensate for the additional implementation cost of more complex MIMO modes.

Among the considered operating parameters, transmission distance provides a natural starting point for the analysis, since it directly affects path loss, effective received SNR and, consequently, packet reliability and retransmission behavior. The analysis therefore begins by investigating the distance-driven evolution of the reliability–energy trade-off.

5.1.2 Distance-Driven Retransmission Energy and Diversity Gains

Transmission distance constitutes one of the most critical parameters governing the reliability–energy behavior of MIMO systems. By directly affecting path loss and effective received SNR, distance strongly influences packet reliability, retransmission behavior and ultimately the energy required for successful communication. Consequently, transmission distance provides a natural operating-point variable for determining when the reliability gains of spatial diversity translate into meaningful retransmission-related energy savings.

The obtained results reveal that the energy–reliability trade-off evolves through distinct operating regimes as transmission distance increases. Figure 5.1 illustrates the packet error rate behavior of the considered antenna configurations under the Indoor LOS scenario. As expected, packet-level reliability generally improves with the availability of additional diversity branches, although the relative performance depends on whether diversity is introduced at the transmitter or receiver. The strongest reliability is achieved by the Alamouti 2×2 configuration, followed by SIMO 1×2, Alamouti 2×1, and SISO 1×1. This confirms the expected benefits of spatial diversity under geometry-aware propagation conditions while also demonstrating that transmit- and receive-side diversity do not necessarily provide identical reliability improvements under the considered operating conditions. Notably, SIMO 1×2 consistently outperforms Alamouti 2×1, despite both configurations providing a nominal diversity order of two under idealized conditions. This result highlights that equivalent nominal diversity order does not necessarily translate into equivalent reliability under geometry-dependent propagation, where transmit-

and receive-side spatial conditions may differ.

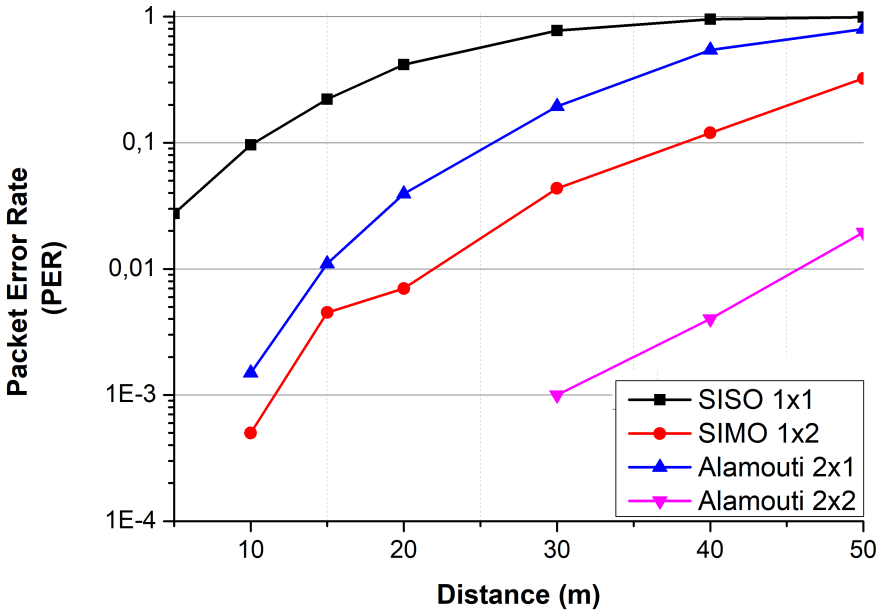


Figure 5.1. PER versus distance for the Indoor LOS scenario.

At short transmission distances, the considered configurations operate under relatively favorable propagation conditions, resulting in limited retransmission activity. Since equal nominal transmit energy per packet is assumed at this stage, the energy per successful packet remains close to the common per-attempt transmission cost. Consequently, the additional reliability provided by diversity produces only limited retransmission-related energy savings in this operating region.

As transmission distance increases, the system progressively enters a transition regime in which packet error rates rise significantly, particularly for lower-diversity configurations. In this region, retransmission-related energy expenditure becomes increasingly important. The reliability gains provided by spatial diversity therefore translate directly into energy savings, since fewer transmission attempts are required for successful packet delivery.

This behavior becomes more evident in Table 5.2 and Figure 5.2, which present the energy per successfully delivered packet under an equal per-attempt transmit-energy assumption. At short distances, the energy values of the considered configurations remain close because retransmissions are infrequent. As distance increases, however, the energy cost of lower-diversity configurations grows rapidly as their packet error rates increase. Higher-diversity schemes, and particularly the Alamouti 2×2 configuration, maintain a substantially lower retransmission burden over a wider distance range and therefore require less energy for successful packet delivery.

At larger transmission distances, lower-diversity configurations progressively approach a reliability-limited operating regime as severe propagation loss drives their packet error probabilities toward unity. Higher-diversity configurations delay this transition substantially,

Table 5.2. Energy per successful packet transmission for different antenna configurations

Distance (m)	SISO	SIMO 1×2	Alamouti 2×1	Alamouti 2×2	Best mode
5	102.82	100.00	100.00	100.00	1×2
10	110.68	100.05	100.15	100.00	2×2
15	128.36	100.45	101.11	100.00	2×2
20	171.23	100.70	104.11	100.00	2×2
30	441.50	104.54	124.14	100.10	2×2
40	2197.80	113.63	218.81	100.40	2×2

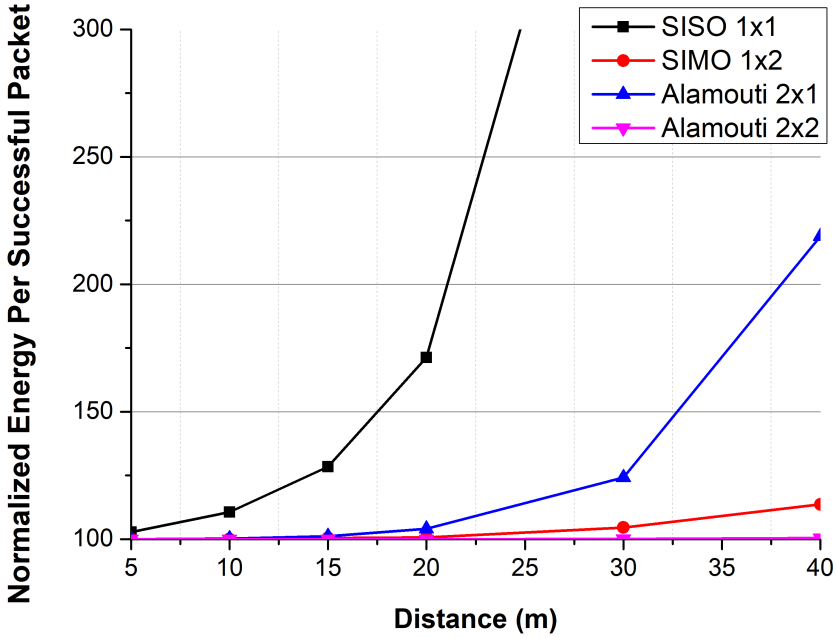


Figure 5.2. Energy per successful packet versus distance for the Indoor LOS scenario.

with the Alamouti 2×2 scheme maintaining comparatively low retransmission-related energy expenditure over a considerably wider distance range. Eventually, however, sufficiently adverse propagation conditions would also limit the effectiveness of higher-diversity transmission.

The importance of realistic propagation modeling is further demonstrated through comparison with a conventional i.i.d. Rayleigh fading model, shown in Figure 5.3. Simplified fading models neglect spatial correlation and geometry-dependent propagation effects, effectively assuming ideal diversity conditions. As a result, such models tend to overestimate the achievable reliability and energy-efficiency gains of diversity techniques. In contrast, the adopted geometry-aware framework captures geometry-dependent propagation limitations that significantly influence energy-optimal behavior, particularly at larger transmission distances.

Overall, the results reveal three distinct distance-driven regimes in the retransmission-related reliability–energy trade-off. Under short-range favorable conditions, retransmission penalties are limited and the energy per successful packet remains close to the common nominal transmission cost. At intermediate distances, the system enters a reliability-transition regime

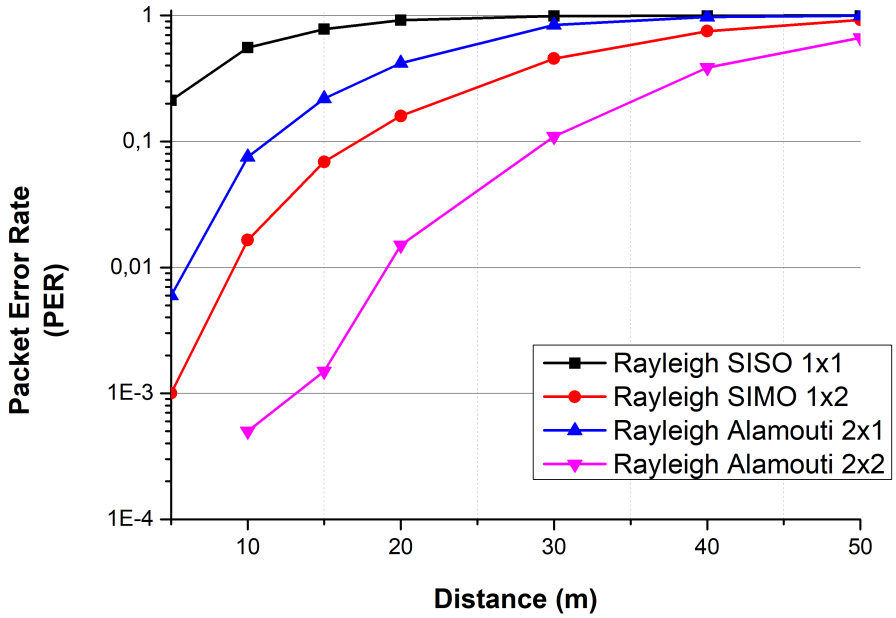


Figure 5.3. PER versus distance under the i.i.d. Rayleigh fading model.

in which diversity becomes increasingly valuable because reduced packet error probability translates directly into fewer retransmissions and lower energy expenditure. At larger distances, lower-diversity configurations progressively enter a reliability-limited regime, while higher-diversity schemes extend the range over which successful communication remains energetically viable. These results establish the reliability-driven component of the energy trade-off; the additional impact of configuration-dependent hardware and processing costs is examined subsequently.

Impact of Operating Conditions

The distance-driven analysis of the previous subsection revealed the existence of distinct operating regimes governing the energy efficiency of diversity-based MIMO systems. However, these operating regions are not fixed. Their boundaries depend strongly on the prevailing operating conditions, which directly influence channel reliability, retransmission behavior and achievable diversity gain.

To further investigate this behavior, the analysis is extended to three key operating parameters: operating SNR, antenna spacing and propagation environment. Each parameter affects the reliability–energy trade-off through different physical mechanisms, including link-quality variation, spatial correlation and large-scale propagation conditions. The objective of this analysis is to determine how these factors modify the transition boundaries between energy-optimal antenna configurations under the considered propagation conditions.

Impact of SNR

Among the considered operating parameters, SNR has a direct influence on the reliability–energy trade-off, since changes in link quality directly affect packet reliability and, consequently, the expected retransmission burden. SNR therefore acts as a primary boundary-shifting parameter for the reliability-driven energy operating regions.

Figure 5.4 illustrates the energy per successful packet of the SIMO 1×2 and Alamouti 2×2 configurations across different SNR conditions.

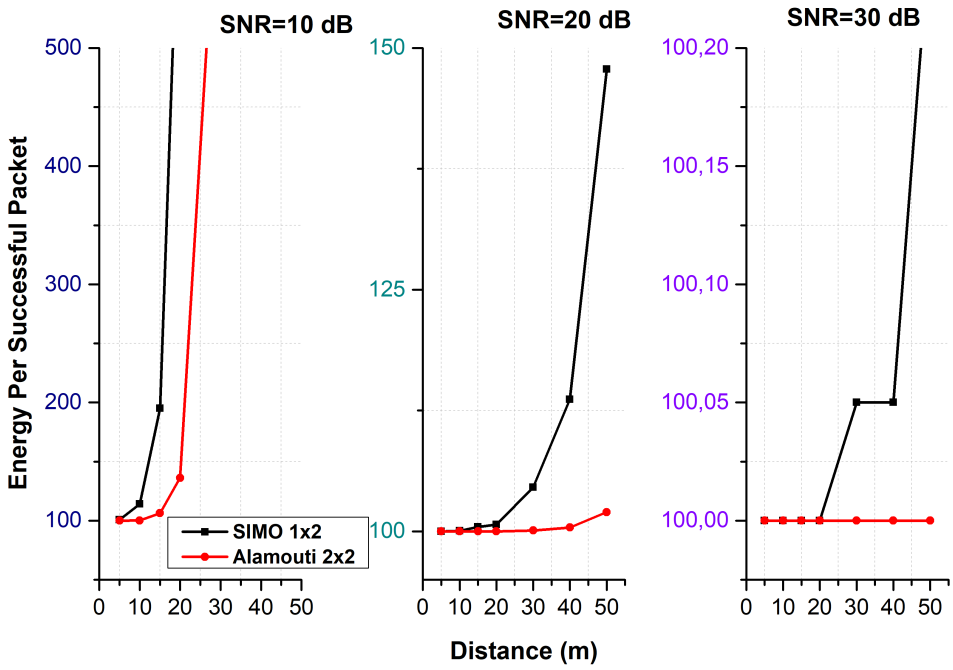


Figure 5.4. Impact of SNR on energy per successful packet versus distance.

At low SNR, the system transitions rapidly toward a reliability-limited operating regime as transmission distance increases. Under these conditions, packet errors produce a rapidly increasing retransmission burden, causing the energy per successful packet to rise sharply. Higher-order diversity delays this transition by maintaining lower packet error probability over a wider distance range, thereby limiting retransmission-related energy expenditure.

As SNR increases, the onset of this energy increase shifts toward larger transmission distances. At intermediate SNR, the difference between the considered configurations becomes pronounced primarily at larger distances, where the lower-diversity configuration begins to experience a substantial retransmission penalty. Under high-SNR conditions, packet errors remain negligible over most of the examined distance range, causing the energy per successful packet of both configurations to remain close to the common nominal per-attempt energy.

These observations demonstrate that SNR primarily controls the location of the reliability-driven energy transition boundaries. Lower SNR causes retransmission-related energy penalties to emerge at shorter distances, whereas increasing SNR extends the operating range over which successful packet delivery can be achieved with little or no retransmission penalty. The

relative energy benefit of diversity therefore becomes most pronounced near the reliability-transition region, where differences in packet error probability translate directly into differences in the expected energy required for successful delivery.

Impact of Antenna Spacing

The impact of antenna spacing is evaluated under Indoor LOS conditions at a fixed transmission distance of 20 m and a reference SNR of 20 dB. Unlike SNR, antenna spacing influences the reliability–energy trade-off indirectly by modifying the spatial characteristics of the MIMO channel. Figure 5.5 illustrates the PER behavior of the considered diversity configurations as a function of antenna spacing.

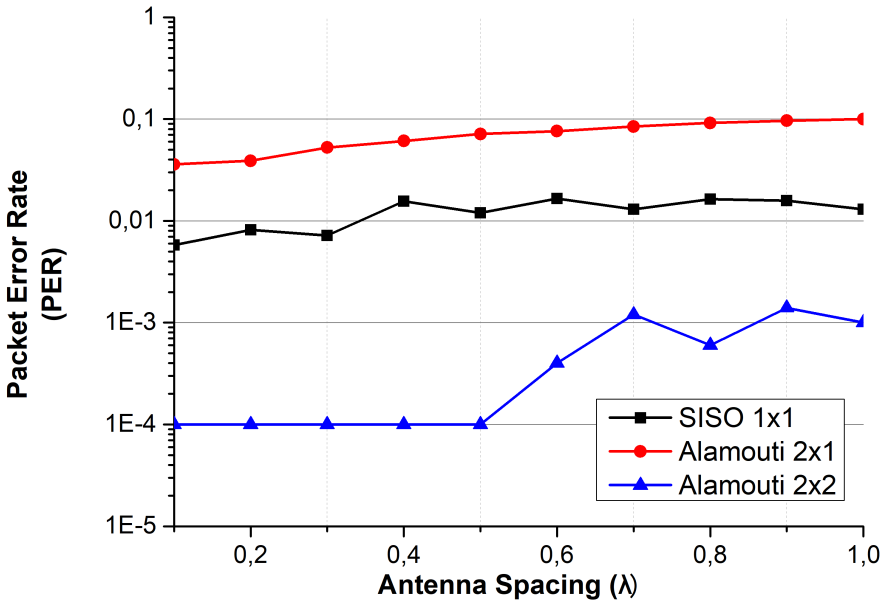


Figure 5.5. PER versus antenna spacing.

The results show that antenna spacing affects the considered configurations differently. The Alamouti 2×1 configuration exhibits a gradual increase in PER as antenna spacing increases over the examined range, whereas SISO shows comparatively small fluctuations. The Alamouti 2×2 configuration maintains the lowest PER throughout the entire spacing range, although some variation becomes visible at larger antenna separations. These results indicate that antenna geometry can modify the reliability achieved by diversity-based transmission, while the magnitude and direction of this effect depend on the specific antenna configuration and the resulting channel structure.

The corresponding energy behavior is presented in Figure 5.6. Since equal nominal per-attempt energy is assumed in this stage of the analysis, the observed energy trends directly reflect the corresponding PER behavior. The Alamouti 2×2 configuration remains close to the nominal energy level throughout the examined spacing range, whereas the increasing PER

of the Alamouti 2×1 configuration produces a progressively larger retransmission-related energy penalty.

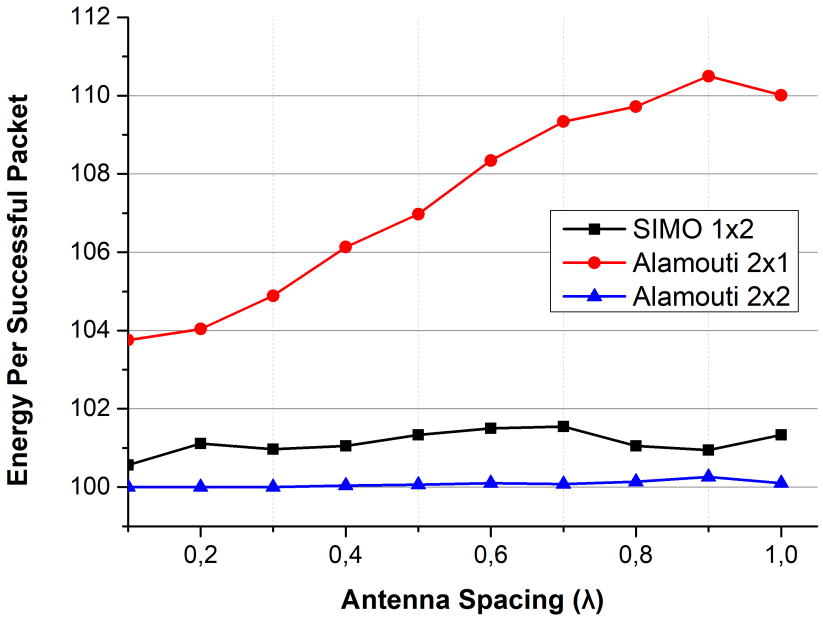


Figure 5.6. Energy per successful packet versus antenna spacing.

Overall, the results indicate that antenna spacing has only a limited influence on the reliability–energy trade-off under the examined operating conditions. Although some configuration-dependent variation in PER is observed, particularly for the Alamouti 2×1 scheme, these changes do not alter the relative ordering of the considered configurations or produce an energy-optimal mode transition. The Alamouti 2×2 configuration maintains both its reliability and energy advantage throughout the entire spacing range. In contrast to transmission distance and operating SNR, antenna spacing therefore does not emerge as a dominant factor governing the energy-optimal operating regions in the present scenario.

Impact of Propagation Environment

The propagation environment represents an important external factor affecting the reliability–energy behavior of MIMO operation, as changes in propagation conditions modify path loss, channel characteristics and, consequently, packet reliability. The impact of the propagation environment on packet-level reliability is summarized in Table 5.3.

The results reveal a pronounced dependence of packet reliability on the propagation environment. Under the examined LOS conditions, diversity-based configurations provide substantial reliability improvements over SISO operation, with several configurations achieving very low or zero observed packet errors over the simulated packet ensemble. Under Indoor NLOS conditions, however, packet reliability deteriorates sharply for all configurations. Although the Alamouti 2×2 configuration retains the lowest PER among the examined schemes, its

Table 5.3. PER across propagation environments

Scenario	SISO 1×1	SIMO 1×2	Alamouti 2×1	Alamouti 2×2
Indoor LOS	0.0988	0.0002	0.0022	0.0000
Indoor NLOS	0.9998	0.9652	0.9999	0.9092
UMi LOS	0.0246	0.0000	0.0000	0.0000
UMi NLOS	1.0000	1.0000	1.0000	1.0000

PER remains high, indicating that the available diversity gain is insufficient to compensate for the severe channel degradation.

The UMi NLOS scenario represents the most adverse propagation condition considered in this analysis. All configurations exhibit a PER of unity over the simulated packet ensemble, indicating that no successful packet delivery was observed at the examined operating point. Consequently, the success probability $1 - \text{PER}$ becomes zero and the adopted energy-per-successful-packet metric does not yield a finite value. Under these conditions, the system therefore lies outside the reliability-feasible operating region, and retransmission alone cannot provide sustainable packet delivery.

Overall, the results demonstrate that the reliability–energy operating regime is strongly dependent on the prevailing operating conditions. Transmission distance and SNR determine when retransmission penalties begin to dominate, while the propagation environment can produce an even more fundamental transition between reliability-feasible, reliability-limited, and infeasible operation. In contrast, antenna spacing produces comparatively limited and configuration-dependent variations within the examined range and does not alter the identity of the best-performing mode. These findings demonstrate that the energy consequences of spatial diversity cannot be assessed independently of the prevailing propagation and operating conditions and establish the reliability-driven baseline for the subsequent introduction of configuration-dependent implementation costs.

5.1.3 Hardware-Aware Operating Region Analysis

The previous analysis demonstrated that the energy-optimal behavior of diversity-based MIMO systems strongly depends on transmission distance and operating conditions. However, energy-efficient operation is not determined solely by propagation-related factors. Practical implementation constraints, particularly circuit-related and signal-processing energy consumption, also play a critical role in shaping the energy–reliability trade-off.

To explicitly investigate these effects, this subsection examines the impact of hardware-related energy overhead on the operating-region structure and the resulting energy-optimal antenna configuration. Particular emphasis is placed on understanding how circuit and processing energy reshape the balance between retransmission-related energy savings and implementation-related energy costs.

Circuit and processing overhead are modeled using the normalized parameters α_m and β_m,

introduced in Chapter 3. These parameters capture the relative increase in hardware-related energy consumption associated with increasing antenna configuration complexity, including RF chain activation and baseband processing requirements.

Accordingly, the per-attempt energy consumption of configuration m can be written in normalized form as

$$E_{\text{pkt}}^{(m)} = E_{\text{tx}} + \alpha_m + \beta_m, \tag{5.4}$$

where E_{tx} denotes the nominal transmission energy, while α_m and β_m represent the circuit-related and processing-related energy contributions, respectively. This formulation allows the reliability benefit of each MIMO configuration to be evaluated jointly with its implementation-related energy cost.

Combining the per-attempt hardware-aware energy model with the packet success probability yields the corresponding expected energy per successfully delivered packet:

$$E_{\text{succ}}^{(m)} = \frac{E_{\text{tx}} + \alpha_m + \beta_m}{1 - \text{PER}_m}. \tag{5.5}$$

This expression explicitly captures the two competing mechanisms governing energy-optimal operation. The numerator represents the configuration-dependent implementation cost of each transmission attempt, whereas the denominator captures the retransmission penalty associated with imperfect packet reliability. Consequently, a more complex diversity configuration becomes energy advantageous only when its reduction in packet errors is sufficient to compensate for its additional circuit and processing energy cost.

Table 5.4 summarizes the adopted parameter values for three representative hardware-overhead regimes: low, moderate and high. These regimes represent progressively increasing dominance of implementation-related energy consumption.

Table 5.4. Normalized circuit (α_m) and processing (β_m) energy scaling

Configuration	α_m (Low)	β_m (Low)	α_m (Moderate)	β_m (Moderate)	α_m (High)	β_m (High)
SISO 1×1	0.10	0.00	0.50	0.00	1.00	0.00
SIMO 1×2	0.18	0.02	0.75	0.05	1.50	0.08
Alamouti 2×1	0.20	0.03	0.80	0.08	1.60	0.12
Alamouti 2×2	0.30	0.05	1.10	0.12	2.20	0.18

The influence of hardware overhead on energy efficiency is illustrated in Figure 5.7, which presents the energy per successful packet as a function of transmission distance under different overhead conditions.

The results demonstrate that hardware overhead substantially modifies the balance between implementation cost and retransmission-related energy consumption. At short transmission distances, where packet failures remain limited, the additional reliability provided by more complex diversity configurations is generally insufficient to compensate for their higher circuit and processing costs. Consequently, lower-complexity configurations are favored in this

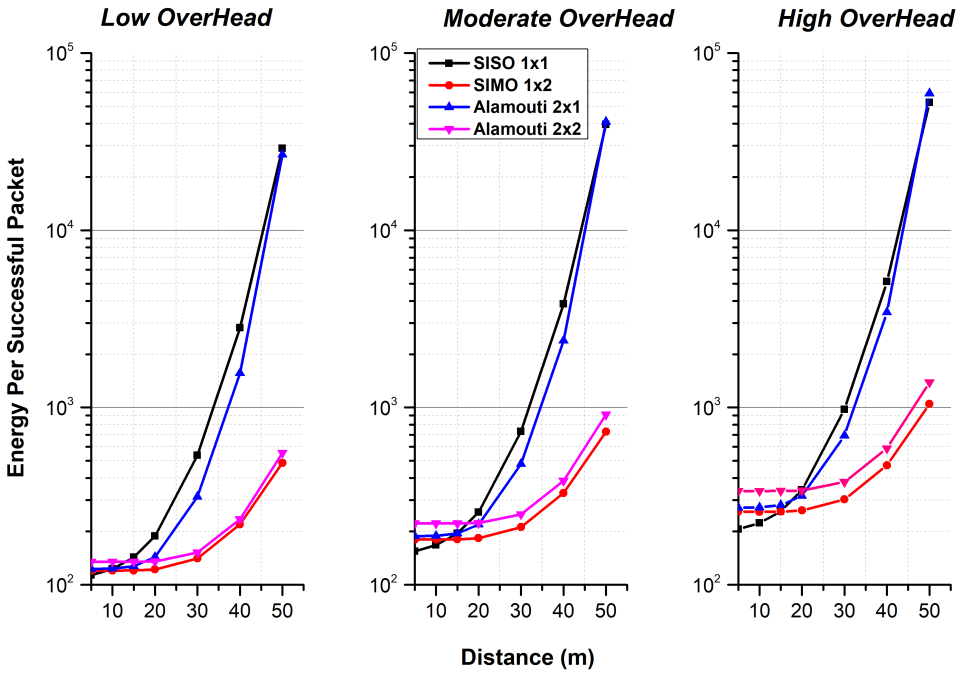


Figure 5.7. Energy per successful packet versus distance under different hardware-overhead regimes.

region.

As transmission distance increases, the reliability differences between configurations become increasingly important. The rapidly increasing retransmission burden of less reliable configurations can eventually outweigh their lower implementation cost, allowing diversity-based schemes to become more energy efficient. Importantly, this transition does not imply that the configuration providing the highest reliability is necessarily energy optimal. Instead, the preferred configuration is the one whose reliability improvement is sufficient to compensate for its additional hardware and processing overhead.

Increasing the hardware-overhead regime shifts this balance further toward lower-complexity configurations. In particular, SIMO 1×2 becomes highly competitive over a broad range of operating distances because it combines a substantial reliability improvement with a comparatively limited increase in implementation cost. By contrast, the additional reliability offered by higher-complexity configurations does not always compensate for their larger hardware overhead.

This behavior is examined in greater detail in Figure 5.8, which focuses separately on short- and long-distance operating regimes.

At short transmission distances, retransmission-related energy remains small and the differences between configurations are therefore governed primarily by their implementation overhead. Under low-overhead conditions, the transition from SISO to SIMO occurs only after the reliability advantage of receive diversity becomes sufficient to compensate for its additional cost, whereas under moderate and high overhead the lower-complexity SISO configuration remains preferable throughout the examined short-distance interval. This behavior characterizes a hardware-dominated operating region.

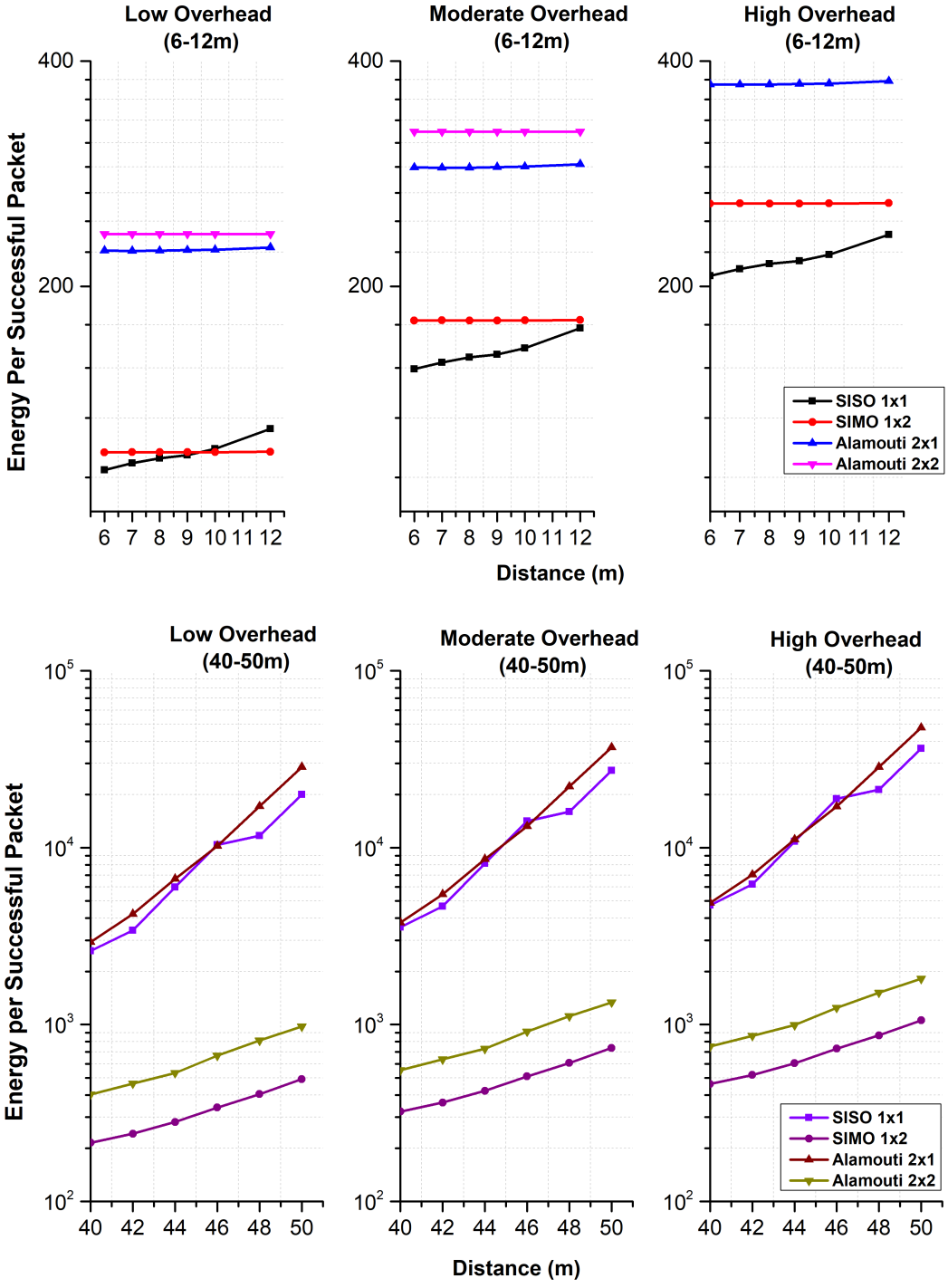


Figure 5.8. Energy per successful packet under different overhead conditions: (a) short-distance regime and (b) long-distance regime.

The long-distance results reveal a different operating regime. As packet reliability deteriorates, retransmission-related energy becomes increasingly important and configurations with improved reliability can outperform lower-complexity alternatives despite their higher implementation cost. In the examined conditions, SIMO 1×2 provides the most favorable balance between reliability improvement and hardware overhead, whereas SISO suffers from increasing retransmission cost and the additional implementation cost of the Alamouti-based configurations is not sufficiently compensated by their reliability advantage.

Overall, the results identify a hardware-aware transition between two competing energy mechanisms. Under favorable channel conditions, implementation overhead dominates and simpler configurations are preferred. As channel conditions deteriorate, retransmission-related energy becomes increasingly important and additional diversity becomes beneficial when the resulting reliability gain exceeds its implementation cost. Under sufficiently severe propagation conditions, however, reliability degradation ultimately dominates the energy behavior of all configurations.

These observations demonstrate that increasing diversity capability does not necessarily translate into improved energy efficiency. Instead, the energy-optimal configuration is jointly determined by channel-dependent packet reliability and configuration-dependent implementation cost. Hardware overhead therefore acts as a major boundary-shifting parameter, altering both the location of configuration transitions and the range of operating conditions over which each MIMO mode remains energy efficient.

5.1.4 Energy-Optimal Operating Regions and Design Insights

The analyses presented in the previous subsections collectively reveal that the energy-efficient operation of diversity-based MIMO systems is governed by a structured optimization landscape characterized by distinct operating behaviors and configuration-dependent transition boundaries. Rather than exhibiting uniform behavior across all operating conditions, the energy-preferred antenna configuration changes according to the combined effects of transmission distance, SNR, propagation environment and hardware-related energy overhead.

The first characteristic behavior is observed under favorable channel conditions and short transmission distances. In this region, packet error rates remain low and the retransmission burden is therefore limited. Under the equal-energy baseline, the energy differences between configurations are correspondingly small because reliability improvements provide only limited retransmission-related savings. When configuration-dependent implementation costs are subsequently introduced, this region increasingly favors lower-complexity configurations, since the additional reliability provided by higher-order diversity may be insufficient to compensate for the associated circuit and processing overhead.

A second characteristic behavior emerges as channel conditions deteriorate and packet errors become increasingly significant. In this region, the expected retransmission burden grows more rapidly for lower-diversity configurations, increasing the energetic value of improved reliability. Consequently, a higher-diversity configuration can become energy-preferable when the

reduction in packet failures is sufficiently large to compensate for its additional per-attempt implementation cost. This region therefore contains the most important configuration transitions observed in the reliability–energy analysis.

A third characteristic behavior appears under severely degraded propagation conditions. As PER approaches very high values, the expected energy required for successful packet delivery increases rapidly for all configurations. Higher-order diversity can extend the useful operating range by maintaining improved reliability, but sufficiently adverse channel conditions eventually reduce the effectiveness of all considered configurations and may lead to outage-like operation. The exact onset of this behavior is condition-dependent and varies with SNR, propagation environment and the considered antenna configuration.

The transition boundaries between energy-preferred configurations follow directly from the reliability-aware energy metric. For two candidate configurations i and j, a transition occurs when their expected energy per successfully delivered packet becomes equal, i.e.,

$$E_{\text{succ}}^{(i)} = E_{\text{succ}}^{(j)}, \tag{5.6}$$

or, using the hardware-aware energy model,

$$\frac{E_{\text{tx}} + \alpha_i + \beta_i}{1 - \text{PER}_i} = \frac{E_{\text{tx}} + \alpha_j + \beta_j}{1 - \text{PER}_j}. \tag{5.7}$$

This condition provides a direct interpretation of the reliability–energy trade-off: a more complex diversity configuration becomes energy-preferable only when the reduction in retransmission burden resulting from its lower PER is sufficient to compensate for its additional circuit and processing energy cost.

Design Insight 1: Distance-Driven Operating-Region Evolution

Transmission distance acts as the primary driver of the operating-region evolution by modifying path loss, packet reliability and the resulting retransmission burden. Under favorable short-range conditions, reliability is already high and the energetic value of additional diversity remains limited, particularly when implementation overhead is considered. As distance increases, retransmission-related energy becomes progressively more important and higher-diversity configurations can become energy-preferable. Under sufficiently severe conditions, however, the energy required for successful delivery increases rapidly for all configurations and the system may eventually approach outage-like operation. Distance therefore determines the progression through the main reliability–energy behaviors and the configuration transitions that occur between them.

Design Insight 2: Operating-Condition-Dependent Boundary Shifting

The transition boundaries between energy-preferred configurations are not fixed. SNR acts as a primary boundary-shifting parameter by modifying the link-quality margin and

retransmission probability, while the propagation environment can substantially reshape the feasible operating space and, under severe NLOS conditions, compress or even eliminate useful operating regions. Antenna spacing, in contrast, produces only limited and configuration-dependent variations within the examined range and does not induce a change in the energy-preferred configuration. The energy-optimal configuration is therefore determined not by transmission distance alone, but by the joint propagation and operating conditions under which the link operates.

Design Insight 3: Hardware–Reliability Trade-Off

Hardware-related energy overhead fundamentally changes the value of additional diversity. Increasing the number of active antenna and RF resources can reduce PER and retransmission-related energy, but simultaneously increases circuit and signal-processing cost. As implementation overhead increases, a larger reliability improvement is required for higher-diversity configurations to become energy beneficial, shifting their transition boundaries toward more demanding operating conditions and restricting the regions in which their additional complexity is energetically justified. The energy value of diversity is therefore determined by whether its reliability gain is sufficiently large to compensate for its additional per-attempt implementation cost, as expressed directly by (5.7).

Design Insight 4: Need for Adaptive Configuration Selection

The combined results demonstrate that the relationship between diversity order and energy efficiency is inherently non-monotonic. Neither the lowest-complexity nor the highest-diversity configuration remains universally energy-optimal across the investigated operating conditions. Instead, the preferred antenna mode changes according to channel quality, propagation conditions and hardware-energy characteristics. Consequently, a static MIMO configuration cannot generally maintain energy-optimal operation across varying conditions, providing direct motivation for an adaptive strategy capable of selecting the appropriate antenna configuration according to the current operating region.

Overall, these findings extend the characterization results of Chapter 4 from performance behavior to reliability-aware energy optimization. While the previous chapter demonstrated that MIMO performance is strongly condition-dependent, the present analysis shows that this condition dependence translates directly into configuration-specific energy-optimal operating regions and transition boundaries. These results establish a general principle: energy-optimal operation depends on the prevailing operating conditions and on the cost of the available reliability-enhancement mechanisms. This provides the physical and analytical basis for the formal operating-region classification and adaptive MIMO selection framework developed in the following chapter.

5.2 Energy Optimization in Constrained LoRa MIMO Systems

The previous section established the fundamental energy–reliability optimization principles governing diversity-based MIMO systems under conventional wireless operating conditions. The analysis revealed that energy-efficient operation is governed by structured operating regions and configuration-dependent transition boundaries, shaped by the interaction between propagation conditions, retransmission behavior and hardware-related energy overhead.

This section extends the analysis to a fundamentally different wireless communication regime, namely Low-Power Wide-Area Networks (LPWANs), with particular focus on LoRa-type systems. Unlike conventional wireless systems, LoRa-type communication is designed for energy-constrained, low-data-rate and extended-coverage operation, making energy efficiency a primary design objective. These characteristics introduce a different optimization landscape, in which the balance between communication reliability and energy consumption is additionally influenced by spreading-factor-dependent transmission characteristics and low-SNR operation.

A key distinguishing feature of LoRa-type systems is the role of the spreading factor (SF) in shaping the reliability and energy characteristics of communication. Higher SF values are generally associated with increased robustness and extended communication range, while also modifying the transmission characteristics relevant to energy consumption. Consequently, SF selection introduces an additional dimension in the reliability–energy trade-off, and improved link robustness through more conservative spreading settings does not necessarily imply improved energy efficiency. In this context, multi-antenna techniques offer an alternative mechanism for improving communication reliability. By exploiting spatial diversity, the considered MIMO configurations can reduce packet errors and improve link robustness without relying exclusively on more robust spreading-factor settings. The resulting reduction in packet failures may reduce the expected energy required for successful packet delivery. The relevant question is therefore whether the reliability improvement provided by spatial diversity is sufficient to compensate for the energy expenditure associated with repeated unsuccessful transmissions.

An additional challenge arises from channel state information uncertainty. While diversity gains are maximized under accurate CSI, practical receivers rely on channel estimation, which is inherently imperfect. Estimation errors may significantly degrade the achievable performance of diversity schemes, particularly under low-SNR conditions, thereby directly affecting packet reliability and the resulting energy required for successful packet delivery.

Compared to the conventional MIMO systems examined in the previous section, the optimization problem considered here is governed by a different set of dominant parameters. In addition to SNR, the spreading factor and CSI quality emerge as critical variables, jointly influencing packet reliability and, consequently, the energy required for successful packet delivery.

The primary objective of this section is to characterize the energy-optimal operating regions of LoRa MIMO systems under both perfect and imperfect CSI conditions and to identify the key parameters governing mode selection, including SNR, spreading factor and channel estimation quality. Particular emphasis is placed on understanding the switching behavior between single-antenna and multi-antenna operation under the considered constrained LPWAN operating conditions. These results complement the general MIMO energy optimization framework developed in the previous section and provide deeper insight into energy-efficient communication under highly constrained wireless environments.

5.2.1 System Model and LoRa Energy Framework

This subsection defines the evaluation framework used to analyze the energy efficiency of LoRa MIMO systems under realistic LPWAN operating conditions. The objective is to characterize how antenna configuration, spreading factor and channel estimation accuracy jointly influence packet reliability and energy consumption, and to identify the operating conditions under which multi-antenna transmission becomes energy efficient. Particular emphasis is placed on the resulting mode-switching behavior between single-antenna and diversity-based MIMO operation under reliability and energy constraints.

The analysis considers a representative set of diversity-oriented LoRa configurations, namely 1×1, 1×2, 2×1 and 2×2, enabling a compact yet sufficiently expressive comparison between conventional single-antenna transmission and diversity-based multi-antenna communication. The considered configurations include both receive-diversity and transmit-diversity schemes, allowing the analysis to capture different forms of diversity gain under LPWAN constraints.

The performance evaluation is carried out over a broad range of representative LoRa operating conditions. In particular, the spreading factor is varied across $\mathrm{SF} = \{8, 10, 12\}$ to capture different spreading-related reliability conditions, while the SNR is swept from -10 dB to 18 dB in steps of 2 dB in order to examine system behavior from highly degraded to favorable channel conditions. Both perfect and imperfect CSI conditions are considered, enabling systematic evaluation of channel estimation uncertainty on energy-efficient operation.

Two imperfect-CSI models are adopted. The first model (CEEM-I) represents estimation uncertainty through additive Gaussian estimation error with variance $\sigma^2 = 0.05$, while the second model (CEEM-II) models estimation quality as a function of pilot overhead using a pilot parameter of $L_p = 4$. These two models allow the analysis to capture both fixed-error and pilot-dependent CSI uncertainty effects.

System performance is evaluated through Monte Carlo simulations under uplink transmission conditions. For each operating point, BER performance is averaged over 40 Monte Carlo runs, each consisting of 250 transmitted blocks. A fixed packet length of 128 bits is used for BER-to-PER conversion, allowing packet-level reliability to be consistently evaluated across all antenna configurations and operating conditions. To ensure numerical stability, the measured BER is lower-bounded by the minimum detectable error rate associated with the total

number of simulated bits.

The primary performance metric is the expected energy per successfully delivered packet, defined using the reliability-aware energy framework introduced earlier in this chapter. For each antenna configuration, spreading factor and SNR operating point, the estimated BER is first mapped to packet-level reliability and subsequently incorporated into the energy-per-successful-packet calculation. In this way, differences in communication reliability are directly reflected in the expected retransmission burden and, consequently, in the energy required for successful packet delivery. The resulting metric provides a common basis for comparing the considered LoRa MIMO configurations and identifying energy-optimal operating regions and mode-transition behavior across different SNR, spreading-factor and CSI conditions.

The main simulation parameters are summarized in Table 5.5.

Table 5.5. Main simulation parameters for LoRa MIMO energy-efficiency evaluation

Parameter	**Value**
Link direction	Uplink
Carrier frequency	868 MHz
Bandwidth	125 kHz
SNR range	-10 dB to 18 dB
SNR step	2 dB
SNR type	E_s/N_0
Spreading factors (SF)	8, 10, 12
MIMO configurations	1×1, 1×2, 2×1, 2×2
Transmission scheme	SISO/SIMO, Alamouti ($N_t = 2$)
Monte Carlo runs	40
Blocks per run	250
Packet length	128 bits
Noise figure	6 dB
Implementation loss	0 dB
CSI conditions	Perfect, Imperfect
CSI model (imperfect)	CEEM-I, CEEM-II
CEEM-I parameter	$\sigma_e^2 = 0.05$
CEEM-II parameter	$L_p = 4$

5.2.2 SNR-Driven Reliability Transition under Imperfect CSI

The first step in characterizing energy-efficient LoRa MIMO operation is to examine how the considered antenna configurations behave in terms of physical- and packet-level reliability.

In LoRa systems, the SNR region in which the link transitions from unreliable to reliable operation is particularly important, since this transition directly determines retransmission behavior and, consequently, the energy per successfully delivered packet.

Figure 5.9 presents the BER performance versus SNR for the considered MIMO configurations under perfect and imperfect CSI conditions for SF = 10.

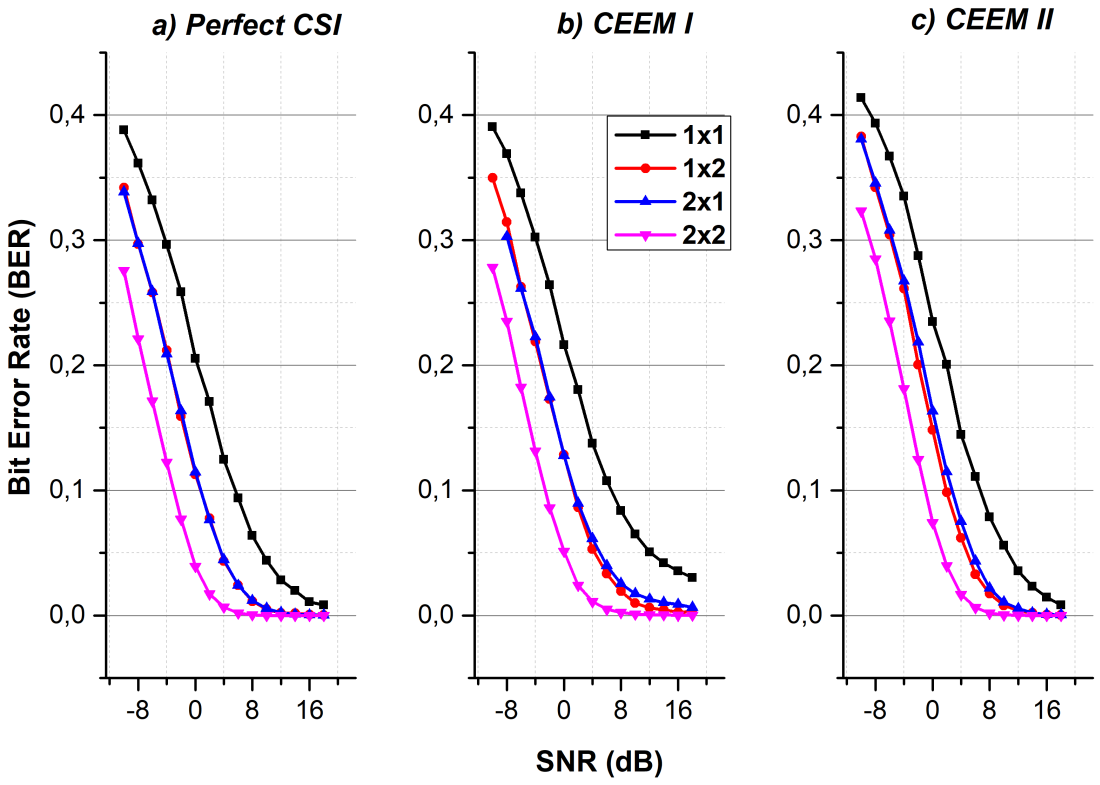


Figure 5.9. BER versus SNR for MIMO configurations under perfect and imperfect CSI (SF = 10): (a) Perfect CSI, (b) CEEM-I, (c) CEEM-II.

Under perfect CSI, the expected diversity advantage is clearly observed. The 2×2 configuration achieves the lowest BER over most of the investigated SNR range, while the 1×2 and 2×1 schemes provide substantial and broadly comparable improvements over the 1×1 configuration. This confirms that spatial diversity improves LoRa link robustness by accelerating the BER reduction as SNR increases.

The impact of imperfect CSI on BER depends strongly on the adopted channel-estimation error model. Under CEEM-I, where the estimation-error variance remains fixed independently of SNR, the BER reduction progressively slows at high SNR, resulting in residual performance degradation for several configurations. This behavior is particularly evident for the 1×1, 1×2 and 2×1 schemes, whereas the 2×2 configuration retains substantially stronger robustness. Under CEEM-II, where estimation quality improves with SNR according to the pilot-dependent model, the BER curves continue to decrease and remain considerably closer to the perfect-CSI behavior. Thus, CSI uncertainty affects not only the position of the reliability transition but also its evolution with increasing SNR.

The corresponding packet-level behavior is shown in Figure 5.10. Since packet error probability depends strongly on the underlying BER, the PER curves exhibit a characteristic waterfall behavior, where each configuration transitions from an unreliable region to a low-error region as SNR increases.

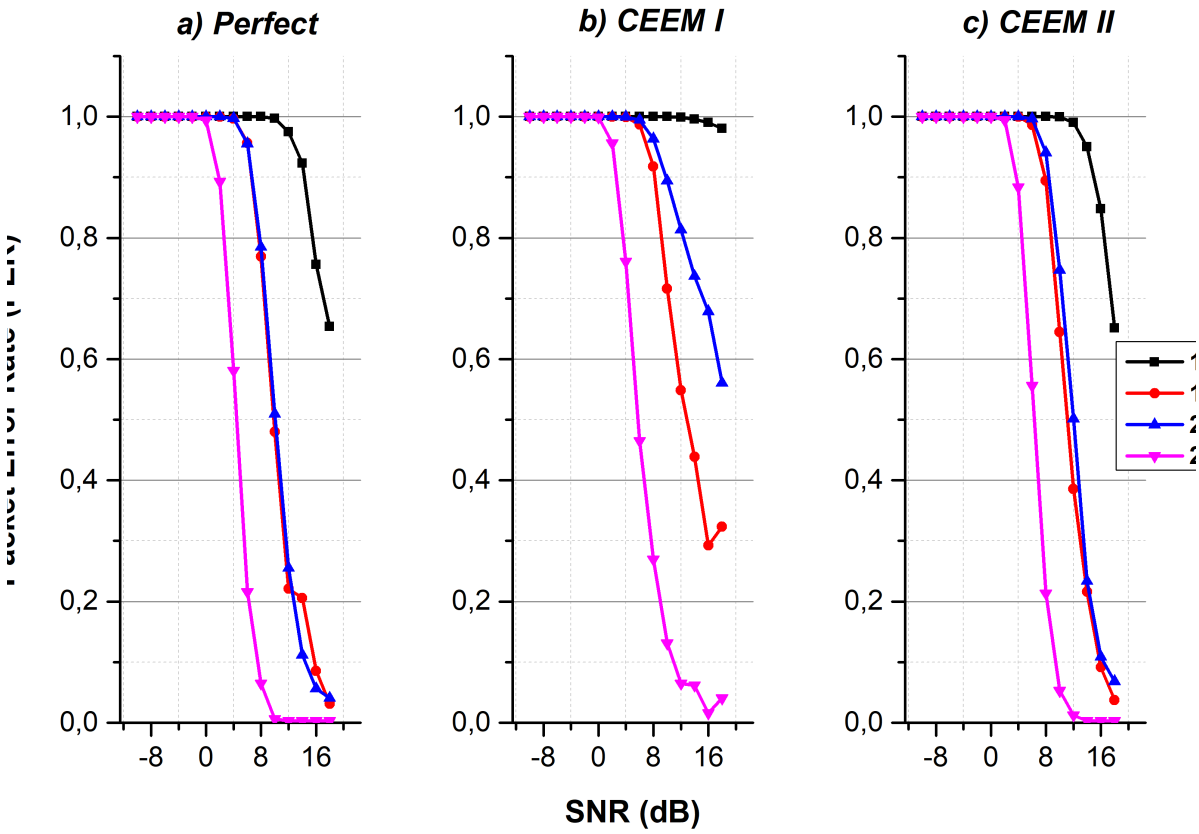


Figure 5.10. PER versus SNR for MIMO configurations under perfect and imperfect CSI (SF = 10): (a) Perfect CSI, (b) CEEM-I, (c) CEEM-II.

Under perfect CSI, diversity-enabled configurations reach the low-PER region earlier than the single-antenna case. In particular, the 2×2 configuration achieves the earliest reliability transition, while the 1×1 configuration requires significantly higher SNR to approach comparable packet-level reliability. This behavior is critical from an energy perspective, because configurations that enter the low-PER region earlier can reduce retransmission-related energy consumption.

Under imperfect CSI, the packet-level behavior depends strongly on the adopted channel-estimation error model. Under CEEM-I, the fixed estimation-error variance produces a persistent reliability degradation at high SNR, preventing several configurations from fully reaching the low-PER region within the investigated SNR range. The 2×2 configuration remains considerably more robust and preserves a substantially earlier reliability transition than the lower-diversity alternatives. Under CEEM-II, in contrast, the PER behavior remains much closer to the perfect-CSI case, since the improving estimation quality with increasing SNR allows the diversity gains to be progressively recovered.

Overall, the BER and PER results reveal an SNR-driven reliability transition whose position

and shape depend jointly on diversity order and CSI quality. Spatial diversity shifts this transition toward lower SNR values by reducing packet errors and the associated retransmission burden. However, the effect of imperfect CSI is strongly model dependent. Fixed estimation uncertainty, as represented by CEEM-I, can impose a residual reliability limitation even as SNR increases, whereas the SNR-dependent estimation model of CEEM-II allows the system to progressively recover much of the diversity benefit observed under perfect CSI. This distinction is particularly important from an energy perspective, because it determines whether increasing SNR can eventually suppress retransmission-related energy or whether residual CSI uncertainty continues to constrain energy-efficient operation.

5.2.3 SNR-Driven Energy–Reliability Trade-Off and Mode Switching

Following the reliability analysis, the next step is to investigate how the observed BER and PER behavior translates into energy efficiency. In LoRa systems, the energy cost per successfully delivered packet is strongly dependent on the operating SNR, since packet failures directly increase retransmission-related energy consumption. Consequently, the transition from unreliable to reliable communication plays a central role in determining the energy-optimal antenna configuration.

Figure 5.11 presents the normalized energy consumption per successful packet as a function of SNR for the considered MIMO configurations under perfect and imperfect CSI conditions for SF = 10.

The results reveal a strong SNR dependence of energy efficiency across all configurations. Under low-SNR conditions, all schemes require significantly higher energy due to the high probability of packet failure and repeated transmissions. As the SNR increases, the energy consumption decreases rapidly, reflecting the improvement in packet-level reliability and the corresponding reduction in retransmission-related energy cost.

Under perfect CSI, the 2×2 configuration achieves substantially lower energy consumption than the other schemes in the low- and moderate-SNR regime in which retransmissions remain significant. This behavior is directly linked to its earlier transition into the low-PER region, allowing it to suppress retransmission-related energy more effectively than the lower-diversity configurations. As SNR increases further and packet errors become rare, the retransmission advantage of diversity progressively diminishes and the energy curves converge toward their configuration-dependent per-attempt energy levels.

Under imperfect CSI, the energy behavior depends strongly on the adopted estimation-error model. Under CEEM-I, residual channel-estimation uncertainty limits the reliability improvement of several configurations and therefore maintains a higher retransmission-related energy cost over a wider SNR range. The 2×2 configuration remains comparatively robust and reaches the low-energy region substantially earlier. Under CEEM-II, the energy behavior approaches the perfect-CSI case as SNR increases, reflecting the progressive improvement in channel-estimation quality. Thus, CSI uncertainty affects the energy landscape primarily through its impact on packet reliability and the resulting retransmission burden.

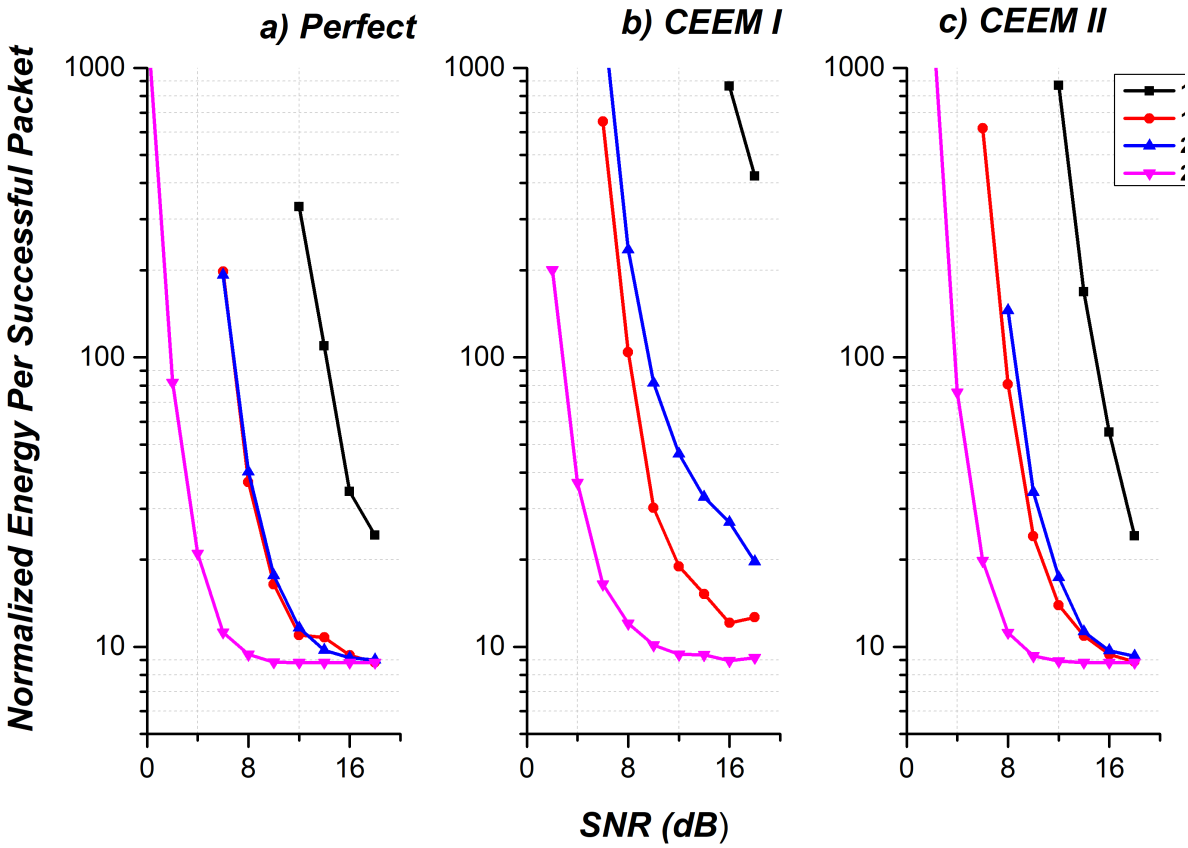


Figure 5.11. Normalized energy per successful packet versus SNR for different MIMO configurations under perfect and imperfect CSI (SF = 10): (a) Perfect CSI, (b) CEEM-I, (c) CEEM-II.

The relationship between energy efficiency and packet reliability is illustrated more directly in Figure 5.12, which shows the normalized energy per successful packet as a function of PER.

A clear energy–reliability coupling is observed across all antenna configurations. In the low-PER regime, the energy consumption of all configurations converges to similar values, since successful transmission is achieved with high probability and retransmissions become negligible. In contrast, as PER increases toward unity, the required energy rises sharply due to repeated unsuccessful transmissions.

Although the general increase in energy with PER follows directly from the reliability-aware energy metric, the figure highlights the strong nonlinear amplification of energy expenditure as packet reliability deteriorates. Differences between antenna configurations arise primarily because each configuration reaches a given PER at different SNR conditions, reflecting its corresponding diversity and CSI robustness.

The results therefore reveal an SNR-driven evolution of the energy-optimal operating regime rather than a monotonic preference for increasing diversity. At very low SNR, packet reliability is severely degraded and some configurations may become effectively infeasible because retransmission requirements grow excessively. As SNR enters the reliability-transition region, diversity becomes particularly valuable: configurations such as 2×2 can reach acceptable packet reliability substantially earlier and thereby avoid the large retransmission-energy penalty experienced by lower-diversity schemes. At sufficiently high SNR, however, packet errors be-

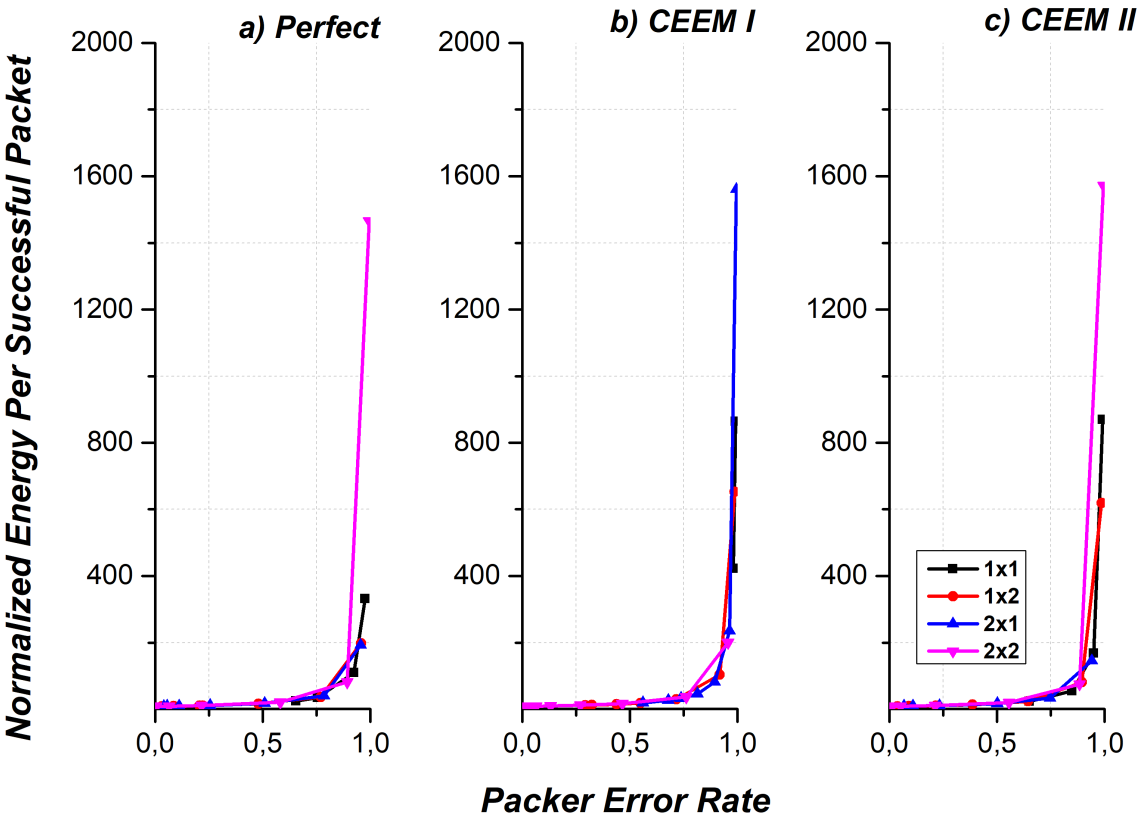


Figure 5.12. Normalized energy per successful packet as a function of PER under perfect and imperfect CSI (SF = 10): (a) Perfect CSI, (b) CEEM-I, (c) CEEM-II.

come infrequent for multiple configurations and the retransmission-related benefit of additional diversity progressively diminishes. In this region, configuration-dependent transmission and implementation costs increasingly determine the energy-optimal mode. Imperfect CSI modifies the location and extent of these regions, with CEEM-I imposing a stronger residual reliability limitation than CEEM-II.

This SNR-driven evolution establishes the basis for the energy-optimal operating regions examined in the following subsections, where the additional effects of spreading factor, CSI quality and implementation overhead are incorporated into the mode-selection problem.

5.2.4 Impact of System Parameters

The energy-efficient operation of LoRa MIMO systems is governed not only by the antenna configuration itself, but also by a set of critical system parameters that directly influence communication reliability and energy consumption. Among these parameters, channel state information (CSI) quality and spreading factor (SF) play a particularly important role. CSI quality determines the effective diversity gain and the resulting retransmission burden, whereas SF affects both link robustness and transmission time-on-air, thereby introducing a direct reliability–energy trade-off. This subsection investigates how these parameters reshape the energy-optimal operating regions and alter the mode-switching behavior identified in the

previous analysis.

Impact of CSI Accuracy

The impact of channel state information (CSI) accuracy on energy efficiency is strongly dependent on both the operating SNR and the selected antenna configuration. Since the energy efficiency of LoRa MIMO systems is tightly coupled to packet-level reliability, CSI uncertainty directly affects the retransmission burden and, consequently, the energy required for successful packet delivery. This effect is illustrated in Figure 5.13.

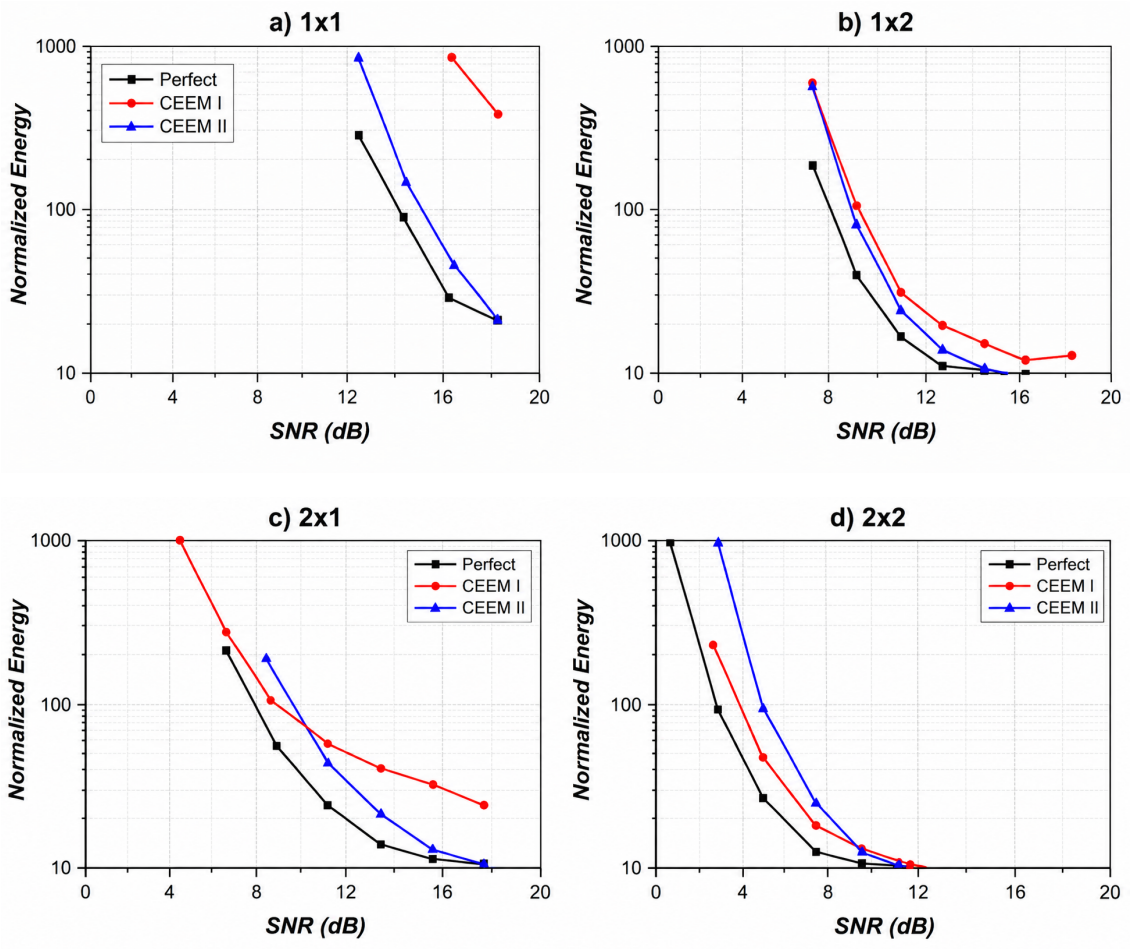


Figure 5.13. Impact of CSI accuracy on the normalized energy per successful packet versus SNR for different MIMO configurations (SF = 10): (a) 1×1, (b) 1×2, (c) 2×1, (d) 2×2.

The results show that CSI uncertainty affects both the position and the shape of the energy transition toward reliable operation, although its impact differs across antenna configurations and estimation models. Under perfect CSI, the energy required per successful packet decreases rapidly as SNR increases, reflecting the reduction in retransmission-related energy consumption. Under CEEM-I, the fixed estimation uncertainty produces a persistent energy penalty for several configurations, particularly at higher SNR, where the corresponding curves remain above the perfect-CSI levels. Under CEEM-II, the energy penalty is more pronounced at lower and intermediate SNR values, but progressively diminishes as SNR increases because the

estimation quality improves with the operating SNR. The effect is therefore configuration and estimation-model dependent rather than strictly proportional to diversity order. Nevertheless, the 2×2 configuration remains comparatively robust, reaching the low-energy region at lower SNR values than the other configurations under all considered CSI conditions.

An important implication is that CSI quality directly modifies the boundaries of energy-efficient operation. Imperfect channel estimation generally requires stronger channel conditions before the retransmission burden becomes sufficiently small, thereby shifting the transition toward the low-energy operating region. The magnitude of this shift depends on both the antenna configuration and the adopted estimation-error model. At sufficiently high SNR, the energy curves tend to approach their configuration-dependent minimum levels as packet errors become negligible and retransmission-related energy vanishes. CSI uncertainty therefore primarily influences the transition region, where differences in packet reliability translate directly into differences in retransmission-related energy consumption, and consequently plays a direct role in determining the SNR range over which each configuration approaches energy-efficient operation.

Impact of Spreading Factor

The spreading factor (SF) plays a fundamental role in determining the energy efficiency of LoRa systems, since it directly affects both communication reliability and transmission duration. Unlike antenna diversity, which improves reliability through spatial processing, the spreading factor improves reliability through increased symbol duration and processing gain, at the cost of longer airtime. This creates a fundamentally different energy–reliability trade-off, illustrated in Figure 5.14.

A clear SF-dependent energy ordering is observed for both antenna configurations, with SF = 12 exhibiting the highest energy consumption, followed by SF = 10 and SF = 8. This ordering persists throughout the investigated SNR range, although the absolute energy levels remain dependent on the employed MIMO configuration. As SNR increases and retransmission-related energy progressively decreases, the curves approach distinct SF-dependent energy floors. These differences reflect the persistent transmission-duration cost associated with increasing the spreading factor.

Although increasing the spreading factor improves communication robustness, the results clearly show that this reliability enhancement comes at a substantial energy cost, in agreement with the well-established airtime–reliability trade-off of LoRa systems [57, 58]. This observation highlights an important distinction between spatial and temporal reliability enhancement mechanisms: while diversity improves reliability through parallel spatial paths, higher SF values achieve reliability improvements by extending transmission duration.

This distinction has important implications for energy-optimal LoRa MIMO operation. As retransmission-related energy decreases with improving channel conditions, the airtime penalty associated with higher SF values does not disappear; instead, it remains embedded in the per-attempt transmission cost and produces distinct SF-dependent energy floors. Conse-

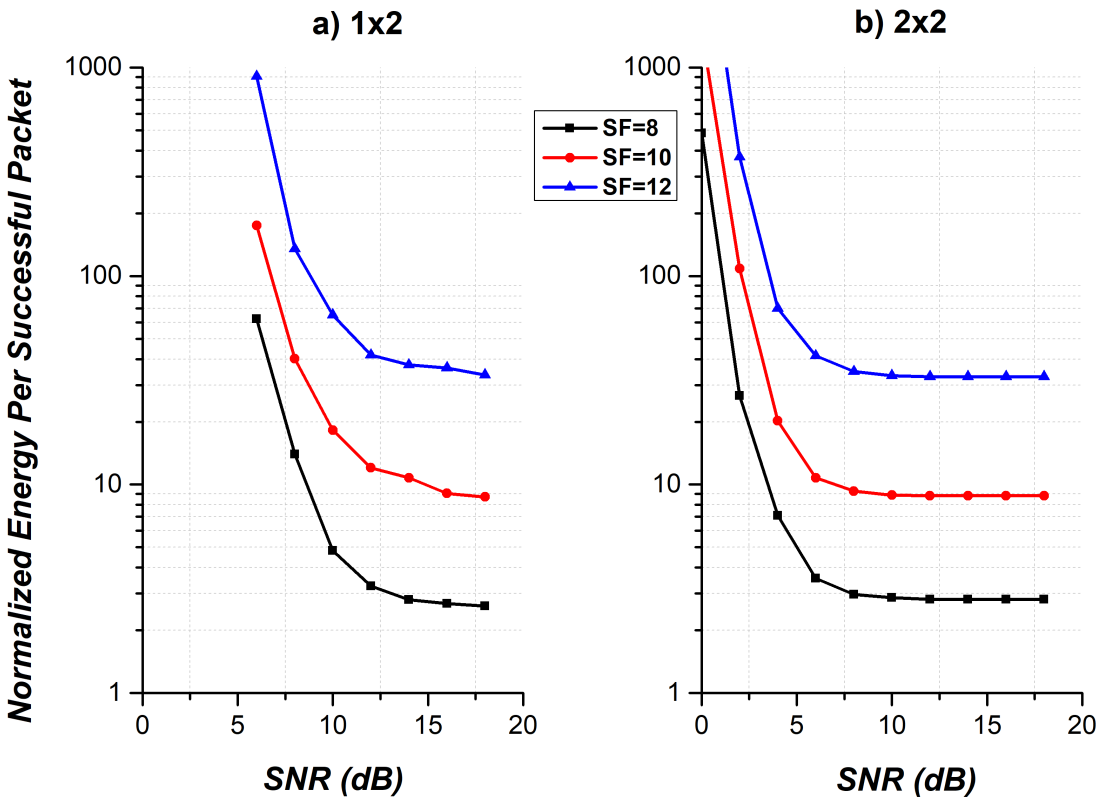


Figure 5.14. Effect of the spreading factor on the normalized energy per successful packet versus SNR for selected MIMO configurations under perfect CSI: (a) 1×2, (b) 2×2.

quently, increasing the SF cannot be treated as an energetically neutral means of improving reliability. Energy-efficient operation therefore requires a joint balance between spreading-factor selection and spatial diversity: reliability may be improved either through longer airtime or through additional antenna resources, but each mechanism introduces a different energy cost. The resulting operating point is therefore jointly determined by SNR, antenna configuration, CSI quality and spreading factor.

5.2.5 Energy-Optimal Operating Regions and Design Insights

The preceding analyses collectively reveal that the energy-efficient operation of LoRa MIMO systems is governed by a structured optimization landscape determined by the interaction between packet reliability, implementation-related energy cost, channel estimation quality and spreading-factor-dependent airtime. As in the conventional MIMO framework examined previously, no antenna configuration is universally energy-optimal. However, the highly constrained LPWAN operating regime produces a distinct mode-selection structure in which the energy-optimal configuration is primarily determined by the balance between retransmission avoidance and the additional cost of spatial diversity.

Figure 5.15 summarizes the resulting energy-optimal operating regions for the considered antenna configurations under different CSI conditions.

A clear operating-region structure emerges. Within the considered parameter range, the

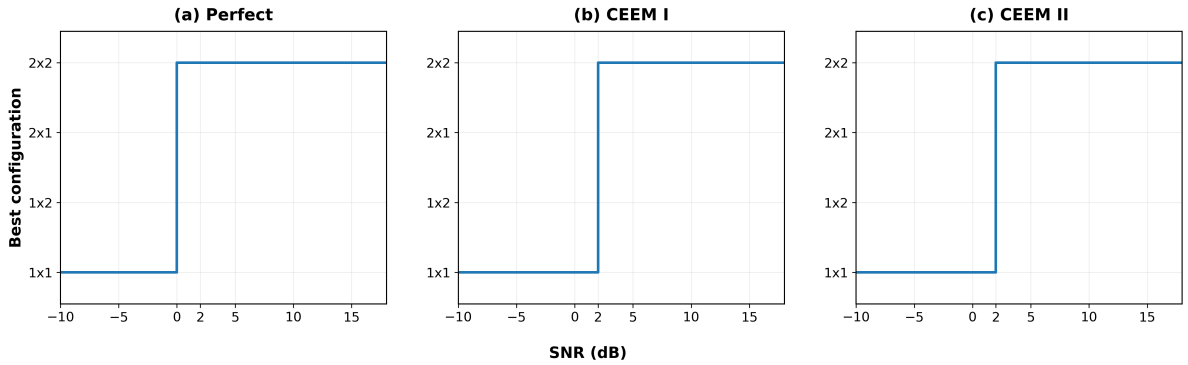


Figure 5.15. Energy-optimal MIMO configuration as a function of SNR under different CSI conditions (SF = 10): (a) Perfect CSI, (b) CEEM-I, (c) CEEM-II.

optimization is dominated by two configurations, namely the single-antenna 1×1 mode and the full-diversity 2×2 mode. At low SNR, the 1×1 configuration is energy-optimal, since the additional reliability provided by spatial diversity is not yet sufficient to compensate for the increased per-attempt energy associated with multi-antenna operation. This defines a single-antenna operating region in which minimizing implementation-related energy cost is more beneficial than activating additional spatial diversity.

As SNR increases, a configuration-dependent transition boundary is reached beyond which the 2×2 mode becomes energy-optimal. In this region, the improvement in packet-delivery probability provided by full spatial diversity becomes sufficiently large to offset its additional hardware and processing cost. The reduction in retransmission-related energy therefore outweighs the increased per-attempt energy, defining a full-diversity operating region.

A particularly important result is that, for the considered SF = 10 scenarios and adopted energy model, the intermediate 1×2 and 2×1 configurations do not define distinct energy-optimal regions. Although both configurations improve reliability relative to 1×1, their reliability gains are not sufficient to produce a lower overall energy per successful packet than both competing modes. The resulting optimization landscape therefore reduces, for the investigated operating conditions, to a two-mode structure characterized by a transition from 1×1 to 2×2 operation. This result should not be interpreted as a universal property of LoRa MIMO systems, but rather as a consequence of the considered reliability characteristics, implementation costs and system parameters.

The physical origin of this transition can be interpreted directly through the adopted energy-efficiency metric. For configuration m, the normalized energy per successfully delivered packet is given by (5.1).

In the LoRa framework, $E_{\mathrm{pkt}}^{(m)}$ incorporates the transmission-related energy, configuration-dependent hardware and processing cost, and the airtime contribution associated with the selected spreading factor.

For two competing configurations, such as 1×1 and 2×2, full-diversity operation becomes energy beneficial when

$$E_{\text{succ}}^{(2\times2)} < E_{\text{succ}}^{(1\times1)}, \tag{5.8}$$

or equivalently,

$$\frac{E_{\text{pkt}}^{(2\times2)}}{1-\text{PER}_{2\times2}} < \frac{E_{\text{pkt}}^{(1\times1)}}{1-\text{PER}_{1\times1}}. \tag{5.9}$$

The equality between the two sides of (5.9) defines the mode-transition boundary. Below this boundary, the additional per-attempt energy required by full-diversity operation is not sufficiently compensated by its reliability gain, and 1×1 remains energy-optimal. Beyond the boundary, the reduction in packet failures and retransmissions becomes sufficiently large for the 2×2 configuration to provide lower overall energy consumption. The transition is therefore governed by the balance between the additional implementation cost of spatial diversity and the retransmission energy avoided through improved packet reliability.

Design Insight 1: SNR-Driven Mode Switching

SNR acts as the primary driver of the observed mode-switching behavior. Rather than a single antenna configuration remaining optimal throughout the operating range, the preferred mode changes when the reliability gain of spatial diversity becomes sufficiently large to compensate for its additional per-attempt energy cost. For the investigated conditions, this produces a transition between a low-SNR 1×1 operating region and a higher-SNR 2×2 operating region. The energy-optimal configuration is therefore determined not by diversity order alone, but by the operating point relative to the mode-transition boundary.

Design Insight 2: CSI-Dependent Boundary Shifting

The position of the mode-transition boundary is not fixed. CSI quality modifies the effective reliability gain provided by spatial diversity and therefore changes the balance between implementation cost and retransmission reduction. The different behavior observed under perfect CSI, CEEM-I and CEEM-II demonstrates that channel-estimation uncertainty affects not only BER and PER, but also the SNR conditions under which multi-antenna operation becomes energy beneficial. CSI quality therefore acts as a boundary-shifting parameter, with the resulting transition determined by the characteristics of the adopted estimation-error model.

Design Insight 3: Airtime–Diversity Trade-Off

The spreading factor introduces a second, LoRa-specific dimension to the energy optimization problem. Both increased SF and spatial diversity can improve communication reliability, but they do so through fundamentally different mechanisms and incur different energy costs. Increasing the SF improves robustness through additional processing gain but increases transmission duration and therefore introduces a persistent airtime-related energy penalty. Spatial diversity, in contrast, improves reliability through additional spatial paths while increasing

RF-chain activation and processing cost. Energy-efficient LoRa operation therefore requires balancing temporal and spatial reliability enhancement rather than maximizing either spreading factor or diversity order independently.

Design Insight 4: Need for Joint Adaptive Operation

The combined results demonstrate that the energy-optimal operating point is jointly determined by SNR, CSI quality, spreading factor and antenna configuration. A static MIMO mode or a fixed spreading-factor policy cannot therefore remain universally energy-optimal as operating conditions change. Instead, energy-efficient operation requires adaptation across the available reliability-enhancement mechanisms, selecting the antenna configuration and spreading factor according to the current channel and estimation conditions. This provides the direct motivation for an adaptive mode-selection framework capable of tracking the corresponding energy-optimal operating region.

Overall, the LoRa analysis reveals a simpler but highly parameter-sensitive operating-region structure compared with the conventional MIMO case. Within the investigated conditions, the dominant antenna-selection problem reduces to switching between low-complexity 1×1 operation and full-diversity 2×2 operation, while CSI quality and spreading factor modify the energy landscape and the location of the corresponding transition boundary. Together with the conventional MIMO analysis presented previously, these findings establish that energy-optimal antenna operation is inherently condition dependent and provide the physical and analytical foundation for the adaptive configuration-selection framework developed in the following chapter.

5.3 Summary and Conclusions

This chapter investigated the reliability–energy trade-off governing MIMO operation and examined how this trade-off determines the energy-preferred antenna configuration under different operating conditions. Building upon the performance characterization developed in Chapter 4, the analysis moved beyond the question of how propagation conditions and antenna configurations affect communication performance and addressed a different design problem: whether the reliability improvement provided by additional diversity is energetically sufficient to justify its associated implementation cost. The central principle underlying the analysis is that improved reliability reduces packet failures and the resulting retransmission burden, whereas additional antenna resources increase the per-attempt energy through RF-chain activation and signal-processing requirements. Energy-optimal operation therefore emerges from the balance between these competing effects rather than from reliability or diversity order alone.

The first part of the chapter examined diversity-based MIMO systems under geometry-aware propagation conditions. The results showed that the energetic value of diversity changes substantially with the operating point. Under favorable short-range conditions, packet errors and retransmissions remain limited, and the additional reliability provided by higher-order diver-

sity produces relatively small energy savings. When configuration-dependent hardware costs are considered, simpler antenna configurations therefore become increasingly competitive. As channel conditions deteriorate, the retransmission burden of lower-diversity configurations increases and improved reliability acquires greater energetic value. Higher-diversity modes can then become energy-preferable when the avoided retransmission cost is sufficient to compensate for their additional circuit and processing overhead. Under sufficiently severe propagation conditions, however, PER becomes high for all configurations and the energy required for successful packet delivery increases rapidly, eventually leading to outage-like behavior.

The conventional MIMO analysis further demonstrated that the boundaries between these operating behaviors are not fixed. Transmission distance drives their evolution through its direct effect on path loss and packet reliability, while SNR and propagation environment substantially modify the conditions under which configuration transitions occur. Antenna spacing introduces a secondary influence through spatial correlation and achievable diversity gain. Hardware-related overhead plays an equally important role: increasing implementation cost shifts the energy balance toward lower-complexity configurations and restricts the operating conditions under which additional diversity remains energetically justified. These results demonstrate that diversity order and energy efficiency are not monotonically related and that neither minimum-complexity nor maximum-diversity operation is universally energy-optimal.

The second part of the chapter extended the same reliability–energy optimization principle to LoRa MIMO systems, where the energy landscape is further shaped by LPWAN-specific constraints. In this case, energy consumption depends not only on packet reliability and hardware activation, but also strongly on transmission duration. The spreading factor therefore introduces an additional reliability mechanism with a fundamentally different energy cost: increasing SF improves robustness through increased processing gain but simultaneously increases airtime and the energy consumed per transmission attempt. Spatial diversity, in contrast, improves reliability through additional spatial resources while introducing RF-chain and processing overhead. LoRa MIMO operation is therefore governed by the joint balance between retransmission avoidance, spatial-diversity cost and spreading-factor-dependent airtime.

Within the investigated LoRa operating conditions, a particularly clear mode-selection structure emerged. For SF = 10 and the adopted energy model, the dominant energy-preferred configurations were 1×1 and 2×2, whereas the intermediate 1×2 and 2×1 configurations did not form distinct energy-optimal operating regions. The preferred mode changes as SNR varies because the relative energy benefit of the reliability improvement provided by full diversity changes with the retransmission burden. A transition occurs when the reduction in packet failures achieved by the 2×2 configuration becomes sufficient to compensate for its higher per-attempt energy cost. The investigated LoRa case therefore exhibits an effectively two-mode energy-selection structure, with the transition location determined by the prevailing SNR and CSI conditions.

Channel-estimation accuracy was shown to directly influence this transition by modifying

the effective reliability benefit of spatial diversity. The comparison between perfect CSI, CEEM-I and CEEM-II demonstrated that CSI uncertainty affects not only BER and PER, but also the location and characteristics of the energy-relevant mode-transition region. Fixed estimation uncertainty can maintain a residual reliability limitation even as SNR increases, whereas an SNR-dependent estimation model can allow a larger part of the diversity benefit to be progressively recovered. Spreading factor introduces a complementary effect: although larger SF values can improve reliability, their longer transmission duration produces a persistent airtime-related energy penalty. The LoRa results therefore reveal that spatial diversity and spreading factor constitute two distinct reliability-enhancement mechanisms whose energetic costs must be jointly considered.

Taken together, the two analyses establish a common optimization principle across substantially different wireless operating regimes. For any candidate MIMO configuration, additional reliability has energetic value only when the corresponding reduction in packet failures and retransmissions compensates for the additional energy required to obtain that reliability. In conventional MIMO systems, this balance is primarily shaped by propagation conditions, SNR and hardware overhead. In LoRa MIMO systems, the same fundamental balance remains valid but is additionally influenced by CSI quality and spreading-factor-dependent airtime. The specific energy-optimal configurations and transition boundaries therefore differ between the two systems, while the underlying reliability–energy principle remains common.

Beyond the individual simulation results, the broader contribution of this chapter is the establishment of an operating-region perspective for reliability-aware MIMO energy optimization. The analysis identifies configuration-dependent transition boundaries at which the reliability benefit of additional diversity becomes sufficient to compensate for its additional energy cost and demonstrates that these boundaries are not static. Instead, they move as propagation conditions, SNR, CSI quality, hardware overhead and transmission-related costs change. A configuration that is energy-preferred at one operating point may therefore become suboptimal when the underlying conditions change. Energy-efficient MIMO design should consequently not be interpreted as the search for a universally optimal antenna configuration, but as the identification of the configuration that provides the most favorable reliability–energy balance under the prevailing operating conditions.

Overall, the findings demonstrate that energy-efficient MIMO operation cannot be determined independently of communication reliability or implementation cost. The relevant design objective is neither to maximize reliability through permanent use of the strongest available diversity configuration nor to minimize the energy expenditure of an individual transmission attempt through minimum-complexity operation. Instead, the energy-optimal solution emerges from the balance between the energy required for each transmission attempt and the retransmission burden resulting from unsuccessful packet delivery. This interpretation provides a common framework for understanding the configuration transitions observed in both conventional and LoRa MIMO systems and reinforces the broader thesis premise that MIMO design must account for the operating conditions under which communication actually takes

place.

The findings of this chapter therefore provide the direct motivation for adaptive MIMO operation. Chapter 4 established that MIMO performance is strongly condition-dependent, while the present chapter demonstrated that this condition dependence translates into moving reliability–energy transition boundaries and changes in the energy-preferred antenna configuration. The remaining design problem is consequently not simply to identify the best MIMO mode, but to determine how the system should select and switch between available configurations as operating conditions evolve. The next chapter addresses this problem by developing an adaptive MIMO selection framework that uses the identified reliability–energy relationships and operating-region structure to dynamically select the transmission configuration according to the prevailing channel conditions, reliability requirements and energy constraints.

6 Structured Adaptive Diversity Selection for Energy-Aware MIMO Systems

The preceding chapters established that the performance and energy efficiency of MIMO systems are strongly influenced by propagation conditions, CSI uncertainty and communication reliability requirements. The characterization analysis under realistic wireless environments demonstrated that MIMO performance varies significantly across different channel conditions, antenna configurations and user distributions. In parallel, the energy-aware optimization analysis revealed that stronger diversity configurations do not necessarily lead to lower overall energy consumption, since the reliability gains achieved through diversity must be balanced against increased hardware activation and signal-processing overhead.

Under favorable operating conditions, low-complexity configurations may provide sufficient reliability with minimal energy expenditure. As channel conditions deteriorate and the retransmission burden increases, stronger diversity configurations may become energy-preferable when their reliability gain is sufficient to compensate for the associated implementation cost. Under severely degraded conditions, however, the feasible operating space may become increasingly restricted. These observations indicate that fixed MIMO operation is generally suboptimal under realistic wireless conditions.

This operating-region dependence naturally motivates the need for adaptive MIMO operation, where the transmission configuration is dynamically selected according to the prevailing operating conditions. Rather than relying on static transmission strategies, MIMO systems should adaptively exploit the most energy-efficient operating mode as channel conditions, reliability constraints and implementation costs vary. Such adaptive operation enables wireless systems to balance communication reliability and energy efficiency while avoiding both unnecessary complexity and insufficient diversity protection.

Motivated by these observations, this chapter investigates adaptive energy-aware diversity selection for MIMO systems operating under imperfect CSI and heterogeneous hardware-overhead conditions. The proposed framework translates the operating-region perspective established in the previous chapter into a dynamic mode-selection mechanism. Multiple receive- and transmit-diversity configurations are evaluated at each operating point, and the most energy-efficient feasible mode is selected according to the prevailing channel and reliability conditions. The adaptive decision process is based on the expected energy-per-successful-packet criterion and therefore jointly accounts for communication reliability, retransmission burden, RF-chain activation cost and processing overhead. Beyond adaptive mode selection itself, this chapter further investigates the structural behavior of adaptive diversity evolution across the SNR–distance operating space. Particular emphasis is placed on understanding how adaptive operating decisions evolve under changing propagation conditions, how transitions occur between diversity modes and how robust the adaptive behavior remains under CSI uncertainty. The analysis shows that adaptive operation exhibits structured operating regions

characterized by progressive diversity activation, predominantly local transitions between neighboring diversity layers, and coherent operating-region redistribution under increasing CSI uncertainty. Overall, this chapter demonstrates that adaptive diversity selection enables robust and energy-efficient MIMO operation under realistic wireless conditions, establishing adaptive optimization as an effective strategy for scenario-dependent wireless environments.

6.1 Adaptive Optimization Framework for Diversity Selection

This section presents the theoretical framework underlying the proposed adaptive diversity-selection methodology. The framework is designed to dynamically exploit the energy-optimal operating regions identified in the previous chapter by performing feasibility-aware adaptive mode selection across varying propagation and channel conditions. Figure 6.1 illustrates the overall architecture of the proposed framework, which integrates propagation-aware channel modeling, CSI-aware reliability evaluation, feasibility-aware energy optimization and adaptive mode selection in order to identify the most energy-efficient MIMO operating mode under each operating condition.

In addition to adaptive mode selection, transition, stability and learnability analyses are incorporated in order to characterize the structural behavior, robustness and predictability of the resulting adaptive operating policy across the considered operating space.

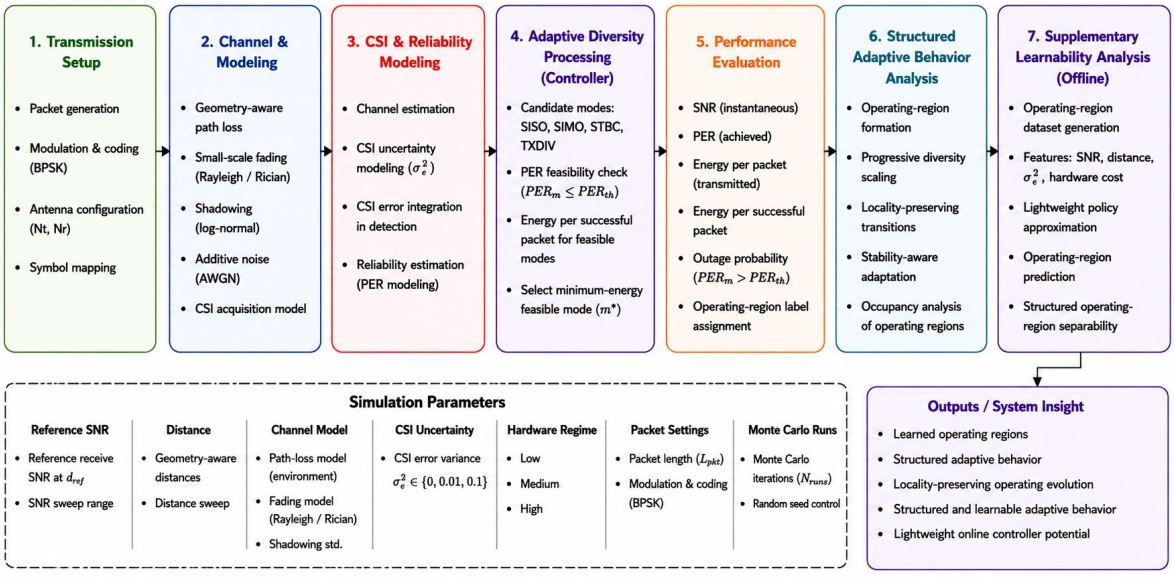


Figure 6.1. Overall architecture of the proposed adaptive diversity-selection framework with structured operating-region evolution and supplementary policy characterization.

For each operating point, the proposed framework evaluates the PER of all candidate diversity configurations, determines their feasibility status, estimates the corresponding packet-level energy expenditure and finally selects the most energy-efficient feasible operating mode according to the underlying adaptive policy. Consequently, the proposed framework enables a

comprehensive evaluation of adaptive diversity-selection behavior under varying propagation conditions, CSI uncertainty and hardware-overhead assumptions.

6.1.1 System Model

The proposed framework investigates adaptive diversity-selection behavior in wireless MIMO environments under imperfect CSI and heterogeneous hardware-overhead conditions. Multiple receive- and transmit-diversity configurations are evaluated under varying propagation, reliability and channel-uncertainty conditions in order to identify the most energy-efficient feasible operating mode at each point of the considered SNR–distance operating space.

The considered diversity set is defined as

$$\mathcal{M} = \{\text{SISO}, \text{SIMO}, \text{STBC/Alamouti}, \text{TXDIV}\} . \tag{6.1}$$

More specifically, the framework considers SISO 1×1, SIMO 1×2, SIMO 1×4, SIMO 1×8, STBC 2×1, STBC 2×2, TXDIV 4×2 and TXDIV 8×4 configurations. These operating modes provide different diversity gains, reliability characteristics and hardware-complexity requirements, thereby forming a representative adaptive operating space.

Communication reliability is evaluated using the packet error rate (PER), which serves as the primary feasibility and retransmission-efficiency metric of the framework. The PER of each operating mode depends on the operating SNR, transmission distance, propagation attenuation and CSI quality.

To account for channel uncertainty, imperfect CSI is modeled through the estimation-error variance

$$\sigma_e^2 \tag{6.2}$$

where higher values of σ_e^2 correspond to progressively degraded channel knowledge and reduced estimation accuracy.

6.1.2 Energy Consumption Model

To evaluate the energy efficiency of the considered diversity configurations, the proposed framework employs a normalized packet-level energy model. Rather than targeting detailed circuit-level power modeling, the adopted formulation captures the relative energy cost associated with activating different antenna and diversity configurations, which is sufficient for analyzing adaptive mode-selection behavior.

For each operating mode m, the total packet-level energy consumption is defined as

$$E_{\text{pkt},m} = E_{\text{tx}} + \alpha_m + \beta_m \tag{6.3}$$

where E_{tx} denotes the baseline transmission energy, while α_m and β_m represent mode-dependent hardware and processing overhead terms, respectively. In the present formulation, E_{tx} is assumed identical for all operating modes, allowing configuration selection to be deter-

mined by the trade-off between reliability improvement and mode-dependent implementation-energy overhead.

The parameter α_m represents the normalized mode-dependent hardware overhead, including the relative cost associated with additional active RF resources, whereas β_m represents the corresponding normalized processing-related overhead. These terms are not intended as circuit-level power measurements, but as relative implementation-cost parameters that enable controlled evaluation of hardware-aware adaptive mode selection. To investigate the impact of different hardware assumptions on adaptive operating behavior, three hardware-overhead regimes are considered:

$$r \in \{\text{Low}, \text{Moderate}, \text{High}\} \tag{6.4}$$

Each regime corresponds to different values of α_m and β_m, while preserving the same fundamental principle: higher-complexity diversity configurations require progressively larger hardware and processing overhead. Table 6.1 summarizes the normalized hardware-overhead parameters considered for all diversity modes.

Table 6.1. Normalized hardware-overhead parameters for the considered diversity configurations under different hardware-overhead regimes.

Mode	α_m	β_m	α_m	β_m	α_m	β_m
	Low	**Low**	**Moderate**	**Moderate**	**High**	**High**
SISO 1×1	0.10	0.00	0.50	0.00	1.00	0.00
SIMO 1×2	0.18	0.02	0.75	0.05	1.50	0.08
SIMO 1×4	0.30	0.05	1.20	0.12	2.40	0.20
SIMO 1×8	0.55	0.10	2.00	0.25	4.20	0.45
STBC 2×1	0.20	0.03	0.80	0.08	1.60	0.12
STBC 2×2	0.30	0.05	1.10	0.12	2.20	0.18
TXDIV 4×2	0.90	0.25	3.20	0.70	7.00	1.40
TXDIV 8×4	1.80	0.60	6.50	1.60	14.00	3.20

Consequently, a diversity mode with lower PER is not necessarily the most energy-efficient operating solution if its additional implementation overhead outweighs the energy savings obtained through reduced retransmissions. Conversely, lower-complexity configurations may remain preferable when their reliability is sufficient and additional diversity does not provide enough retransmission-related energy reduction to justify its higher per-attempt cost. This balance between packet reliability, retransmission burden and mode-dependent implementation energy constitutes the fundamental decision principle of the proposed adaptive diversity-selection mechanism.

6.1.3 Feasibility-Aware Adaptive Selector

The proposed adaptive selector constitutes the core decision mechanism of the framework and is independently applied to each operating point of the considered SNR–distance operating space. For every operating point, the selector evaluates the PER of all candidate diversity configurations and determines the most energy-efficient feasible operating mode. The overall decision flow of the proposed feasibility-aware adaptive selection mechanism is illustrated in Figure 6.2.

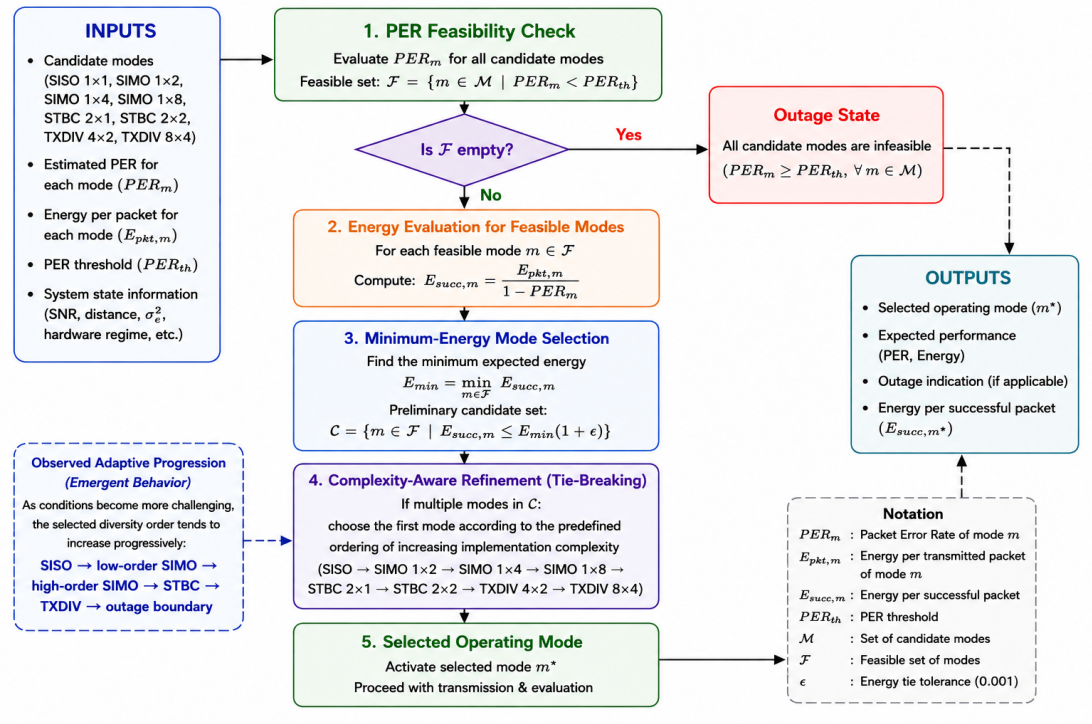


Figure 6.2. Decision flow of the proposed feasibility-aware adaptive diversity-selection policy.

Initially, each operating mode $m \in \mathcal{M}$ is evaluated according to the packet-error feasibility criterion

$$PER_m < PER_{\text{th}} \tag{6.5}$$

where PER_m denotes the packet error rate of mode m, while PER_{th} represents the feasibility threshold. In the present framework, the following value is considered:

$$PER_{\text{th}} = 0.99 \tag{6.6}$$

The selected threshold does not represent a strict QoS reliability target, but rather an outage-feasibility boundary used to distinguish feasible from practically infeasible communication conditions. This formulation enables the adaptive behavior of the framework to be examined up to edge-of-coverage operating states without prematurely classifying challenging operating points as outage.

The feasible operating-mode set is therefore defined as

$$\mathcal{F} = \{m \in \mathcal{M} : PER_m < PER_{\text{th}}\} \tag{6.7}$$

For each feasible mode, the selector computes the expected energy per successful packet transmission:

$$E_{\text{succ},m} = \frac{E_{\text{pkt},m}}{1 - PER_m} \tag{6.8}$$

where $E_{\text{pkt},m}$ denotes the packet-level energy consumption of mode m. This metric jointly captures packet-level energy expenditure, communication reliability and retransmission burden.

The primary mode-selection criterion is given by

$$E_{\min} = \min_{m \in \mathcal{F}} E_{\text{succ},m} \tag{6.9}$$

and the selected operating mode is

$$m^\star = \arg\min_{m \in \mathcal{F}} E_{\text{succ},m} \tag{6.10}$$

where $m^\star$ denotes the operating mode selected by the adaptive framework.

To avoid unnecessary activation of higher-complexity diversity configurations for negligible energy gains, a near-optimality refinement criterion is additionally applied. Specifically, all modes satisfying

$$E_{\text{succ},m} \leq E_{\min}(1 + \epsilon) \tag{6.11}$$

are treated as energetically near-equivalent. In the present framework,

$$\epsilon = 0.001 \tag{6.12}$$

corresponding to a maximum energy deviation of 0.1% from the minimum-energy solution.

Among the near-equivalent candidates, the selector chooses the lowest-complexity operating mode according to the predefined ordering of diversity configurations. This refinement mechanism prevents unnecessary complexity escalation and improves the practical stability of adaptive operation.

If no operating mode satisfies the feasibility criterion, namely

$$\mathcal{F} = \emptyset \tag{6.13}$$

the corresponding operating point is classified as outage.

Overall, the proposed selector performs feasibility-aware energy minimization with complexity-aware refinement, enabling the framework to jointly balance communication reliability, retransmission burden, energy efficiency and hardware complexity.

6.1.4 Transition and Stability Characterization Framework

The feasibility-aware adaptive selector described in the previous subsection determines the energy-efficient operating mode at each point of the considered SNR–distance operating space. Beyond the mode-selection outcome itself, it is important to examine how adaptive operating decisions evolve across neighboring operating points. The objective of this analysis is to quantify transition behavior, operating continuity and switching activity of the adaptive policy.

For each operating scenario, the adaptive operating space is represented through a discrete mode map

$$\mathbf{M}(i, j) \tag{6.14}$$

where each element corresponds to the diversity mode selected by the adaptive selector at the operating point (SNR, d).

Adaptive operating evolution is analyzed through transitions between neighboring operating points along both the SNR and distance axes. For two neighboring operating points, a transition is defined as

$$m_i \rightarrow m_j \tag{6.15}$$

where m_i denotes the operating mode associated with the initial operating point and m_j denotes the mode selected at the neighboring point.

Transition behavior is quantified through the transition distance

$$D(i, j) = |m_i - m_j| \tag{6.16}$$

where the mode indices follow the predefined ordering of the candidate configurations used by the adaptive framework. The resulting quantity does not represent a physical distance between MIMO schemes, but rather provides a discrete measure of how far the adaptive decision moves within the ordered mode set between neighboring operating points.

This formulation enables the distinction between local and non-local operating transitions. Since transition analysis considers operating-mode switches between distinct modes, transitions satisfying

$$D(i, j) = 1 \tag{6.17}$$

are classified as local transitions, as they occur between directly neighboring adaptive layers. Conversely, transitions satisfying

$$D(i, j) > 1 \tag{6.18}$$

are classified as non-local transitions and correspond to changes across multiple adaptive layers. To characterize the continuity of adaptive operating evolution, the average transition distance is defined as

$$D_{\text{avg}} = \frac{1}{N_t} \sum_{k=1}^{N_t} D_k \tag{6.19}$$

where N_t denotes the total number of detected mode transitions and D_k is the transition

distance associated with the k-th transition.

In parallel, the locality ratio is defined as

$$L_{\text{loc}} = \frac{N_{\text{local}}}{N_{\text{switch}}}, \qquad N_{\text{switch}} > 0, \tag{6.20}$$

where N_{local} denotes the number of local mode transitions and N_{switch} is the total number of detected mode switches. The complementary non-local transition ratio is therefore given by

$$A = 1 - L_{\text{loc}}. \tag{6.21}$$

To quantify the overall switching activity of the adaptive policy, the Stability Index is defined as

$$S = 1 - \frac{N_{\text{switch}}}{N_{\text{neighbors}}} \tag{6.22}$$

where $N_{\text{neighbors}}$ denotes the total number of neighboring operating-point comparisons performed across the SNR–distance map. Higher values of S indicate greater spatial persistence of the selected operating mode across neighboring operating conditions, whereas lower values indicate more frequent changes in the adaptive decision.

Collectively, these metrics characterize complementary aspects of adaptive behavior. The transition-distance and locality metrics describe the magnitude and structure of mode changes when switching occurs, whereas the Stability Index quantifies how frequently such switching occurs across the operating space. They therefore provide a quantitative basis for evaluating the continuity, locality and stability of the adaptive mode-selection policy.

6.1.5 Learnability Characterization Framework

The transition and operating-region analyses presented in the previous subsections indicate that the adaptive policy may exhibit structured and regular decision patterns across the considered operating space. To further investigate this property, the resulting adaptive behavior is formulated as a supervised mapping between propagation- and hardware-aware operating features and the corresponding adaptive decision produced by the feasibility-aware selector.

The objective of this analysis is not to replace or modify the adaptive selector, but to provide a supplementary offline characterization of the structure of the resulting policy. In particular, the analysis examines whether the decisions generated by the deterministic energy-aware selection mechanism can be approximated using lightweight machine-learning models. Accurate approximation would indicate that the adaptive decision boundaries exhibit a degree of regularity and predictability that can be captured from a compact set of operating-state features.

The considered feature space includes transmission distance, reference SNR, CSI uncertainty variance, path loss, large-scale received SNR and hardware-overhead regime information. These features jointly represent the propagation, channel-estimation and implementation conditions that influence the adaptive selection process. Supervised classification is then

performed using labels derived directly from the decisions generated across the evaluated operating space.

Policy approximation is examined using lightweight tree-based supervised learning models, specifically decision trees and bagged tree ensembles. These models provide a suitable balance between predictive capability, computational complexity and interpretability. A decision tree provides a compact rule-based representation of the decision structure, whereas bagged ensembles combine multiple tree learners trained on bootstrap samples in order to improve predictive robustness and reduce sensitivity to individual training realizations.

The learnability evaluation is performed through supervised train/test partitioning, confusion-matrix analysis and classification-accuracy metrics. The resulting performance is interpreted as a measure of how consistently the adaptive decision structure can be recovered from the considered operating-state features rather than as a direct measure of the performance of the underlying communication system.

Consequently, the learnability analysis complements the operating-region and transition characterization without forming part of the online adaptive decision mechanism. While the feasibility-aware selector determines the energy-efficient operating mode directly from reliability and energy criteria, the supervised-learning analysis evaluates, offline, whether the resulting policy exhibits sufficiently structured decision boundaries to admit a compact predictive approximation. This provides an additional characterization of the regularity and potential implementability of the proposed adaptive framework.

6.1.6 Simulation Setup

The proposed framework was evaluated using the Vienna LTE-A Downlink System Level Simulator (v2.0 Q3) under geometry-aware wireless propagation conditions and PER-based operating analysis. The evaluation considers multiple receive- and transmit-diversity configurations under imperfect CSI and heterogeneous hardware-overhead regimes in order to investigate the adaptive behavior of the proposed framework across a broad range of operating conditions.

The analysis is performed over the SNR–distance operating space, where each operating point represents a specific combination of transmission distance and reference SNR. Separate operating scenarios are generated for different CSI uncertainty levels and hardware-overhead regimes, allowing the adaptive policy to be evaluated under progressively different estimation and implementation conditions.

The resulting adaptive policy is evaluated through three complementary analysis layers. First, the effectiveness of adaptive diversity selection is examined through operating-region analysis and energy-efficiency evaluation. Second, the structural behavior of the adaptive policy is characterized through occupancy redistribution, transition analysis and stability evaluation. Finally, robustness under CSI uncertainty is examined together with a learnability assessment that investigates whether the resulting adaptive decision structure can be accurately approximated using lightweight supervised-learning models. Table 6.2 summarizes the main

simulation parameters and operating assumptions considered throughout the evaluation.

Table 6.2. Simulation and evaluation parameters.

Parameter	Value / Description
Simulator	Vienna LTE-A SLS-based simulation framework
Evaluation type	PER-based adaptive operating analysis
Selection metric	Expected energy per successful packet
Operating space	SNR–distance grid
Reference distance	$d_{\text{ref}} = 5$ m
Distance values	$\{5, 10, 15, 20, 30, 40, 50\}$ m
Reference SNR values	$\{0, 5, 10, 20, 25, 30\}$ dB
Reference calibration	5000 channel realizations at d_{ref}
Carrier frequency	2.5 GHz
Propagation environment	Indoor LOS
LOS K-factor	6 dB
Shadowing model	Disabled
Channel model	Correlated Rician MIMO fading channel
Large-scale propagation	Distance-dependent path loss
CSI uncertainty variance	$\sigma_e^2 = \{0, 0.01, 0.1\}$
PER feasibility threshold	$PER_{\text{th}} = 0.99$
Hardware-overhead regimes	Low, Moderate, High
Near-optimality tolerance	$\epsilon = 10^{-3}$
Diversity families	SISO, SIMO, STBC/Alamouti, TXDIV
Antenna configurations	1×1, 1×2, 1×4, 1×8, 2×1, 2×2, 4×2, 8×4
Modulation	BPSK

6.2 Adaptive Operating Behavior and Energy-Efficiency Evaluation

6.2.1 Adaptive Operating Region Analysis

Following the development of the proposed adaptive framework, the first step of the analysis is to investigate how diversity-mode selection evolves across different propagation and operating

conditions. To this end, the adaptive behavior of the framework is examined over the SNR–distance operating space through operating-region maps that visualize the mode selected by the feasibility-aware energy-minimization policy at each operating point.

Figure 6.3 presents a representative operating-region map for the Moderate hardware-overhead regime with CSI uncertainty variance $\sigma_e^2 = 0.01$. This scenario represents an intermediate operating case in which neither hardware cost nor CSI degradation dominates the selection process, allowing the interaction between propagation conditions, reliability and diversity-related energy overhead to be clearly observed.

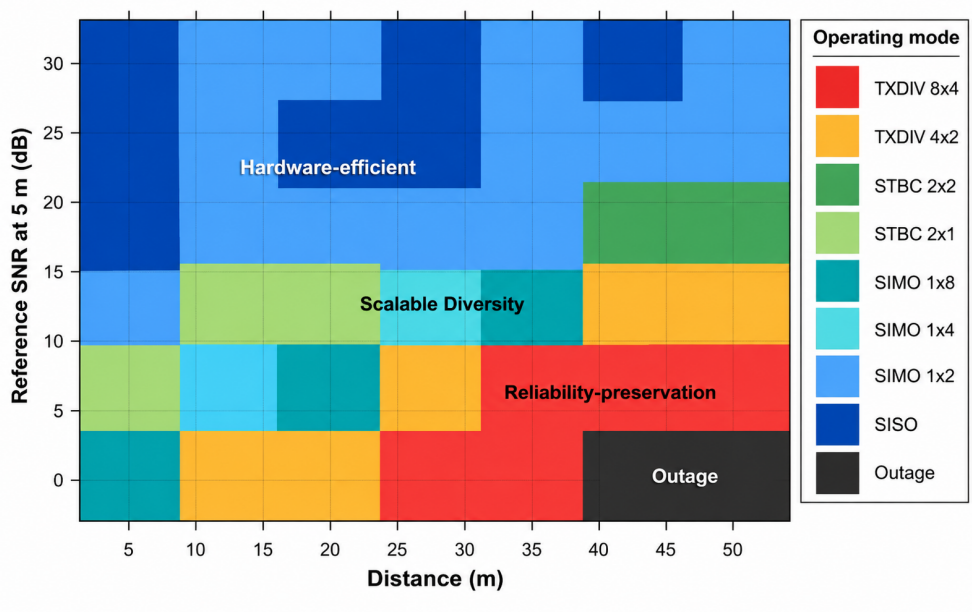


Figure 6.3. Adaptive operating-region map of the proposed framework for the representative Moderate hardware-overhead regime with CSI uncertainty variance $\sigma_e^2 = 0.01$.

The resulting map reveals a structured adaptive policy across the considered operating space. Under favorable propagation conditions, particularly at shorter transmission distances and higher reference-SNR values, the selector predominantly favors SISO and low-order SIMO operation. In these conditions, the available link quality is sufficient to satisfy the feasibility criterion without requiring the additional hardware and processing overhead associated with stronger diversity configurations. The adaptive policy therefore avoids unnecessary diversity activation when its reliability benefit does not justify its additional energy cost.

As propagation conditions deteriorate through increasing distance or decreasing reference SNR, the selected mode progressively shifts toward configurations providing stronger diversity protection. This behavior reflects the reliability–energy trade-off established in Chapter 5: additional diversity becomes energetically justified when the resulting reduction in packet failures and retransmission burden compensates for the higher per-packet hardware and processing cost.

For interpretation purposes, the resulting operating space can be organized into four characteristic regions:

$$\text{Hardware-Efficient} \rightarrow \text{Scalable Diversity} \rightarrow \text{Reliability-Preservation} \rightarrow \text{Outage}. \quad (6.23)$$

The *Hardware-Efficient* region corresponds to operating conditions in which SISO or low-order diversity provides sufficient reliability at comparatively low implementation cost. The *Scalable Diversity* region represents the intermediate adaptation regime, where progressively stronger receive-diversity configurations, particularly SIMO modes, become energy-preferred as propagation conditions deteriorate. The *Reliability-Preservation* region occurs closer to the feasibility boundary, where stronger diversity configurations, including TXDIV modes, are selected because maintaining packet-level reliability becomes increasingly important despite their larger hardware overhead. Finally, the *Outage* region contains operating points for which no candidate configuration satisfies the adopted feasibility condition $PER_m < PER_{\text{th}}$.

An important feature of the representative map is therefore the progressive activation of diversity resources rather than universal dominance of either the simplest or the strongest configuration. Low-complexity modes occupy favorable parts of the operating space, intermediate SIMO configurations become relevant as link conditions deteriorate, and high-diversity TXDIV configurations are primarily activated near the reliability boundary. This spatial organization provides an initial qualitative indication that the adaptive policy evolves through structured diversity layers. The extent to which these transitions are local or abrupt is quantified separately through the transition-characterization framework presented in the following analysis.

Among the individual configurations, SIMO 1×2 occupies a substantial portion of the representative operating space and acts as an important intermediate diversity layer between SISO operation and stronger diversity configurations. This illustrates that moderate receive diversity can provide a favorable compromise between reliability improvement and implementation overhead. Conversely, the higher-order TXDIV modes are concentrated mainly in more demanding parts of the operating space, where their additional reliability gain becomes sufficient to justify their higher energy cost.

Overall, the representative operating-region map demonstrates the central principle of the proposed adaptive framework: the energy-preferred MIMO configuration is not fixed, but changes systematically with the operating conditions. The resulting policy therefore transforms the static reliability–energy transition boundaries identified in Chapter 5 into an adaptive mode-selection structure over the SNR–distance space. The following analyses examine whether this structure persists across CSI and hardware-overhead scenarios and quantify its occupancy, transition and stability characteristics.

6.2.2 Adaptive Occupancy Redistribution

While the operating-region maps provide a spatial representation of the adaptive policy, additional insight can be obtained by quantifying how frequently each diversity configuration is selected. Figure 6.4 presents the occupancy distribution of the proposed framework across the examined CSI uncertainty and hardware-overhead conditions. Each stacked bar represents the percentage of the operating space occupied by a particular diversity configuration.

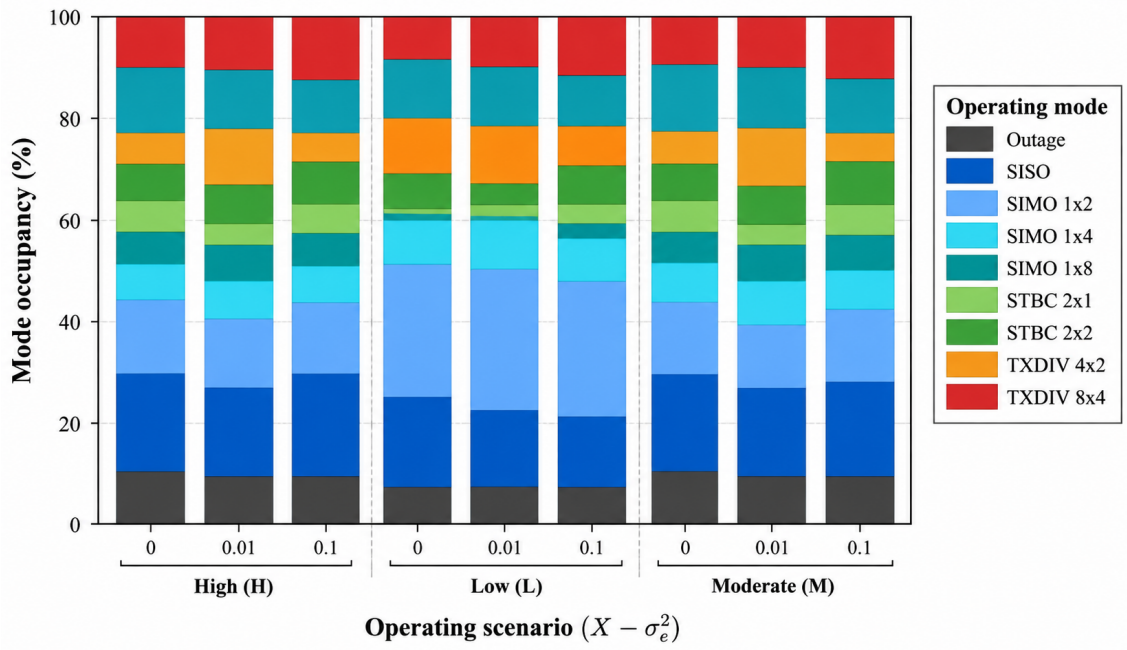


Figure 6.4. Adaptive occupancy redistribution of the proposed framework under different operating scenarios. The operating scenarios are denoted as X-σ_e^2, where $X \in \{L, M, H\}$ represents the hardware-overhead regime (Low, Moderate, High), while $\sigma_e^2 \in \{0, 0.01, 0.1\}$ denotes the CSI uncertainty variance.

The obtained results demonstrate that the proposed framework does not converge toward a single universally dominant diversity configuration. Instead, the adaptive policy redistributes operating-space occupancy among different diversity modes according to the prevailing CSI uncertainty and hardware-overhead conditions.

A particularly important observation is that the SIMO 1×2 configuration maintains the largest occupancy across most examined scenarios, effectively emerging as the dominant scalable-diversity layer of the framework. This result indicates that low-order receive diversity provides a highly favorable energy–reliability tradeoff while requiring relatively limited RF-chain activation and processing overhead. In parallel, SISO operation continues to occupy a considerable portion of the operating space, particularly under favorable operating conditions and lower CSI uncertainty levels. This behavior is consistent with the objective of the adaptive controller to avoid unnecessary diversity activation whenever reliable communication can be maintained through lower-complexity operation. Importantly, this behavior is consistently observed across nearly all examined operating scenarios, indicating that the dominance of the SIMO 1×2 configuration is not scenario-specific but rather a robust characteristic of the proposed adaptive policy. This observation further highlights the role of low-order receive diversity as the principal scalable operating layer of the framework under wireless conditions.

A further insight emerges from the way occupancy changes across the examined scenarios. As CSI quality deteriorates, the distribution of selected modes shifts because lower-complexity configurations become less capable of maintaining reliable communication, increasing the relevance of stronger diversity modes and, under sufficiently adverse conditions, outage. Hardware overhead modifies this tendency in the opposite direction by penalizing configurations with

larger implementation cost. The resulting occupancy patterns therefore reflect the competing influence of reliability degradation, which increases the value of diversity, and hardware cost, which discourages unnecessary complexity.

As operating conditions vary due to changes in CSI uncertainty and hardware-overhead assumptions, the adaptive policy redistributes part of the operating space among higher-order SIMO and TXDIV configurations. This behavior indicates that stronger diversity layers are selectively activated when their additional reliability benefit becomes sufficient to justify their increased energy cost. The observed occupancy redistribution therefore provides further evidence that the preferred diversity level depends jointly on channel reliability and hardware-related energy overhead.

An additional observation is that the STBC configurations exhibit heterogeneous occupancy behavior. In particular, the STBC 2×1 mode occupies only a limited portion of the operating space across most scenarios, whereas STBC 2×2 remains active in selected operating regions but does not emerge as a dominant operating layer. This indicates that, under the adopted PER-constrained energy criterion, STBC operation remains positioned between scalable receive-diversity operation and stronger TXDIV reliability-preservation layers.

Finally, the outage occupancy remains relatively limited across the examined scenarios, indicating that feasible communication is preserved over a large portion of the operating space despite variations in CSI uncertainty and hardware-overhead conditions.

Overall, Figure 6.4 confirms that the proposed framework redistributes diversity-mode utilization according to the prevailing operating conditions rather than converging toward a fixed dominant operating mode. These results further support the central motivation of Chapter 6, namely that efficient MIMO optimization naturally requires adaptive rather than static operating strategies.

6.2.3 Transition and Stability Analysis

While the previous analysis identified the dominant diversity modes under different CSI uncertainty and hardware-overhead conditions, it is equally important to examine how the adaptive operating policy evolves across neighboring operating points. In particular, the objective of this analysis is to determine whether the adaptive evolution occurs through structured neighboring transitions or through abrupt operating-mode switching.

To this end, Figure 6.5 presents the dominant adaptive operating transitions observed across neighboring operating points in the SNR–distance operating space.

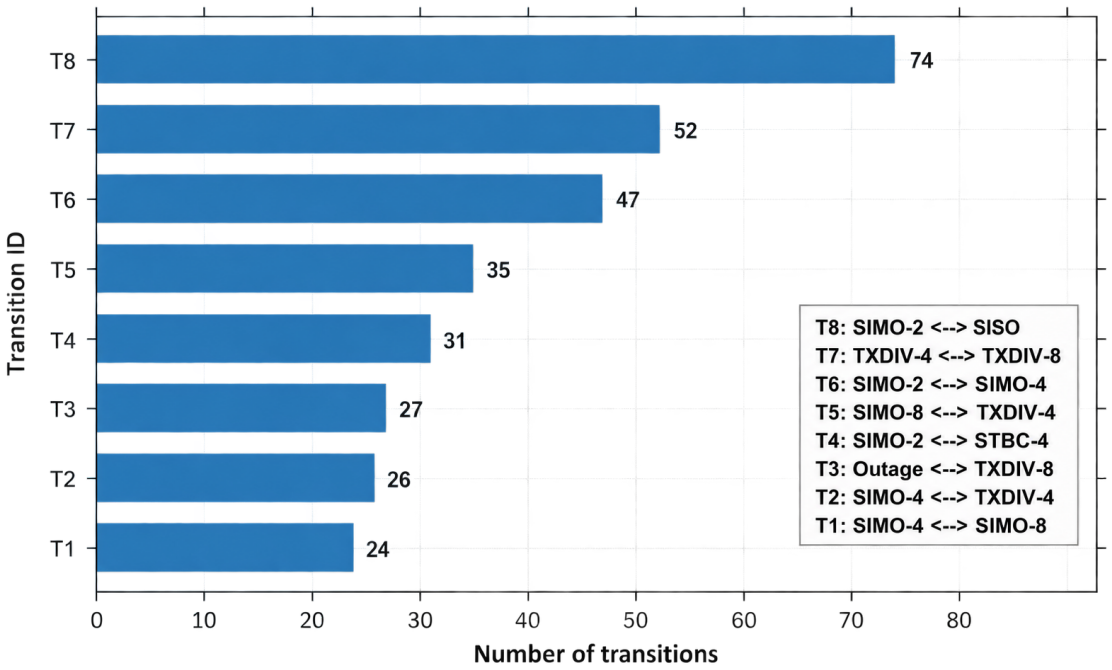


Figure 6.5. Observed transition frequencies between adaptive operating modes.

The obtained results reveal that transition activity is not uniformly distributed across all available diversity configurations. Instead, the adaptive operating evolution is concentrated around a limited set of dominant transition patterns. The strongest transition activity is observed between SISO and SIMO 1×2, indicating frequent adaptation between hardware-efficient operation and the first receive-diversity layer of the framework.

A second dominant transition cluster is formed by neighboring receive-diversity transitions, particularly between SIMO 1×2 and SIMO 1×4, as well as between SIMO 1×4 and SIMO 1×8. Together with the dominant SISO-to-SIMO 1×2 transition, these results indicate that the proposed framework primarily performs progressive receive-diversity scaling through adjacent operating layers.

In addition, significant transition activity is observed between TXDIV 4×2 and TXDIV 8×4, indicating that even within the high-diversity reliability-preservation region the adaptive evolution remains localized rather than exhibiting abrupt operating-mode changes.

Additional transitions are observed between SIMO 1×8 and TXDIV 4×2, between SIMO 1×4 and TXDIV 4×2, and between SIMO 1×2 and STBC 2×2. These transitions reveal occasional reliability-driven escalations toward stronger diversity configurations. Such transitions are associated with more demanding operating conditions, where stronger diversity configurations become energetically preferable or necessary for preserving feasibility under the adopted PER constraint.

The presence of transitions between Outage and TXDIV 8×4 further indicates that the strongest transmit-diversity configuration operates near the feasibility boundary and functions as the final adaptive reliability layer before outage occurs.

Overall, Figure 6.5 demonstrates that the adaptive operating policy does not rely on arbi-

trary operating-mode switching. Instead, the adaptive evolution is dominated by neighboring diversity-layer transitions, complemented by a smaller set of reliability-driven escalations toward stronger protection layers. This transition structure suggests favorable implementation characteristics for the proposed adaptive policy, since most operating-mode changes occur through gradual complexity adjustments rather than abrupt global reconfigurations.

To quantify the magnitude of adaptive mode changes, each operating state is represented by the mode index used by the adaptive selector, including the outage state and all candidate diversity configurations. The transition distance between two neighboring operating points is then defined as

$$d_{ij} = |i - j|, \tag{6.24}$$

where i and j denote the corresponding selector indices. This quantity is therefore interpreted as an index-based measure of the magnitude of the operating-state change rather than as a physical distance between MIMO configurations.

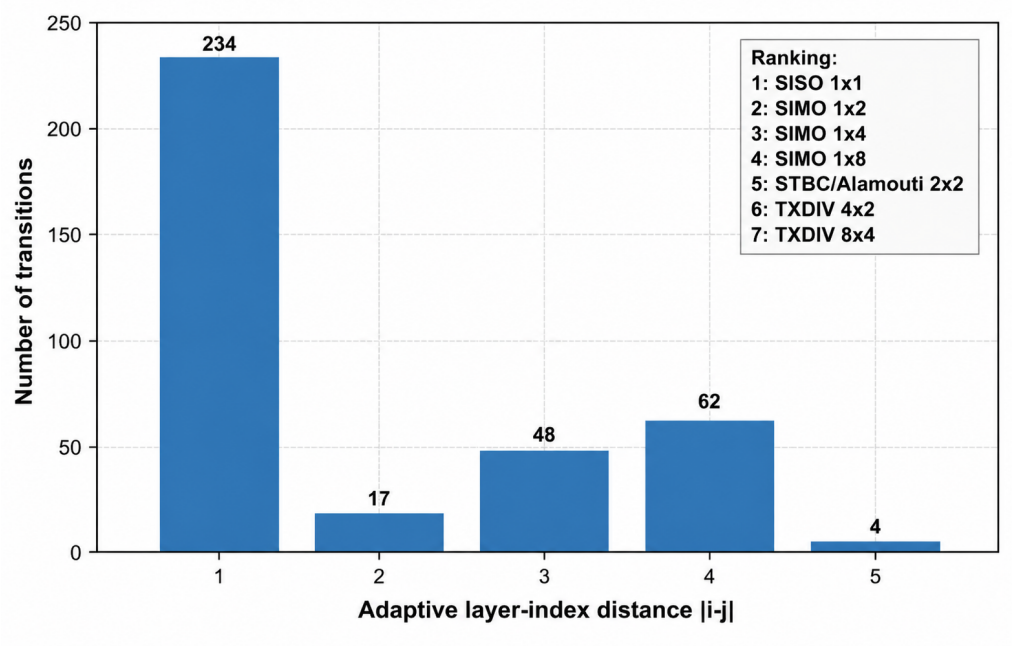


Figure 6.6. Aggregated distribution of adaptive transition distances between neighboring operating points across all examined CSI uncertainty levels and hardware-overhead regimes, computed from the operating-state indices used by the adaptive selector.

Figure 6.6 presents the aggregated distribution of adaptive transition distances across all examined CSI uncertainty levels and hardware-overhead regimes. The results reveal that the largest concentration of adaptive transitions occurs at $d_{ij} = 1$, indicating that a substantial fraction of mode changes take place between adjacent selector states. This observation indicates a clear tendency toward localized adaptive evolution, although transitions between more distant selector states also occur under specific operating conditions. This result indicates that complexity escalation within the adaptive framework occurs progressively in most cases, with additional diversity resources activated when their reliability benefit justifies the corresponding

increase in hardware and processing cost.

A smaller number of transitions is also observed for larger transition distances, particularly around $d_{ij} = 3$ and $d_{ij} = 4$. These larger transitions are fully consistent with the reliability-driven transition pairs observed previously, especially those involving transitions between moderate-diversity SIMO configurations and stronger TXDIV protection layers.

Importantly, no transitions corresponding to $d_{ij} = 6$ are observed. Therefore, the framework never directly switches between the lowest-diversity and highest-diversity operating layers within the examined operating space. This provides additional evidence that the adaptive policy generally preserves operating continuity, even though larger non-local transitions remain possible near demanding operating regions.

Overall, the combined observations of Figures 6.5 and 6.6 demonstrate that the proposed adaptive framework exhibits predominantly localized and continuity-preserving operating evolution across the SNR–distance operating space. The adaptive policy is therefore governed by structured neighboring-layer transitions, while larger operating jumps appear only selectively near feasibility-boundary regions where stronger diversity protection becomes unavoidable. These results further reinforce the central premise of Chapter 6 that efficient MIMO optimization is naturally achieved through adaptive and progressively evolving operating strategies.

6.2.4 Adaptive Energy Efficiency Analysis

The previous analyses characterized the adaptive operating behavior and transition properties of the proposed framework under varying CSI uncertainty and hardware-overhead conditions. The next step is to evaluate whether this adaptive behavior translates into measurable energy-efficiency gains. To this end, the energy performance of the framework is examined at three complementary levels: scenario-level adaptive energy behavior, mode-level energy comparison and statistical characterization of adaptive energy gains across the operating space.

Figure 6.7 summarizes the mean adaptive energy per successful packet transmission under the examined CSI uncertainty and hardware-overhead scenarios.

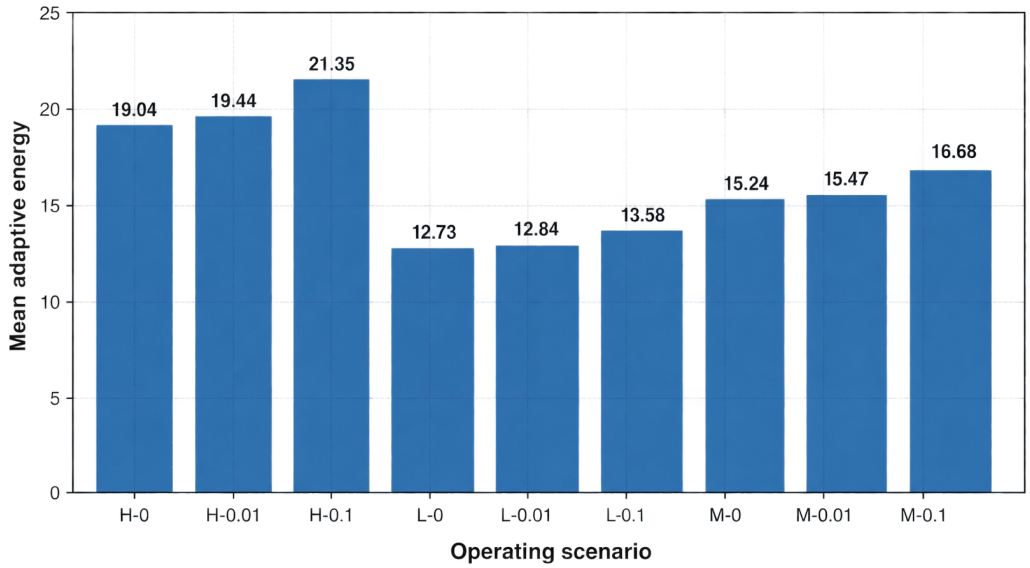


Figure 6.7. Mean adaptive energy per successful packet transmission of the proposed framework under different CSI uncertainty and hardware-overhead conditions. The operating scenarios are denoted as $X - \sigma_e^2$, where $X \in \{L, M, H\}$ represents the hardware-overhead regime (Low, Moderate, High), while $\sigma_e^2 \in \{0, 0.01, 0.1\}$ denotes the CSI uncertainty variance.

The results demonstrate that adaptive energy consumption depends strongly on both the CSI uncertainty level and the hardware-overhead regime. Across all hardware-overhead scenarios, increasing CSI uncertainty leads to higher average energy expenditure. This behavior is consistent with the occupancy trends observed previously, where degraded channel knowledge progressively shifts the adaptive policy toward stronger diversity configurations in order to preserve communication reliability.

Although stronger diversity layers reduce retransmission burden, they also introduce additional RF-chain activation and processing overhead, leading to higher overall energy consumption. A similar trend is observed across the hardware-overhead regimes, where high-overhead scenarios consistently exhibit the largest adaptive energy values. This result confirms that diversity activation becomes progressively more expensive as RF-chain and processing costs increase.

Nevertheless, the increase in adaptive energy consumption remains substantially smaller than would be expected under permanent operation with strong diversity configurations. This behavior indicates that the proposed framework successfully balances retransmission reduction, reliability preservation and hardware complexity through selective diversity activation rather than permanently aggressive diversity utilization. This observation directly reinforces the central premise of Chapter 6: MIMO optimization cannot rely on static diversity activation, since both under-provisioning and over-provisioning of diversity resources lead to energy inefficiency under varying operating conditions.

To further investigate the energy characteristics of the individual diversity configurations, Figure 6.8 presents a representative mode-level energy comparison for the low-overhead regime with $\sigma_e^2 = 0.01$.

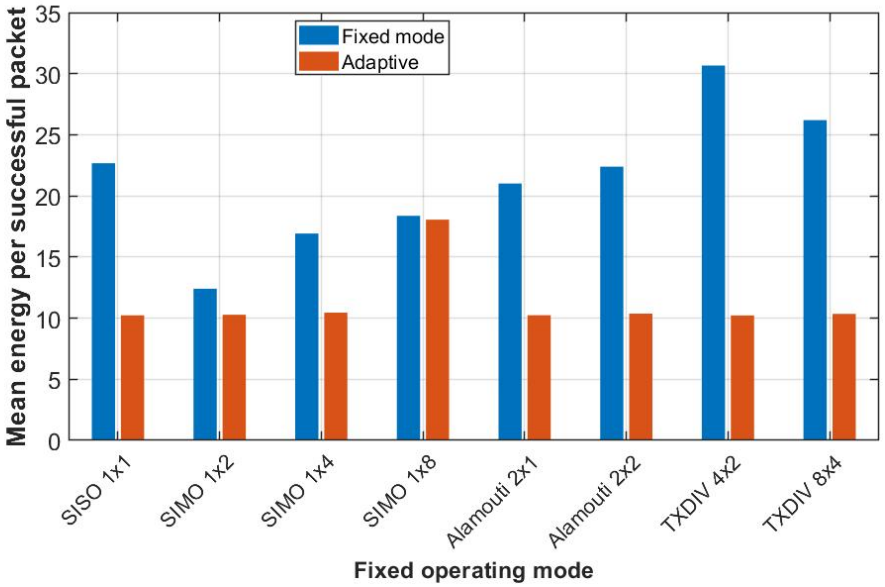


Figure 6.8. Pairwise comparison of the mean energy per successful packet between each fixed diversity configuration and the proposed adaptive framework under low-overhead operation ($\sigma_e^2 = 0.01$). For each pair, the mean values are evaluated over the common set of operating points for which both the fixed configuration and the adaptive framework remain feasible.

The results show that the mean energy per successful packet differs considerably across the available fixed diversity modes. To ensure a consistent comparison, each fixed configuration is evaluated against the adaptive framework over the same subset of operating points for which both alternatives remain feasible. Therefore, the adaptive mean shown for each pair may differ, since the corresponding common feasible subset depends on the fixed mode being considered.

Although SISO operation has the lowest hardware complexity, it exhibits substantially higher mean energy than the adaptive framework over their common feasible operating points, as its lower reliability increases the retransmission burden. SIMO 1×2 provides the closest energy performance to the adaptive framework among the lower-order fixed configurations, confirming that low-order receive diversity can provide an efficient reliability–energy trade-off when it remains feasible. As the fixed configurations become more hardware-intensive, the additional diversity protection does not necessarily translate into lower energy consumption, since the associated RF-chain and processing costs increasingly contribute to the total energy expenditure.

A particularly important observation is that the proposed adaptive framework achieves lower mean energy than each fixed diversity configuration over their respective common feasible operating points. The advantage is especially pronounced relative to the more hardware-intensive transmit-diversity configurations, whereas the difference becomes considerably smaller relative to SIMO 1×2 and SIMO 1×8 in the operating regions where these modes remain feasible. This behavior reflects the central advantage of adaptive selection: the framework does not permanently incur the cost of a single diversity configuration, but instead selects the energy-preferred feasible mode according to the prevailing operating conditions.

These results highlight a key advantage of adaptive diversity selection over fixed-mode op-

eration: energy efficiency is achieved through selective mode activation rather than permanent reliance on either low-complexity or high-diversity operation. To determine whether these energy-efficiency gains remain localized or persist systematically across broader operating conditions, a statistical analysis is performed next.

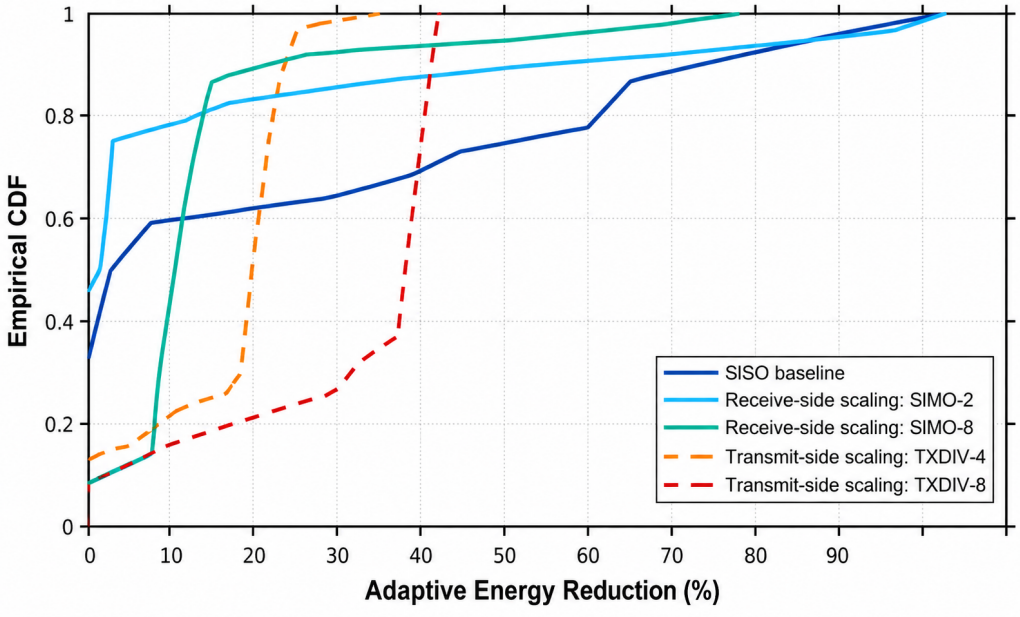


Figure 6.9. ECDF of the adaptive energy reduction relative to selected fixed operating-mode baselines across the considered operating space.

The ECDF results indicate that the proposed adaptive framework achieves predominantly positive energy reduction relative to most fixed diversity configurations across a large portion of the operating space. This observation demonstrates that the energy-efficiency gains identified previously are not confined to isolated operating points, but instead persist systematically across diverse propagation and CSI conditions.

The smallest separation is observed relative to the SIMO 1×2 configuration, indicating that low-order receive diversity already provides an efficient energy–reliability tradeoff under a broad range of operating conditions. This result is fully consistent with the occupancy analysis of Section 6.2.2, where SIMO 1×2 emerged as the most frequently selected diversity mode and occupied a substantial fraction of the operating space.

In contrast, significantly larger adaptive energy reductions are observed relative to fixed TXDIV configurations. This result does not imply that TXDIV modes are inherently energy inefficient. Rather, it indicates that maintaining strong transmit-diversity protection across the entire operating space introduces unnecessary hardware and processing overhead in regions where lower-complexity diversity solutions remain sufficient.

Consequently, the observed adaptive gains originate primarily from selective diversity activation according to the prevailing operating conditions rather than from permanent operation in a single high-diversity mode.

Overall, the combined observations of Figures 6.7, 6.8 and 6.9 demonstrate that the proposed adaptive framework provides substantial energy-efficiency benefits across a broad range of

propagation and CSI conditions. The results confirm that adaptive diversity selection enables energy-efficient operation by dynamically balancing communication reliability, retransmission burden and hardware complexity, while activating stronger diversity protection only when required.

6.2.5 Robustness Analysis under CSI Uncertainty

The previous analyses demonstrated that the proposed adaptive framework achieves structured operating behavior and systematic energy-efficiency gains across the considered operating space. However, a critical question concerns whether the resulting adaptive policy preserves its underlying decision structure when channel knowledge becomes progressively less accurate. Since practical wireless systems rarely operate under perfect CSI conditions, the robustness of the proposed framework must also be examined under imperfect channel estimation.

To investigate this aspect, the adaptive operating maps are compared for three CSI uncertainty levels, namely $\sigma_e^2 = 0$, 0.01, and 0.1. Figure 6.10 illustrates how the selected operating modes evolve across distance and reference-SNR conditions as CSI uncertainty increases.

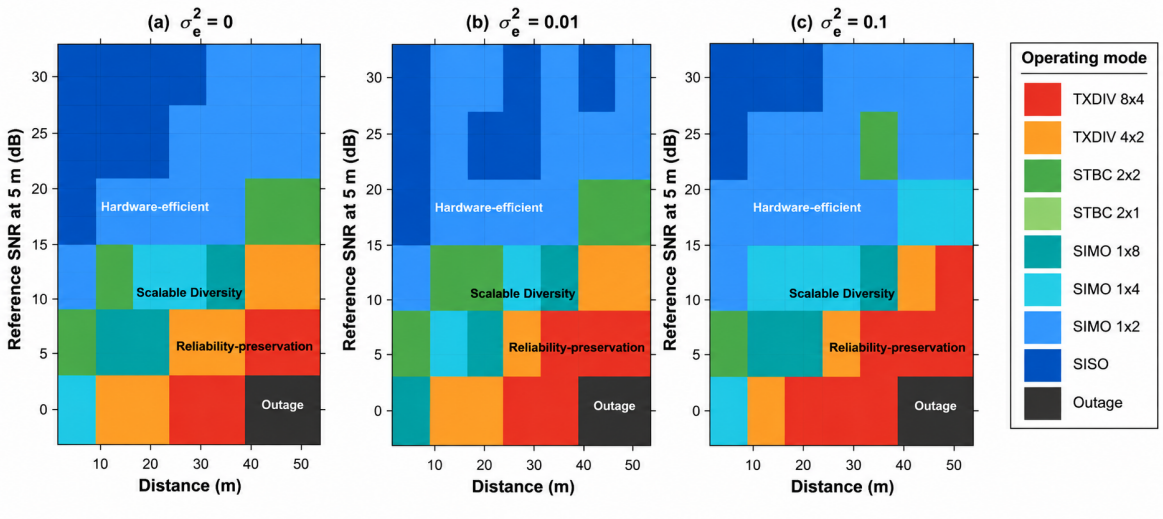


Figure 6.10. Adaptive operating-mode maps under increasing CSI uncertainty variance ($\sigma_e^2 = 0$, 0.01, and 0.1), illustrating the redistribution of selected diversity configurations across distance and reference-SNR conditions.

The operating maps reveal a progressive redistribution of the selected MIMO configurations as CSI uncertainty increases. Under perfect CSI, a substantial portion of the favorable operating space is served by low-complexity SISO and low-order SIMO configurations, forming a broad hardware-efficient region. As channel estimation becomes less accurate, the boundaries between operating regions shift and stronger diversity configurations are selected over a larger portion of the operating space.

This evolution is particularly visible at moderate and unfavorable SNR–distance combinations, where increasing CSI uncertainty causes the selector to move progressively from lower-order receive diversity toward stronger receive- and transmit-diversity configurations. Such behavior is consistent with the reliability–energy criterion underlying the proposed framework:

degradation of channel knowledge reduces the reliability achievable by simpler configurations, making additional diversity resources necessary at operating points where lower-complexity modes were previously sufficient.

Importantly, the increasing CSI uncertainty does not fundamentally alter the organization of the adaptive operating space. Across all three CSI conditions, favorable operating points remain predominantly associated with lower-complexity configurations, intermediate conditions are characterized by scalable receive-side diversity and increasingly demanding conditions lead to stronger reliability-preserving diversity modes and eventually to outage when no candidate configuration satisfies the imposed reliability requirement. The principal effect of imperfect CSI is therefore a displacement of the operating-region boundaries rather than a loss of the underlying decision structure.

The comparison also shows that the adaptive selector responds to CSI degradation in a systematic manner. Rather than producing an unstructured redistribution of operating modes, increasing uncertainty progressively extends the regions in which stronger diversity protection becomes energetically justified. This behavior indicates that the proposed policy retains its basic operating logic while adapting the required diversity level to the degradation in channel knowledge.

Overall, the robustness analysis demonstrates that the proposed adaptive framework preserves a coherent and interpretable operating-region structure under increasing CSI uncertainty. Imperfect channel knowledge modifies the location and extent of the individual operating regions and promotes stronger diversity activation, but the fundamental progression from hardware-efficient operation to scalable diversity, reliability-preserving operation, and eventual outage remains identifiable. These observations support the robustness of the proposed adaptive selection strategy under imperfect CSI conditions.

6.2.6 Learnability and Policy Approximation

The previous analyses demonstrated that the proposed adaptive framework exhibits structured operating regions, predominantly localized transitions and a coherent redistribution of operating modes under increasing CSI uncertainty. These observations suggest that the resulting adaptive policy may possess regular and predictable decision patterns across the operating space. To further investigate this property, an additional learnability analysis is performed to assess whether the adaptive policy can be accurately approximated using lightweight machine-learning models.

The objective of this analysis is not to replace the proposed adaptive selector itself, but rather to examine the extent to which the resulting adaptive behavior can be represented through compact data-driven approximations. Successful approximation would provide additional evidence that the adaptive policy exhibits structured, predictable and compressible decision behavior across varying propagation and hardware conditions.

The learnability analysis is formulated as a supervised classification problem, where propagation-aware operating features are mapped to the final adaptive operating decision of

the framework. The considered feature space includes transmission distance, reference SNR, CSI uncertainty variance, path loss, large-scale received SNR and hardware-overhead regime information. These features jointly capture both the propagation-related and hardware-related factors governing adaptive operating behavior.

To evaluate policy approximation capability, lightweight tree-based supervised learning models are considered, specifically decision trees and bagged ensemble tree learners. These models are selected because they provide a favorable balance between prediction performance, computational complexity and interpretability. Decision trees offer transparent rule-based approximations of the adaptive policy, while bagged ensemble trees improve prediction robustness through bootstrap aggregation of multiple independently trained models.

The learnability evaluation is performed using train/test partitioning, confusion-matrix analysis and prediction-accuracy metrics associated with the operating-region prediction task. Figure 6.11 summarizes the classification performance of the considered lightweight machine-learning models.

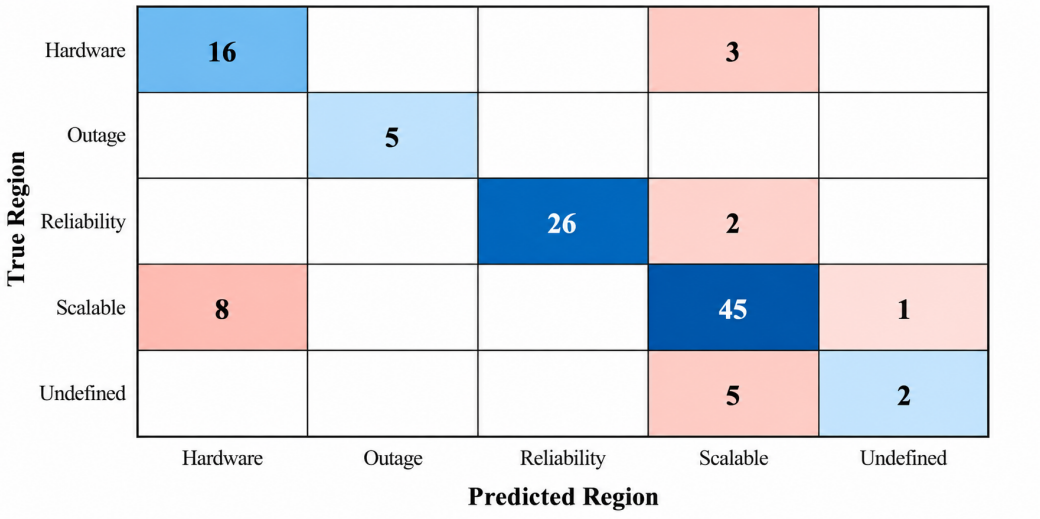


Figure 6.11. Classification performance of lightweight machine-learning models for adaptive policy approximation.

The confusion-matrix results indicate that the adaptive operating-region structure can be approximated with good classification accuracy using a lightweight learning model. Specifically, 94 out of 113 test samples are correctly classified, corresponding to an overall accuracy of approximately 83.2%. The Hardware-Efficient, Reliability-Preservation and Scalable-Diversity regions are predominantly identified correctly, while the Outage region is correctly classified for all test samples belonging to that class.

A particularly informative observation is that the largest classification ambiguity occurs between the Hardware-Efficient and Scalable-Diversity regions. Eight Scalable-Diversity samples are classified as Hardware-Efficient, while three Hardware-Efficient samples are classified as Scalable-Diversity. Smaller classification errors are observed between the Reliability-Preservation and Scalable-Diversity regions and between the Scalable-Diversity and Undefined classes. This error structure suggests that most classification ambiguity is concentrated around

related operating regions rather than being distributed arbitrarily across the decision space.

These results indicate that the adaptive policy exhibits a sufficiently structured decision geometry to permit effective approximation using a lightweight data-driven classifier. Although the approximation is not exact, the achieved classification accuracy and the concentration of errors among related operating regions provide additional evidence that the adaptive decision structure is regular and learnable.

Overall, the learnability analysis serves as an additional validation of the structural regularity identified in the preceding operating-region and transition analyses. The ability of lightweight models to reproduce the selector decisions with high accuracy, together with the predominantly localized nature of the remaining classification errors, provides further evidence that the proposed adaptive policy follows consistent and predictable decision patterns rather than arbitrary operating-state changes.

6.3 Summary and Conclusions

This chapter investigated adaptive energy-aware diversity selection as a response to the scenario-dependent behavior of MIMO systems established in the preceding analysis. The central problem was whether a fixed diversity configuration can remain energetically preferable as propagation quality, CSI uncertainty and implementation cost vary, or whether efficient operation requires dynamic adaptation of the employed diversity resources. To address this problem, a feasibility-aware adaptive framework was developed in which candidate receive- and transmit-diversity configurations are evaluated according to their expected energy per successful packet. The resulting decision therefore jointly reflects packet reliability, retransmission burden, RF-chain activation and processing overhead, while configurations that fail to satisfy the imposed reliability requirement are excluded from selection.

The operating-region analysis demonstrated that the resulting adaptive behavior is strongly dependent on the prevailing wireless conditions. The selected configuration changes systematically across the SNR–distance operating space, with lower-complexity configurations dominating favorable regions and progressively stronger diversity becoming preferable as operating conditions deteriorate. CSI uncertainty and hardware overhead further modify these regions, showing that the preferred configuration cannot be determined from propagation quality alone. Rather, the energy-optimal decision emerges from the interaction between channel conditions, reliability degradation and the implementation cost associated with each diversity configuration.

The occupancy analysis provided a complementary view of this behavior by quantifying how frequently the different configurations become energetically preferable across the examined operating space. A particularly important observation was the prominent role of low-order receive diversity, especially SIMO 1×2, which was selected over a substantial range of operating conditions. This behavior indicates that a relatively small increase in diversity can often provide sufficient reliability improvement to reduce retransmission cost without

introducing the considerably larger hardware burden associated with stronger configurations. Higher-order receive diversity extends this principle as conditions become more demanding, whereas strong transmit-diversity configurations are used more selectively, particularly when additional reliability protection becomes necessary to preserve feasible communication.

These observations clarify that the energetic role of diversity cannot be characterized independently of the conditions under which it is employed. Increasing diversity introduces two competing effects: improved reliability can reduce the energy wasted through unsuccessful transmissions and retransmissions, whereas additional RF chains and signal-processing requirements increase the energy cost of each transmission attempt. The energy-preferred configuration is therefore determined by the balance between these two effects rather than by diversity order itself.

The transition analysis further examined how the preferred operating configuration evolves as the underlying operating point changes. The results showed that adaptation does not occur through arbitrary switching among unrelated configurations. Instead, mode changes are predominantly concentrated among nearby operating states, while larger transitions appear more selectively under demanding or feasibility-limited conditions. The resulting evolution therefore reflects a progressive allocation of diversity resources, with additional complexity introduced as the operating conditions make stronger reliability protection necessary. This transition behavior complements the operating-region and occupancy results by demonstrating that the adaptive policy is organized not only in terms of which configuration is selected, but also in terms of how the preferred configuration evolves across neighboring operating conditions.

The energy analysis then examined whether this structured adaptive behavior translates into an actual energetic advantage relative to fixed diversity operation. At the scenario level, adaptive energy expenditure increases as CSI uncertainty becomes more severe and as hardware overhead increases, reflecting the greater cost of maintaining reliable communication under increasingly demanding conditions. This observation is important because adaptation does not eliminate the physical energy consequences of degraded channel knowledge or expensive hardware. Instead, its role is to identify the most favorable reliability–energy compromise available under each set of conditions.

The fixed-mode comparison further clarified this role. When the adaptive framework and each fixed configuration are evaluated over common feasible operating points, the adaptive strategy provides a lower mean energy per successful packet by retaining lower-complexity operation where it remains sufficient and activating stronger diversity only where its additional reliability becomes energetically justified. The statistical distribution of the energy reductions further showed that the magnitude of this advantage varies across operating points and fixed baselines. Low-order receive diversity can remain highly competitive in parts of the operating space, whereas permanent activation of stronger diversity may introduce unnecessary hardware and processing cost in regions where its additional reliability is not required. Consequently, the benefit of adaptation should not be interpreted as evidence for the superiority of a partic-

ular diversity configuration, but as evidence for the value of selecting among configurations according to the prevailing conditions.

The analysis under increasing CSI uncertainty provided an additional test of whether the resulting adaptive behavior preserves its underlying organization when channel knowledge deteriorates. Increasing CSI uncertainty progressively redistributes the selected configurations toward stronger diversity and modifies the boundaries separating the different operating regions. Nevertheless, the overall organization of the operating space remains identifiable: favorable conditions continue to support lower-complexity operation, intermediate conditions increasingly require scalable diversity, and more demanding regions promote stronger reliability-preserving configurations before feasibility is eventually lost. Imperfect CSI therefore modifies the location and extent of the operating regions without fundamentally altering the logic through which the framework responds to deteriorating conditions.

The learnability analysis provided a supplementary and independent validation of this structural property. Its purpose was not to introduce a machine-learning replacement for the proposed adaptive selector, but to determine whether the decisions generated by the optimization framework exhibit sufficient regularity to be recovered by a lightweight data-driven approximation. The classifier reproduced 94 of the 113 test-region decisions, corresponding to an accuracy of approximately 83.2%, while the remaining classification errors were concentrated primarily among related operating regions. This result supports the structural interpretation obtained from the operating-region and transition analyses by showing that a substantial part of the resulting decision structure can be recovered from the underlying operating conditions.

Taken together, the analyses performed throughout this chapter lead to four principal insights regarding energy-aware adaptive MIMO operation:

Insight 1: Energy-optimal MIMO operation is inherently scenario-dependent. No single diversity configuration provides a universal energy optimum across the considered operating space. The preferred operating mode changes with propagation conditions, CSI uncertainty and hardware-overhead characteristics. Energy-efficient MIMO operation must therefore be determined within its specific operating context rather than through a universally fixed antenna configuration.

Insight 2: The energetic value of diversity is conditional rather than intrinsic. Additional diversity becomes energy-beneficial only when the resulting reliability improvement and retransmission reduction are sufficient to compensate for the additional RF-chain activation and processing cost. Diversity order alone therefore cannot determine the energy-preferred configuration; its energetic value depends on the reliability–energy balance prevailing at each operating point.

Insight 3: The energy advantage of adaptation originates from selective movement between operating modes. Adaptive operation achieves its energy advantage by avoiding permanent commitment to any single diversity configuration. It reduces the retransmission penalty associated with insufficient diversity when stronger protection is required, while avoiding the

persistent implementation cost associated with excessive diversity when simpler configurations remain adequate. The energy optimum should therefore be viewed as a moving operating point rather than a fixed MIMO configuration.

Insight 4: Adaptive diversity evolution is structured and remains structurally robust under imperfect CSI. Adaptive decisions evolve predominantly through organized changes among related operating states rather than arbitrary mode switching. Increasing CSI uncertainty shifts the regions in which stronger diversity becomes necessary without fundamentally altering the organization of the adaptive response. The supplementary learnability analysis provides independent supporting evidence that this organization reflects a regular and predictable decision structure.

Overall, these findings demonstrate that the energy-optimal operating point of a MIMO system is neither a fixed point of maximum reliability nor a fixed point of minimum implementation complexity. Instead, it moves across diversity configurations as the balance among propagation quality, CSI uncertainty, retransmission burden and hardware cost changes. The role of adaptation is precisely to track this changing balance and allocate only the level of diversity that is energetically justified by the prevailing conditions. In this sense, adaptation is not merely an additional optimization mechanism, but a direct consequence of the scenario-dependent behavior identified throughout the preceding chapters. Energy-aware MIMO design therefore requires operating mechanisms capable of adjusting communication resources according to the conditions under which the system actually operates.

While the present chapter established this principle for adaptive optimization in single-link MIMO systems, it also raises a natural question regarding more complex distributed communication scenarios. If additional diversity is beneficial only when its reliability gain compensates for its associated cost, the same principle must be examined when diversity is provided through cooperation and relay-assisted transmission, where additional links, processing stages and imperfect channel knowledge introduce further sources of cost and uncertainty. This motivates the next chapter, where the analysis is extended to cooperative MIMO systems in order to investigate when cooperation remains beneficial, when it may become detrimental and how cooperative operation can be optimized under imperfect CSI and realistic operating constraints.

7 Cooperative MIMO under Realistic Operating Impairments

The preceding chapters demonstrated that MIMO system performance and optimization are fundamentally shaped by realistic propagation conditions, imperfect channel knowledge and communication reliability requirements. The characterization analysis showed that wireless channel conditions significantly influence achievable system performance, while the optimization analyses revealed that neither fixed diversity configurations nor static operating strategies can efficiently support the full range of operating conditions. Instead, robust and energy-efficient operation requires adaptive and context-aware transmission mechanisms. This progressive transition from characterization to adaptive optimization naturally raises the question of whether cooperation itself can be regarded as an effective optimization mechanism under realistic operating conditions.

Beyond adaptive diversity selection, cooperative communication represents an additional optimization mechanism for improving wireless system performance. By exploiting relay-assisted transmission and distributed spatial diversity, cooperative MIMO systems can improve communication reliability, extend coverage and enhance spectral efficiency, particularly under challenging propagation conditions. For this reason, cooperative transmission has emerged as a promising component of beyond-5G and 6G wireless networks, where distributed and collaborative communication architectures are expected to play an increasingly important role.

Under ideal operating assumptions, cooperative transmission is generally considered beneficial because relay-assisted diversity can improve signal reliability and reduce communication outages. In practice, however, cooperative MIMO operation is strongly influenced by realistic system impairments that may fundamentally alter the expected cooperation gains. In particular, imperfect channel state information introduces channel uncertainty and residual interference, while Decode-and-Forward relaying introduces the additional risk of relay decoding errors and error propagation.

The combined impact of these impairments creates a critical challenge for cooperative MIMO operation. Although imperfect CSI and relay reliability have each been studied extensively in the literature, their combined influence on the conditions under which cooperative transmission remains beneficial requires further investigation under realistic operating conditions. More importantly, these impairments raise a fundamental question regarding whether cooperation can always be considered beneficial in MIMO systems. Consequently, the validity of cooperation as an optimization strategy can no longer be taken for granted.

Motivated by this challenge, this chapter investigates whether cooperation can be considered an effective optimization mechanism for MIMO systems operating under realistic impairments. Particular emphasis is placed on the joint impact of imperfect CSI and relay decoding errors on cooperative transmission reliability relative to direct MIMO transmission.

The analysis demonstrates that cooperative transmission is not inherently beneficial under

all operating conditions. Instead, the effectiveness of cooperation depends strongly on the prevailing SNR regime, CSI uncertainty level, relay reliability and system dimension. In particular, the analysis reveals the existence of a harmful cooperation region, namely the operating regime in which cooperative transmission underperforms direct MIMO communication due to the combined effects of CSI-induced interference and relay error propagation.

To address this limitation, a reliability-aware relay activation mechanism is investigated in order to selectively enable cooperation according to the estimated source–relay channel quality. The activation threshold is subsequently optimized across different SNR and CSI uncertainty conditions in order to determine the reliability-preferred degree of relay participation for each operating point. In addition, the impact of antenna scaling is examined in order to evaluate how system dimension affects robustness against CSI uncertainty and harmful cooperation effects.

Overall, this chapter extends the central condition-dependent design perspective developed throughout the dissertation to cooperative MIMO operation. While the previous chapters showed that the preferred MIMO configuration depends on the prevailing propagation, reliability, energy and CSI conditions, the present chapter examines whether cooperation itself should also be treated as a condition-dependent communication resource. Specifically, it investigates when relay participation improves communication reliability, when it becomes harmful, how relay activation should be adapted to the prevailing operating conditions, and how antenna configuration influences robustness against CSI uncertainty.

7.1 Reliability-Aware Cooperative MIMO Framework and Evaluation Methodology

This section presents the theoretical framework underlying the cooperative reliability analysis developed in this chapter. The framework integrates cooperative MIMO signal modeling, imperfect CSI characterization, relay error propagation analysis and reliability-aware relay activation in order to evaluate whether cooperative transmission remains beneficial under realistic operating impairments. Particular emphasis is placed on identifying the operating conditions under which cooperation improves communication reliability and those under which cooperation becomes detrimental.

Figure 7.1 illustrates the considered cooperative relay-assisted MIMO communication framework. The system consists of a source (S), a relay (R) and a destination (D), with communication supported through both direct and relay-assisted transmission paths. Transmission follows a two-phase Decode-and-Forward (DF) protocol.

During Phase 1, the source transmits simultaneously to both the relay and the destination through the source–relay and source–destination links, respectively. During Phase 2, provided that relay participation is enabled, the relay forwards the decoded signal toward the destination through the relay–destination link. The destination therefore receives information through both direct and relay-assisted transmission paths.

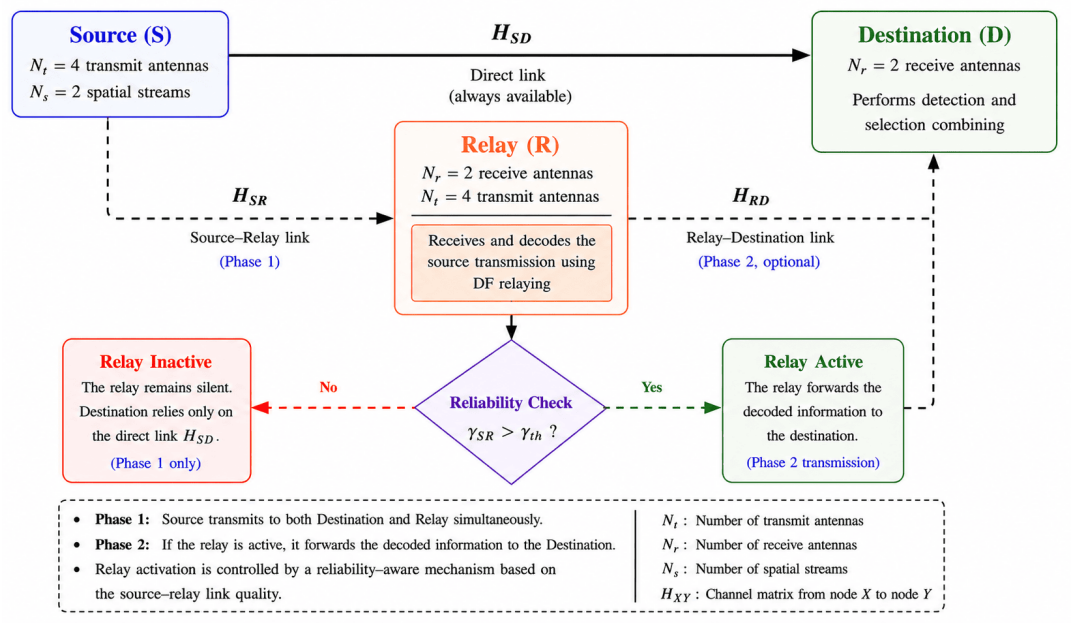


Figure 7.1. Architecture of the considered cooperative relay-assisted MIMO system with reliability-aware relay activation under imperfect CSI.

For the baseline configuration, the source employs $N_t = 4$ transmit antennas, while both the relay and destination employ $N_r = 2$ receive antennas. Spatial multiplexing with $N_s = 2$ transmitted streams is considered.

The transmitted symbol vector is defined as

$$\mathbf{s} \in \mathbb{C}^{N_s \times 1}, \qquad \mathbb{E}[\mathbf{s}\mathbf{s}^H] = \mathbf{I} \tag{7.1}$$

During Phase 1, the received signals at the destination and relay are respectively given by

$$\mathbf{y}_{SD} = \mathbf{H}_{SD}\mathbf{F}\mathbf{s} + \mathbf{n}_{SD} \tag{7.2}$$

$$\mathbf{y}_{SR} = \mathbf{H}_{SR}\mathbf{F}\mathbf{s} + \mathbf{n}_{SR} \tag{7.3}$$

During Phase 2, the relay forwards its detected signal to the destination according to

$$\mathbf{y}_{RD} = \mathbf{H}_{RD}\mathbf{F}\hat{\mathbf{s}}_R + \mathbf{n}_{RD} \tag{7.4}$$

where $\mathbf{H}_{SD}$, $\mathbf{H}_{SR}$ and $\mathbf{H}_{RD}$ denote the source–destination, source–relay and relay–destination channel matrices, respectively.

At the destination, the final detected signal is obtained using gain-based selection combining between the direct and relay-assisted transmission branches. This receiver structure enables branch-level reliability comparison and provides a computationally efficient cooperative detection framework for evaluating the impact of imperfect CSI and relay error propagation.

All communication links are assumed to operate under imperfect CSI conditions. Channel estimation uncertainty is modeled as

$$\hat{\mathbf{H}} = \mathbf{H} + \mathbf{E} \tag{7.5}$$

where $\mathbf{E}$ represents the channel estimation error matrix with variance σ_e^2.

Under imperfect CSI, signal detection is performed using estimated rather than true channel matrices. Consequently, residual interference is introduced due to channel mismatch. The received signal can therefore be expressed as

$$\mathbf{y} = \hat{\mathbf{H}}\mathbf{x} + (\mathbf{H} - \hat{\mathbf{H}})\mathbf{x} + \mathbf{n} \tag{7.6}$$

The second term represents residual interference caused by channel estimation uncertainty. Unlike thermal noise, this interference does not vanish with increasing SNR and may lead to SINR saturation and BER error floors under high-SNR conditions.

In the considered DF cooperative framework, the relay performs signal detection and forwards the decoded information during the second transmission phase. Under ideal relay operation, cooperative transmission provides additional diversity gain and improves communication reliability.

In practical operation, however, relay decoding errors may occur due to imperfect channel conditions and CSI uncertainty. In such cases, incorrectly detected symbols are forwarded to the destination, introducing an additional source of structured interference during cooperative transmission.

As a result, cooperative transmission becomes affected by two simultaneous impairment mechanisms:

- Residual interference caused by imperfect CSI
- Error propagation caused by relay decoding errors

The combined effect of these impairments may significantly degrade cooperative transmission performance.

A key objective of this chapter is to determine whether cooperative transmission remains beneficial under realistic operating impairments. To evaluate cooperation effectiveness, the BER difference is defined as

$$\Delta\text{BER} = \text{BER}_{\text{coop}} - \text{BER}_{\text{direct}}, \tag{7.7}$$

where $\text{BER}_{\text{direct}}$ denotes the BER of direct MIMO transmission and BER_{coop} denotes the BER under cooperative transmission. Positive values of ΔBER indicate harmful cooperation, whereas negative values indicate beneficial cooperation.

The harmful cooperation region is therefore defined as the operating region in which the combined effects of CSI-induced interference and relay error propagation render cooperative transmission detrimental relative to direct MIMO communication.

To mitigate harmful cooperation, a reliability-aware relay activation mechanism is considered. Instead of permanently enabling cooperative transmission, relay participation is activated

only when the source–relay link satisfies a reliability criterion.

The relay activation decision is based on the estimated source–relay channel quality metric

$$\gamma_{SR} = \|\hat{\mathbf{H}}_{SR}\mathbf{F}_S\|_F^2, \tag{7.8}$$

Relay participation is enabled according to

$$\text{Relay Active} = \begin{cases} 1, & \gamma_{SR} > \gamma_{\text{th}}, \\ 0, & \text{otherwise}, \end{cases} \tag{7.9}$$

where γ_{th} denotes the activation threshold.

This mechanism suppresses relay participation under unreliable source–relay conditions, thereby reducing relay error propagation and mitigating harmful cooperation.

A deeper analytical interpretation of the harmful cooperation phenomenon can be obtained by examining the post-detection behavior of the cooperative system under imperfect CSI. Under linear detection, the effective detection error consists of two main components: thermal noise and impairment-induced interference.

Considering the imperfect CSI model, the residual interference introduced by channel estimation uncertainty after linear detection can be expressed as

$$\mathbf{i}_{\text{CSI}} = \mathbf{WEFs} \tag{7.10}$$

where $\mathbf{W}$ denotes the linear detection matrix. This term represents residual self-interference caused by channel mismatch during signal detection.

Accordingly, the effective post-detection SINR can be approximated as

$$\text{SINR}_{\text{eff}} = \frac{P_s}{P_{\text{CSI}} + P_n} \tag{7.11}$$

where P_s denotes the desired signal power, P_{CSI} represents the residual interference power caused by imperfect CSI and P_n denotes the post-detection noise power.

As the operating SNR increases, the thermal noise contribution progressively decreases, whereas the CSI-induced interference remains non-negligible due to channel estimation uncertainty. Since the residual interference power scales proportionally with the transmitted signal power, increasing transmit power alone cannot eliminate this impairment. Consequently, the effective SINR no longer increases unboundedly with SNR, but instead approaches a finite limit determined by CSI uncertainty.

This behavior explains the BER saturation and error-floor phenomena observed under imperfect CSI conditions, where communication performance gradually transitions from a noise-limited regime to an interference-limited regime.

In cooperative DF transmission, this behavior becomes further aggravated by relay decoding errors. Due to imperfect detection at the relay, the forwarded signal can be modeled as

$$\hat{\mathbf{s}}_R = \mathbf{s} + \mathbf{e}_R \tag{7.12}$$

where $\mathbf{e}_R$ denotes the relay decoding error vector.

The relay-assisted received signal therefore contains an additional structured interference component associated with relay error propagation. Unlike thermal noise, this impairment originates from erroneous symbol forwarding and may remain significant even under moderate-to-high SNR conditions when CSI uncertainty is present.

As a result, cooperative transmission under realistic impairments is affected by compounded interference originating from both CSI uncertainty and relay error propagation. Under favorable operating conditions, the diversity gain provided by cooperation dominates and cooperative transmission remains beneficial. However, under specific operating conditions where impairment-induced interference exceeds the achievable diversity gain, cooperative transmission may underperform direct MIMO communication.

This transition defines the harmful cooperation region and provides the analytical explanation for the central hypothesis investigated in this chapter, namely that cooperation under realistic operating impairments is inherently operating-condition dependent rather than universally beneficial. Overall, the proposed framework enables a systematic evaluation of cooperative MIMO operation under realistic impairments and provides the analytical basis for identifying harmful cooperation regions, quantifying cooperation reliability and assessing the effectiveness of reliability-aware cooperative transmission.

The proposed cooperative reliability framework was evaluated through controlled Monte Carlo link-level simulations. The objective of the evaluation is to investigate whether cooperative transmission remains beneficial under realistic operating impairments and to identify the operating conditions under which cooperation becomes harmful.

The simulation study focuses on three complementary evaluation scenarios: direct MIMO transmission, conventional always-on cooperative transmission and reliability-aware cooperative transmission with selective relay activation. This comparative evaluation enables systematic characterization of the harmful cooperation region, assessment of the effectiveness of the proposed relay activation mechanism and evaluation of cooperative robustness under different system dimensions.

Particular emphasis is placed on the joint impact of imperfect CSI and relay decoding errors across different SNR regimes. To this end, BER performance is evaluated over a broad SNR range under multiple CSI uncertainty levels and antenna configurations. In addition, larger MIMO dimensions are considered in order to investigate how antenna scaling influences robustness against harmful cooperation effects.

Table 7.1 summarizes the main simulation parameters used throughout the analysis.

Table 7.1. Simulation parameters.

Parameter	Value	Description
Simulation Method	Monte Carlo link-level simulation	Controlled numerical evaluation
Evaluation Cases	Direct / Coop / Relay-aware	Compared transmission strategies
Transmission Scheme	Spatial Multiplexing ($N_s = 2$)	Two spatial streams
Transmit/Receive Antennas	$(N_t, N_r) = (4,2), (8,2), (8,4)$	Evaluated configurations
Relay Protocol	Decode-and-Forward (DF)	Half-duplex relaying
Channel Model	Rayleigh fading	i.i.d. fading
Precoding	Semi-unitary DFT precoding	Precoding matrix $\mathbf{F}$
CSI Model	$\hat{\mathbf{H}} = \mathbf{H} + \mathbf{E}$	Estimation error model
CSI Error Variance	$\sigma_e^2 \in \{0, 0.01, 0.05, 0.1\}$	CSI uncertainty
Detection Method	ZF	Linear detection
Noise Model	AWGN: $\mathcal{CN}(0, \sigma_n^2\mathbf{I})$	Gaussian noise
Combining Scheme	Selection Combining	Gain-based selection
SNR Range	0–30 dB	Operating range
Modulation	QPSK	Two bits per symbol
Activation Metric	$\gamma_{SR} = \|\hat{\mathbf{H}}_{SR}\mathbf{F}_S\|_F^2$	Source–relay reliability metric
Threshold (γ_{th})	Swept and optimized	Operating-condition-dependent relay activation criterion

7.2 Cooperative Reliability Analysis and Relay-Activation Evaluation

7.2.1 Interference-Limited Cooperative Behavior under Imperfect CSI

The first step of the analysis is to investigate how imperfect CSI affects relay reliability, since relay decoding accuracy directly determines the effectiveness of cooperative transmission.

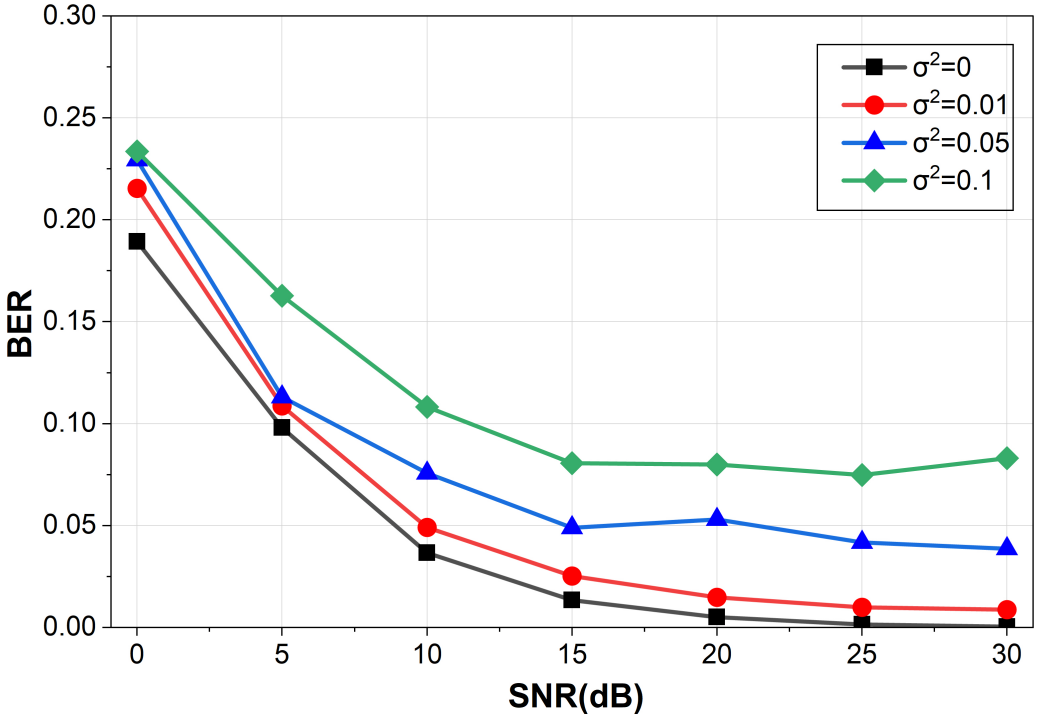


Figure 7.2. BER performance of the source–relay link under different CSI error variances.

Figure 7.2 illustrates the BER performance of the source–relay link under different CSI error variances. Under perfect CSI conditions, relay decoding performance improves continuously with increasing SNR, approaching near-error-free operation in the high-SNR regime. In contrast, under imperfect CSI conditions, BER improvement gradually saturates and clear error floors emerge.

The severity of this error-floor behavior increases with CSI uncertainty variance. For moderate CSI uncertainty, relay BER remains non-negligible even at high SNR, while severe CSI uncertainty leads to persistent decoding errors across the entire operating range. These results confirm that imperfect CSI fundamentally limits relay decoding reliability and may prevent the relay from achieving sufficiently accurate symbol detection even under otherwise favorable operating conditions.

As a result, relay decoding errors remain present even in medium-to-high SNR regimes, increasing the probability of erroneous symbol forwarding during cooperative transmission. This behavior directly intensifies the impact of relay error propagation and constitutes a key mechanism behind the degradation of cooperative reliability. Consequently, relay-assisted transmission cannot always provide the expected diversity benefit, since unreliable relay decisions may increasingly offset the gains offered by cooperation.

The impact of relay error propagation on the overall cooperative system performance is illustrated in Figure 7.3.

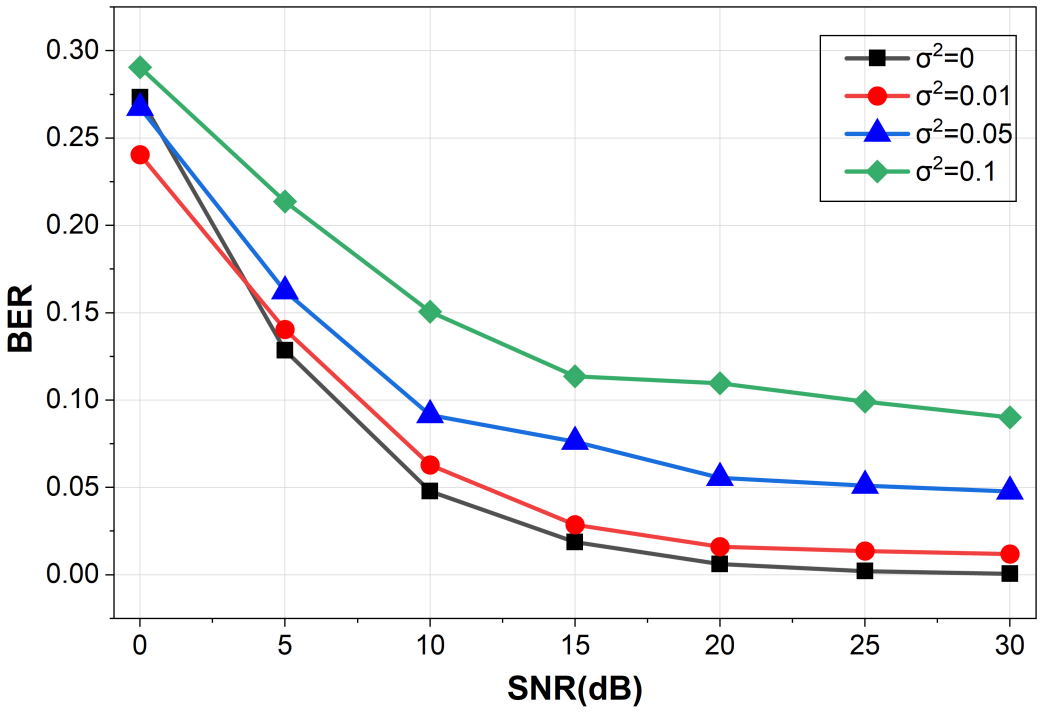


Figure 7.3. BER performance of cooperative DF MIMO under imperfect relay decoding for different CSI error variances.

Figure 7.3 presents the BER performance of the cooperative DF MIMO system when relay decoding errors are explicitly taken into account. Compared to ideal relay operation, the inclusion of relay decoding errors leads to significantly degraded BER performance, particularly in the medium-to-high SNR regime.

A clear performance saturation behavior is observed as SNR increases under imperfect CSI conditions. While cooperative transmission exhibits improving BER performance at low-to-moderate SNR levels, further performance improvement progressively diminishes as residual CSI-induced interference and relay error propagation become dominant.

As CSI uncertainty increases, the cooperative BER curves exhibit increasingly pronounced error floors, indicating that system performance gradually transitions from noise-limited operation toward interference-limited behavior. Under these conditions, relay forwarding no longer contributes purely beneficial diversity gain. Instead, erroneous relay transmissions introduce structured interference that directly degrades destination detection performance.

Overall, the analysis demonstrates that cooperative MIMO systems operating under imperfect CSI progressively transition from noise-limited behavior toward interference-limited operation as the SNR increases. In this regime, residual CSI-induced interference together with relay error propagation fundamentally limits the achievable cooperative performance. These observations establish the physical mechanisms responsible for cooperative performance degradation. The next step is therefore to determine whether these mechanisms are sufficiently strong to reverse the expected cooperation gain, causing cooperative transmission to underperform direct MIMO communication under specific operating conditions.

7.2.2 Comparative Behavior of Direct and Cooperative MIMO under Ideal and Impaired Conditions

Having established the interference-limited behavior of cooperative transmission under realistic operating impairments, the next step is to compare the performance evolution of direct and cooperative MIMO transmission under ideal and impaired operating conditions. This comparison provides the reference required to evaluate whether cooperation remains an effective reliability-enhancement mechanism once imperfect CSI and relay decoding errors are introduced.

The performance of the baseline direct 4×2 MIMO system is first evaluated under perfect CSI in order to establish a reference for the subsequent cooperative analysis.

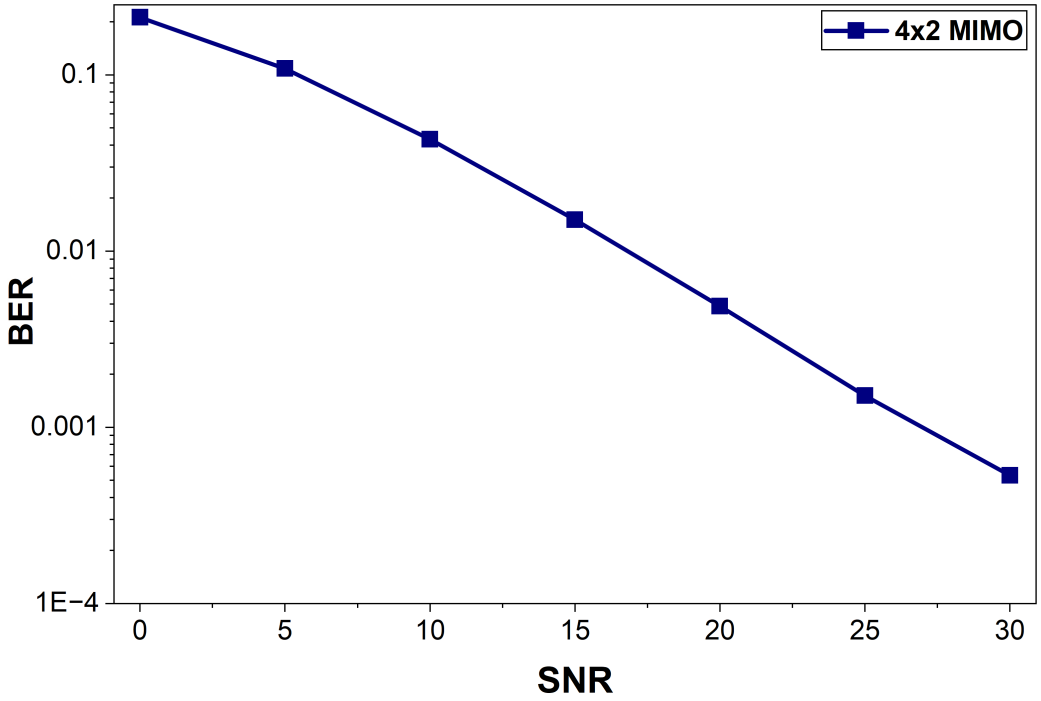


Figure 7.4. BER performance of direct 4×2 MIMO transmission with ZF detection under perfect CSI.

Figure 7.4 illustrates the BER performance of direct 4×2 MIMO transmission under perfect CSI conditions. As expected, the BER decreases steadily as the operating SNR increases, indicating noise-limited behavior without observable error-floor effects within the examined SNR range. This curve serves as the direct-transmission baseline against which cooperative transmission is subsequently compared.

To establish an ideal performance benchmark for cooperative transmission, cooperative DF relaying is next evaluated under ideal operating conditions, assuming perfect CSI and error-free relay decoding. This ideal-performance benchmark represents the conventional assumption under which cooperative transmission is expected to provide additional reliability through relay-assisted diversity.

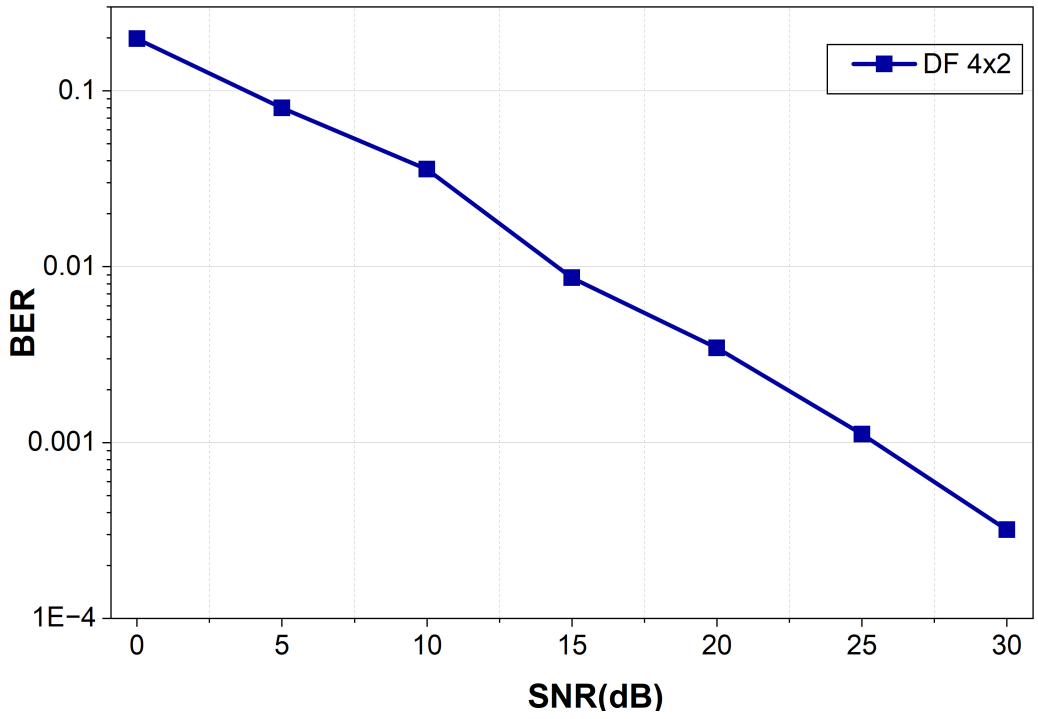


Figure 7.5. BER performance of cooperative DF 4×2 MIMO transmission under ideal relay operation and perfect CSI.

As shown in Figure 7.5, cooperative transmission improves BER performance relative to direct MIMO transmission under ideal operating conditions. The additional relay-assisted transmission path provides a diversity contribution and improves communication reliability across the examined SNR range.

Although the achieved gain remains moderate due to the use of spatial multiplexing, linear detection and selection combining, cooperative transmission remains consistently beneficial under ideal assumptions and no BER error floor is observed. Therefore, under perfect CSI and error-free relay decoding, cooperative DF transmission behaves as expected and provides a reliability advantage over direct MIMO communication.

The cooperative behavior changes significantly once realistic impairments are introduced.

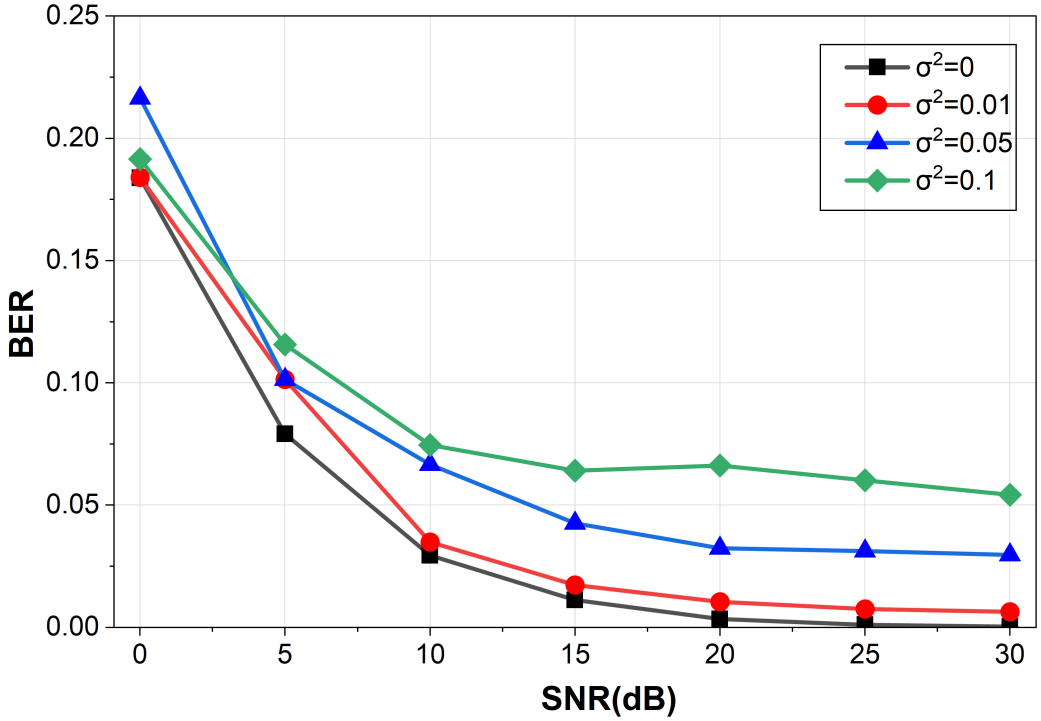


Figure 7.6. BER performance of cooperative DF 4 × 2 MIMO transmission under imperfect CSI for different CSI error variances.

Figure 7.6 presents the BER performance of cooperative DF transmission under imperfect CSI conditions. In contrast to the ideal scenario, BER saturation and error-floor behavior emerge under non-zero CSI uncertainty levels, indicating the onset of interference-limited operation.

This degradation becomes increasingly severe as the CSI error variance increases. While BER initially improves with increasing SNR, further performance improvement progressively diminishes at higher SNR due to the combined effects of residual CSI-induced interference and relay error propagation.

Compared with the ideal cooperative benchmark, the imperfect-CSI results demonstrate that realistic operating impairments can fundamentally alter the behavior of cooperative transmission. In particular, cooperative performance depends not only on destination-side detection quality, but also on the reliability of relay decoding. As a result, erroneous relay forwarding may reduce or even offset the expected diversity benefit of cooperation.

Overall, the comparison demonstrates that the effectiveness of cooperative transmission cannot be assessed solely under ideal operating assumptions. While cooperation remains beneficial under perfect CSI and error-free relay operation, realistic impairments progressively reduce the achievable cooperation gain. This observation provides the basis for the next stage of the analysis, where direct and cooperative transmission are compared explicitly in order to identify the operating regions in which cooperation becomes beneficial or harmful.

7.2.3 Harmful Cooperation Region Analysis

The previous results demonstrated that the combined effects of CSI-induced interference and relay decoding errors can substantially reduce the benefits of cooperative transmission under operating impairments. The next step is therefore to determine whether the effectiveness of cooperation as an optimization mechanism can be completely reversed under realistic operating impairments, causing cooperative transmission to become detrimental relative to direct MIMO communication. To address this question, the concept of the harmful cooperation region is introduced.

The harmful cooperation region is quantified using the BER difference defined in (7.7). Positive values of ΔBER indicate harmful cooperation, since cooperative transmission becomes less reliable than direct MIMO communication, whereas negative values indicate beneficial cooperation.

From an effective SINR perspective, harmful cooperation emerges whenever the additional interference introduced by relay participation exceeds the achievable diversity gain, causing cooperative transmission to operate with lower effective reliability than direct MIMO transmission. Consequently, the harmful cooperation region represents the operating regime in which the expected optimization gain of cooperation is completely offset by impairment-induced interference.

The emergence of this phenomenon is first illustrated through representative BER comparisons under different CSI uncertainty conditions.

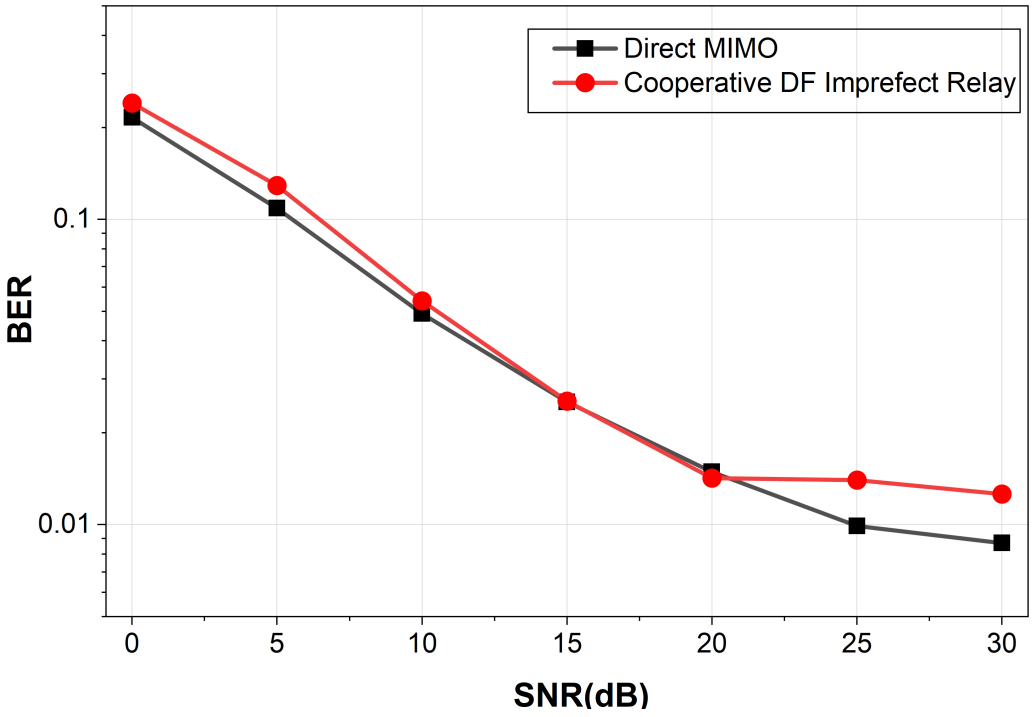


Figure 7.7. BER comparison of direct MIMO and cooperative DF with imperfect relay decoding for $\sigma_e^2 = 0.01$.

Figure 7.7 illustrates the BER comparison between direct and cooperative transmission under moderate CSI uncertainty. The results show that the relative benefit of cooperation varies with SNR. Cooperative transmission underperforms direct MIMO at low SNR, approaches comparable performance in the intermediate SNR range, and provides a limited benefit around 20 dB. At higher SNR, however, cooperative transmission again becomes less reliable than direct MIMO communication, indicating the re-emergence of harmful cooperation.

The degradation becomes substantially more severe under stronger CSI uncertainty.

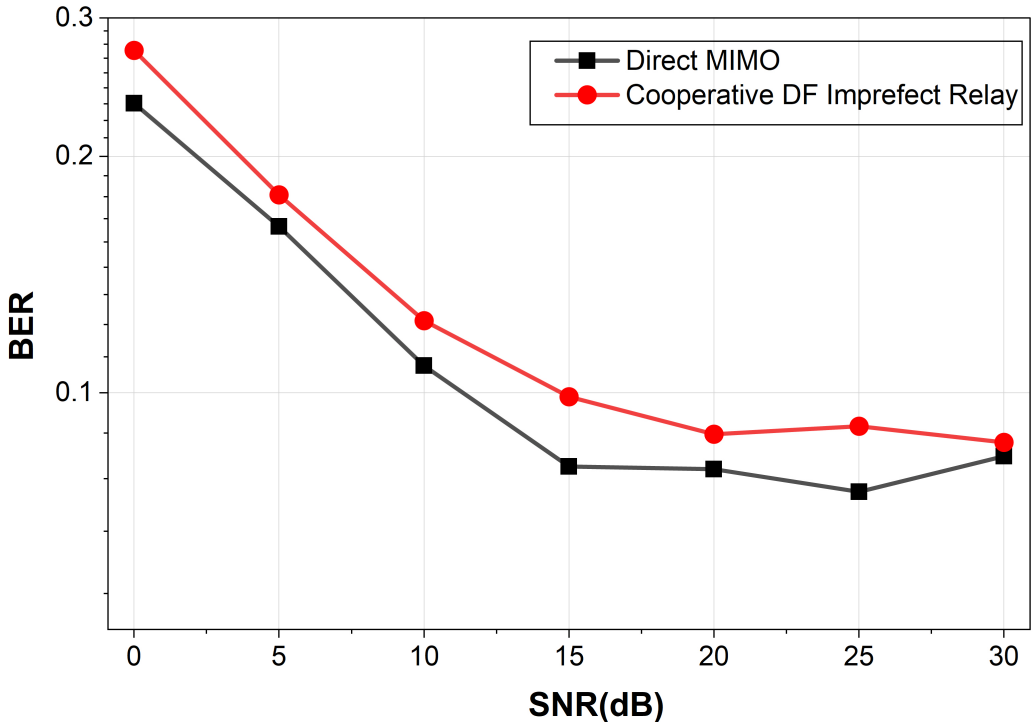


Figure 7.8. BER comparison of direct MIMO and cooperative DF with imperfect relay decoding for $\sigma_e^2 = 0.1$.

As shown in Figure 7.8, severe CSI uncertainty significantly amplifies the impact of residual interference and relay error propagation. Under these conditions, cooperative transmission consistently underperforms direct MIMO communication across a wide SNR range. The relay no longer improves link reliability, but instead introduces additional structured interference through erroneous forwarding.

The harmful cooperation region is explicitly characterized in Figure 7.9, which provides the central result of this chapter.

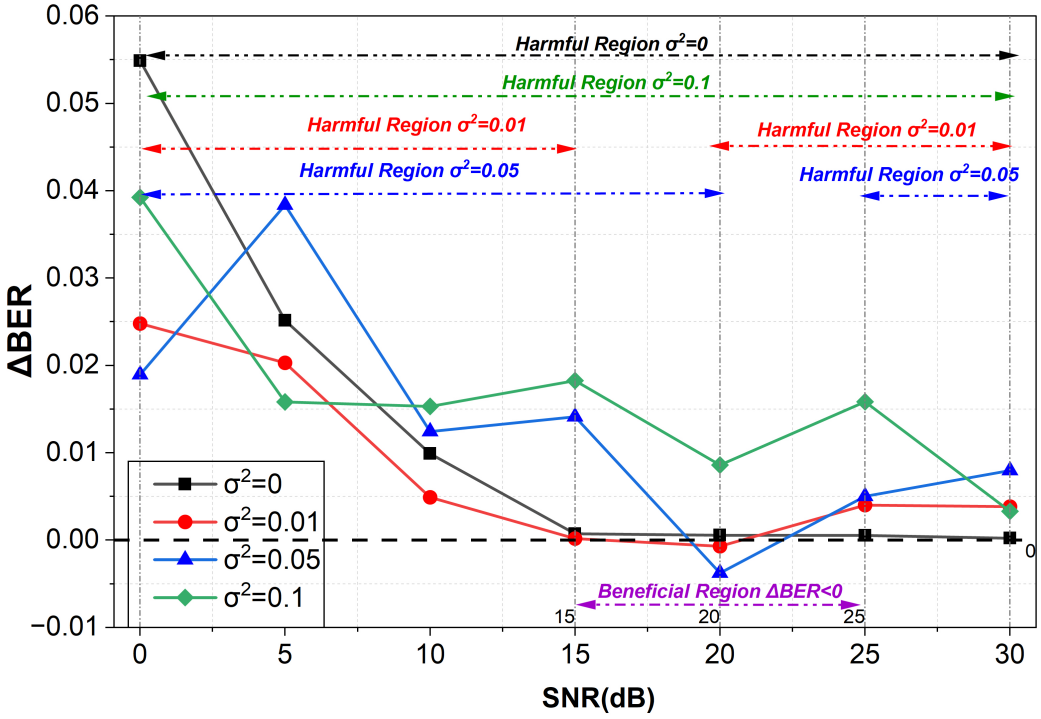


Figure 7.9. Harmful cooperation region, defined by $\Delta\text{BER} = \text{BER}_{\text{coop}} - \text{BER}_{\text{direct}}$, as a function of SNR for different CSI error variances σ_e^2. Positive values indicate harmful cooperation. The horizontal dashed line indicates the boundary at $\Delta\text{BER} = 0$, separating beneficial and harmful cooperation regions.

Figure 7.9 provides the central operating-region interpretation of the harmful cooperation phenomenon. By plotting the difference between cooperative and direct BER, the figure explicitly separates beneficial cooperation regions, where $\Delta\text{BER} < 0$, from harmful cooperation regions, where $\Delta\text{BER} > 0$. For low CSI uncertainty, harmful cooperation is observed over substantial portions of the examined SNR range, although limited beneficial operating points may also emerge. As the CSI error variance increases, the harmful-cooperation behavior becomes increasingly pronounced, showing that the combined impact of CSI-induced residual interference and relay error propagation can fully offset the diversity gain of cooperation.

This result demonstrates that cooperative transmission is not inherently beneficial under realistic operating impairments. Instead, cooperation effectiveness is strongly operating-condition dependent and highly sensitive to CSI uncertainty and relay decoding reliability. Therefore, cooperation can no longer be treated as a universally advantageous transmission strategy; it must be activated selectively according to the prevailing reliability conditions.

It should be noted that the present analysis assumes statistically identical average channel conditions for all communication links and does not explicitly incorporate relay placement or distance-dependent path loss effects. This modeling choice was adopted in order to isolate the impact of CSI uncertainty and relay error propagation on cooperative MIMO performance. Consequently, the identified harmful cooperation region reflects the effects of realistic operating impairments rather than a specific relay topology.

To further examine whether the harmful cooperation phenomenon is merely an artifact of uncoded BER evaluation, an additional coded-system validation was performed using the same cooperative DF framework under imperfect CSI with $\sigma_e^2 = 0.1$.

The coded harmful-region metric is defined as

$$\Delta\text{BER}_{\text{coded}} = \text{BER}_{\text{coop,coded}} - \text{BER}_{\text{direct,coded}} \tag{7.13}$$

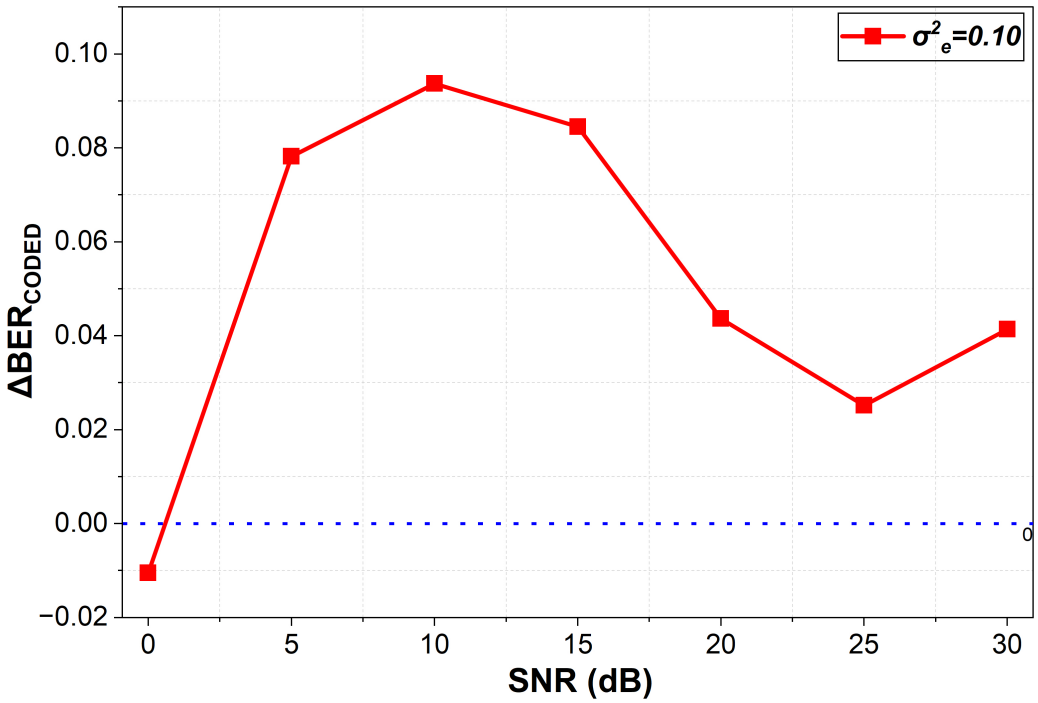


Figure 7.10. Coded harmful cooperation region for $\sigma_e^2 = 0.1$, expressed through $\Delta\text{BER}_{\text{coded}} = \text{BER}_{\text{coop,coded}} - \text{BER}_{\text{direct,coded}}$. Positive values indicate harmful cooperation, while negative values indicate beneficial cooperation. The horizontal dashed line indicates the boundary at $\Delta\text{BER}_{\text{coded}} = 0$.

Figure 7.10 shows that the harmful cooperation phenomenon remains clearly observable even under coded transmission. The coded performance metric remains positive throughout most of the examined SNR range, confirming that harmful cooperation is not merely an artifact of uncoded BER evaluation.

This result provides strong validation of the central hypothesis of this chapter. The harmful cooperation phenomenon originates from the underlying impairment mechanisms identified in this work, namely residual CSI-induced interference and relay error propagation and persists even when practical coding mechanisms are employed.

Overall, this section establishes harmful cooperation as the fundamental operating phenomenon governing cooperative MIMO systems under realistic impairments. Rather than constituting a universally beneficial transmission strategy, cooperation is shown to exhibit distinct operating regimes in which its effectiveness depends on the interplay between CSI

uncertainty, relay reliability and SNR. This observation transforms cooperative communication from a conventionally assumed performance-enhancement technique into an adaptive optimization mechanism whose activation must itself depend on realistic operating conditions, thereby providing the foundation for the reliability-aware relay control framework developed in the following section.

7.2.4 Reliability-Aware Relay Activation

The previous sections established that cooperative transmission cannot be regarded as a universally effective optimization mechanism under realistic operating impairments. Instead, the achievable cooperation gain was shown to depend strongly on the prevailing operating conditions, with the harmful cooperation region identifying the operating regime in which relay-assisted transmission becomes detrimental relative to direct MIMO communication. These observations indicate that continuously maintaining relay participation is no longer an appropriate operating strategy for cooperative MIMO systems.

Rather than abandoning cooperation altogether, the results suggest that relay participation should itself become adaptive. The objective is therefore not to maximize relay utilization, but to preserve the reliability benefits of cooperative diversity whenever favorable operating conditions exist while suppressing relay participation whenever unreliable forwarding is likely to degrade the overall communication performance. Consequently, cooperation is transformed from a static transmission strategy into an adaptive operating mechanism whose activation depends on the instantaneous reliability of the communication process.

Based on this design principle, a reliability-aware relay activation mechanism is investigated. Since the harmful cooperation phenomenon originates primarily from relay decoding errors under imperfect CSI conditions, relay activation is performed according to the estimated reliability of the source–relay transmission link. The underlying objective is to prevent unreliable relay participation before error propagation occurs, thereby reducing the detrimental effects of CSI-induced interference while preserving the achievable diversity gain whenever relay decoding is sufficiently reliable.

To quantify relay reliability, the proposed approach employs the source–relay channel-quality metric defined in (7.8), where $\hat{\mathbf{H}}_{SR}$ denotes the estimated source–relay channel matrix and $\mathbf{F}_S$ is the source precoding matrix.

The proposed metric represents the effective strength of the estimated source–relay channel and serves as an indicator of relay decoding reliability. Since the metric is computed directly from the estimated channel already available at the relay for signal detection, no additional channel statistics, relay BER estimation or destination feedback are required. Because the metric relies on estimated CSI, its reliability is naturally affected by the CSI uncertainty considered throughout this chapter.

Based on the estimated channel quality, relay participation is controlled according to the activation rule defined in (7.9).

According to this rule, the relay forwards the decoded information only when the estimated

source–relay channel quality exceeds the prescribed threshold. Otherwise, relay participation is suppressed and communication relies exclusively on the direct MIMO transmission path. Consequently, relay activation becomes directly coupled to the estimated reliability of the source–relay link, allowing cooperation to adapt automatically to the prevailing operating conditions.

The squared Frobenius norm is selected because it provides a simple and computationally efficient reliability indicator that depends solely on locally available CSI. Although alternative reliability metrics could also be considered, the proposed metric offers an attractive compromise between implementation complexity and relay reliability estimation while remaining readily applicable across different antenna configurations.

The relay activation threshold represents the key design parameter governing the balance between cooperative diversity gain and relay-induced error propagation. Small threshold values increase relay participation and closely approximate conventional always-on cooperation, whereas larger threshold values progressively suppress unreliable relay forwarding at the expense of reduced cooperative diversity. Consequently, the threshold controls the transition between aggressive cooperation and conservative relay utilization.

As an initial operating point, a threshold value of $\gamma_{\text{th}} = 4$ is considered in order to illustrate the fundamental behavior of reliability-aware relay activation under imperfect CSI conditions. This threshold results in selective relay participation, suppressing source–relay realizations whose estimated channel quality does not satisfy the prescribed reliability criterion.

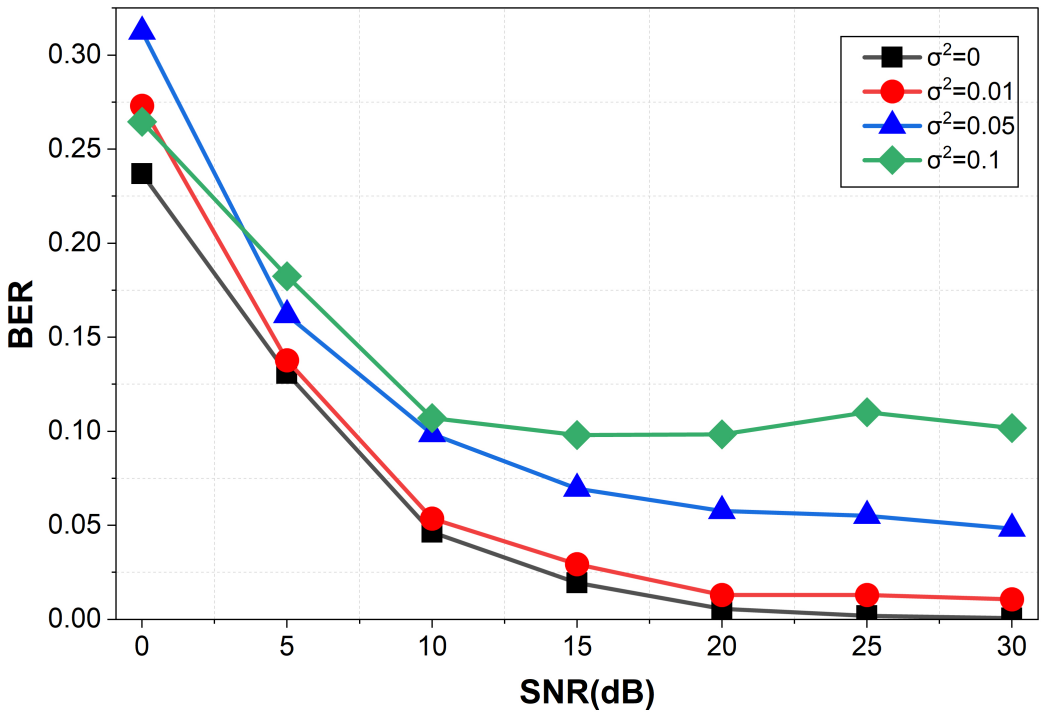


Figure 7.11. BER performance of reliability-aware cooperative DF ($\gamma_{\text{th}} = 4$) under different CSI uncertainty levels.

Figure 7.11 demonstrates the BER behavior of the reliability-aware activation strategy under different CSI uncertainty levels. Under perfect CSI, BER decreases continuously with increasing SNR, whereas imperfect CSI progressively limits the achievable reliability improvement and leads to pronounced high-SNR saturation. The severity of this behavior increases with CSI uncertainty, indicating that reliability-aware relay activation remains strongly dependent on the prevailing CSI conditions.

Overall, the proposed relay activation mechanism constitutes the first step toward adaptive cooperative optimization under realistic wireless impairments. Rather than assuming that relay participation is always beneficial, cooperation is activated only when the estimated source–relay link quality indicates that relay forwarding is likely to improve overall communication reliability. The following section further investigates the selection of the activation threshold and examines how the operating point of the proposed adaptive cooperative mechanism can be optimized under different CSI uncertainty conditions.

7.2.5 Relay-Activation Threshold Optimization

The previous section introduced the reliability-aware relay activation mechanism as an adaptive cooperative strategy for mitigating harmful cooperation under realistic operating impairments. Although the proposed mechanism provides a means of selectively controlling relay participation, its effectiveness depends critically on the selection of the relay activation threshold. Consequently, optimizing the activation threshold becomes an essential design step for achieving reliable cooperative operation under varying channel conditions.

The relay activation threshold directly governs the balance between two competing objectives. Small threshold values favor frequent relay participation and maximize the exploitation of cooperative diversity. However, they also increase the probability of forwarding erroneously decoded symbols under imperfect CSI conditions, thereby intensifying relay error propagation. Conversely, large threshold values suppress unreliable relay participation and improve transmission reliability, but simultaneously reduce the achievable diversity gain by limiting cooperative operation. The activation threshold therefore defines the operating point of the proposed adaptive mechanism and determines the trade-off between diversity exploitation and impairment mitigation.

The threshold-selection problem can be expressed as

$$\gamma_{\text{th}}^{\star}(\rho, \sigma_e^2) = \arg \min_{\gamma_{\text{th}} \in \Gamma} \text{BER}_{\text{RA}} \left(\rho, \gamma_{\text{th}}; \sigma_e^2 \right), \tag{7.14}$$

where Γ denotes the set of examined relay activation thresholds and ρ represents the operating SNR. The term $\text{BER}_{\text{RA}}(\rho, \gamma_{\text{th}}; \sigma_e^2)$ denotes the BER of the reliability-aware cooperative scheme for a given SNR, activation threshold and CSI uncertainty variance. Therefore, $\gamma_{\text{th}}^{\star}(\rho, \sigma_e^2)$ corresponds to the activation threshold that minimizes the BER for each specific combination of SNR and CSI uncertainty.

Table 7.2 summarizes the corresponding relay activation rates for the examined threshold

Table 7.2. Impact of Relay-Activation Threshold Selection for $\sigma_e^2 = 0.05$

Threshold (γ_{th})	**Activation Rate**	**Interpretation**
1	$\sim$ 0.98–0.99	Near-always-on cooperation
2	$\sim$ 0.87–0.94	High relay participation
4	$\sim$ 0.43–0.49	Selective relay participation
6	$\sim$ 0.16–0.19	Conservative relay participation
8	$\sim$ 0.04–0.06	Limited relay participation
10	< 0.02	Near-direct operation
12	$\sim$ 0–0.01	Near-direct operation

values. For very low thresholds, the relay remains active for almost all channel realizations, closely approximating conventional always-on cooperative transmission. Although relay participation is maximized, persistent relay error propagation limits the achievable BER improvement.

As the activation threshold increases, relay participation becomes progressively more selective, suppressing unreliable relay forwarding and improving communication reliability. An intermediate operating region emerges in which relay activation remains sufficiently frequent to preserve cooperative diversity while effectively limiting relay-induced performance degradation. The best BER performance is achieved within this operating region, corresponding to relay activation rates of approximately 40–50%.

For excessively large threshold values, relay participation becomes infrequent and the cooperative transmission gradually approaches direct MIMO operation. Although relay error propagation is largely eliminated, the reduced utilization of cooperative diversity results in a gradual loss of the achievable cooperation gain.

Figure 7.12 illustrates the BER performance obtained for different relay-activation thresholds under a representative CSI uncertainty level of $\sigma_e^2 = 0.05$. The results reveal a clear dependence of the preferred threshold on the operating SNR. Lower threshold values promote frequent relay participation, whereas higher thresholds progressively restrict relay activation. Importantly, the BER curves intersect across the examined SNR range, indicating that no single threshold provides uniformly superior reliability performance. Instead, the reliability-preferred activation threshold varies with the operating point, motivating the operating-condition-dependent threshold formulated in (7.14).

The obtained results also suggest that the preferred activation threshold should not be interpreted as a universal fixed parameter, since the optimal operating point is expected to depend on CSI uncertainty, relay reliability and the operating SNR range. Consequently, relay activation threshold selection constitutes an operating-condition-dependent optimization problem rather than a fixed system parameter.

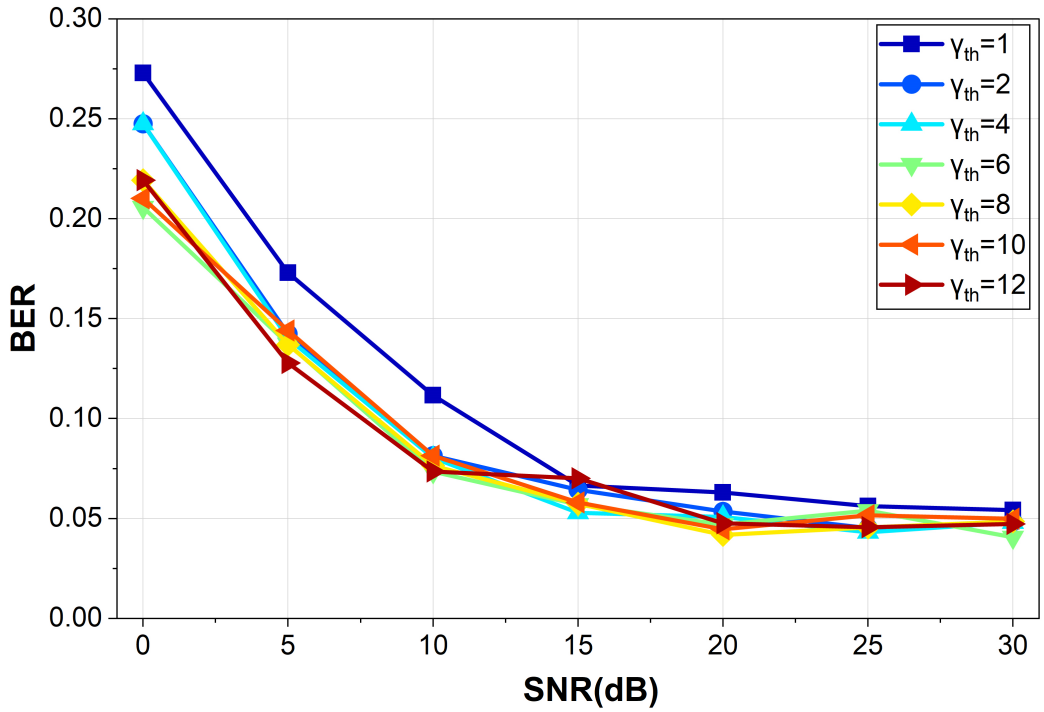


Figure 7.12. BER vs. SNR for different activation thresholds γ_{th} ($\sigma_e^2 = 0.05$).

Overall, this optimization establishes the preferred operating region of the proposed reliability-aware relay activation mechanism. Having established the operating-condition dependence of the preferred activation threshold, the following section evaluates the overall communication performance achieved when the reliability-preferred threshold is selected for each operating point.

7.2.6 Performance Evaluation of Adaptive Cooperative Operation

The previous sections established the reliability-aware relay activation mechanism and identified its preferred operating region through threshold optimization. Having designed and optimized the proposed adaptive cooperative strategy, the remaining objective is to evaluate its overall effectiveness under realistic operating impairments. In particular, the present analysis examines whether adaptive relay participation is capable of recovering part of the reliability advantage of cooperative transmission while mitigating the harmful cooperation phenomenon identified earlier in this chapter.

To provide a comprehensive performance assessment, three representative transmission strategies are compared: conventional direct MIMO transmission, cooperative DF transmission with continuous relay participation (always-on cooperation), and the proposed adaptive cooperative strategy employing optimized reliability-aware relay activation. This comparison allows the performance degradation associated with conventional cooperative transmission to be directly contrasted with the improvements achieved through adaptive relay control.

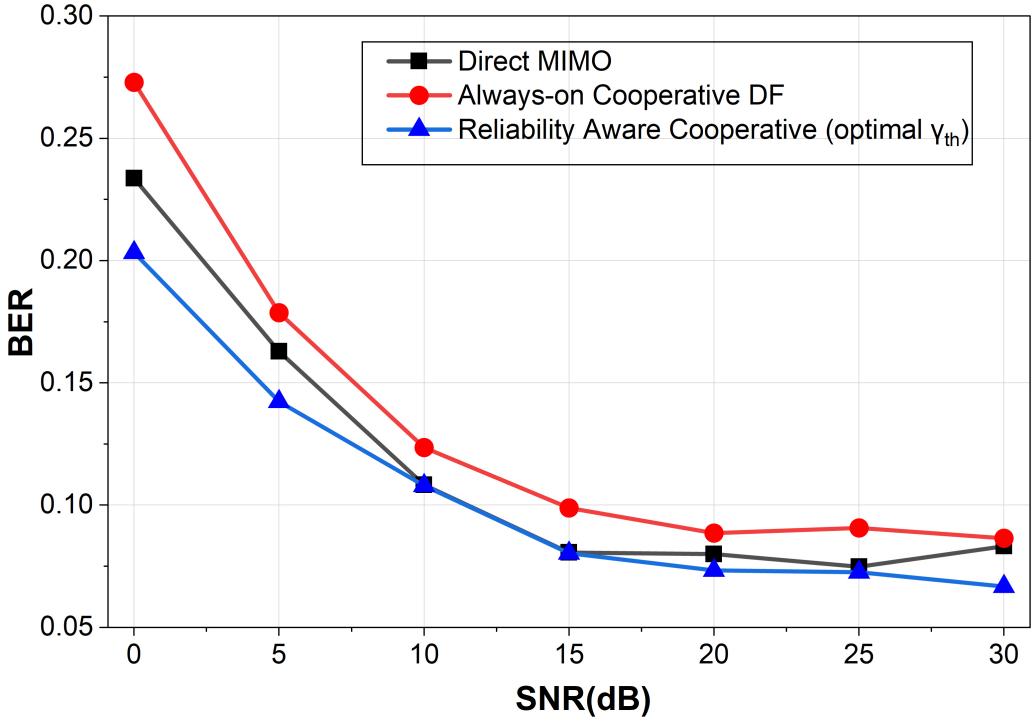


Figure 7.13. BER comparison of direct MIMO, always-on cooperative DF and adaptive reliability-aware cooperative transmission under $\sigma_e^2 = 0.1$ using the optimized relay activation threshold.

Figure 7.13 compares the BER performance of the three transmission strategies under severe CSI uncertainty. Conventional always-on cooperative transmission exhibits significant performance degradation in the medium-to-high SNR regime due to the combined effects of relay error propagation and residual CSI-induced interference. As the SNR increases, these impairment mechanisms progressively dominate the cooperative transmission process, leading to the harmful cooperation behavior identified in the previous sections.

In contrast, the proposed adaptive cooperative strategy substantially improves communication reliability by selectively suppressing unreliable relay participation. Rather than maintaining continuous cooperation, relay forwarding is enabled only when the estimated source–relay channel quality satisfies the reliability criterion established in the previous section. Consequently, the probability of relay-induced error propagation is reduced while the potential benefits of relay-assisted diversity are preserved under favorable source–relay conditions.

Compared with conventional always-on cooperation, the proposed adaptive strategy consistently achieves lower BER throughout the medium-to-high SNR region. Furthermore, the adaptive cooperative scheme also outperforms direct MIMO transmission over a substantial portion of the examined operating range, demonstrating that selective relay participation effectively restores the performance advantages of cooperative diversity under realistic operating impairments.

Beyond the observed BER improvement, the proposed adaptive mechanism substantially reduces the extent of the harmful cooperation region. Instead of allowing unreliable relay

transmissions to dominate system performance, adaptive relay activation confines cooperative operation to channel conditions where relay participation is expected to provide a net reliability benefit. Consequently, cooperation is transformed from a potentially detrimental transmission strategy into an adaptive operating mechanism whose effectiveness depends on the prevailing communication conditions.

From a computational perspective, the proposed strategy maintains low complexity. Relay activation requires only the evaluation of the locally available source–relay channel quality metric followed by a simple threshold comparison, introducing negligible computational overhead compared with the matrix operations already required for MIMO signal detection.

Overall, the obtained results demonstrate that adaptive relay activation successfully restores the effectiveness of cooperative transmission under realistic operating impairments. Rather than relying on continuous relay participation, the proposed strategy adaptively exploits cooperative diversity only when it is expected to improve communication reliability, thereby mitigating harmful cooperation while preserving the principal advantages of relay-assisted MIMO transmission. These observations establish adaptive relay control as an effective optimization strategy for cooperative MIMO systems operating under imperfect CSI conditions.

7.2.7 Antenna Scaling and Cooperative Robustness

The previous sections demonstrated that reliability-aware relay activation substantially improves cooperative MIMO operation under realistic operating impairments by suppressing harmful cooperation while preserving the benefits of cooperative diversity. The remaining question concerns the generality of these conclusions across different MIMO system dimensions. As future wireless networks are expected to employ progressively larger antenna arrays, it becomes important to investigate whether the operating principles established throughout this chapter remain valid as the system dimension increases.

Increasing the number of antennas influences cooperative communication in several ways. Larger MIMO configurations provide additional spatial diversity and increased receive-side redundancy, potentially improving robustness against CSI uncertainty. At the same time, however, residual CSI-induced interference and relay error propagation remain present. This raises the important question of whether antenna scaling alone is sufficient to mitigate harmful cooperation or whether adaptive relay control remains an essential component of robust cooperative operation.

To investigate these effects, the impact of antenna scaling is evaluated for several cooperative MIMO configurations while maintaining identical transmission assumptions. The objective is to quantify the influence of system dimension on communication reliability and to examine how the robustness of cooperative transmission evolves under imperfect CSI conditions.

To quantitatively evaluate the sensitivity of the system to channel estimation errors, the CSI sensitivity metric is defined as

$$S_{\mathrm{CSI}} = \frac{\mathrm{BER}_{\sigma_e^2} - \mathrm{BER}_0}{\mathrm{BER}_0} \tag{7.15}$$

where BER_0 denotes the BER obtained under the baseline case of perfect CSI ($\sigma_e^2 = 0$), while $\mathrm{BER}_{\sigma_e^2}$ corresponds to the BER obtained under imperfect CSI conditions.

The relative formulation normalizes the impact of CSI uncertainty with respect to the baseline system performance, thereby enabling fair robustness comparisons across different antenna configurations and transmission schemes. Since extremely small BER values may lead to numerical instability when the reference BER approaches zero, a stabilized version of the metric is additionally introduced:

$$S_{\mathrm{CSI}}^{\mathrm{safe}} = \frac{\mathrm{BER}_{\sigma_e^2} - \mathrm{BER}_0}{\max(\mathrm{BER}_0, \epsilon)} \tag{7.16}$$

where ϵ denotes a small BER floor introduced to avoid numerical instability when $\mathrm{BER}_0 \to 0$.

Based on the stabilized CSI sensitivity metric, the robustness gain is defined as

$$G_R^{\mathrm{safe}} = S_{\mathrm{CSI,direct}}^{\mathrm{safe}} - S_{\mathrm{CSI,coop}}^{\mathrm{safe}}. \tag{7.17}$$

Positive values of G_R^{safe} indicate that cooperative transmission is less sensitive to CSI uncertainty than direct MIMO communication, whereas negative values indicate that cooperative transmission is more sensitive to CSI imperfections.

To examine the effect of system dimension, simulations are performed for three representative MIMO configurations (4×2, 8×2 and 8×4), while maintaining the same number of transmitted spatial streams and identical system parameters. The corresponding BER performance is presented in Figure 7.14.

Figure 7.14 shows that antenna scaling can lead to substantial BER improvement when it provides additional receive-side spatial redundancy. This behavior becomes especially pronounced for the 8×4 configuration in the medium-to-high SNR regime under severe CSI uncertainty.

Although the BER curves clearly demonstrate the robustness improvement achieved through antenna scaling, they do not directly explain the underlying physical mechanism. To gain further insight into the observed behavior, the conditioning of the effective channel matrix is additionally investigated.

The effective channel matrix is given by

$$\hat{\mathbf{G}} = \hat{\mathbf{H}}\mathbf{F}, \tag{7.18}$$

where $\hat{\mathbf{H}}$ denotes the estimated channel matrix and $\mathbf{F}$ is the transmit precoding matrix. The channel conditioning is quantified through the condition number

$$\kappa(\hat{\mathbf{G}}) = \frac{\sigma_{\max}(\hat{\mathbf{G}})}{\sigma_{\min}(\hat{\mathbf{G}})}, \tag{7.19}$$

where smaller values correspond to a better-conditioned detection problem. Under severe CSI uncertainty ($\sigma_e^2 = 0.1$), the median condition number is approximately 2.82–2.96 for the

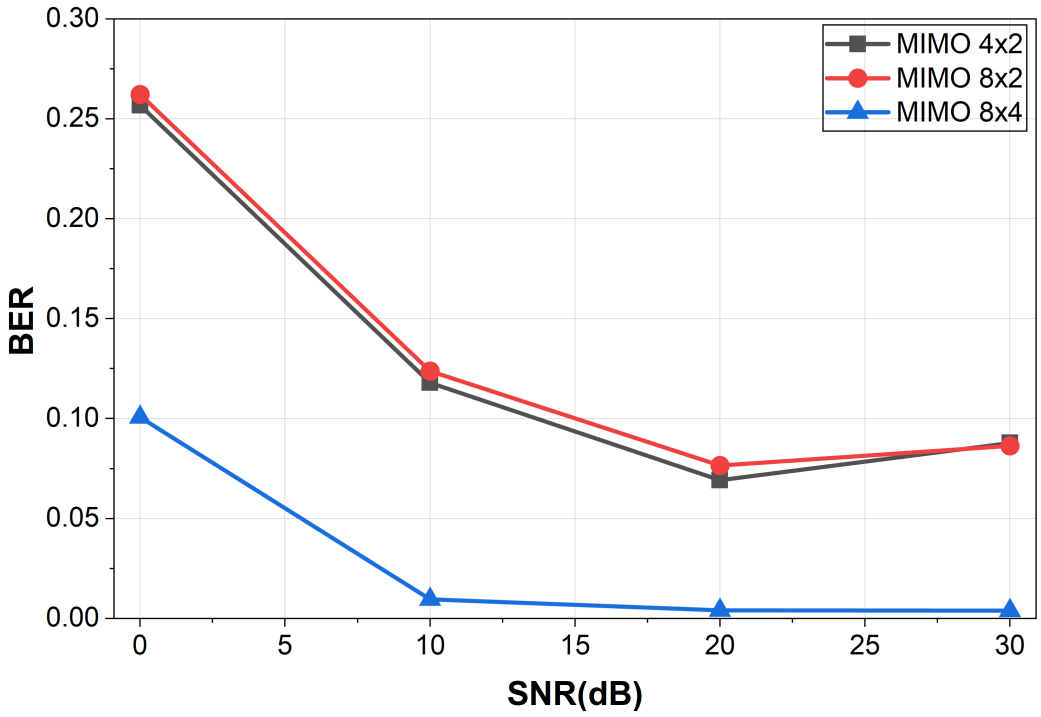


Figure 7.14. BER comparison across different antenna configurations under imperfect CSI ($\sigma_e^2 = 0.1$).

4×2 configuration and 2.83–3.02 for the 8×2 configuration, whereas it decreases significantly to approximately 1.86–1.87 for the 8×4 configuration.

The observed robustness improvement originates primarily from the overdetermined effective channel structure of the 8×4 configuration ($N_r = 4 > N_s = 2$), which provides additional receive-side spatial redundancy. Consequently, the pseudo-inverse operation becomes better conditioned, reducing noise enhancement and making the receiver considerably less sensitive to CSI perturbations. This explains the substantially improved robustness observed for larger receive dimensions under imperfect CSI conditions. The improvement observed through the condition number analysis is further reflected by the robustness gain metric shown in Figure 7.15, which provides a unified comparison of the sensitivity of direct and cooperative transmission to CSI uncertainty across different antenna configurations.

Figure 7.15 summarizes the impact of antenna scaling on the relative robustness of cooperative and direct MIMO transmission. For the smaller antenna configurations (4×2 and 8×2), the robustness gain remains predominantly negative over the examined range of CSI uncertainty. This indicates that, despite the diversity benefits provided by relay-assisted transmission, cooperative operation remains more sensitive to CSI imperfections due to the combined effects of relay error propagation and residual CSI-induced interference.

A markedly different behavior is observed for the 8×4 configuration. In this case, the robustness gain becomes positive over a wide range of CSI error variances, demonstrating that cooperative transmission can become more resilient than direct MIMO communication when sufficient receive-side spatial redundancy is available. These results are fully consistent with

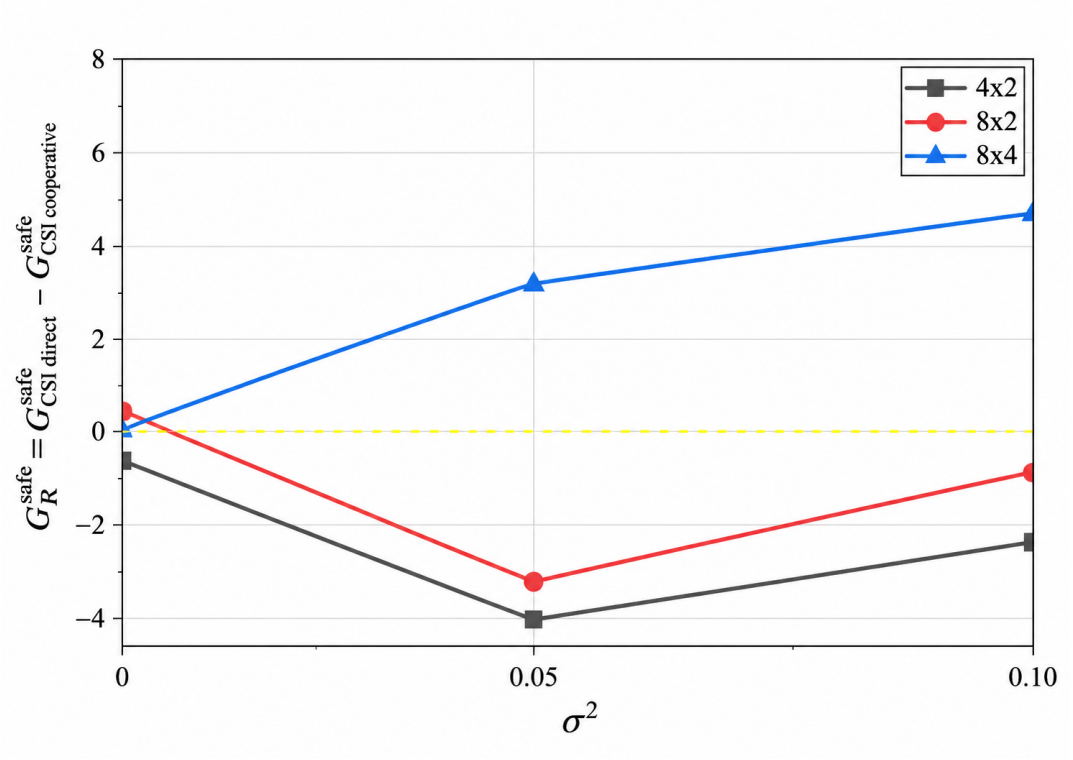


Figure 7.15. Robustness gain versus CSI error variance for different antenna configurations at 20 dB. The metric is defined as $G_R^{safe} = S_{CSI,direct}^{safe} - S_{CSI,coop}^{safe}$. Positive values indicate robustness improvement, whereas negative values indicate robustness degradation.

the condition number analysis presented earlier, confirming that improved channel conditioning significantly reduces the sensitivity of the receiver to CSI perturbations.

The obtained results indicate that antenna scaling influences not only the achievable BER performance but also the fundamental robustness characteristics of cooperative MIMO systems. Increasing receive-side spatial redundancy can shift the operating region toward improved resilience against CSI uncertainty, thereby reducing the relative impact of relay-induced impairments. Nevertheless, the underlying mechanisms responsible for harmful cooperation are not completely eliminated. Residual CSI-induced interference and relay decoding errors remain present, although their influence becomes progressively weaker as the receive dimension increases.

These observations demonstrate that antenna scaling and adaptive relay activation address complementary aspects of robust cooperative communication. Increasing the number of antennas provides structural robustness by improving spatial diversity and receiver conditioning, whereas reliability-aware relay activation provides adaptive robustness by preventing unreliable relay participation under unfavorable operating conditions. Consequently, neither mechanism should be regarded as a complete replacement for the other. Instead, both operate synergistically to improve cooperative communication reliability under realistic wireless impairments.

Overall, the analysis presented in this section generalizes the conclusions established throughout this chapter. Larger MIMO configurations can substantially improve robustness

against CSI uncertainty, especially when the receive dimension provides additional redundancy relative to the number of transmitted streams. However, antenna scaling does not remove the underlying impairment mechanisms responsible for harmful cooperation. Residual CSI-induced interference and relay error propagation remain present, although their relative impact may be reduced as the system dimension increases. Robust cooperative MIMO operation therefore requires the combined application of structural robustness, achieved through appropriate antenna configuration, and adaptive robustness, achieved through reliability-aware relay activation. Together, these design principles establish a comprehensive framework for cooperative MIMO systems operating under realistic wireless conditions.

7.3 Summary and Conclusions

This chapter investigated the reliability of cooperative MIMO communication under realistic operating impairments and examined whether relay-assisted transmission can be regarded as an inherently beneficial extension of conventional MIMO operation. Building upon the condition-dependent design perspective developed in the preceding chapters, the analysis addressed cooperation as an additional communication resource whose effectiveness must be evaluated relative to the prevailing channel, CSI and relay conditions. The central question was therefore not simply whether cooperation can provide additional diversity, but under which operating conditions relay participation remains beneficial when channel estimation uncertainty and relay decoding errors are explicitly taken into account.

The analysis began by establishing direct MIMO transmission as the reference operating mode and subsequently introduced cooperative Decode-and-Forward transmission under progressively more realistic assumptions. Under ideal conditions, relay-assisted transmission provides an additional diversity opportunity and can improve communication reliability. However, once imperfect CSI is introduced, the estimated channel matrices deviate from the actual propagation channels, producing residual channel-mismatch effects during signal detection. The analysis further incorporated imperfect decoding at the relay, allowing erroneous symbol decisions to be re-modulated and forwarded toward the destination. This extension was particularly important because it captured the error-propagation mechanism inherent to Decode-and-Forward operation rather than assuming an error-free relay.

The source–relay analysis demonstrated that increasing SNR alone cannot guarantee reliable relay decoding when CSI uncertainty remains present. Under imperfect CSI, relay BER progressively exhibits high-SNR saturation, showing that channel-estimation errors can remain influential even when the contribution of thermal noise is reduced. Once these relay decoding errors are propagated through the relay–destination transmission phase, the resulting cooperative BER is affected jointly by CSI-induced residual interference and erroneous relay forwarding. Consequently, the expected reliability advantage of cooperative diversity becomes strongly dependent on the operating point rather than being guaranteed by relay participation itself.

Direct comparison between cooperative and direct MIMO operation revealed the resulting harmful-cooperation phenomenon. Harmful cooperation was defined as the operating condition in which the BER achieved through cooperative transmission exceeds that of the corresponding direct MIMO link. The results showed that beneficial and harmful cooperative regions depend jointly on SNR and CSI uncertainty and need not evolve monotonically across the operating range. Under relatively limited CSI uncertainty, cooperation may remain beneficial at selected operating points while becoming detrimental at others. As CSI uncertainty increases, harmful cooperation becomes increasingly pronounced, and under severe estimation errors conventional always-on cooperation may underperform direct transmission over most or all of the examined SNR range. Coded-system validation further confirmed that this behavior persists when channel coding is introduced, demonstrating that harmful cooperation is not restricted to the uncoded transmission model.

These observations motivated the introduction of reliability-aware relay activation. Rather than allowing the relay to participate continuously, the proposed mechanism evaluates the estimated source–relay effective-channel quality through the metric defined in (7.8) and activates relay participation only when this metric exceeds a prescribed threshold γ_{th}.

The activation threshold therefore controls the degree of relay selectivity: low threshold values result in frequent relay participation and approach always-on cooperative operation, whereas progressively larger thresholds restrict relay activation and move the system toward predominantly direct transmission. The proposed mechanism introduces only limited additional computational complexity, since relay control requires the evaluation of a locally available channel-quality metric followed by a simple threshold comparison.

The threshold-sweep analysis demonstrated that relay selectivity cannot be determined by a universally fixed threshold. The examined values $\gamma_{\text{th}} \in \{1, 2, 4, 6, 8, 10, 12\}$ produced substantially different relay-activation rates, ranging from near-continuous relay participation at low thresholds to near-direct operation at the largest thresholds. More importantly, the corresponding BER curves intersected across the examined SNR range, demonstrating that no individual threshold provides uniformly superior reliability performance. The reliability-preferred threshold therefore depends on the operating point. This observation motivated operating-condition-dependent threshold selection, in which the value $\gamma_{\text{th}}^{\star}$ is selected according to the combination of SNR and CSI uncertainty in order to minimize the resulting BER.

The effectiveness of this approach was subsequently evaluated through direct comparison among three representative operating strategies: direct MIMO transmission, conventional always-on cooperative DF transmission and reliability-aware cooperative transmission using the optimized activation threshold. Under severe CSI uncertainty, always-on cooperation exhibited the expected harmful-cooperation behavior and produced higher BER than direct transmission over the examined operating range. In contrast, reliability-aware operation consistently improved performance relative to always-on cooperation and achieved performance comparable to or better than direct MIMO across the investigated conditions. These results demonstrate that the reliability limitation does not originate from cooperation alone, but from

indiscriminate relay participation under conditions in which the relay cannot contribute sufficiently reliable information. Selective relay control can therefore recover useful cooperative gains while substantially mitigating the harmful effects associated with unreliable forwarding.

The final part of the chapter examined whether these conclusions remain valid as the antenna configuration changes. Three representative configurations, 4×2, 8×2 and 8×4, were evaluated while maintaining two transmitted spatial streams. The results revealed that antenna scaling does not provide uniform robustness improvement merely through an increase in the number of antennas. In particular, increasing the transmit dimension from 4×2 to 8×2 produced relatively limited improvement, whereas the 8×4 configuration exhibited a substantial BER reduction under severe CSI uncertainty. This behavior demonstrated the particular importance of receive-side spatial redundancy relative to the number of transmitted streams.

The underlying mechanism was further examined through the conditioning of the estimated effective channel matrix. For the 4×2 and 8×2 configurations, the effective detection problem remains determined by two receive dimensions and two transmitted streams. In contrast, the 8×4 configuration provides four receive dimensions for the detection of two spatial streams, producing an overdetermined effective channel structure. The corresponding reduction in condition number indicates improved numerical conditioning of the pseudo-inverse detector, reducing noise enhancement and limiting the sensitivity of detection to CSI perturbations. The robustness-gain analysis confirmed this behavior: while the smaller configurations remained comparatively sensitive to CSI uncertainty, the 8×4 configuration exhibited positive robustness gain over a substantial range of CSI error variance, indicating that sufficient receive-side spatial redundancy can fundamentally improve the resilience of cooperative MIMO operation.

The combined results lead to four principal insights.

Insight 1: Cooperation is a condition-dependent reliability resource rather than an inherently beneficial transmission mechanism. The additional diversity offered by relay-assisted transmission does not guarantee improved end-to-end reliability. Under imperfect CSI and imperfect relay decoding, relay participation may either improve or degrade performance depending on SNR, channel-estimation uncertainty and relay reliability. The emergence of harmful cooperation therefore demonstrates that the value of cooperative diversity must be assessed relative to the prevailing operating conditions.

Insight 2: The effectiveness of cooperation depends critically on selective relay participation. The comparison between always-on and reliability-aware operation shows that the principal limitation of cooperative transmission is not relay assistance itself, but the indiscriminate use of the relay when its contribution is unreliable. Screening relay participation through a source–relay reliability criterion substantially reduces error propagation and allows cooperative diversity to be exploited selectively when the estimated relay-link conditions justify participation.

Insight 3: The preferred degree of relay selectivity is itself operating-condition dependent. The threshold-sweep results show that neither aggressive cooperation nor highly

conservative relay activation is universally optimal. Different activation thresholds become reliability-preferred as SNR and CSI uncertainty change. Consequently, relay control should not rely on a universally fixed activation rule; the activation threshold represents an adaptive design parameter whose preferred value moves with the operating point.

Insight 4: Receive-side spatial redundancy and adaptive relay control provide complementary forms of robustness. Antenna scaling improves cooperative reliability most effectively when it increases the receive dimension relative to the number of transmitted streams, thereby improving effective-channel conditioning and reducing sensitivity to CSI perturbations. This structural robustness does not eliminate the mechanisms responsible for harmful cooperation, just as adaptive relay activation does not replace the benefits of an appropriately dimensioned MIMO architecture. Robust cooperative operation therefore emerges from the complementary use of spatial redundancy and condition-dependent relay control.

Overall, this chapter demonstrates that cooperation should not be treated as a static extension of MIMO diversity whose reliability benefit can be assumed a priori. Instead, relay-assisted transmission represents an additional communication resource whose usefulness depends on the prevailing operating conditions. Imperfect CSI and relay decoding errors determine when cooperation may become harmful; reliability-aware activation determines when the relay should participate; operating-point-dependent threshold selection determines how selectively this resource should be exploited; and receive-side spatial redundancy provides an additional structural mechanism for improving robustness.

More broadly, these findings complete the progression developed throughout this dissertation. The initial characterization of MIMO systems established that the value of spatial resources depends strongly on propagation conditions, antenna configuration and channel knowledge. The subsequent energy analysis showed that additional diversity is beneficial only when its reliability improvement justifies the associated transmission, hardware and processing costs, while the adaptive MIMO framework demonstrated that the preferred antenna configuration should therefore change with the operating point. The present chapter extends this same condition-dependent design principle to cooperative communication, showing that relay-assisted diversity must likewise be activated selectively rather than employed unconditionally. Taken together, these results establish a unified design perspective in which MIMO configuration, energy consumption and cooperative resources are jointly governed by adaptation to the prevailing operating conditions. MIMO design therefore evolves from the static use of available diversity toward the adaptive selection of when, where and to what extent additional communication resources should be employed, balancing reliability gains against their associated energy, implementation and impairment costs.

8 General Conclusions and Future Research Directions

The analyses developed throughout this dissertation converge toward a central conclusion: the behavior and optimization of MIMO systems cannot be understood independently of the wireless conditions under which they operate. Realistic propagation effects, imperfect channel knowledge, communication reliability requirements, energy consumption and implementation constraints jointly determine system performance and influence the suitability of different transmission strategies.

For this reason, the dissertation adopted a characterization-driven research methodology. Rather than treating system characterization, performance optimization, adaptive transmission and cooperative communication as independent topics, the presented studies examined them as successive and interconnected stages of MIMO system design. Realistic system characterization was first used to identify the mechanisms governing wireless performance. This understanding was then used to analyze reliability–energy trade-offs, define operating regions, develop adaptive transmission strategies and extend the same reasoning to cooperative MIMO communication under imperfect CSI.

This final chapter synthesizes the main scientific outcomes of the dissertation. It summarizes the principal findings, highlights the main research contributions, discusses the broader design implications of the obtained results, outlines the scope and limitations of the work and identifies future research directions enabled by the proposed characterization-driven approach.

8.1 Principal Scientific Findings

The principal findings of the dissertation are summarized in this section. Although the individual studies addressed different aspects of wireless communication , their results form a coherent scientific sequence. The characterization analyses identify the dominant mechanisms governing system behavior, while the subsequent optimization, adaptive transmission and cooperative communication studies demonstrate how this understanding can be translated into improved MIMO system operation.

Rather than representing independent research outcomes, the findings collectively demonstrate the close relationship between realistic system characterization and effective optimization under wireless operating conditions.

Finding 1: Realistic Characterization Reveals the Dominant Performance-Limiting Mechanisms

The first principal finding of this dissertation is that the behavior of wireless systems is governed by multiple interacting mechanisms that are not fully captured under idealized communication

assumptions. The characterization studies demonstrated that realistic propagation environments, channel asymmetries, imperfect channel state information, implementation constraints and communication reliability requirements collectively shape achievable system performance. Rather than acting independently, these factors interact in complex ways that fundamentally influence communication reliability, spectral efficiency and energy consumption.

The investigations further demonstrated that these mechanisms are present across different wireless communication scenarios, including both broadband MIMO systems operating under standardized propagation models and low-power wide-area communication networks. Although the underlying communication technologies differ substantially, the obtained results consistently highlighted the importance of realistic system modeling for accurately evaluating wireless performance.

Beyond providing a detailed performance assessment, the characterization analyses revealed how realistic propagation conditions, channel characteristics and system parameters shape wireless performance and established the scientific foundation for the optimization studies developed throughout the remainder of the dissertation. This understanding allows the subsequent optimization strategies to be interpreted in relation to the physical and practical factors affecting system performance rather than solely through idealized communication metrics.

Overall, this finding demonstrates that realistic system characterization provides the necessary understanding of the factors that shape wireless system performance under realistic operating conditions.

Finding 2: Wireless Optimization is Governed by the Reliability–Energy Trade-Off

The second principal finding of this dissertation is that the optimization of wireless systems cannot be based solely on conventional transmission-performance metrics. The conducted analyses demonstrated that communication reliability, transmission energy, hardware-related power consumption and signal-processing overhead jointly determine overall operating efficiency. Consequently, effective optimization requires balancing multiple performance objectives rather than maximizing a single communication metric.

The obtained results further revealed that the interaction between communication reliability and total energy expenditure gives rise to distinct operating trade-offs. While higher-order diversity schemes generally improve communication reliability, they may simultaneously increase RF-chain activation costs and signal-processing energy. Conversely, lower-complexity transmission modes reduce implementation cost but may require additional retransmissions under unfavorable channel conditions. These competing effects demonstrate that optimization inherently involves balancing reliability and energy efficiency according to the prevailing operating conditions and system constraints.

By explicitly incorporating both communication reliability and total energy consumption into the optimization process, the analyses identified operating regions in which different trans-

mission strategies become preferable. The energetic value of additional diversity was therefore shown to be conditional: its reliability benefit becomes energetically advantageous only when the resulting reduction in packet failures and retransmissions is sufficient to compensate for the additional implementation and processing cost. Rather than indicating a universally optimal configuration, these results demonstrate that the energy-preferred transmission strategy depends on the prevailing operating conditions, reliability requirements and implementation constraints. The extension of the analysis to energy-constrained LPWAN scenarios further confirmed that reliability–energy trade-offs remain critical in resource-limited wireless environments.

Overall, this finding demonstrates that effective wireless optimization requires the joint consideration of communication reliability, total energy consumption and implementation-related constraints in order to achieve balanced system operation.

Finding 3: Operating-Condition Dependence Motivates Adaptive MIMO Operation

The third principal finding of this dissertation is that the operating-condition-dependent behavior identified during the optimization analyses naturally motivates the adoption of adaptive transmission strategies. Since different MIMO configurations become preferable under different channel conditions, reliability requirements and energy constraints, no fixed transmission mode can consistently provide the preferred reliability–energy operating point across the entire operating range.

Building upon the operating regions identified in the previous analyses, the proposed adaptive framework demonstrated that dynamic transmission-mode selection enables the communication system to adjust its operation according to the prevailing wireless conditions. By jointly accounting for communication reliability and the energy cost associated with the available MIMO configurations, the adaptive strategy was shown to select different transmission modes across the examined operating conditions rather than relying on a single predefined configuration.

The obtained results further demonstrated that adaptive operation provides an effective mechanism for balancing communication reliability and energy efficiency under realistic operating conditions. Rather than optimizing individual transmission modes in isolation, the adaptive framework dynamically exploits the strengths of different diversity configurations according to the current operating regime, avoiding both the retransmission burden associated with insufficient diversity and the unnecessary energy overhead associated with excessive diversity.

Unlike the previous optimization analyses, which identified the preferred operating regions of individual transmission schemes, the adaptive framework translates these observations into an operating strategy capable of responding to changing wireless environments. In this sense, the proposed adaptive operation represents the operational realization of the operating-condition-aware optimization approach developed throughout the dissertation.

Overall, this finding demonstrates that adaptive MIMO operation can translate condition-dependent reliability–energy trade-offs into dynamic transmission-mode selection, allowing the system to exploit the configuration that is most appropriate for each operating regime rather than relying on a universally fixed transmission strategy.

Finding 4: Reliability-Aware Adaptive Cooperative Communication

The fourth principal finding of this dissertation is that the operating-condition-dependent optimization approach established for individual MIMO links naturally extends to cooperative communication systems. While cooperative transmission is traditionally regarded as an effective mechanism for improving communication reliability, the conducted analyses demonstrated that its effectiveness strongly depends on the prevailing operating conditions and cannot be assumed a priori under realistic wireless impairments.

The investigation revealed that the combined effects of imperfect channel state information and relay decoding errors fundamentally alter the behavior of cooperative MIMO systems. Rather than providing consistent diversity gains, cooperative transmission may under certain operating conditions become less reliable than direct communication, leading to the emergence of the harmful cooperation region. This observation demonstrates that cooperative operation itself is governed by operating-condition-dependent behavior similar to that identified previously for diversity-based optimization.

Building upon this observation, the proposed reliability-aware relay activation strategy demonstrated that harmful cooperation can be substantially mitigated by selectively controlling relay participation according to the estimated source–relay channel quality. The threshold-optimization analysis further demonstrated that the preferred degree of relay selectivity is itself operating-condition dependent, since no single activation threshold provides uniformly superior reliability across the examined SNR and CSI uncertainty conditions. Furthermore, the robustness analysis showed that antenna scaling provides substantial resilience against CSI uncertainty when it introduces additional receive-side spatial redundancy, while structural improvements alone do not eliminate the effects of relay error propagation and therefore do not remove the need for adaptive cooperative control.

Rather than treating cooperation as a permanently enabled transmission mechanism, the obtained results support a more adaptive operating philosophy in which relay participation is determined according to the prevailing communication conditions. In this way, the condition-dependent design perspective developed throughout the dissertation is extended from adaptive MIMO configuration selection to the selective use of cooperative communication resources.

Overall, this finding demonstrates that cooperation itself should be treated as a condition-dependent communication resource, whose activation and degree of selectivity must adapt to the prevailing operating conditions in order to preserve its reliability benefits under realistic wireless impairments.

8.2 Scientific Contributions and Research Outcomes

The investigations presented throughout this dissertation contribute to the understanding, characterization and optimization of MIMO communication systems operating under realistic wireless conditions. Rather than addressing a single isolated aspect of wireless communications, the research progressively examined system behavior under realistic and non-ideal operating conditions, reliability–energy trade-offs, adaptive transmission operation and cooperative communication under imperfect channel knowledge. Collectively, the obtained results establish a coherent framework for analyzing and improving wireless system operation under realistic and non-ideal operating conditions.

The principal scientific contributions of this dissertation are summarized as follows.

Contribution 1: Systematic Characterization of Wireless Systems under Realistic Operating Conditions

This dissertation establishes a comprehensive characterization framework for wireless communication systems operating under realistic conditions, with emphasis on both broadband MIMO and energy-constrained LPWAN scenarios. Through the use of standardized propagation models, advanced system-level simulations and complementary low-power communication analyses, the presented investigations demonstrate how realistic propagation conditions, deployment characteristics, channel uncertainty and implementation assumptions jointly influence system behavior. The obtained results demonstrate how wireless performance varies with propagation conditions, deployment characteristics and system configuration, providing a systematic and realistic basis for evaluating wireless system behavior beyond idealized communication assumptions.

Contribution 2: Characterization of Reliability–Energy Trade-offs for Wireless Optimization

A central contribution of this work is the systematic investigation of the reliability–energy trade-off across both conventional MIMO and energy-constrained LPWAN communication scenarios. For conventional MIMO operation, the analysis explicitly incorporates retransmission behavior, hardware-related energy consumption and signal-processing overhead, demonstrating that improved communication reliability does not necessarily translate into lower total energy consumption. In the LPWAN context, the investigation further examines how transmission configuration, communication reliability and airtime-related energy expenditure interact under resource-constrained operating conditions. Across both communication scenarios, the obtained results identify distinct reliability–energy trade-offs and operating regions in which different transmission strategies become energetically preferable, demonstrating that the energy-preferred operating strategy depends on the prevailing communication conditions and implementation constraints.

Contribution 3: Development of an Adaptive Operating Framework for MIMO Systems

Building upon the identified reliability–energy operating regions, this dissertation develops an adaptive MIMO operating framework that dynamically selects among alternative diversity configurations according to the prevailing operating conditions. Rather than relying on a fixed transmission strategy, the proposed framework jointly considers communication reliability and the energy cost associated with each available MIMO configuration, allowing the preferred transmission mode to change as propagation conditions, CSI uncertainty and implementation overhead vary. The resulting adaptive operation avoids both the retransmission burden associated with insufficient diversity and the unnecessary hardware and processing energy associated with excessive diversity, demonstrating how condition-dependent reliability–energy trade-offs can be translated into dynamic MIMO configuration selection.

Contribution 4: Reliability-Aware Cooperative MIMO Operation under Realistic Wireless Impairments

Extending the condition-dependent design perspective to cooperative communication, this dissertation investigates relay-assisted MIMO operation under imperfect CSI and relay decoding uncertainty. The presented analyses identify the harmful cooperation phenomenon arising from the combined effects of channel estimation uncertainty and relay decoding errors, demonstrating that relay participation does not inherently improve communication reliability under all operating conditions. To address this limitation, a reliability-aware relay activation strategy is developed to selectively control relay participation according to the estimated source–relay channel quality. The subsequent threshold-optimization analysis demonstrates that the reliability-preferred degree of relay participation is itself operating-condition dependent, with the preferred activation threshold varying across SNR and CSI uncertainty conditions. Furthermore, the antenna-scaling analysis demonstrates that additional receive-side spatial redundancy can substantially improve robustness against CSI uncertainty. Collectively, these contributions establish cooperation as a condition-dependent communication resource whose reliability benefits can be preserved through selective relay activation and appropriate system configuration.

Taken together, these contributions establish a unified research framework in which realistic system characterization, reliability–energy analysis, adaptive transmission and cooperative communication are treated as complementary components of wireless system design. Collectively, the dissertation demonstrates that understanding the mechanisms governing wireless behavior under the considered non-ideal operating conditions provides the foundation upon which robust, adaptive and energy-efficient communication strategies can be systematically developed for next-generation wireless networks.

8.3 Design Implications for MIMO Systems

The investigations presented throughout this dissertation extend beyond the analysis of individual MIMO communication problems and provide broader implications for the design of wireless systems. Collectively, the obtained results demonstrate that robust and efficient MIMO operation should not rely solely on idealized theoretical assumptions, static transmission configurations or isolated performance metrics. Instead, system design requires a systematic understanding of the mechanisms governing wireless communication behavior and the adoption of adaptive operating strategies capable of responding to realistic deployment conditions. Based on the findings of this dissertation, several engineering design guidelines for MIMO systems can be identified.

Design Guideline 1: Characterization Precedes Optimization

The presented analyses demonstrate that effective optimization cannot be separated from realistic system characterization. Propagation conditions, deployment characteristics, channel uncertainty and implementation constraints fundamentally influence communication performance and must therefore be explicitly considered before optimization strategies are developed. Accurate characterization consequently represents the foundation upon which wireless optimization should be built.

Design Guideline 2: Reliability as a Central Design Variable

Rather than representing only a performance metric, communication reliability should be regarded as a primary system-design variable. The analyses performed throughout this dissertation demonstrate that reliability is closely linked to retransmission behavior and total energy consumption, while also serving as a key criterion in adaptive transmission and cooperative relay decisions. Consequently, reliability should be jointly considered with energy efficiency and implementation complexity during MIMO system design. Importantly, reliability improvements should not be pursued independently of their associated cost, since the additional resources required to increase reliability may introduce energy and implementation overhead that outweighs the resulting performance benefit.

Design Guideline 3: Adaptive Operation Instead of Static Configuration

The obtained results consistently demonstrate that no single transmission strategy remains optimal under all operating conditions. Instead, different transmission configurations become preferable within different operating regions determined by propagation conditions, channel uncertainty, reliability requirements and implementation constraints. MIMO systems therefore benefit from adaptive operating mechanisms capable of selecting transmission configurations according to the prevailing wireless conditions. Adaptive operation consequently represents a natural response to the operating-condition-dependent behavior identified throughout this

dissertation.

Design Guideline 4: Adaptive Cooperative Operation

The investigations of cooperative communication demonstrate that relay-assisted transmission should not be regarded as a permanently enabled communication mechanism. Instead, relay participation should be adaptively controlled according to prevailing channel conditions and communication reliability in order to avoid harmful cooperation and preserve the benefits of cooperative diversity. Consequently, cooperation should be treated as an adaptive network resource rather than as a fixed transmission strategy.

Taken together, these engineering design guidelines express the broader design philosophy emerging from this dissertation. MIMO optimization should not be viewed as an isolated algorithmic problem, but as the outcome of a progressive process in which realistic system characterization provides the knowledge required to identify performance-limiting mechanisms, understand reliability–energy trade-offs and develop adaptive transmission strategies capable of responding to realistic wireless operating conditions.

This perspective reinforces the central scientific message of the dissertation: robust MIMO system design emerges from characterization-driven and reliability-aware optimization rather than from static transmission configurations or isolated performance objectives. By exploiting the operating regions identified under realistic wireless conditions, adaptive decision mechanisms can support reliable, energy-efficient and robust operation across diverse deployment scenarios.

8.4 Limitations and Scope of the Present Work

Although the studies presented throughout this dissertation systematically investigate the characterization and optimization of MIMO communication systems, they were intentionally conducted within a well-defined research scope. The adopted assumptions enabled the focused investigation of key factors affecting practical wireless operation while maintaining analytical consistency across the different studies. Consequently, several aspects of practical wireless communication remain beyond the scope of the present work.

First, the MIMO characterization was conducted over a representative but necessarily limited set of propagation conditions, antenna configurations and deployment scenarios. The analysis was not intended to cover the full range of emerging MIMO architectures and deployment paradigms, such as massive MIMO, cell-free MIMO and highly distributed or ultra-dense multi-user systems. Extending the characterization to such architectures would require the consideration of additional factors, including inter-user interference, distributed coordination, resource allocation and large-scale antenna management.

Second, the adaptive transmission strategies developed in this dissertation are based on performance characterization and operating-region identification. The proposed adaptive mechanisms therefore rely on deterministic decision criteria rather than data-driven optimiza-

tion techniques such as machine learning or reinforcement learning. While this choice provides clear physical interpretation and low implementation complexity, learning-based adaptation represents an important complementary research direction for highly dynamic wireless environments.

Moreover, the adaptive mechanisms are evaluated primarily under quasi-static operating conditions and do not explicitly model rapid temporal channel variations, feedback delays or configuration-switching costs. In highly dynamic environments, these effects may influence the practical responsiveness of the adaptive decision process and the achievable gains from operating-condition-dependent transmission selection.

Furthermore, the presented investigations focus primarily on communication-system performance and do not explicitly incorporate higher-layer networking aspects, including scheduling, traffic modeling, latency-aware optimization or cross-layer resource management. Similarly, hardware implementation issues such as RF impairments, hardware non-linearities, synchronization effects and real-time processing constraints are not explicitly considered.

Finally, the obtained results have been extensively evaluated through simulation studies using standardized communication models and realistic operating assumptions. Although this methodology provides controlled performance evaluation and enables the systematic investigation of individual physical mechanisms, experimental validation using software-defined radio platforms or practical wireless testbeds would provide additional insight into implementation-related effects that cannot be fully captured through simulation alone.

These limitations, however, should be viewed as deliberate modeling choices rather than shortcomings of the presented research. By carefully restricting the scope of the investigation, the dissertation isolates the principal mechanisms governing wireless system behavior under the considered non-ideal conditions and establishes a coherent scientific framework upon which more advanced communication scenarios, adaptive decision mechanisms and implementation aspects can be investigated in future work.

8.5 Future Research Directions

The investigations presented throughout this dissertation provide a systematic basis for the characterization and optimization of MIMO communication systems under realistic wireless conditions.

A first research direction concerns the extension of the proposed characterization-driven optimization approach to emerging large-scale distributed communication architectures, including distributed and cell-free MIMO systems. Such systems introduce additional challenges associated with user-centric communication, distributed signal processing, inter-node coordination and network-wide resource allocation. Addressing these challenges requires extending operating-condition-dependent optimization and adaptive resource-selection strategies to multi-node and spatially distributed communication scenarios.

A second direction involves the integration of learning-based adaptive decision mech-

anisms. The adaptive frameworks developed in this dissertation rely on performance-based operating regions and deterministic decision criteria. Future research may investigate how machine learning and reinforcement learning techniques can use the proposed characterization framework to support adaptive transmission decisions in highly dynamic wireless environments, while preserving the physical interpretability and low-complexity characteristics of the obtained solutions.

Another important extension concerns the joint optimization of communication reliability, energy efficiency and additional quality-of-service requirements. Future wireless systems will increasingly require the simultaneous consideration of latency, computational complexity, spectrum utilization, communication reliability and energy consumption. Extending the proposed reliability-aware optimization philosophy toward multi-objective optimization frameworks therefore represents an important direction for future investigation, particularly in heterogeneous wireless environments with diverse service requirements.

The cooperative communication framework developed in this dissertation may also be extended to more advanced cooperative architectures, including multi-relay systems, relay selection strategies, distributed antenna systems and heterogeneous cooperative networks. Investigating whether the harmful cooperation phenomenon persists under these more complex communication scenarios may provide further insight into the robustness limits of cooperative communications under realistic operating conditions and the conditions under which relay-assisted transmission should be adaptively activated.

Finally, experimental validation represents an important continuation of the present work. Although the proposed methodologies have been extensively evaluated through system-level simulations under realistic operating conditions, implementation using software-defined radio platforms or practical wireless testbeds would enable the investigation of hardware impairments, synchronization effects, real-time processing constraints and implementation-related uncertainties that remain difficult to fully capture through simulation alone.

Collectively, these research directions demonstrate that the methodologies developed throughout this dissertation provide not only answers to the investigated research problems but also a flexible scientific foundation upon which future advances in adaptive and reliability-aware MIMO communication systems may be developed.

8.6 Final Remarks

The continuous evolution of wireless communication systems toward increasingly heterogeneous, dynamic and resource-constrained environments demands a corresponding evolution in the way MIMO systems are analyzed, optimized and designed. Although the theoretical foundations of MIMO communications have been established through decades of research, the practical realization of these systems increasingly depends on understanding how realistic propagation conditions, imperfect channel knowledge, communication reliability, energy consumption and adaptive operation interact under wireless conditions.

The investigations presented throughout this dissertation demonstrate that MIMO behavior cannot be fully understood through idealized communication assumptions, nor can it be effectively optimized through static transmission strategies or isolated performance objectives. Instead, robust wireless system design requires a progressive methodology in which realistic system characterization first identifies the mechanisms governing communication performance, then reveals the associated reliability–energy trade-offs and ultimately enables adaptive transmission strategies capable of responding to diverse operating conditions.

Within this framework, communication reliability emerges as a central design parameter rather than merely as a conventional performance metric. The obtained results show that reliability is closely linked to retransmission behavior and total energy expenditure, while also serving as a key criterion in adaptive mode selection and cooperative communication decisions. This perspective is particularly important under imperfect CSI, where channel uncertainty and relay error propagation may fundamentally alter the expected benefits of both diversity-based and cooperative transmission strategies.

A central conclusion of this dissertation is therefore that MIMO optimization is inherently operating-condition-dependent. No single transmission configuration, diversity strategy or cooperative mechanism can be assumed to remain universally beneficial across all wireless environments. Instead, effective system operation requires adaptive decision mechanisms capable of responding to the operating-condition-dependent behavior identified throughout the presented analyses. In this sense, adaptive MIMO operation and reliability-aware cooperative communication are not isolated extensions of conventional MIMO design, but natural consequences of understanding how wireless systems behave under realistic and non-ideal operating conditions.

More broadly, this dissertation supports a characterization-driven view of wireless system design. From this perspective, optimization does not begin with the selection of an algorithm or a transmission mode, but with the systematic understanding of the physical and practical factors that shape system behavior. Once these factors are understood, adaptive and reliability-aware strategies can be developed to translate this understanding into operating decisions. This shift from metric-driven optimization toward characterization-driven and operating-condition-aware design constitutes one of the central messages of the present work.

The methodologies, analyses and design insights developed in this dissertation provide a foundation for further research on MIMO communications, adaptive wireless systems and reliability-aware optimization under increasingly realistic deployment conditions.

Bibliography

[1] A. Goldsmith, *Wireless Communications*. Cambridge University Press, 2005.

[2] J. G. Andrews, S. Buzzi, W. Choi, S. V. Hanly, A. Lozano, A. C. Soong, and J. C. Zhang, "What will 5G be?" *IEEE Journal on Selected Areas in Communications*, vol. 32, no. 6, pp. 1065–1082, 2014.

[3] ITU-R, "IMT vision—framework and overall objectives of the future development of IMT for 2020 and beyond," International Telecommunication Union, Geneva, Switzerland, Recommendation ITU-R M.2083-0, Sep. 2015.

[4] W. Saad, M. Bennis, and M. Chen, "A vision of 6G wireless systems: Applications, trends, technologies, and open research problems," *IEEE Network*, vol. 34, no. 3, pp. 134–142, 2020.

[5] M. Centenaro, L. Vangelista, A. Zanella, and M. Zorzi, "Long-range communications in unlicensed bands: The rising stars in the IoT and smart city scenarios," *IEEE Wireless Communications*, vol. 23, no. 5, pp. 60–67, 2016.

[6] U. Raza, P. Kulkarni, and M. Sooriyabandara, "Low power wide area networks: An overview," *IEEE Communications Surveys & Tutorials*, vol. 19, no. 2, pp. 855–873, 2017.

[7] K. Mekki, E. Bajic, F. Chaxel, and F. Meyer, "A comparative study of LPWAN technologies for large-scale IoT deployment," *ICT Express*, vol. 5, no. 1, pp. 1–7, 2019.

[8] G. J. Foschini and M. J. Gans, "On limits of wireless communications in a fading environment when using multiple antennas," *Wireless Personal Communications*, vol. 6, no. 3, pp. 311–335, 1998.

[9] E. Telatar, "Capacity of multi-antenna Gaussian channels," *European Transactions on Telecommunications*, vol. 10, no. 6, pp. 585–595, 1999.

[10] A. J. Paulraj, D. A. Gore, R. U. Nabar, and H. Bolcskei, "An overview of MIMO communications - a key to gigabit wireless," *Proceedings of the IEEE*, vol. 92, no. 2, pp. 198–218, 2004.

[11] D. Tse and P. Viswanath, *Fundamentals of Wireless Communication*. Cambridge University Press, 2005.

[12] S. M. Alamouti, "A simple transmit diversity technique for wireless communications," *IEEE Journal on Selected Areas in Communications*, vol. 16, no. 8, pp. 1451–1458, 1998.

[13] A. Paulraj, R. Nabar, and D. Gore, *Introduction to Space-Time Wireless Communications*. Cambridge University Press, 2003.

[14] L. Zheng and D. Tse, "Diversity and multiplexing: A fundamental tradeoff in multiple-antenna channels," *IEEE Transactions on Information Theory*, vol. 49, no. 5, pp. 1073–1096, 2003.

[15] A. F. Molisch, *Wireless Communications*, 2nd ed. Wiley, 2012.

[16] 3rd Generation Partnership Project (3GPP), "Study on 3D Channel Model for LTE," 3GPP, Technical Report TR 36.873, 2017.

[17] ——, "Study on Channel Model for Frequencies from 0.5 to 100 GHz," 3GPP, Technical Report TR 38.901, 2020.

[18] M. Temiz, E. Alsusa, L. Danoon, and Y. Zhang, "On the impact of antenna array geometry on indoor wideband massive MIMO networks," *IEEE Transactions on Antennas and Propagation*, vol. 69, no. 1, pp. 406–416, 2021.

[19] COST 2100, "COST 2100 channel model," 2012, Geometry-Based Stochastic Channel Model for MIMO Communications.

[20] P. Kyösti, J. Meinilä, L. Hentilä, X. Zhao, T. Jämsä, C. Schneider, M. Narandžić, M. Milojević, A. Hong, J. Ylitalo, V.-M. Holappa, M. Alatossava, R. Bultitude, Y. de Jong, and T. Rautiainen, "WINNER II channel models, Part I: Channel models," IST-4-027756 WINNER II Consortium, Deliverable D1.1.2 V1.1, 2007.

[21] M. Biguesh and A. B. Gershman, "Training-based MIMO channel estimation: A study of estimator tradeoffs and optimal training signals," *IEEE Transactions on Signal Processing*, vol. 54, no. 3, pp. 884–893, 2006.

[22] B. Hassibi and B. M. Hochwald, "How much training is needed in multiple-antenna wireless links?" *IEEE Transactions on Information Theory*, vol. 49, no. 4, pp. 951–963, 2003.

[23] D. J. Love, R. W. Heath, V. K. N. Lau, D. Gesbert, B. D. Rao, and M. Andrews, "An overview of limited feedback in wireless communication systems," *IEEE Journal on Selected Areas in Communications*, vol. 26, no. 8, pp. 1341–1365, 2008.

[24] G. Caire, N. Jindal, M. Kobayashi, and N. Ravindran, "Multiuser MIMO achievable rates with downlink training and channel state feedback," *IEEE Transactions on Information Theory*, vol. 56, no. 6, pp. 2845–2866, 2010.

[25] G. Ku and J. M. Walsh, "Resource allocation and link adaptation in LTE and LTE advanced: A tutorial," *IEEE Communications Surveys & Tutorials*, vol. 17, no. 3, pp. 1605–1633, 2015.

[26] M. J. Taghiyar, S. Muhaidat, J. Liang, and M. Dianati, "Relay selection with imperfect CSI in bidirectional cooperative networks," *IEEE Communications Letters*, vol. 16, no. 1, pp. 57–59, 2012.

[27] P. Popovski, J. J. Nielsen, C. Stefanovic, E. De Carvalho, E. Strom, K. F. Trillingsgaard, A.-S. Bana, D. M. Kim, R. Kotaba, J. Park, and R. B. Sorensen, "Wireless access for ultra-reliable low-latency communication: Principles and building blocks," *IEEE Network*, vol. 32, no. 2, pp. 16–23, 2018.

[28] M. Bennis, M. Debbah, and H. V. Poor, "Ultra-reliable and low-latency wireless communication: Tail, risk, and scale," *Proceedings of the IEEE*, vol. 106, no. 10, pp. 1834–1853, 2018.

[29] G. Durisi, T. Koch, and P. Popovski, "Toward massive, ultrareliable, and low-latency wireless communication with short packets," *Proceedings of the IEEE*, vol. 104, no. 9, pp. 1711–1726, 2016.

[30] C. Isheden, Z. Chong, E. Jorswieck, and G. Fettweis, "Framework for link-level energy efficiency optimization with informed transmitter," *IEEE Transactions on Wireless Communications*, vol. 11, no. 8, pp. 2946–2957, 2012.

[31] G. Miao, N. Himayat, G. Y. Li, and S. Talwar, "Energy-efficient link adaptation in frequency-selective channels," *IEEE Transactions on Communications*, vol. 58, no. 2, pp. 545–554, 2010.

[32] S. Cui, A. J. Goldsmith, and A. Bahai, "Energy-constrained modulation optimization," *IEEE Transactions on Wireless Communications*, vol. 4, no. 5, pp. 2349–2360, 2005.

[33] Z. Hasan, H. Boostanimehr, and V. Bhargava, "Green cellular networks: A survey," *IEEE Communications Surveys & Tutorials*, vol. 13, no. 4, pp. 524–540, 2011.

[34] A. Goldsmith and S.-G. Chua, "Variable-rate variable-power MQAM for fading channels," *IEEE Transactions on Communications*, vol. 45, no. 10, pp. 1218–1230, 1997.

[35] A. J. Goldsmith and S. G. Chua, "Adaptive coded modulation for fading channels," *IEEE Transactions on Communications*, vol. 46, no. 5, pp. 595–602, 1998.

[36] D. Gesbert, M. Kountouris, R. W. Heath, C.-B. Chae, and T. Sälzer, "Shifting the MIMO paradigm," *IEEE Signal Processing Magazine*, vol. 24, no. 5, pp. 36–46, 2007.

[37] D. J. Love, R. W. Heath, Jr., and T. Strohmer, "Grassmannian beamforming for multiple-input multiple-output wireless systems," *IEEE Transactions on Information Theory*, vol. 49, no. 10, pp. 2735–2747, 2003.

[38] S. Sanayei and A. Nosratinia, "Antenna selection in MIMO systems," *IEEE Communications Magazine*, vol. 42, no. 10, pp. 68–73, 2004.

[39] J. N. Laneman, D. N. C. Tse, and G. W. Wornell, "Cooperative diversity in wireless networks: Efficient protocols and outage behavior," *IEEE Transactions on Information Theory*, vol. 50, no. 12, pp. 3062–3080, 2004.

[40] A. Sendonaris, E. Erkip, and B. Aazhang, "User cooperation diversity—Part I: System description and Part II: Implementation aspects and performance analysis," *IEEE Transactions on Communications*, vol. 51, no. 11, pp. 1927–1948, 2003.

[41] A. Nosratinia, T. Hunter, and A. Hedayat, "Cooperative communication in wireless networks," *IEEE Communications Magazine*, vol. 42, no. 10, pp. 74–80, 2004.

[42] I. F. Akyildiz, W. Su, Y. Sankarasubramaniam, and E. Cayirci, "Wireless sensor networks: A survey," *Computer Networks*, vol. 38, no. 4, pp. 393–422, 2002.

[43] D. Gesbert, H. Bölcskei, D. A. Gore, and A. J. Paulraj, "Outdoor MIMO wireless channels: Models and performance prediction," *IEEE Transactions on Communications*, vol. 50, no. 12, pp. 1926–1934, 2002.

[44] M. K. Simon and M.-S. Alouini, *Digital Communication over Fading Channels*, 2nd ed. Hoboken, NJ: Wiley, 2005.

[45] T. S. Rappaport, *Wireless communications: Principles and practice, 2/E*. Pearson Education India, 2010.

[46] COST 207, "Digital Land Mobile Radio Communications," Commission of the European Communities, Final Report, 1989.

[47] COST 259, "Wireless Flexible Personalised Communications," European Cooperation in Science and Technology (COST 259), Tech. Rep., 2001.

[48] J. C. Ikuno, M. Wrulich, and M. Rupp, "System level simulation of LTE networks," in *2010 IEEE 71st Vehicular Technology Conference*. IEEE, 2010, pp. 1–5.

[49] M. K. Müller, F. Ademaj, T. Dittrich, A. Fastenbauer, B. R. Elbal, A. Nabavi, L. Nagel, S. Schwarz, and M. Rupp, "Flexible multi-node simulation of cellular mobile communications: The Vienna 5G system level simulator," *EURASIP Journal on Wireless Communications and Networking*, vol. 2018, no. 1, p. 227, 2018.

[50] Q. Zhu, C.-X. Wang, B. Hua, K. Mao, S. Jiang, and M. Yao, "3GPP TR 38.901 channel model," in *Wiley 5G Ref: The Essential 5G Reference Online*. Wiley, 2021, pp. 1–35.

[51] S. Yang and L. Hanzo, "Fifty years of MIMO detection: The road to large-scale MIMOs," *IEEE Communications Surveys & Tutorials*, vol. 17, no. 4, pp. 1941–1988, 2015.

[52] D. G. Riviello, F. Di Stasio, and R. Tuninato, "Performance analysis of multi-user MIMO schemes under realistic 3GPP 3-D channel model for 5G mmWave cellular networks," *Electronics*, vol. 11, no. 3, p. 330, 2022.

[53] M. Rupp, S. Schwarz, and M. Taranetz, Eds., *The Vienna LTE-Advanced Simulators*. Springer, 2016.

[54] C. Sudhamani, M. Roslee, L. L. Chuan, A. Waseem, A. F. Osman, and M. H. Jusoh, "Performance analysis of a millimeter wave communication system in urban micro, urban macro, and rural macro environments," *Energies*, vol. 16, p. 5358, 2023.

[55] J. Hu, L. Wang, J. Wu, Q. Pei, F. Liu, and B. Li, "A comparative measurement study of cross-layer 5G performance under different mobility scenarios," *Computer Networks*, vol. 257, p. 110952, 2025.

[56] L. Wei, S. S. Yuan, C. Huang, J. Zhang, F. Bader, Z. Zhang, S. Muhaidat, M. Debbah, and C. Yuen, "Electromagnetic channel modeling and capacity analysis for HMIMO communications," *IEEE Transactions on Wireless Communications*, 2025.

[57] F. Adelantado, X. Vilajosana, P. Tuset-Peiró, B. Martinez, J. Melia-Segui, and T. Watteyne, "Understanding the limits of LoRaWAN," *IEEE Communications Magazine*, vol. 55, no. 9, pp. 34–40, 2017.

[58] A. Augustin, J. Yi, T. Clausen, and W. M. Townsley, "A study of LoRa: Long range & low power networks for the Internet of Things," *Sensors*, vol. 16, no. 9, p. 1466, 2016.

[59] L. Rugini, K. Sardar, and G. Baruffa, "Coherent detection of MIMO LoRa with increased data rate," *IEEE Open Journal of the Communications Society*, vol. 5, pp. 5652–5666, 2024.

[60] A. Ghosh, S. Chandan, and S. Misra, "Implementing LoRa MIMO system for Internet of Things," *arXiv preprint arXiv:2501.07148*, 2025.

[61] A. Hoeller, R. D. de Souza, O. L. Alcaraz López, H. Alves, M. de Noronha Neto, and G. Brante, "Analysis and performance optimization of LoRa networks with time and antenna diversity," *IEEE Access*, vol. 6, pp. 32 820–32 829, 2018.

[62] O. T. Ozdogan and E. Bjornson, "Massive MIMO with dual-polarized antennas," *IEEE Transactions on Wireless Communications*, vol. 22, no. 3, pp. 1448–1463, 2023.

[63] T. Yunita, H. H. Ryanu, and A. A. Pramudita, "Effect of antenna polarization arrangement on MIMO channel capacity," *Emerging Science Journal*, vol. 9, pp. 1076–1088, 2025.

[64] V. Ezzati, F. Farzaneh, and M. Fakharzadeh, "A study of the effect of array geometry on improving channel hardening in mmWave massive MIMO systems," *Physical Communication*, vol. 66, p. 102402, 2024.

[65] P. Wang, Y. Li, Y. Peng, S. C. Liew, and B. Vucetic, "Non-uniform linear antenna array design and optimization for millimeter-wave communications," *IEEE Transactions on Wireless Communications*, vol. 15, no. 11, pp. 7343–7356, 2016.

[66] C. Hou, Q. Li, J. Zhang, Z. Wu, Y. Zhang, L. Guo, X. Zhu, and P. Du, "A three-dimensional fully polarized millimeter-wave hybrid propagation channel model for urban microcellular environments," *Electronics*, vol. 13, p. 3629, 2024.

[67] H. Lu, Y. Zeng, C. You, Y. Han, J. Zhang, Z. Wang, Z. Dong, S. Jin, C.-X. Wang, T. Jiang, X. You, and R. Zhang, "A tutorial on near-field XL-MIMO communications toward 6G," *IEEE Communications Surveys & Tutorials*, vol. 26, no. 4, pp. 2213–2257, 2024.

[68] X. Shao, Q. Jiang, and R. Zhang, "6D movable antenna based on user distribution: Modeling and optimization," *IEEE Transactions on Wireless Communications*, vol. 24, no. 1, pp. 355–370, 2024.

[69] E. Björnson, L. Sanguinetti, J. Hoydis, and E. G. Larsson, "Massive MIMO networks: Spectral, energy, and hardware efficiency," *Foundations and Trends in Signal Processing*, vol. 11, no. 3–4, pp. 154–655, 2017.

[70] Y. Liu, B. Ai, and J. Zhang, "Downlink spectral efficiency of massive MIMO systems with mutual coupling," *Electronics*, vol. 12, no. 6, p. 1364, 2023.

[71] Y. Chen, S. Zhang, S. Xu, and G. Y. Li, "Fundamental trade-offs on green wireless networks," *IEEE Communications Magazine*, vol. 49, no. 6, pp. 30–37, 2011.

[72] T. Wang, W. Heinzelman, and A. Seyedi, "Link energy minimization for wireless networks," *Ad Hoc Networks*, vol. 10, no. 3, pp. 569–585, 2012.

[73] S. Cui, A. J. Goldsmith, and A. Bahai, "Energy-efficiency of MIMO and cooperative MIMO techniques in sensor networks," *IEEE Journal on Selected Areas in Communications*, vol. 22, no. 6, pp. 1089–1098, 2004.

[74] S. Cui, R. Madan, A. J. Goldsmith, and S. Lall, "Cross-layer energy and delay optimization in small-scale sensor networks," *IEEE Transactions on Wireless Communications*, vol. 6, no. 10, pp. 3688–3699, 2007.

[75] F. Meshkati, H. V. Poor, S. C. Schwartz, and R. V. Balan, "Energy-efficient resource allocation in wireless networks with quality-of-service constraints," *IEEE Transactions on Communications*, vol. 57, no. 11, pp. 3406–3414, 2009.

[76] F. Rosas and C. Oberli, "Impact of the channel state information on the energy-efficiency of MIMO communications," *IEEE Transactions on Wireless Communications*, vol. 14, no. 8, pp. 4156–4169, 2015.

[77] B. M. Lee, "Leveraging massive MIMO for enhanced energy efficiency in high-density IoT networks," *Mathematics*, vol. 12, no. 22, p. 3539, 2024.

[78] J. C. Marinello, T. Abrão, A. Amiri, E. De Carvalho, and P. Popovski, "Antenna selection for improving energy efficiency in XL-MIMO systems," *IEEE Transactions on Vehicular Technology*, vol. 69, no. 11, pp. 13 305–13 318, 2020.

[79] G. Wu, Y. Fang, J. Xu, Z. Feng, and S. Cui, "Energy-efficient MIMO integrated sensing and communications with on–off nontransmission power," *IEEE Internet of Things Journal*, vol. 11, no. 7, pp. 12 177–12 191, 2023.

[80] W. B. Abbas, S. Khalid, Q. Z. Ahmed, F. Khalid, T. T. Alade, and P. Sureephong, "Heuristic antenna selection and precoding for a massive MIMO system," *IEEE Open Journal of the Communications Society*, vol. 5, pp. 83–96, 2024.

[81] H. Halbauer, A. Weber, D. Wiegner, and T. Wild, "Energy efficient massive MIMO array configurations," in *2018 IEEE Globecom Workshops (GC Wkshps)*. IEEE, 2018, pp. 1–6.

[82] L. Van der Perre, L. Liu, and E. G. Larsson, "Efficient DSP and circuit architectures for massive MIMO: State of the art and future directions," *IEEE Transactions on Signal Processing*, vol. 66, no. 18, pp. 4717–4736, 2018.

[83] J. Zhang, Y. Wei, E. Bjornson, Y. Han, and X. Li, "Spectral and energy efficiency of cell-free massive MIMO systems with hardware impairments," in *2017 9th International Conference on Wireless Communications and Signal Processing (WCSP)*. IEEE, 2017, pp. 1–6.

[84] A. Biason, C. Pielli, A. Zanella, and M. Zorzi, "On the energy/distortion tradeoff in the IoT," *arXiv preprint arXiv:1702.03695*, 2017.

[85] J. L. Soler-Fernández, O. Romera, A. Diéguez, J. D. Prades, and O. Alonso, "LoRa power model for energy optimization in IoT applications," *Sensors*, vol. 26, no. 1, p. 301, 2026.

[86] H. Taleb, G. Andrieux, A. Nasser, and N. Charara, "Energy-efficient selection of spreading factor in LoRaWAN-based systems," *Internet of Things*, vol. 24, p. 100896, 2023.

[87] F. Nisar, M. Amin, M. Touseef Irshad, H. J. Hadi, N. Ahmad, and M. Ladan, "XGBoost-driven adaptive spreading factor allocation for energy-efficient LoRaWAN networks," *Frontiers in Communications and Networks*, vol. 6, p. 1665262, 2025.

[88] J. A. Azevedo and F. Mendonça, "A critical review of the propagation models employed in LoRa systems," *Sensors*, vol. 24, no. 12, p. 3877, 2024.

[89] H. Kim, C.-B. Chae, G. de Veciana, and R. W. Heath, "A cross-layer approach to energy efficiency for adaptive MIMO systems exploiting spare capacity," *IEEE Transactions on Wireless Communications*, vol. 8, no. 8, pp. 4264–4275, 2009.

[90] S. Marwaha, E. A. Jorswieck, M. S. Jassim, T. Kuerner, D. L. Perez, X. Geng, and H. Bao, "Energy efficient operation of adaptive massive MIMO 5G HetNets," *IEEE Transactions on Wireless Communications*, vol. 23, no. 7, pp. 6889–6904, 2024.

[91] J. Park, C.-B. Chae, and R. W. Heath, "Switch-DFT: Adaptive waveform and MIMO switching for energy-efficient base stations," in *2026 IEEE International Conference on Communications Workshops (ICC Workshops)*. IEEE, 2026, pp. 1–6.

[92] C. Jiang and L. J. Cimini, "Antenna selection for energy-efficient MIMO transmission," *IEEE Wireless Communications Letters*, vol. 1, no. 6, pp. 577–580, 2012.

[93] N. P. Le, F. Safaei, and L. C. Tran, "Antenna selection strategies for MIMO-OFDM wireless systems: An energy efficiency perspective," *IEEE Transactions on Vehicular Technology*, vol. 65, no. 4, pp. 2048–2062, 2016.

[94] X. Yang, J. Qiu, and D. Mo, "Energy-efficient transmit antenna selection with fast-ABC-boost," *Scientific Reports*, vol. 15, no. 1, p. 38735, 2025.

[95] K. Wang, W. Chen, J. Li, and B. Vucetic, "Green MU-MIMO/SIMO switching for heterogeneous delay-aware services with constellation optimization," *IEEE Transactions on Communications*, vol. 64, no. 5, pp. 1984–1995, 2016.

[96] W. Gao, Y. Zhang, L. Liu, R. Fang, J. Sun, L. Zhu, and Z. Zhang, "Robust energy-efficient transmission for cell-free massive MIMO systems with imperfect CSI," *Electronics*, vol. 12, no. 16, p. 3384, 2023.

[97] Y. Sun, H. Shen, W. Xu, N. Hu, and C. Zhao, "Robust MIMO detection with imperfect CSI: A neural network solution," *IEEE Transactions on Communications*, vol. 71, no. 10, pp. 5877–5892, 2023.

[98] C. Kim and J. Lee, "Dynamic rate-adaptive MIMO mode switching between spatial multiplexing and diversity," *EURASIP Journal on Wireless Communications and Networking*, vol. 2012, no. 1, p. 238, 2012.

[99] G. D. Sworo, K. R. Dandekar, and M. Kam, "Reconfigurable antennas and link adaptation algorithms for MIMO-OFDM wireless systems," *EURASIP Journal on Wireless Communications and Networking*, vol. 2015, no. 1, p. 156, 2015.

[100] G. Favier and D. S. Rocha, "Overview of tensor-based cooperative MIMO communication systems—part 1: Tensor modeling," *Entropy*, vol. 25, no. 8, p. 1181, 2023.

[101] D. Darsena, G. Gelli, and F. Verde, "Design and performance analysis of multiple-relay cooperative MIMO networks," *Journal of Communications and Networks*, vol. 21, no. 1, pp. 25–32, 2019.

[102] M. Mohammadi and S. M. Hosseini Andargoli, "Throughput maximization for downlink DF MIMO relay based SWIPT cognitive radio networks," *Computer Communications*, vol. 209, pp. 368–377, 2023.

[103] S. Soni, R. Makkar, D. Rawal, and N. Sharma, "Performance of selective DF-based multiple relayed NOMA system with imperfect CSI and SIC errors," *IEEE Transactions on Green Communications and Networking*, vol. 8, pp. 79–89, 2024.

[104] L.-S. Tsai, S.-L. Shih, P.-K. Liao, and C.-K. Wen, "MIMO evolution toward 6G: End-user-centric collaborative MIMO," *IEEE Communications Magazine*, vol. 62, no. 7, pp. 104–110, 2023.

[105] C.-K. Wen, Y.-C. Chan, T.-H. Huang, H.-J. Zeng, F.-K. Wang, L.-S. Tsai, and P.-K. Liao, "End-user-centric collaborative MIMO: Performance analysis and proof of concept," *IEEE Transactions on Wireless Communications*, vol. 24, no. 9, pp. 7686–7701, 2025.

[106] S. Morimoto, H. Sugai, H. Murata, D. Murayama, T. Nakahira, and T. Ogawa, "Performance of terminal-collaborated MIMO reception system leveraging multiple decision results," in *2024 IEEE 99th Vehicular Technology Conference (VTC2024-Spring)*. IEEE, 2024, pp. 1–5.

[107] H. Murata, "Terminal-collaborated MIMO systems: Initial results of 25.9 GHz collaboration," in *2025 International Symposium on Antennas and Propagation (ISAP)*. IEEE, 2025, pp. 1–2.

[108] T.-Y. Wang and J.-Y. Wu, "Cooperative communications using reliability-forwarding relays," *IEEE Transactions on Communications*, vol. 61, no. 5, pp. 1776–1785, 2013.

[109] G. Amarasuriya, C. Tellambura, and M. Ardakani, "Impact of antenna correlation on a new dual-hop MIMO AF relaying model," *EURASIP Journal on Wireless Communications and Networking*, vol. 2010, p. 956721, 2010.

[110] Y. Zhang, D. Zhao, H. Zhao, Y. Chen, and N. Kang, "Optimization of a MIMO amplify-and-forward relay system with channel state information estimation error and feedback delay," *EURASIP Journal on Advances in Signal Processing*, vol. 2016, no. 1, p. 117, 2016.

[111] B. C. Nguyen, N. N. Thang, X. N. Tran, and L. T. Dung, "Impacts of imperfect CSI, hardware, and self-interference on full-duplex MIMO relay systems," *Sensors*, vol. 20, no. 6, p. 1671, 2020.

[112] S. Beddiaf, K. Abdellatif, F. Khennoufa, F. Kara, H. Kaya, X. Li, K. Rabie, and H. Yanikomeroglu, "A unified performance analysis of cooperative NOMA with practical constraints: Hardware impairment, imperfect SIC and CSI," *IEEE Access*, vol. 10, pp. 132 931–132 948, 2022.

[113] N. Varshney, A. V. Krishna, and A. K. Jagannatham, "Selective DF protocol for MIMO STBC based single/multiple relay cooperative communication: End-to-end performance and optimal power allocation," *IEEE Transactions on Communications*, vol. 63, no. 7, pp. 2458–2474, 2015.